State of California
California Natural Resources Agency
DEPARTMENT OF WATER RESOURCES

Methodology for Flow and Salinity Estimates in the Sacramento-San Joaquin Delta and Suisun Marsh

33rd Annual Progress Report to the
State Water Resources Control Board in
Accordance with Water Right Decisions 1485 and 1641

June 2012

Edmund G. Brown Jr.	**John Laird**	**Mark W. Cowin**
Governor	Secretary for Natural Resources	Director
State of California	Natural Resources Agency	Department of Water Resources

If you need this publication in an alternate form, contact the Public Affairs Office, 1-800-272-8869.

Foreword

This is the 33rd annual progress report of the California Department of Water Resources' San Francisco Bay-Delta Evaluation Program, which is carried out by the Delta Modeling Section. This report is submitted annually by the section to the California State Water Resources Control Board pursuant to its Water Right Decision 1485, Term 9, which is still active pursuant to its Water Right Decision 1641, Term 8.

This report documents progress in the development and enhancement of the Bay-Delta Office's Delta Modeling Section's computer models and reports the latest findings of studies conducted as part of the program. This report was compiled under the direction of Tara Smith, program manager for the Bay-Delta Evaluation Program.

Online versions of previous annual progress reports are available at: http://baydeltaoffice.water.ca.gov/modeling/deltamodeling/annualreports.cfm.

For more information contact:

Tara Smith

tara@water.ca.gov

(916) 653-9885

Page left blank for two-sided printing

State of California
Edmund G. Brown Jr., Governor

California Natural Resources Agency
John Laird, Secretary for Natural Resources

Department of Water Resources
Mark W. Cowin, Director

Dale Hoffman-Floerke, Chief Deputy Director

Office of the Chief Counsel Cathy Crothers	Public Affairs Office Nancy Vogel, , Ass't Dir.	Security Operations Sonny Fong
Gov't & Community Liaison Kimberly Johnston-Dodds	Policy Advisor Waiman Yip	Legislative Affairs Office Kasey Schimke, Ass't Dir.

Deputy Directors

Russell Stein, acting — **Delta and Statewide Water Management**
Assistant to Deputy Director: B Harrell

Gary Bardini — **Integrated Water Management**
Assistant to Deputy Director: D Uding and J Marr; Assistant Deputy Director J Andrew, Climate Change

Carl Torgersen, acting — **State Water Project**
Assistant to Deputy Director: D Adachi, P Lecocq, and G Scholl; Assistant Deputy Director M Anderson

John Pacheco, acting — **California Energy Resources Scheduling**
Assistant to Deputy Director R Grix

Kathie Kishaba — **Business Operations**
Assistant to Deputy Director J Cole

Bay Delta Office
Katherine Kelly, Chief

Modeling Support Branch
Francis Chung, Chief

Delta Modeling Section
Tara Smith, Chief

Edited by

Ralph Finch, Bay Delta Office

See individual chapters for author names

Editorial review, graphics, and report production
Supervisor of Technical Publications Patricia Cornelius
Marilee Talley, research writer

Report Contents

Figures

Table

Figures

Table

Figures

Tables

Figures

Figures

Tables

Preface

Chapter 1 Monitoring Station Locations

The authors compared several lists of purported accurate measurement station locations and conducted field measurements of some sites. The lists were analyzed using ESRI products and a script in ArcPython. This chapter describes and summarizes the analysis.

Chapter 2 Improved Geometry Interpolation in DSM2-Hydro

This chapter documents modifications to the DSM2 Delta modeling program that improve the model's internal representation of bathymetry under conditions typical of the Sacramento-San Joaquin River Delta. The authors implemented a more accurate channel cross-sectional calculation scheme based on absolute elevation and also increased the density of geometry samples (number of quadrature points) used when calculating integral quantities such as volume.

Chapter 3 DSM2 Version 8.1 Recalibration

Modifications to the DSM2 program source code that improve channel geometry representation described in Chapter 2 of this report affects results both in DSM2-Hydro and DSM2-Qual. The model has been recalibrated by adjusting Manning's coefficient values in DSM2-Hydro. The recalibrated Hydro results (flow and stage) are very close to the Bay Delta Conservation Plan (BDCP) 2009 Calibration results, although there are significant changes in Manning's coefficient values. Qual was recalibrated in 2011 after changes to improve DSM2-Qual model convergence. Using the recently recalibrated Hydro, we reran the Qual module to check the impacts of the Hydro source code changes and the Hydro recalibration on EC results. The electrical conductivity results are compared with field data and also the 2009 BDCP Calibration results.

Chapter 4 South Delta Null Zone Study

The State Water Resources Control Board (SWRCB) is in the process of reviewing and updating the 2006 Water Quality Control Plan for the San Francisco Bay/Sacramento-San Joaquin Delta Estuary (Bay-Delta Plan). The review may result in the potential amendments to the South Delta salinity objectives in the Bay-Delta Plan. Under the review process, SWRCB states that poor water circulation (null zones) contributes to bad water quality in the South Delta, and that the Central Valley Project (CVP) and State Water Project (SWP) are responsible for improving the water circulation conditions while raising water stage so that the farmers are able to divert water.

The purpose of this study is to analyze through hydrodynamic modeling whether and to what extent CVP and SWP exports and the agricultural temporary barrier actually influence the water levels (stage) and water circulation in South Delta.

Chapter 5 Estimating Delta-wide Bromide Using DSM2-Simulated EC Fingerprints

This chapter compares 6 methods to determine bromide concentrations at select locations in the Sacramento-San Joaquin River Delta (the Delta). The results of the methods are compared to observed grab sample bromide data at those Delta locations. The analysis confirms MWH's conclusion that direct simulation of bromide with DSM2 and the current version of dispersion coefficients is equivalent to estimating bromide based on DSM2-simulated electrical conductivity (EC) and applying multiple linear regressions based on simulated EC fingerprints. However, using observed EC and multiple linear regressions provides significantly better estimates of bromide. Multiple linear regressions based on

Delta regions perform nearly as well as site-specific regressions and allow for converting from EC to bromide at nearly any location in the Delta.

Chapter 6 A Continuous Surface Elevation Map for Modeling

This chapter documents the development of an elevation data set for multidimensional modeling developed under the REALM project, synthesizing LiDAR, single- and multibeam sonar soundings and surveys and integrating them with existing integrated maps that themselves were collated from multiple sources. The result is a continuous surface—terrestrial and water—in meters using the NAVD88 vertical datum. The initial release of this map was in the form of a 10 m Digital Elevation Map (DEM) for the entire Bay-Delta and parts of the coast to the Farallones, supplemented by a 2 m model of the South Delta in a region where the channel features are poorly resolved at 10 m.

Chapter 7 DSM2-PTM Simulations of Particle Movement

The National Marine Fisheries Service requested the California Department of Water Resources Modeling Support Branch perform a DSM2-PTM modeling study to investigate the impact of various factors on salmon/steelhead migration behaviors in the Sacramento-San Joaquin River Delta. Those factors include San Joaquin River flows, exports from the State Water Project and Central Valley Project, and the Head of Old River Barrier (HORB). The report documents the assumptions, model setups, and simulation results and could be used to help studies on HORB installation/operation and export adaptive management for salmonid outmigration protections.

Acronyms and Abbreviations

Bay-Delta Plan	2006 Water Quality Control Plan for the San Francisco Bay/San Joaquin Delta Estuary
BDCP	Bay Delta Conservation Plan
BNSF	Burlington Northern Santa Fe Railway
Br	bromide
CDEC	California Data Exchange Center
cfs	cubic feet per second
CLFCT	Clifton Court Forebay Gates
CVP	Central Valley Project
DC	dispersion coefficient
DCC	Delta Cross Channel
Delta	Sacramento-San Joaquin River Delta
DEM	Digital Elevation Map
DSM2	Delta Simulation Model 2
DWR	California Department of Water Resources
EC	electrical conductivity
GIS	Geographical Information System
GLCB	Grant Line Canal Barrier
HORB	Head of Old River Barrier
IE ratio	inflow/export ratio
Marsh	Suisun Marsh
MIDB	Middle River Barrier
MTZSL	Montezuma Salinity Control Structure
NED	National Elevation Dataset
NMFS	National Marine Fisheries Service
NOAA	National Oceanic and Atmospheric Administration
N-S	Nash-Suttcliffe
OMR	Old and Middle River
ORTB	Old River Barrier at Tracy
PTM	Particle Tracking Model
RPA	Reasonable Prudent Alternative
SAC R.	Sacramento River
SJR	San Joaquin River
SWP	State Water Project
SWRCB	State Water Resources Control Board
TDS	total dissolved solids
USBR	US Bureau of Reclamation
USGS	US Geological Survey
WDL	Water Data Library

Metric Conversion Table

Quantity	*To Convert from Metric Unit*	*To Customary Unit*	*Multiply Metric Unit By*	*To Convert to Metric Unit Multiply Customary Unit By*
Length	millimeters (mm)	inches (in)	0.03937	25.4
	centimeters (cm) for snow depth	inches (in)	0.3937	2.54
	meters (m)	feet (ft)	3.2808	0.3048
	kilometers (km)	miles (mi)	0.62139	1.6093
Area	square millimeters (mm^2)	square inches (in^2)	0.00155	645.16
	square meters (m^2)	square feet (ft^2)	10.764	0.092903
	hectares (ha)	acres (ac)	2.4710	0.40469
	square kilometers (km^2)	square miles (mi^2)	0.3861	2.590
Volume	liters (L)	gallons (gal)	0.26417	3.7854
	megaliters (ML)	million gallons (10*)	0.26417	3.7854
	cubic meters (m^3)	cubic feet (ft^3)	35.315	0.028317
	cubic meters (m^3)	cubic yards (yd^3)	1.308	0.76455
	cubic dekameters (dam^3)	acre-feet (ac-ft)	0.8107	1.2335
Flow	cubic meters per second (m^3/s)	cubic feet per second (ft^3/s)	35.315	0.028317
	liters per minute (L/mn)	gallons per minute (gal/mn)	0.26417	3.7854
	liters per day (L/day)	gallons per day (gal/day)	0.26417	3.7854
	megaliters per day (ML/day)	million gallons per day (mgd)	0.26417	3.7854
	cubic dekameters per day (dam^3/day)	acre-feet per day (ac-ft/day)	0.8107	1.2335
Mass	kilograms (kg)	pounds (lbs)	2.2046	0.45359
	megagrams (Mg)	tons (short, 2,000 lb.)	1.1023	0.90718
Velocity	meters per second (m/s)	feet per second (ft/s)	3.2808	0.3048
Power	kilowatts (kW)	horsepower (hp)	1.3405	0.746
Pressure	kilopascals (kPa)	pounds per square inch (psi)	0.14505	6.8948
	kilopascals (kPa)	feet head of water	0.32456	2.989
Specific capacity	liters per minute per meter drawdown	gallons per minute per foot drawdown	0.08052	12.419
Concentration	milligrams per liter (mg/L)	parts per million (ppm)	1.0	1.0
Electrical conductivity	microsiemens per centimeter (µS/cm)	micromhos per centimeter (µmhos/cm)	1.0	1.0
Temperature	degrees Celsius (°C)	degrees Fahrenheit (°F)	(1.8X°C)+32	0.56(°F-32)

Methodology for Flow and Salinity Estimates in the Sacramento-San Joaquin Delta and Suisun Marsh

33rd Annual Progress Report
June 2012

Chapter 1
Monitoring Station Locations

Authors: Ralph Finch and Jane Schafer-Kramer
Delta Modeling Section
Bay-Delta Office
California Department of Water Resources

Page left blank for two-sided printing

Contents

Figure

Tables

Page left blank for two-sided printing

1 Monitoring Station Locations

1.1 Introduction

In late 2010, the authors began to examine the DSM2 grid and Sacramento-San Joaquin River Delta bathymetry and geometry using ArcMap. Several deficiencies were noted in the current grid, among them the placement of nodes (channel junctions and ends) in the geo-referenced ArcMap. This led to the realization that we did not have accurate locations of the observed data monitoring stations. At that time, we had a single source of locations from the California Data Exchange Center (CDEC), and many were in error by several hundred meters or more. In 2011, both authors acquired lists of purported accurate station locations, and the authors conducted field measurements of some sites. We eventually had 10 lists of station locations including our own field measurements. We analyzed these lists using ESRI products and a script in ArcPython; this chapter describes and summarizes the analysis.

1.2 Procedure

We ended with 9 station lists, other than our measured stations, internally named[1]

- CDEC_Delta
- FlowStations
- NCRO_FlowStation_Oct2011
- Stations_SMayr
- SurfaceWater
- SurfaceWater_fr_GSmith
- USBR_Others
- WaterQuality
- waterquality_Stations_D1641

With so many lists of potentially good locations, two tasks became obvious:

1. estimate which stations and lists have accurate station location, and
2. estimate which stations are duplicated in other lists (in order to consolidate them).

We measured the locations of 10 stations in the North Delta to spot-check stations in other lists, and then found nearby stations—within 100 meters—in other lists using ArcPython and Arc Catalog (Table 1-1). An ArcPython script was written to perform this and other tasks described in this chapter and is reproduced as an appendix at the back of this chapter.

[1] The list names were made when the authors received each list and refer to type and source of data.

Table 1-1 Partial List of Stations and Station-Lists near Measured Stations

Contents | Preview | Description

OBJECTID *	IN_FID	NEAR_FID	NEAR_DIST	StationList	StaListName	BaseStaID
20	1	0	0	None	None	Dlc
1	2	22	11.3424413611733	SurfaceWater	B91120	Emm
6	2	22	11.3423426810068	Stations_SMayr_Proj	B91120	Emm
10	2	15	73.6189000975313	CDEC_Delta_Proj	EMM	Emm
13	2	8	129.353842404674	USBR_Others_Proj	EMMATON	Emm
15	2	56	11.3420830592777	SurfaceWater_fr_GSmith_Proj	B91120	Emm
17	2	24	235.64324379616	waterquality_Stations_D1641_Proj	D22	Emm
18	2	23	79.5521768792677	waterquality_Stations_D1641_Proj	D22A	Emm
21	3	0	0	None	None	Fpt
11	4	20	18.009518605283	CDEC_Delta_Proj	GES	Ges
7	5	31	13.7022597024286	Stations_SMayr_Proj	B91651	Ggs
2	6	32	20.2793525315143	SurfaceWater	B94100	Gsmr
3	7	24	11.132401848978	SurfaceWater	B91212	Rvb
8	7	24	11.1324547238763	Stations_SMayr_Proj	B91212	Rvb
12	7	63	139.979675713814	CDEC_Delta_Proj	SRV	Rvb
14	7	15	310.110796472058	USBR_Others_Proj	RIO VISTA	Rvb
19	8	7	88.4415861668535	waterquality_Stations_D1641_Proj	C3A	Srh
5	9	8	61.2312945804588	WaterQuality_Proj	Three Mile Slough near SJR	Tmsnsjr
16	9	152	61.2318010725615	SurfaceWater_fr_GSmith_Proj	TMS	Tmsnsjr
4	10	38	43.042055640107	SurfaceWater	B95060	Tsl
9	10	39	43.0417589480545	Stations_SMayr_Proj	B95060	Tsl

Table note: the partial listing shown here does not contain all stations and station-lists.

The OBJECTID column is used as a primary key by ArcCatalog. The IN_FID and OUT_FID columns are the primary keys for the measured station and nearby station in another list, respectively. NEAR_DIST is the distance from the measured station to the nearby station in feet; 0 means no nearby station was found in any list. StationList is the name of the list that has the nearby station, and StaListName is the name of the station in the other list. A measured station that has no nearby stations in other lists has a value "None" under each of these columns. Finally, BaseStaID is the name of the measured station.

If a measured station is found to have more than one nearby station from the other lists, each station is listed in a new row. In Table 1-1, there are 10 measured stations. Two have no nearby stations in any lists (DLC and FPT) while EMM had matches in 6 other lists. Nearby stations were found in 7 other lists, with only lists FlowStations and NCRO_FlowStation_Oct2011 failing to have nearby stations. We also know that the CDEC list contains some stations with accurate locations and some inaccurate; our first task is to estimate if other lists might be accurate.

Table 1-2 shows the total number of stations and the number of stations within the legal Delta and Suisun Marsh for each station list we have. There are at least 98 stations in the Delta and Marsh (Figure 1-1), using the highest figure in Table 1-3 (CDEC_Delta). We field-measured the locations of 10 stations (GarminWaypoints), or about 10% of the total Delta stations. For any given list, assuming that its stations are scattered throughout the Delta, we might find the same proportion of stations that match the measured stations. This also assumes that the measured stations are scattered evenly throughout the Delta, when in fact we know they are in the North Delta.

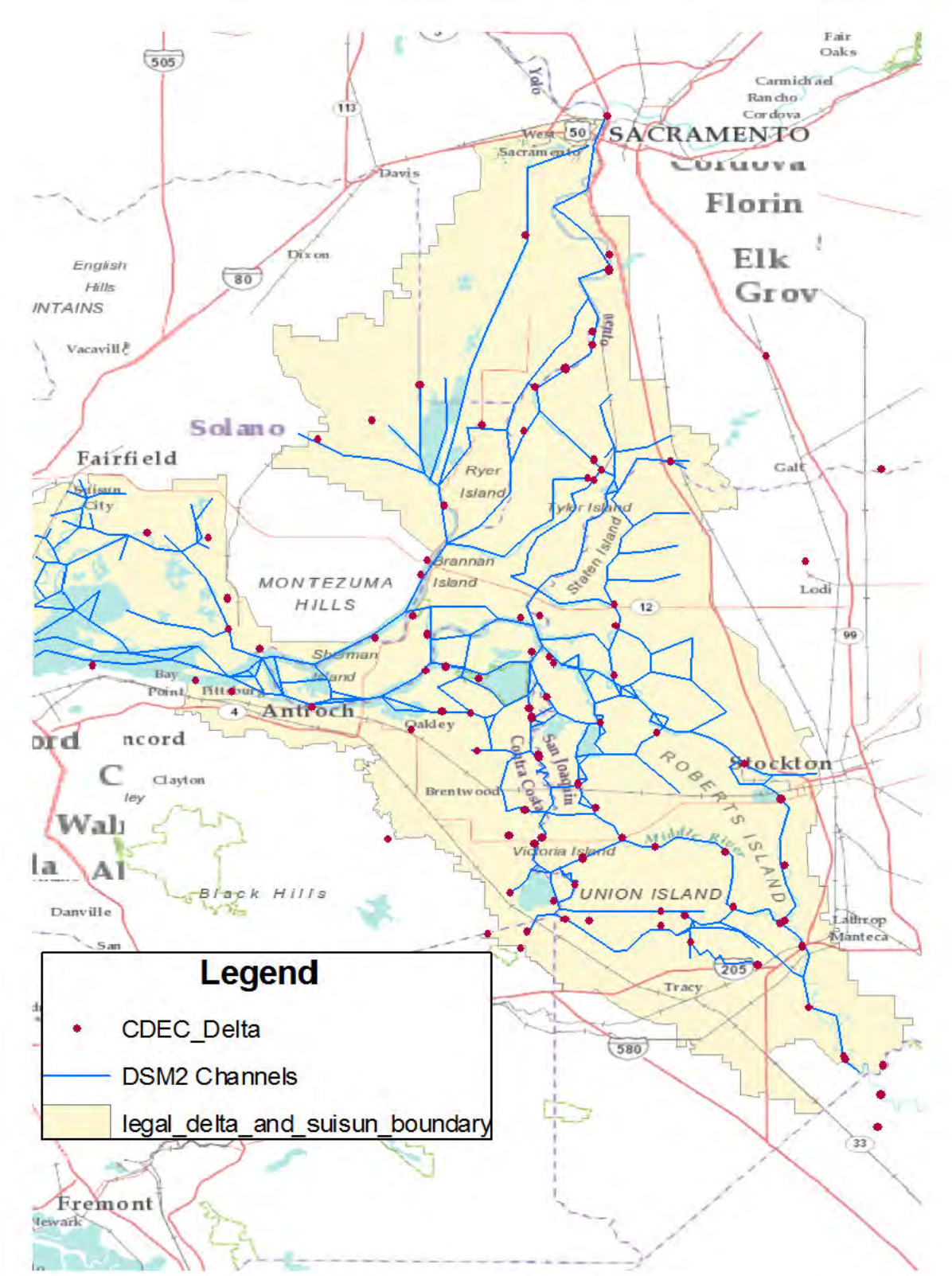

Figure 1-1 Sacramento-San Joaquin Legal Delta, DSM2 Channels, and CDEC Stations

Table 1-2 Station-Lists and Counts

Station-list name	Total number of stations	Number of stations within Delta+Marsh
CDEC_Delta	106	98
FlowStations	11	10
GarminWaypoints	10	10
NCRO_FlowStation_Oct2011	12	11
Stations_SMayr	77	57
SurfaceWater	75	55
SurfaceWater_fr_GSmith	269	60
USBR_Others	24	19
WaterQuality	32	32
waterquality_Stations_D1641	52	49

Table 1-3 is the same as Table 1-1, but sorted on the StationList column. This way it's easier to count how many stations in each list match the measured stations.

Table 1-3 Partial List of Stations and Station-Lists near Measured Stations, Sorted by Station-List

Contents | Preview | Description

OBJECTID *	IN_FID	NEAR_FID	NEAR_DIST	StationList	StaListName	BaseStaID
10	2	15	73.6189000975313	CDEC_Delta_Proj	EMM	Emm
11	4	20	18.009518605283	CDEC_Delta_Proj	GES	Ges
12	7	63	139.979675713814	CDEC_Delta_Proj	SRV	Rvb
20	1	0	0	None	None	Dlc
21	3	0	0	None	None	Fpt
6	2	22	11.3423426810068	Stations_SMayr_Proj	B91120	Emm
7	5	31	13.7022597024286	Stations_SMayr_Proj	B91651	Ggs
8	7	24	11.1324547238763	Stations_SMayr_Proj	B91212	Rvb
9	10	39	43.0417589480545	Stations_SMayr_Proj	B95060	Tsl
1	2	22	11.3424413611733	SurfaceWater	B91120	Emm
2	6	32	20.2793525315143	SurfaceWater	B94100	Gsmr
3	7	24	11.132401848978	SurfaceWater	B91212	Rvb
4	10	38	43.042055640107	SurfaceWater	B95060	Tsl
15	2	56	11.3420830592777	SurfaceWater_fr_GSmith_Proj	B91120	Emm
16	9	152	61.2318010725615	SurfaceWater_fr_GSmith_Proj	TMS	Tmsnsjr
13	2	8	129.353842404674	USBR_Others_Proj	EMMATON	Emm
14	7	15	310.110796472058	USBR_Others_Proj	RIO VISTA	Rvb
5	9	8	61.2312945804588	WaterQuality_Proj	Three Mile Slough near SJR	Tmsnsjr
17	2	24	235.64324379616	waterquality_Stations_D1641_Proj	D22	Emm
18	2	23	79.5521768792677	waterquality_Stations_D1641_Proj	D22A	Emm
19	8	7	88.4415861668535	waterquality_Stations_D1641_Proj	C3A	Srh

Table 1-4 Proportion of Stations near Measured Stations

Station list name	Number of stations within Delta+Marsh	No. of stations near measured stations	Proportion of stations near measured stations
CDEC_Delta	98	3	$\frac{3}{98} * 100 = 3.1\%$
Stations_SMayr	57	4	$\frac{4}{57} * 100 = \mathbf{7.0}\%$
SurfaceWater	55	4	$\frac{4}{55} * 100 = \mathbf{7.3}\%$
SurfaceWater_fr_GSmith	60	2	$\frac{2}{60} * 100 = 3.3\%$
USBR_Others	19	2	$\frac{2}{19} * 100 = \mathbf{10.5}\%$
WaterQuality	32	1	$\frac{1}{32} * 100 = 3.1\%$
waterquality_Stations_D1641	49	3	$\frac{3}{49} * 100 = \mathbf{6.1}\%$

Finally we calculate the proportion of nearby stations to number of Delta and Marsh stations (Table 1-4).

Previously, we reasoned that if a given list had accurate station locations and its stations were uniformly scattered throughout the Delta+Marsh and if the measured stations were uniformly scattered throughout the Delta+Marsh, we would find about 10% of stations in a given list near the measured stations. But we know the measured stations are not uniformly located throughout the Delta and Marsh; they are concentrated in the North Delta. Therefore, we expect a given list with accurate locations to have somewhat less than 10% nearby stations.

From Table 1-4, four lists have 6% to 10% of their stations within 100 m of the measured stations; we conclude those lists have accurate locations unless shown otherwise (Stations_SMayr, SurfaceWater, USBR_Others, waterquality_Stations_D1641).

Table 1-5 is a portion of a larger table produced by the same script that produced Table 1-1 and Table 1-3. The snippet shown in Table 1-5 contains the stations in the SurfaceWater list (which seems to have accurate stations) that are near the WaterQuality list. Note the 4th column, which is the distance in feet between stations in both lists. Of the 6 close stations, 2 are probably from an identical measurement because their distance apart is a small fraction of a foot: numerical round-off. The other 4 nearby stations are within 10s of feet. So for the WaterQuality list, SurfaceWater has 6 close stations out of 55 in the Delta+Marsh, a proportion of 10.9%. In a similar analysis, 6 of 57 stations in the Stations_SMayr list are near, a proportion of 10.5%. We conclude the SurfaceWater list also has accurate stations.

Table 1-5 Partial Water Quality List and nearby Stations in Surface Water List

4	14	50	25.1335008014342	SurfaceWater	B95325	Doughty Cut above GLC
5	16	49	17.4214984379326	SurfaceWater	B95300	GLC at Tracy Road
6	21	64	1.38062553001212E-05	SurfaceWater	B95500	Middle River at Union Point
7	22	53	30.8798041703845	SurfaceWater	B95366	Old River at DMC - Above
8	23	52	4.38219294088364E-05	SurfaceWater	B95365	Old River at DMC - Below
9	25	55	18.10806906965	SurfaceWater	B95400	Old River near Head

In like manner we analyzed the SurfaceWater_fr_GSmith list. Forty-one different stations from the Stations_SMayr list out of 57 Delta+Marsh stations were near (71.9%); 31 of the 41 distances were within round-off error. Forty-two different stations of 55 (76.4%) from the SurfaceWater list were near, and 31 were within round-off error. We conclude that SurfaceWater_fr_GSmith probably has accurate locations, and many are duplicates of other lists.

This leaves only the 2 flow station lists as unknown accuracy (we know CDEC has inaccurate stations). Flow stations are often not located with stage or water quality stations so we will ignore those stations; their location is not needed for the task of re-locating DSM2 nodes.

1.3 Conclusion

We conclude that the station locations in the lists we were given are generally accurate. They will be assumed to be accurate until shown otherwise. The 2 flow station lists have not been checked, but will be in the future.

We know CDEC has a mixture of accurate and inaccurate locations, for reasons unknown. There may be a way of reliably predicting which stations in CDEC are accurately located (involving the number of significant digits in their latitude and longitude values).

The next major step in this project will be to consolidate duplicate stations and generate a list of common and alternate station names. We plan on using CDEC names as the base names, generating names similar to the CDEC style where necessary.

Appendix ArcPy Script

```
import arcpy, os, time
from arcpy.mapping import *
from arcpy.analysis import *
from arcpy.management import *
from arcpy import *
## For GPS-measured stations, find nearby stations in other lists

workspaceDir1 = "D:/delta/GIS/Observed/Monitoring Stations/"
workspaceDir2 = workspaceDir1 + "Jane 20110802/"
commonDir = "C:/Users/rfinch/Documents/ArcGIS/Packages/"
outDir = "Z:/Temp"
scratchWorkspace = "z:/Temp"
overwriteOutput = True

# the GPS-measured stations DB and layer
GPSMeasGDB = workspaceDir2 + "DeltaStationsGPS.gdb/"
GPS_lyr = GPSMeasGDB + "GarminWaypoints"
# the provided lists of station locations to check
StationListsNCRO = workspaceDir1 + "Stations_NCRO/BranchStations.mdb/"
StationListsGDB = workspaceDir2 + "DeltaStationLists.gdb/"
#
SMayr_lyr = StationListsGDB + "Stations_SMayr_Proj"
CDEC_lyr = StationListsGDB + "CDEC_Delta_Proj"
USBR_lyr = StationListsGDB + "USBR_Others_Proj"
SW_lyr = StationListsGDB + "SurfaceWater_fr_GSmith_Proj"
WQD1641_lyr = StationListsGDB + "waterquality_Stations_D1641_Proj"
NCRO_Oct2011_lyr = StationListsGDB + "NCRO_FlowStation_Oct2011_Proj"
NCRO_Flow_lyr = StationListsNCRO + "FlowStations"
NCRO_SW_lyr = StationListsNCRO + "SurfaceWater"
NCRO_WQ_lyr = StationListsNCRO + "WaterQuality_Proj"
# for each station list, which field is the primary station name field
NameFields = {GPS_lyr: "station", SMayr_lyr: 'STA_NO', CDEC_lyr: 'CDEC_ID', USBR_lyr: 'StationDescription',
\
              SW_lyr: 'Site_ID', WQD1641_lyr: 'StationID', NCRO_Oct2011_lyr: "Internal_c", \
              NCRO_Flow_lyr: "Name", NCRO_SW_lyr: "Station_No", NCRO_WQ_lyr: "Station_Na"}
# A generic primary station name field
genericStaID = 'BaseStaID'
# which station lists to check
```

```
StationLyrs = [NCRO_Oct2011_lyr, NCRO_Flow_lyr, NCRO_SW_lyr, NCRO_WQ_lyr, \
               SMayr_lyr, CDEC_lyr, USBR_lyr, SW_lyr, WQD1641_lyr, GPS_lyr]
# where to put output tables
env.workspace = StationListsGDB
# find other stations with searchRadius of each Base list location
searchRadius = '100 Meters'
location = 'NO_LOCATION'
angle = 'NO_ANGLE'
closest = 'ALL'
closestCount = 5
tempTable = GPSMeasGDB + "temp"
for baseLyr in StationLyrs:
    temp = os.path.basename(baseLyr).replace('_lyr','')
    temp = temp.replace('_Proj','')
    outTable = 'Nearest_' + temp
    # get OID field of base table
    BaseOIDFld_lst = ListFields(baseLyr, '', 'OID')
    BaseOIDFld_nm = BaseOIDFld_lst[0].name
    print "Base List:", os.path.basename(baseLyr), "OID:", BaseOIDFld_nm
    # total number of stations in base layer, and nearest stations found
    nStasBase = int(GetCount(baseLyr).getOutput(0))
    nStasFound = 0
    # create nearest table...
    lyrCount = 0
    for lyr in StationLyrs:
        shortLyr = os.path.basename(lyr)
        if lyr == baseLyr:
            continue
        #print 'List: ',shortLyr
        try: Delete(tempTable)
        except: pass
        desc = Describe(lyr)
        if not desc.hasOID:
            print 'No ObjectID field, skipping layer', shortLyr
            continue
        # put the nearest table list into the temporary table...
        # we will add fields to it for the permanent table.
        GenerateNearTable(baseLyr, lyr, tempTable, searchRadius,location, angle, closest, closestCount)
        # now join the Base table to the nearest table...
        # get correct field delimiters
        delmField = arcpy.AddFieldDelimiters(tempTable, 'NEAR_FC')
```

```
        # ...join to get location names
        JoinField(tempTable, 'in_fid', baseLyr, BaseOIDFld_nm, NameFields[baseLyr])
        if lyrCount == 0:
            # Create permanent table
            try: Delete(GPSMeasGDB + outTable)
            except: pass
            CreateTable(GPSMeasGDB, outTable, tempTable, '')
            AddField(GPSMeasGDB + outTable, 'StationList', 'text', '', '', 50, '', '', '', '')
            AddField(GPSMeasGDB + outTable, 'StaListName', 'text', '', '', 254, '', '', '', '')
        # ...join the station name from the target station list
        JoinField(tempTable, 'near_fid', lyr, desc.OIDFieldName, NameFields[lyr])
        AddField(tempTable, 'StationList', 'text', '', '', 50, '', '', '', '')
        rows = UpdateCursor(tempTable, '', '', '', '')
        for row in rows:
            row.StationList = shortLyr[0:49]
            rows.updateRow(row)
        # Create FieldMappings object for append output fields
        fieldMappings = FieldMappings()
        # Add all fields from tempTable
        fieldMappings.addTable(tempTable)
        fldMap_staListName = fieldMappings.getFieldMap(fieldMappings.findFieldMapIndex(NameFields[lyr]))
        # Set name of permanent output field StaListName
        fld_staListName = fldMap_staListName.outputField
        fld_staListName.name = "StaListName"
        fldMap_staListName.outputField = fld_staListName
        fieldMappings.addFieldMap(fldMap_staListName)
        fieldMappings.removeFieldMap(fieldMappings.findFieldMapIndex(NameFields[lyr]))
        Append(tempTable, GPSMeasGDB + outTable, 'NO_TEST', fieldMappings, '')
        lyrCount += 1
    try: arcpy.management.Delete(tempTable)
    except: pass
    # Checking against all station lists is done
    # Check the output table for stations in the base layer that had no near matches
    # and add the generic station id field, deleting the base list station id field
    AddField(GPSMeasGDB + outTable, genericStaID, 'TEXT', '','', '50', '', 'NULLABLE', 'NON_REQUIRED', '')
    staNumListPrev = 0
    missingStas = []
    rows = UpdateCursor(GPSMeasGDB + outTable, '', '', '', 'IN_FID A')
    for row in rows:
        row.setValue(genericStaID,row.getValue(NameFields[baseLyr]))
        rows.updateRow(row)
```

```
        staNumList = long(row.IN_FID)
        if staNumList == staNumListPrev:
            continue
        while staNumList-staNumListPrev > 1:
            missingStas += [staNumListPrev+1]
            staNumListPrev += 1
        staNumListPrev = staNumList
    DeleteField(GPSMeasGDB + outTable, NameFields[baseLyr])
    del row, rows
    rows = InsertCursor(GPSMeasGDB + outTable)
    nStasFound = nStasBase - len(missingStas)
    for sta in missingStas:
        row = rows.newRow()
        rowsBase = SearchCursor(baseLyr, BaseOIDFld_nm+" = "+str(sta), "", NameFields[baseLyr], "")
        for rowBase in rowsBase:    # should be only 1 row
            baseStaID = rowBase.getValue(NameFields[baseLyr])
            row.setValue(genericStaID,baseStaID)
        row.IN_FID = sta
        row.NEAR_FID = 0L
        row.NEAR_DIST = 0.0
        row.StationList = 'None'
        row.StaListName = 'None'
        rows.insertRow(row)
        #print "No near neighbor in", os.path.basename(baseLyr), "for station", baseStaID
    print 'Total stations', nStasBase, 'Stations Nearest', nStasFound
    print
print "Finished"
```

Methodology for Flow and Salinity Estimates in the Sacramento-San Joaquin Delta and Suisun Marsh

33rd Annual Progress Report
June 2012

Chapter 2
Improved Geometry Interpolation in DSM2-Hydro

Authors: Lianwu Liu, Eli Ateljevich, and Prabhjot Sandhu
Delta Modeling Section
Bay-Delta Office
California Department of Water Resources

Page left blank for two-sided printing

Contents

Figures

Page left blank for two-sided printing

2 Improved Geometry Interpolation in DSM2-Hydro

2.1 Introduction

This chapter documents modifications to the DSM2 program source code that improve the model's internal representation of bathymetry under conditions typical of the Sacramento-San Joaquin River Delta (the Delta). In DSM2, geometry is input by means of *cross sections* specified by the user at selected points along a channel. The cross section input represents a lookup table of width, area, and wetted perimeter versus elevation. The geometry is then interpolated along the channel from locations chosen by the user to locations where geometry is needed for computations. This interpolation requires some assumption about the vertical structure of the cross section, and whether properties at upstream and downstream locations should be compared based on "similar height from the bed" or "similar absolute elevation."

The original methods used in DSM2 were based on height from the bed and were suited to long river reaches with consistent slopes. The authors found this assumption to be less accurate in the Delta, which has an undulating bottom due to local scour, channel dredging, berms, and other local geometric features. In the present project, the authors implemented a more accurate scheme based on absolute elevation and also increased the density of geometry samples (number of quadrature points) used when calculating integral quantities such as volume.

2.2 Hydro Geometry Setup and Channel Cross Section Interpolation Methods

DSM2-Hydro uses an adapted version of the FourPt program (DeLong, Thompson, & Lee, 1997), which divides the Delta into discrete computation points along its channels. A contrived example for a single channel is shown in Figure 2-1. Two nodes are shown connected by a channel, and a network of nodes and channels represent the "user" view of the channel network. Additionally, the user must specify a nominal spatial grid size ΔX (usually 5,000 feet in DSM2 practice in the Delta) and some cross section geometry (possible locations of which are shown by thick violet arrows).

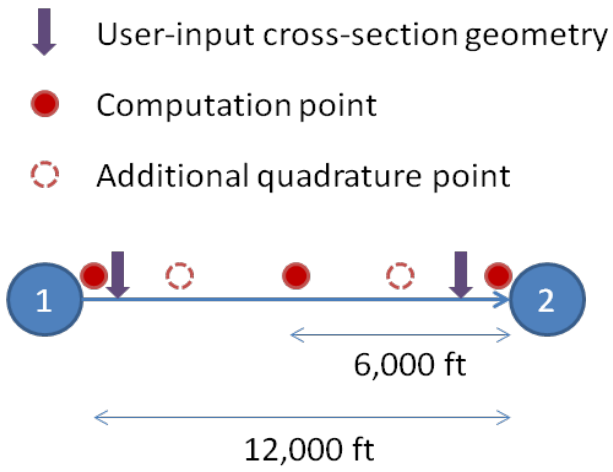

Figure note: The user cross section locations are indicated using thick violet arrows. The computation points and quadrature points where geometry is used in calculations are shown as small (closed and opened) red circles.

Figure 2-1 Computational Grid for a Fictional Channel Connecting Nodes '1' and '2'

The model calculations are based on computational points, which are more densely spaced than channels and nodes. When the computational mesh is constructed internally, channels may be further subdivided to conform better to the requested grid size. Specifically, a channel is subdivided into uniform computational sections no smaller than the requested ΔX. If in the example ΔX is assumed to be 5,000 ft, and the channel is 12,000 ft, the channel will be divided in two computational sections of 6,000 ft.

Finally, Hydro generates *virtual cross sections* not only at the computational point locations but also at quadrature points between the computation points that are used for calculating integral quantities such as volume. The computation and potential quadrature points are indicated with closed and open red circles in Figure 2-1; advanced users can discover their location, but they are not exposed in standard usage.

The basis for assigning values at virtual cross sections is *bilinear interpolation.* User-input cross sections are located downstream and upstream, and a value is obtained by assuming geometry at similar heights is comparable and can be interpolated in the streamwise direction based on distance. Wetted perimeter is similarly interpolated. Area is integrated vertically from width for consistency rather than independently interpolated.

The crux of the interpolation geometry is deciding what a "similar height" is. The original DSM2 geometry module compared the geometry based on height from the bed. In other words, the width of a virtual cross section 10 ft from the lowest point in the cross section was assumed to be comparable to the width of upstream and downstream user cross sections 10 ft from their respective beds. This assumption is clearly problematic when adjacent user cross sections used in interpolation are dramatically different in bottom elevation due to local irregularities.

An applied example that illustrates the issue is given by DSM2 channel 445 (connecting nodes 329 and 366) in Suisun Bay. Figure 2-2 shows user input cross sections in this channel at fractional lengths[1] 0.211, 0.551, and 0.819. The cross sections look symmetrical because they are inverted from width and area, which are the only data used by the model but are insufficient to infer exact geometry.

[1] The relative locations multiplied by the length of the channel will give the distance from the upstream node to the user-input cross sections.

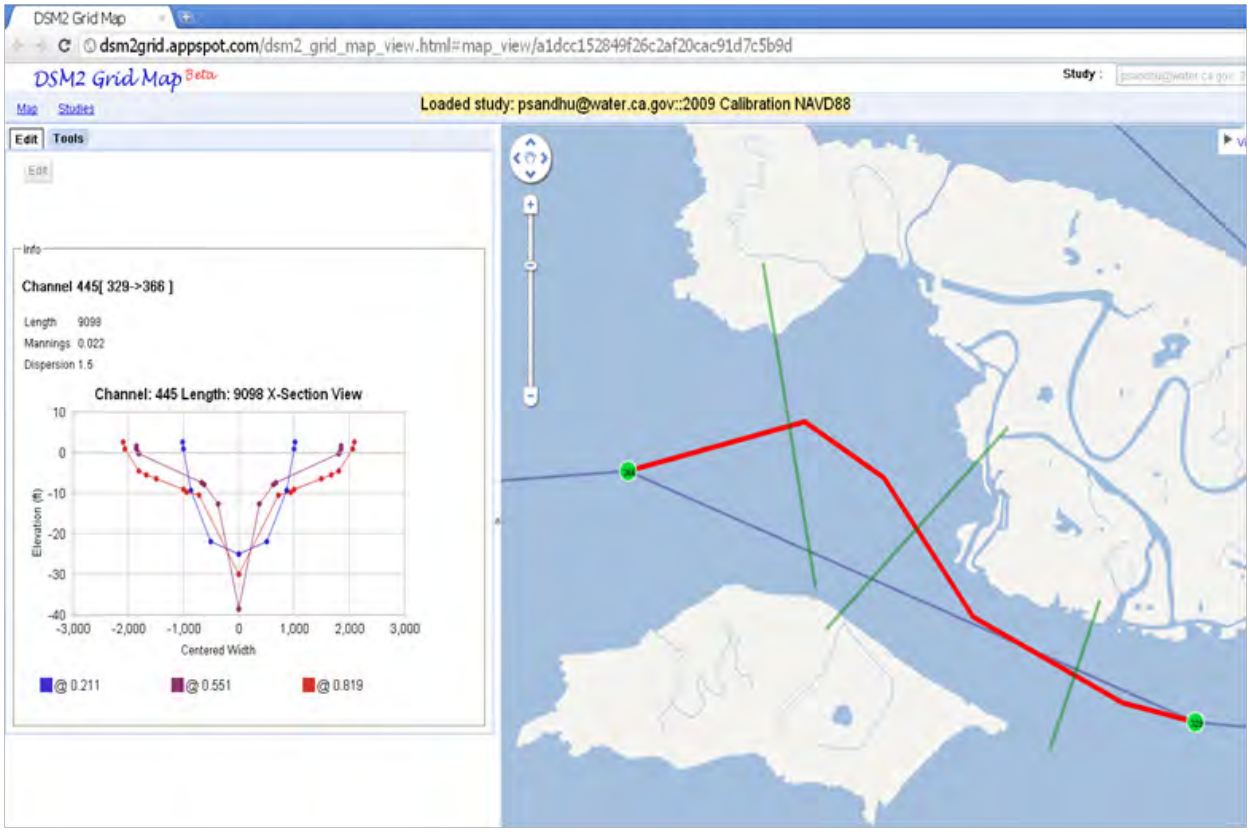

Figure note: Cross sections are shown as symmetric because they are inverted from area and width and do not determine the exact shape of the cross section. Distances are in feet.

Figure 2-2 A Map of User Input Cross Sections of Channel 445 in Suisun Marsh

Figure 2-3 shows the virtual cross sections used in DSM2-Hydro. Because the channel length is 9,098 ft, with a ΔX of 5,000 ft, the channel has only one computational reach. Computational points are located at both ends of the channel. Virtual cross sections at the ends are generated by interpolation with cross sections in channel 445 and adjacent channels. The virtual cross section at the midpoint is interpolated from the cross sections at fractional lengths 0.211 and 0.551.

Figure 2-4 illustrates height-based interpolation. Due to the big difference in bottom elevation, the interpolation layers have a large slope. The interpolation is not accurate. The method assumes that the change in bottom elevation is due to a slope in the channel that is also reflected in the slope of the water surface. For the Delta, this large change in bottom elevation is not a sloping bottom as much as it is an irregularity in the depth.

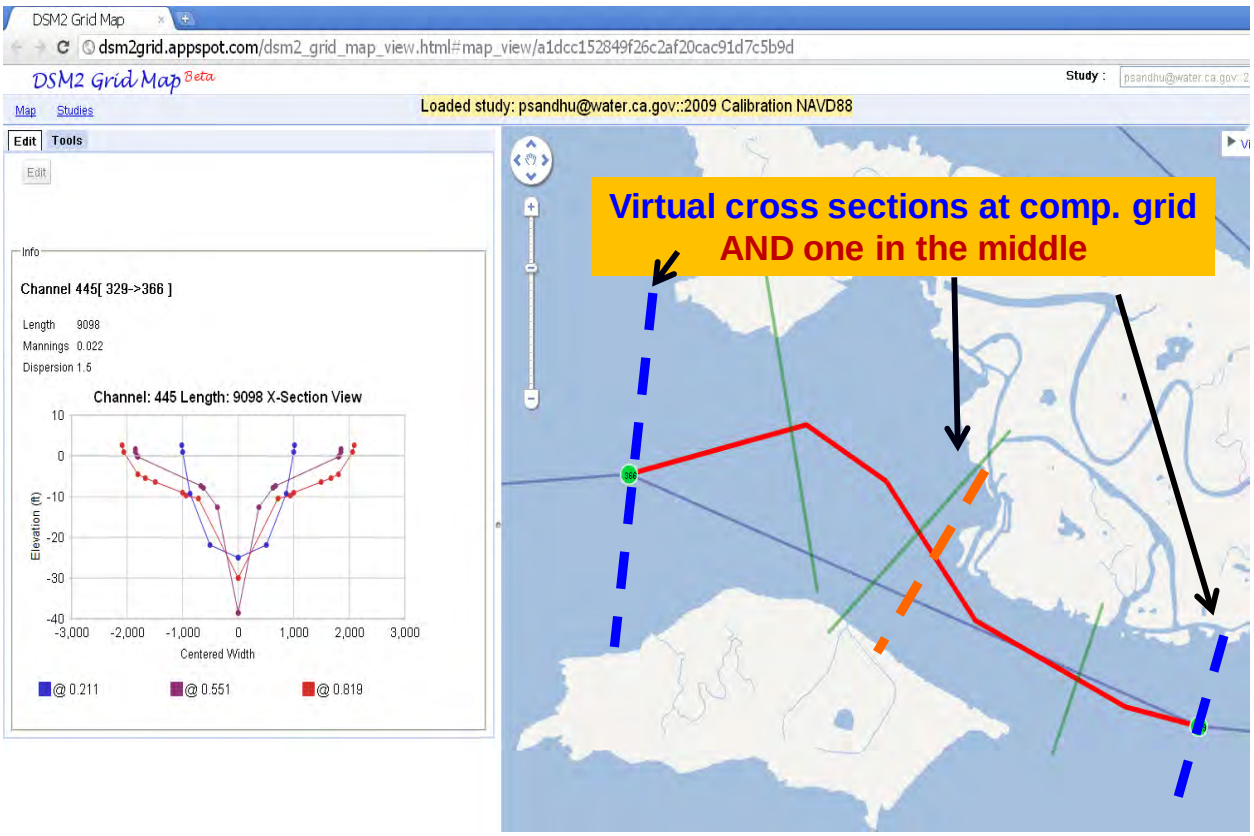

Figure 2-3 Virtual Cross Section Locations at Computational Points and Midpoint

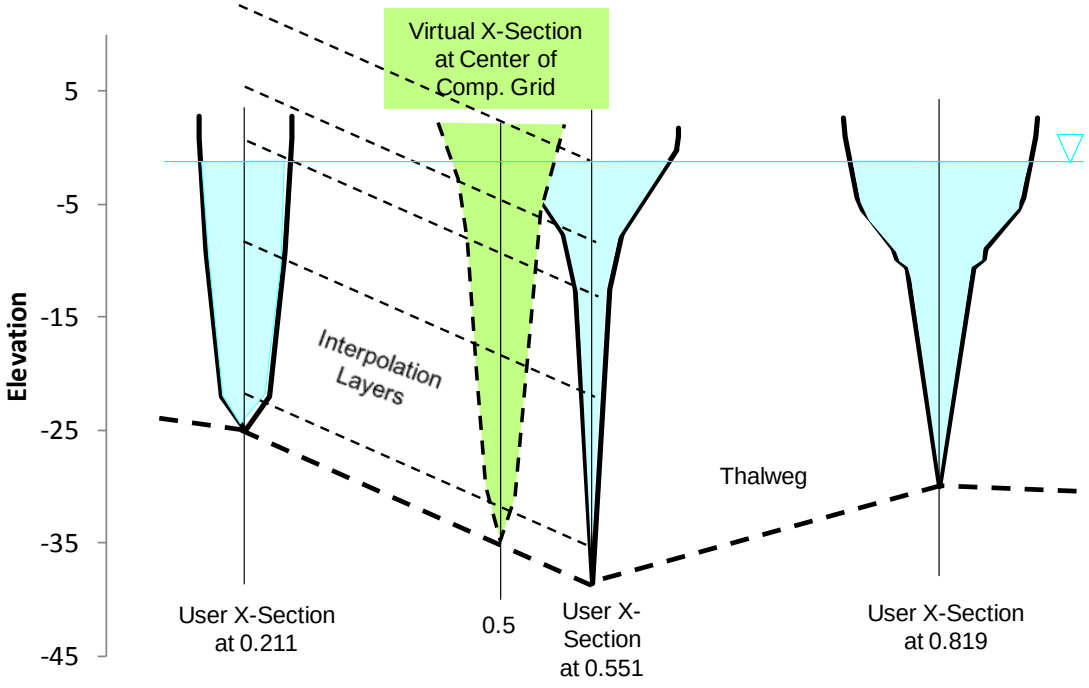

Figure 2-4 Illustration of Height-based Cross Section Interpolation

We have changed the interpolation to an elevation-based method, which is more appropriate for the Delta where the water surface is mostly flat, as shown in Figure 2-5 . Test runs showed this modification changed electrical conductivity (EC) results by only around 1% in most Delta stations. The effect of this modification is not significant.

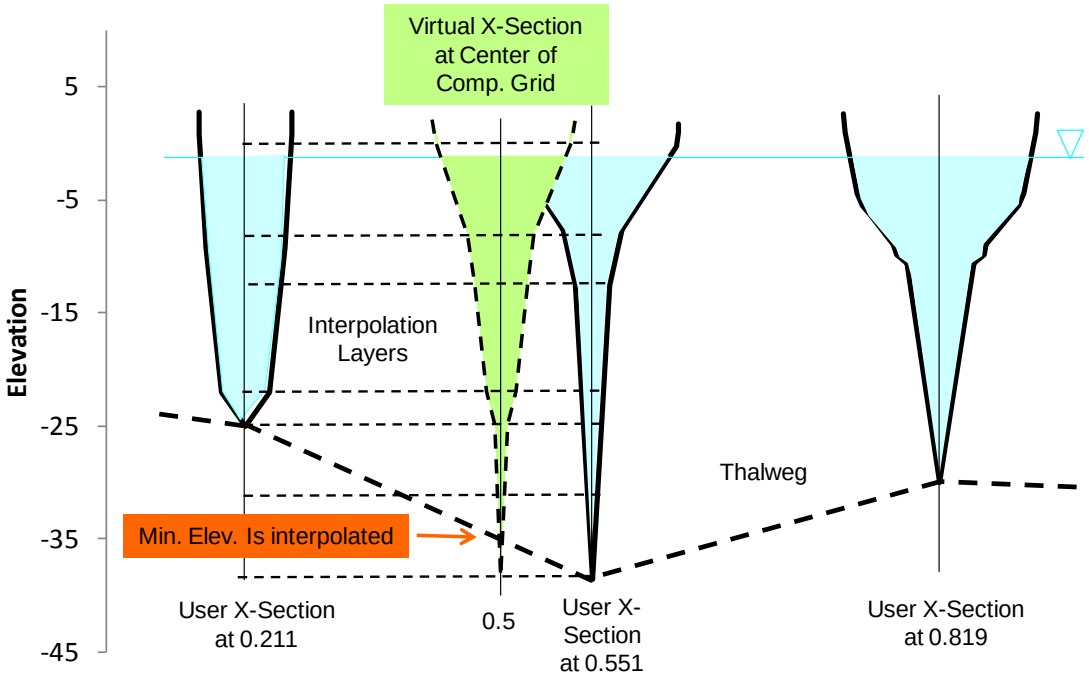

Figure 2-5 Illustration of Elevation-based Cross Section Interpolation

2.3 Improvement in Spatial Integration

Numerical integration in space is accomplished in the model through the use of a general quadrature. For a typical variable, φ, it is expressed by

$$\int_{x1}^{x2} \varphi \, dx \cong \Delta x \sum_{k=1}^{n} \omega_k \, \varphi_{\xi_k}$$

where ω is a weighting function. The number of points n, location ξ_k, and corresponding weight ω_k, in general determine accuracy of the approximation. Weights ω_k must sum to 1.

DSM2-Hydro has been using n = 1 for the simplicity and speed, a decision that was made at a time when relatively little detailed geometry was available. In this case, integrated properties such as the volume of a channel are calculated entirely from one cross section at the middle of the computational reach. When n = 2, a channel is represented by average of two cross sections at computational points. When n = 3, a channel is represented by average of all 3 virtual cross sections in a computational reach.

Results should be more accurate and reliable using n = 3, especially when one cross section is quite different from the others.

2.4 Model State at the Midpoint of a Computational Reach

At some quadrature points, we need to calculate a geometry parameter such as area at a location where there is no model state representing water surface. In this case, the model must interpolate an elevation to use as the basis for the geometry lookup. And an analogous issue arises to the one discussed above, i.e., whether to interpolate height (from bed to surface) or absolute surface relative to a datum.

As an example, DSM2 uses a file called a tidefile to pass data from Hydro to Qual. In the tidefile, average channel area was not calculated accurately in some channels. Because a single quadrature point was being used, average channel area was being calculated as average of areas at the middle of computational reaches. As shown in Figure 2-6, height (same as water depth) was interpolated first to the middle of the computational grid, and then area was calculated based on this interpolated depth. When the bottom elevation of the virtual cross section in the middle is quite different from those on the ends, the true depth is quite different from the interpolated depth; and calculated area is not correct. The problem is that depth is not a good variable to interpolate. Water surface elevation can be safely assumed to change linearly and slowly within a computational reach and should be used in the interpolation. This error affected Qual results because average channel area is used to initialize the volume of the channel. The error also affected Hydro because the same algorithm is used in Hydro to calculate some terms involving channel area. Test runs showed this modification has significant effects on both Hydro and Qual results. Recalibration will be needed for both Hydro and Qual before the change is formally released.

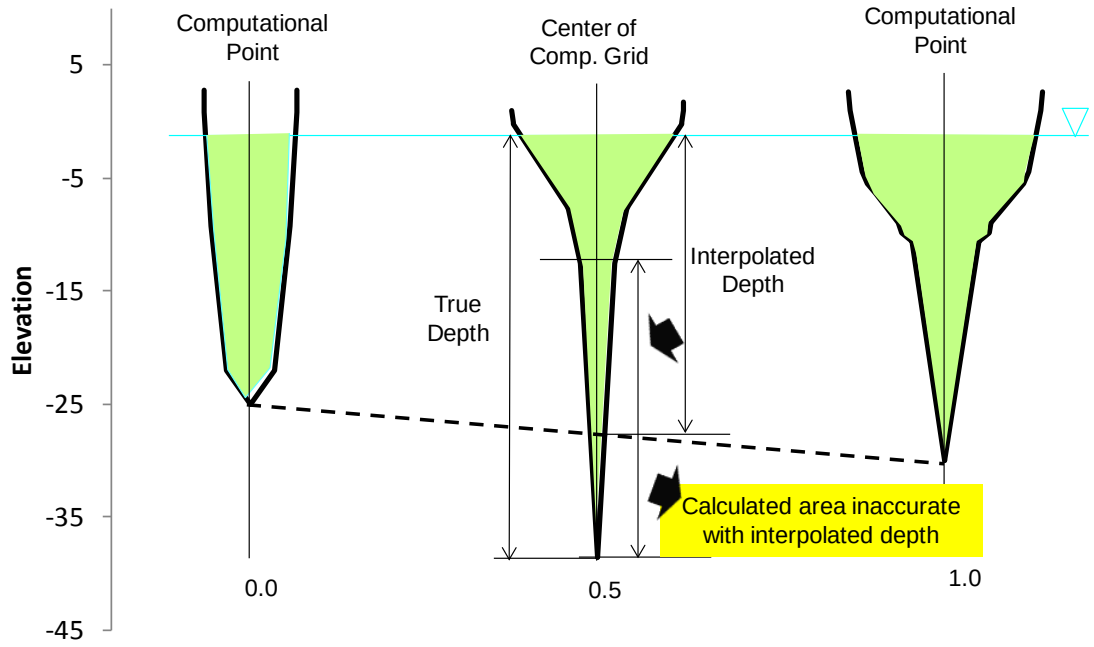

Figure 2-6 Illustration of a Poor Area Calculation

2.5 Summary of Modifications

- Virtual cross sections are generated based on elevation instead of height.
- Interpolated water surface instead of depth for midpoint geometry calculation.
- Quadrature points changed to 3. Results should be more accurate.
- Re-calibration is needed as a result of modifications.

2.6 References

DeLong, L. L., Thompson, D. B., & Lee, J. K. (1997). *The computer program FourPt (Version 95.01)--a model for simulating one-dimensional, unsteady, open-channel flow.* U.S. Geological Survey.

Page left blank for two-sided printing

Methodology for Flow and Salinity Estimates in the Sacramento-San Joaquin Delta and Suisun Marsh

33rd Annual Progress Report
June 2012

Chapter 3
DSM2 Version 8.1 Recalibration

Authors: Lianwu Liu and Prabhjot Sandhu
Delta Modeling Section
Bay-Delta Office
California Department of Water Resources

Page left blank for two-sided printing

Contents

Figures

Table

Page left blank for two-sided printing

3 DSM2 Version 8.1 Recalibration

3.1 Introduction

Modifications to the DSM2 program source code that improve channel geometry representation, presented at a DSM2 Users Group meeting (Liu & Ateljevich, 2011 Oct) and discussed in Chapter 2 of this Report (Liu, Ateljevich, & Sandhu, 2012), affects results both in DSM2-Hydro and DSM2-Qual. The model has been recalibrated by adjusting Manning's coefficient values in DSM2-Hydro. The recalibrated Hydro results (flow and stage) are very close to the Bay Delta Conservation Plan (BDCP) 2009 Calibration results (CH2M Hill, 2009 Oct), although there are significant changes in Manning's coefficient values. Stations for hydro calibration are shown in Figure 3-1. Qual was recalibrated in 2011 after we made changes to improve DSM2-Qual model convergence (Liu & Sandhu, 2011 Aug). Using the recently recalibrated Hydro, we reran the Qual module to check the impacts of the Hydro source code changes and the hydro recalibration on EC results. The electrical conductivity (EC) results are compared with field data and also the 2009 BDCP Calibration results.

3.2 Hydro Recalibration Results

This recalibration is based on the 2009 BDCP Calibration grid (CH2M Hill, 2009 Oct). The Hydro calibration period was from 10/1/2000 to 10/1/2002 and validation period from 10/1/2006 to 10/1/2008. Only Manning's coefficients were adjusted for this brief recalibration. All other model setup and boundary conditions were the same as in the 2009 BDCP Calibration.

The model was primarily calibrated to match observed flows. Modeled stage was also compared to observed stage. The calibration metric is composed of 4 figures for each station:

- **Timeseries comparison of tidally filtered daily-averaged flow.** This plot compares modeled and observed tidally averaged flow, or net flow. Net flow is critical for flow distribution and for salt transport.
- **Linear regression analysis of tidally filtered daily-averaged flow.** This scatterplot with a linear regression trend line shows statistically the comparison of the simulated vs. observed daily averaged flow. R^2 value gives information about the goodness of fit of the model. The trend line shows over- or under-estimating of the model.
- **Timeseries comparison of instantaneous flow.** This plot compares modeled and observed instantaneous flow. We show only 5 days in order to be able to see the tidal process and comparison clearly.
- **Timeseries comparison of instantaneous stage.** This plot compares modeled and observed instantaneous stage for the same period of the instantaneous flow plot.

Because overall the calibrated flow in 2009 BDCP Calibration matched observed data reasonably well, the 2009 calibration was used as a reference. Manning's n values were adjusted by groups. Sixteen adjustments/runs were made to reach the satisfactory result. Comparisons at key stations are plotted in Figure 3-2 to Figure 3-13: RSAC155, RSAC128, RSAC123, RSAC101, RSAN018, RSAN063, ROLD024, ROLD034, SLTRM004, CHDCC000, SLGEO009, and CHGRL009. Because we only adjusted Manning's n values in this brief recalibration, improvement of the calibration is slight. The recalibrated flow and stage results are very close to the 2009 calibration. Other changes in the model may be needed to further improve the calibration, e.g., improved estimates of Delta diversion and return flows and water quality, improved open area representations, better bathymetry, etc.

Due either to the bug fix or to a calibration process different than in the 2009 BDCP Calibration, Manning's n values changed significantly in some areas, as listed in Table 3-1 (for example, in Sutter Slough and Steamboat Slough, Manning's n changed from 0.024 to 0.031; Lower San Joaquin River channels 48 to 51 changed from 0.022 to 0.026; Montezuma Slough area changed from 0.018 to 0.021).

Table 3-1 Recalibrated Manning's Coefficient

GroupName	Channel Number	2009 Mini_Calibration	Recalibrated
SUTTER_SL	379--382	0.024	0.031
STEAMBOAT_SL	383--387	0.024	0.031
LOWER_SJR	48--53, 282--301	0.019--0.037, most 0.022	0.026
THREE MILE SL	307--310	0.033	0.032
FALSE_RIVER	276--279	0.027	0.025
DUTCH_SL	215, 260, 273--275	0.027	0.025
OLD_RIVER	81--124, 214--278	0.027	0.025
MONTEZUMA_SL	455--542	0.018	0.021

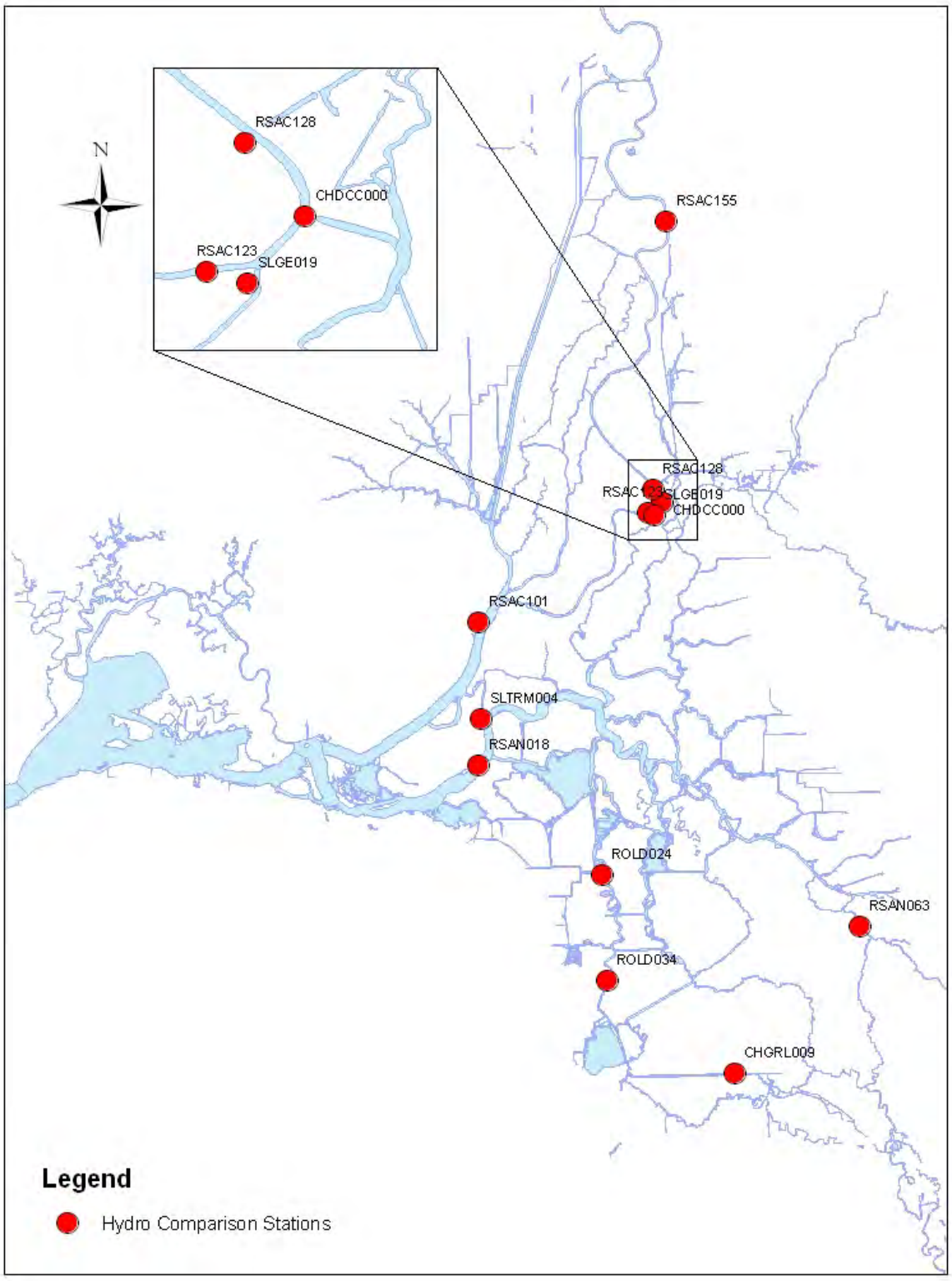

Figure 3-1 Stations for Hydro Calibration

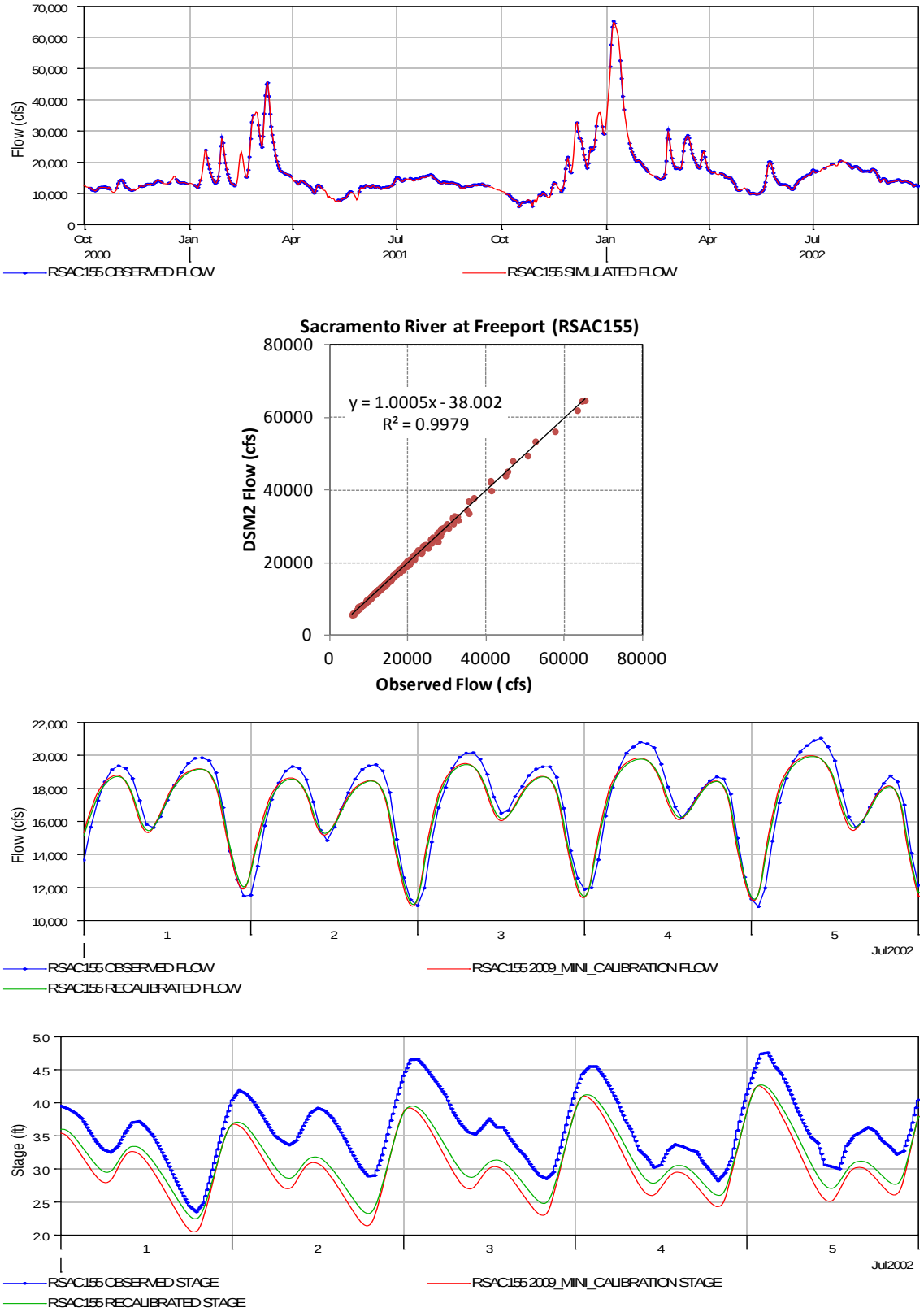

Figure 3-2 Hydro Calibration, Sacramento River at Freeport

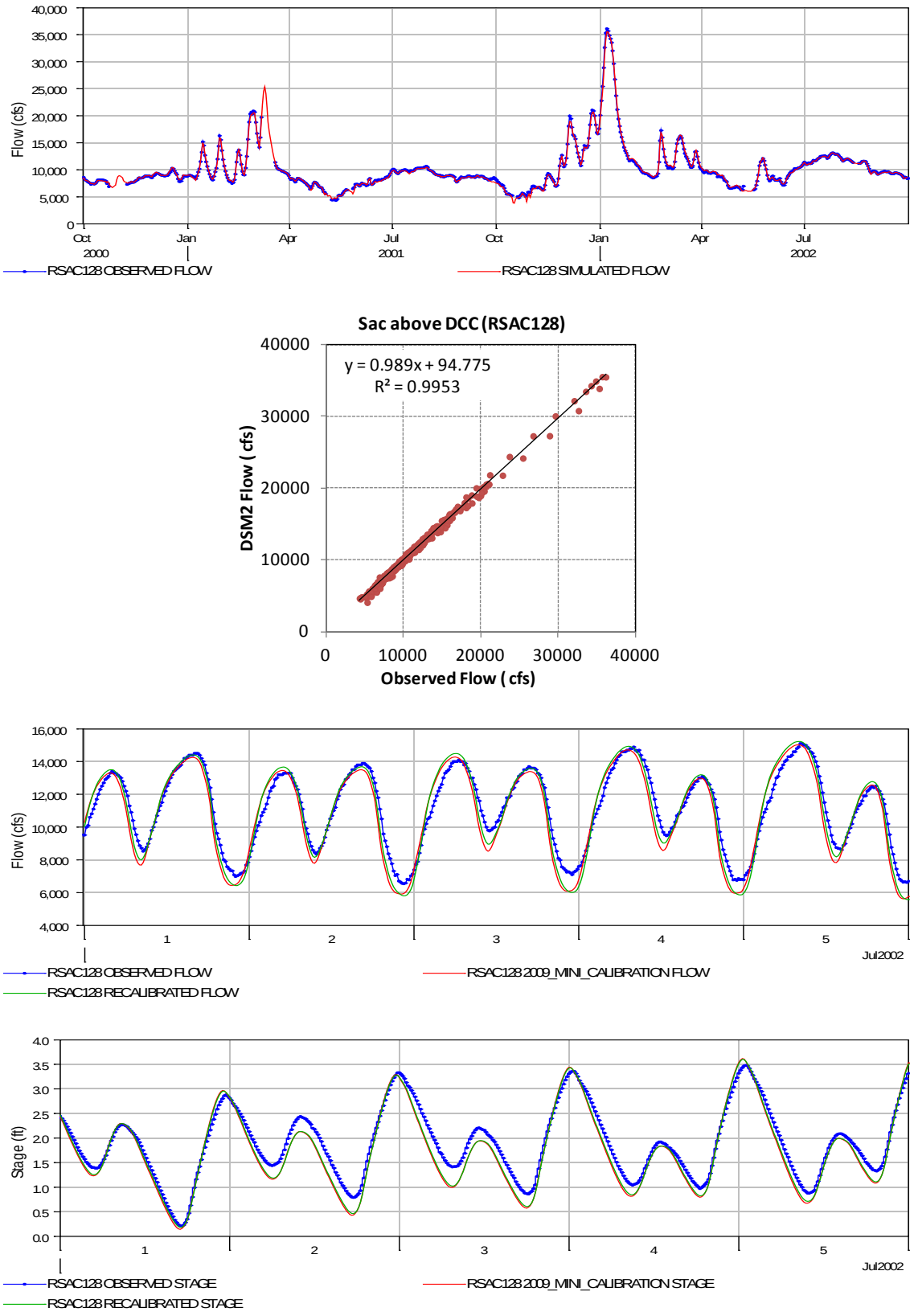

Figure 3-3 Hydro Calibration, Sacramento River above Delta Cross Channel

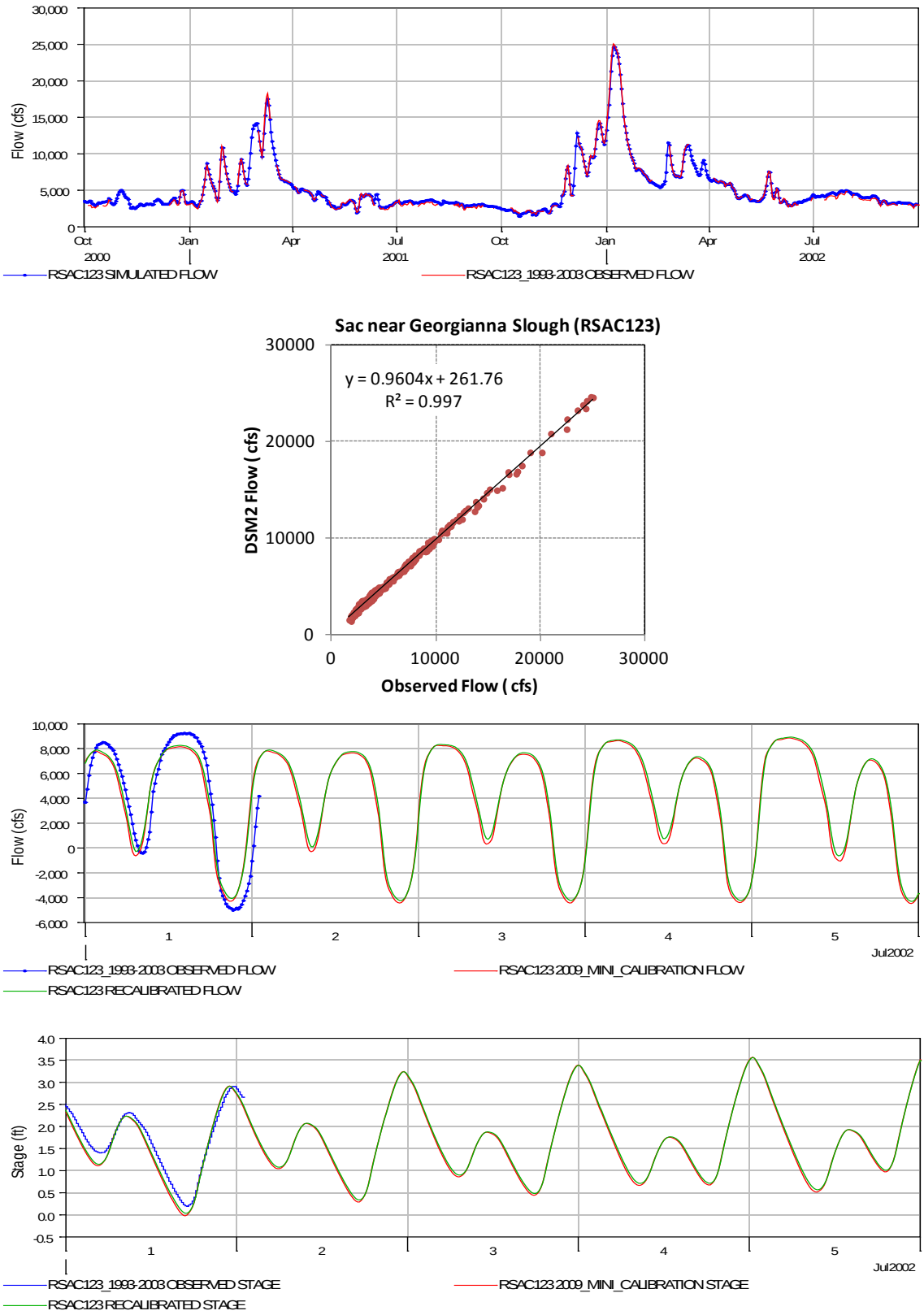

Figure 3-4 Hydro Calibration, Sacramento River downstream of Georgiana Slough

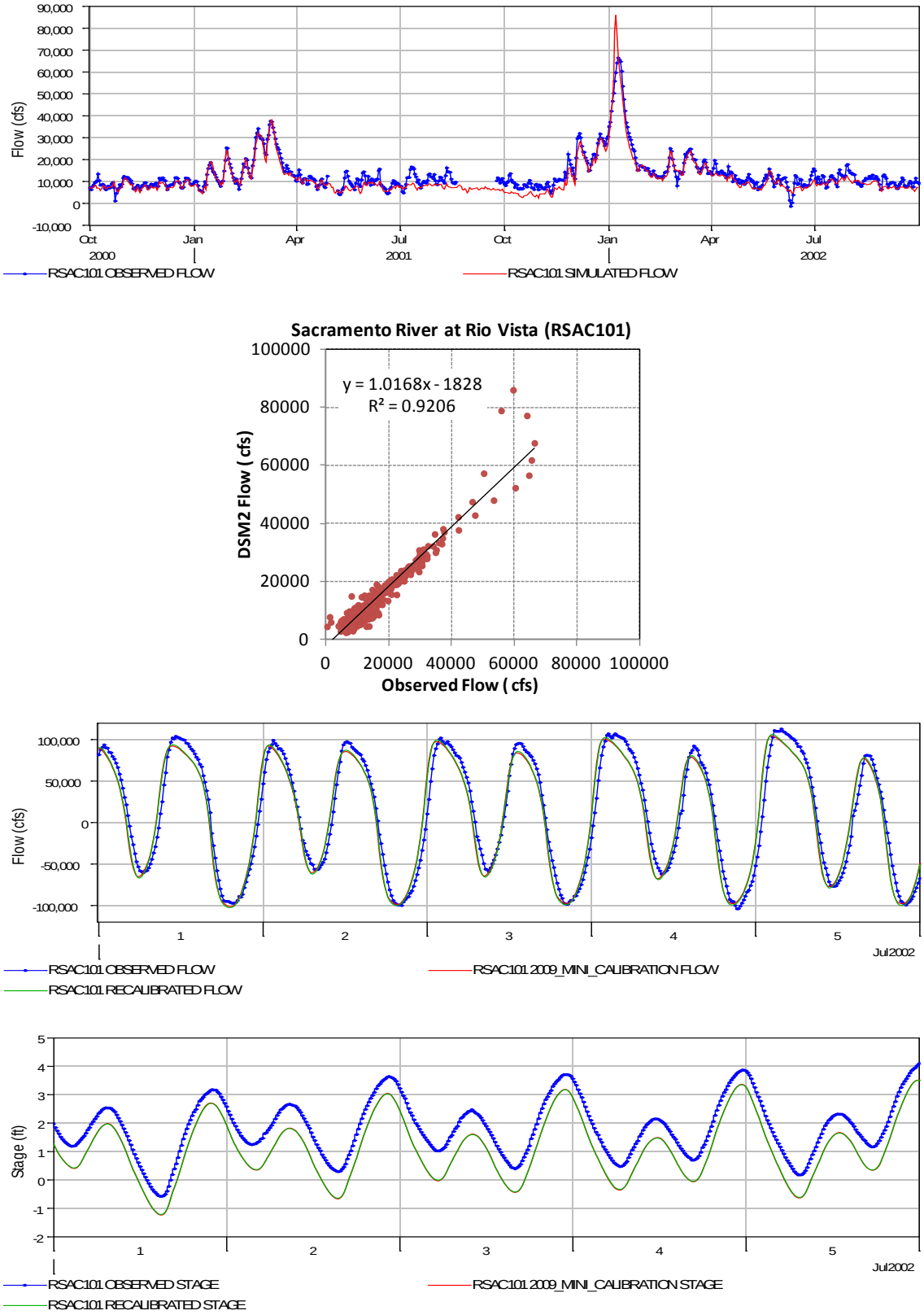

Figure 3-5 Hydro Calibration, Sacramento River at Rio Vista

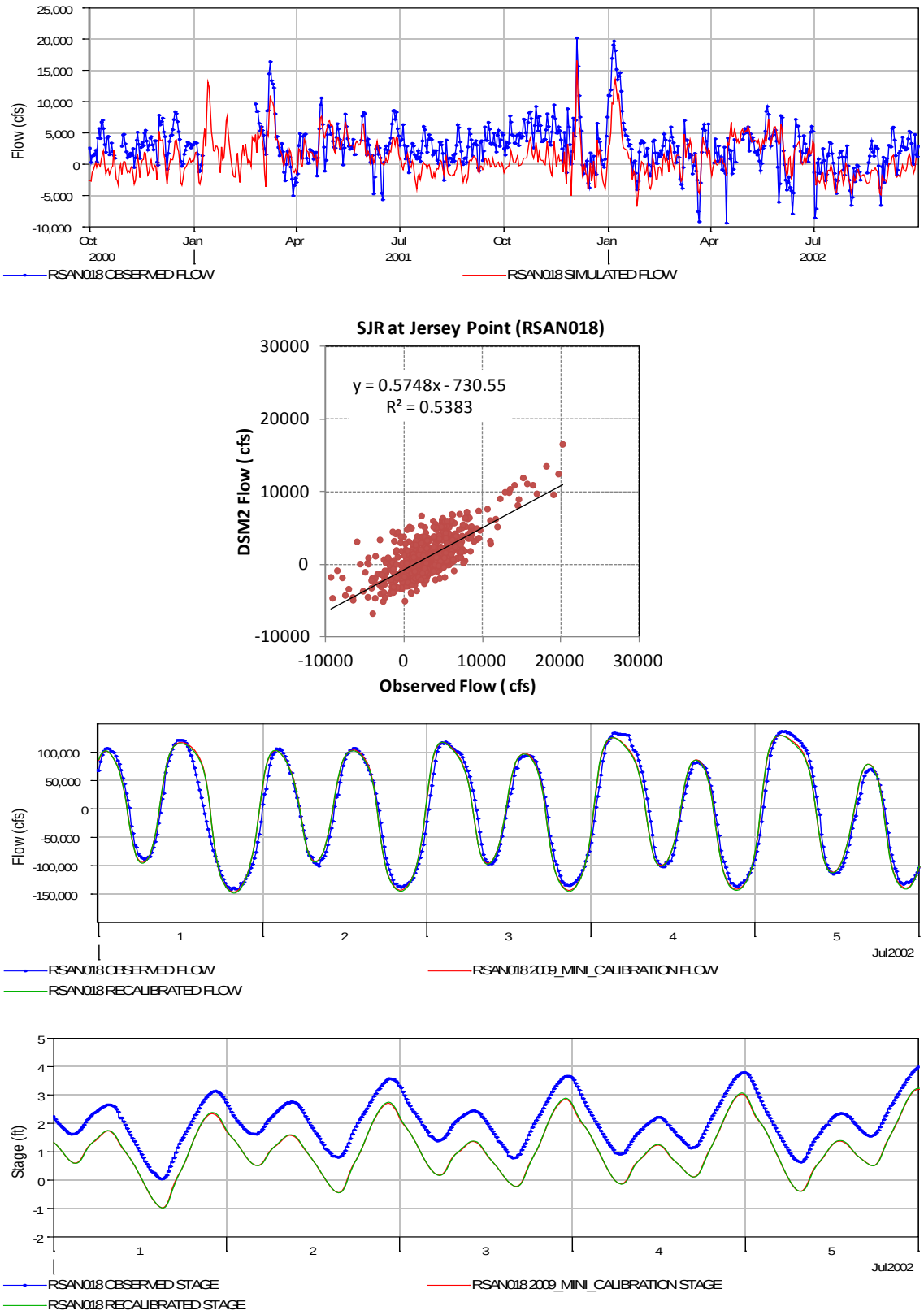

Figure 3-6 Hydro Calibration, San Joaquin River at Jersey Point

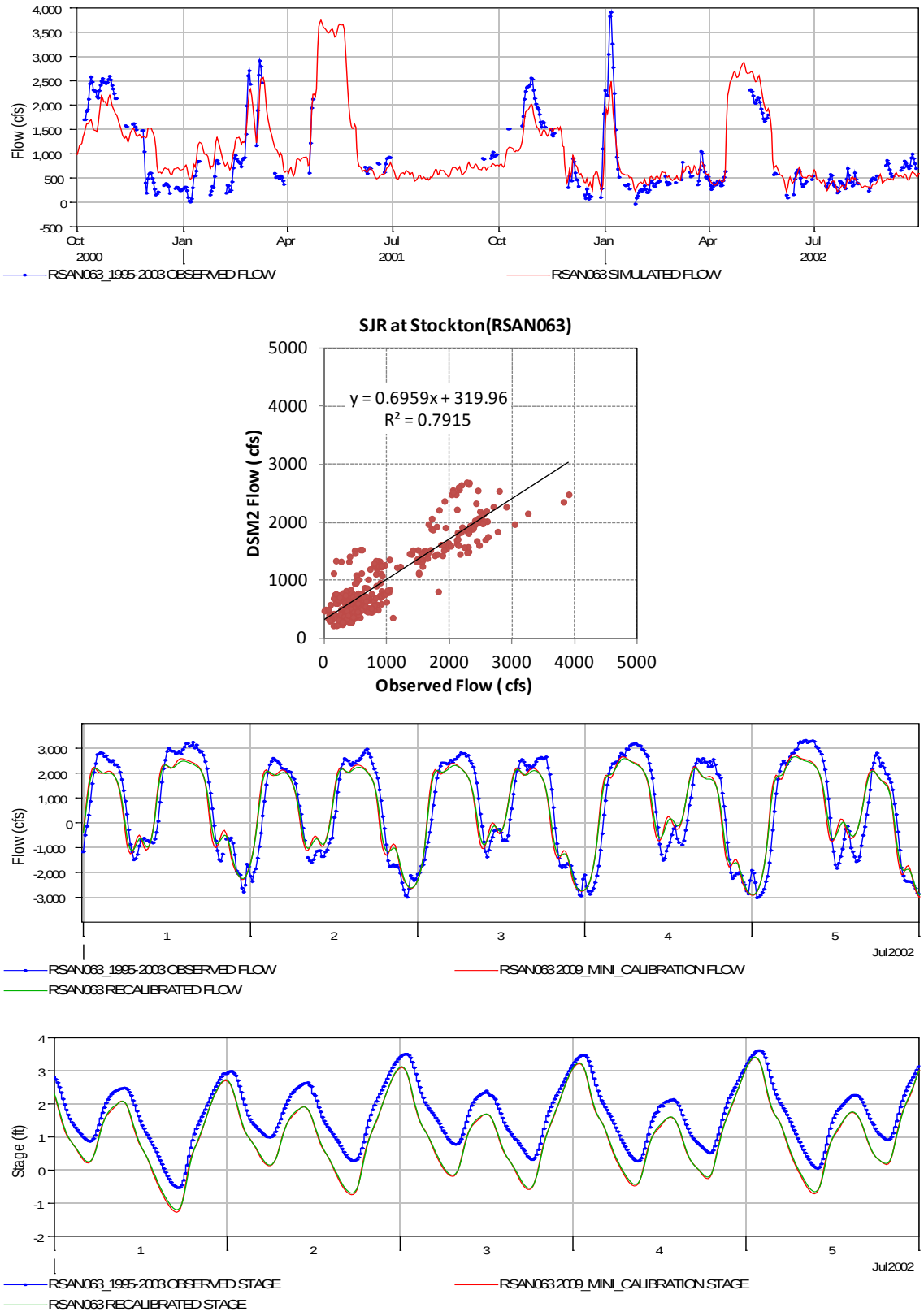

Figure 3-7 Hydro Calibration, San Joaquin River at Stockton

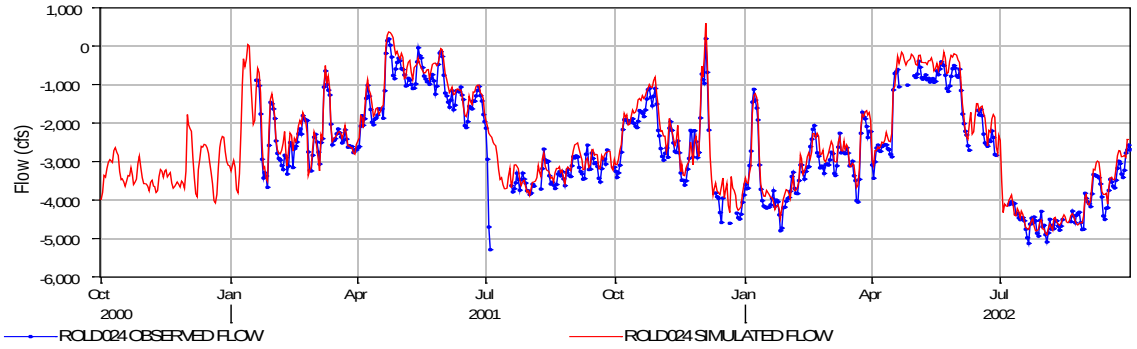

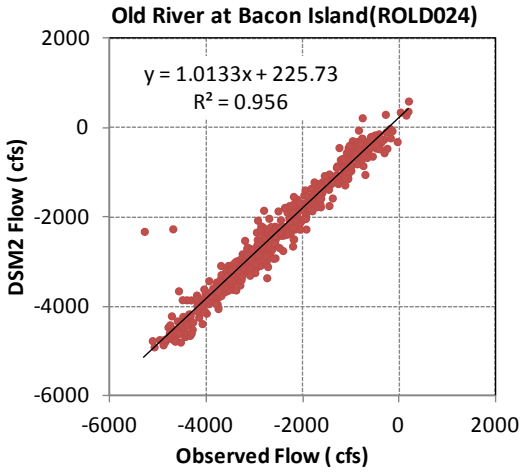

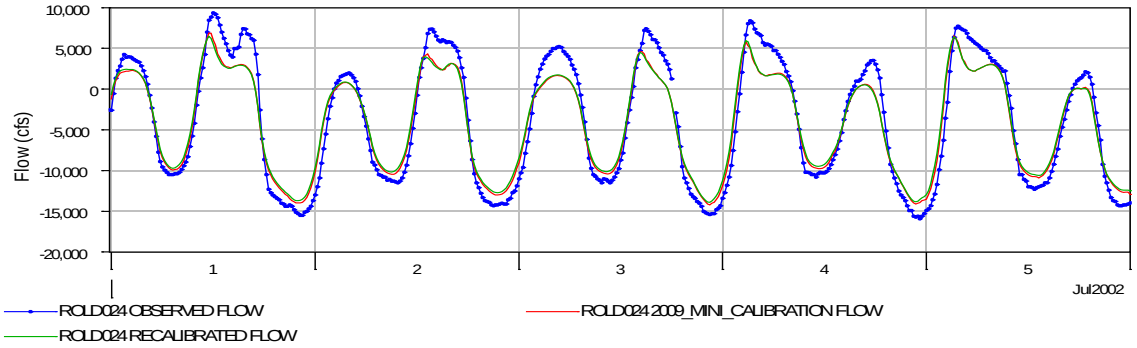

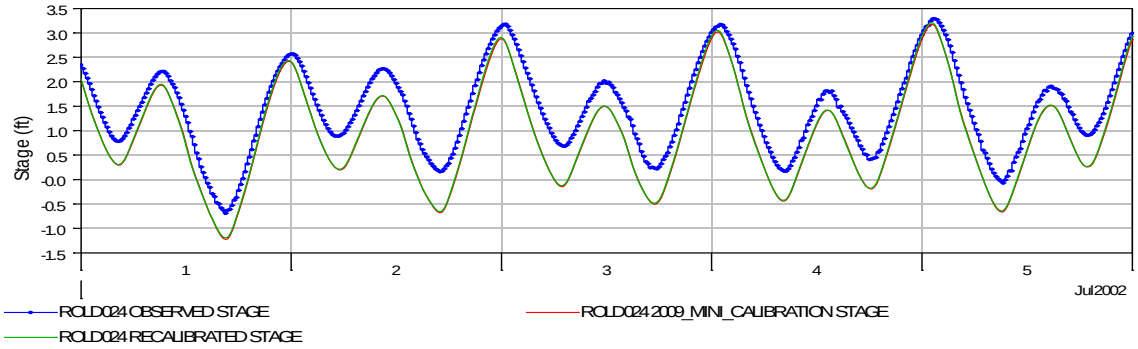

Figure 3-8 Hydro Calibration, Old River at Bacon Island

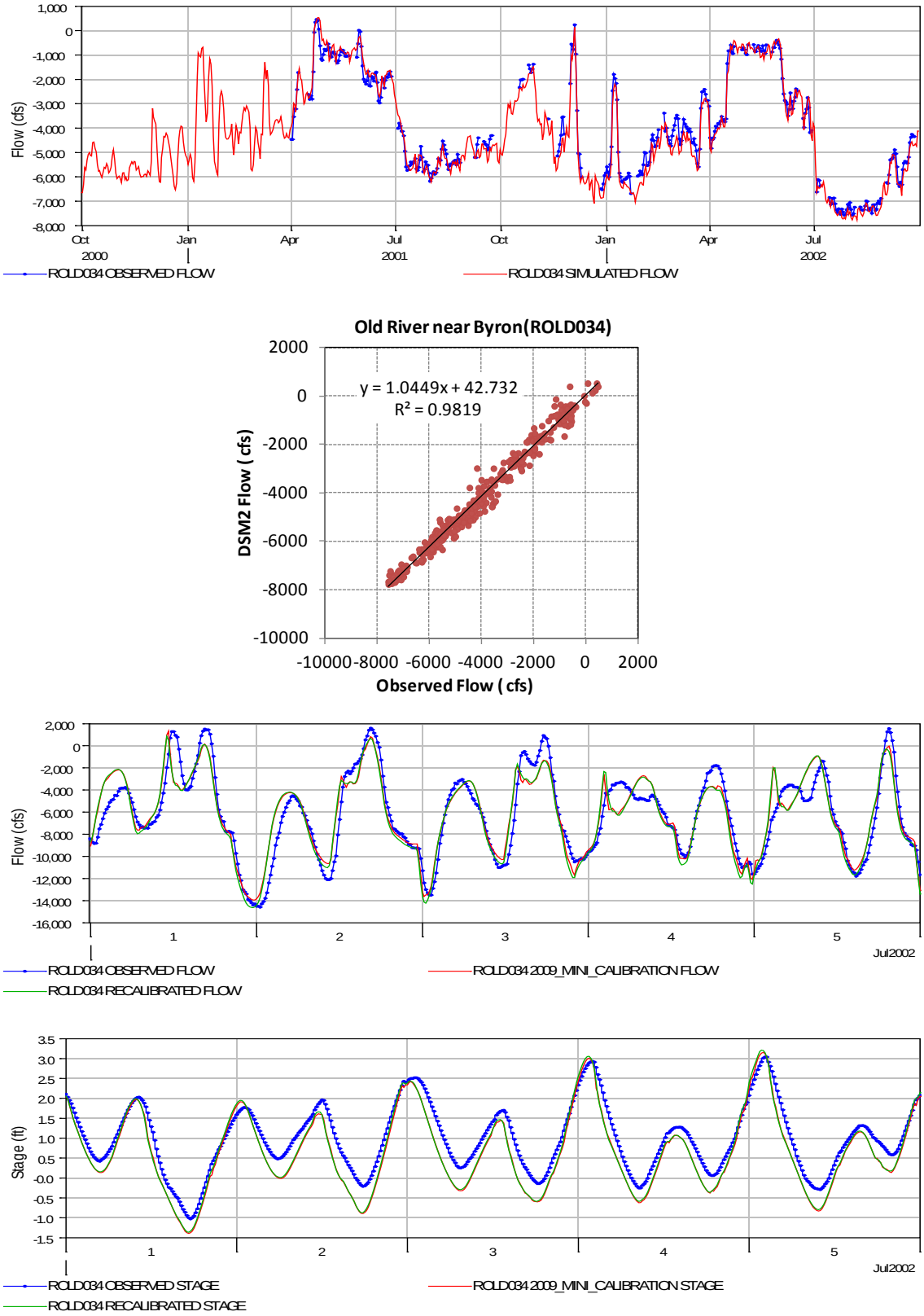

Figure 3-9 Hydro Calibration, Old River near Byron

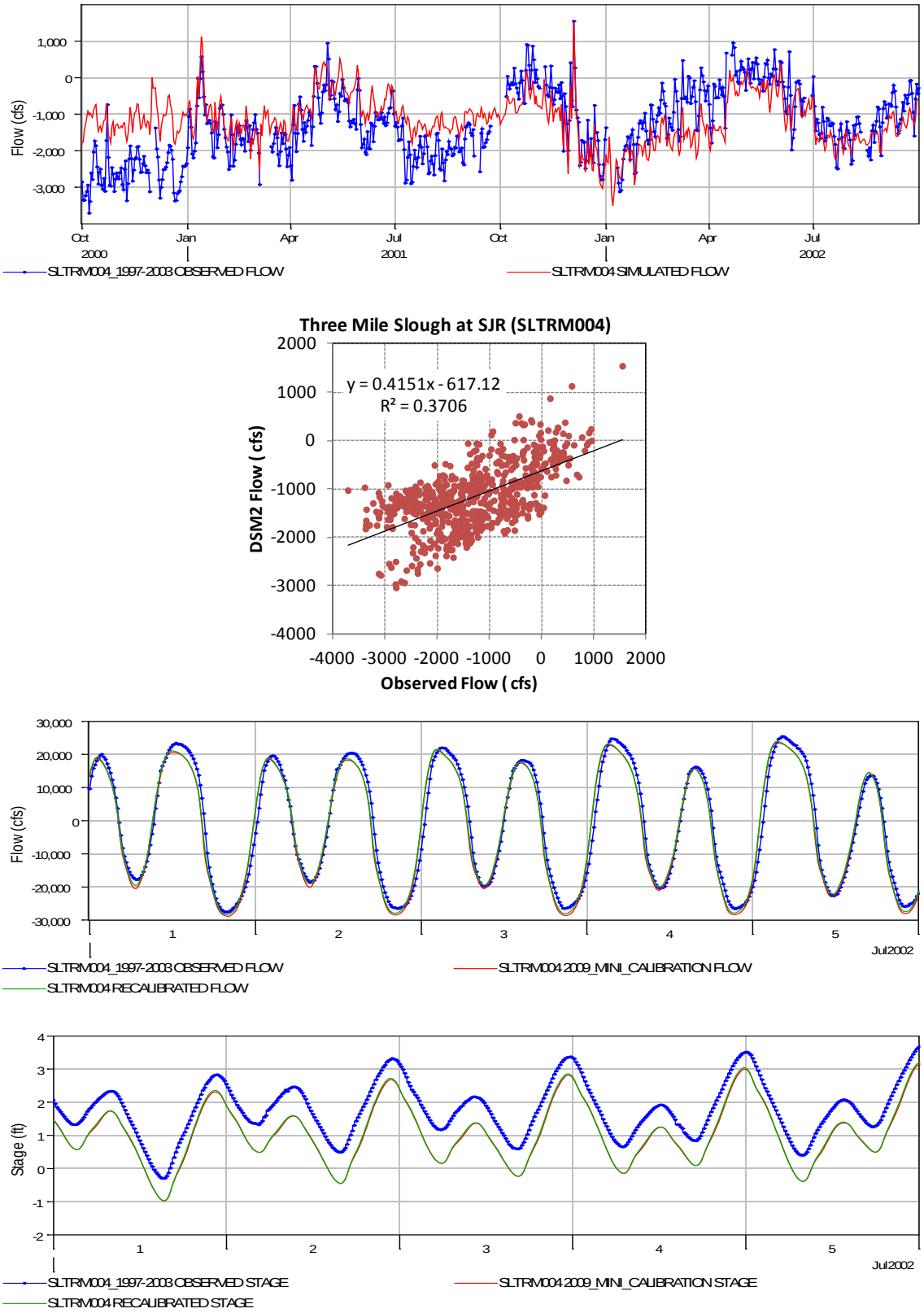

Figure 3-10 Hydro Calibration, Three Mile Slough at SJR

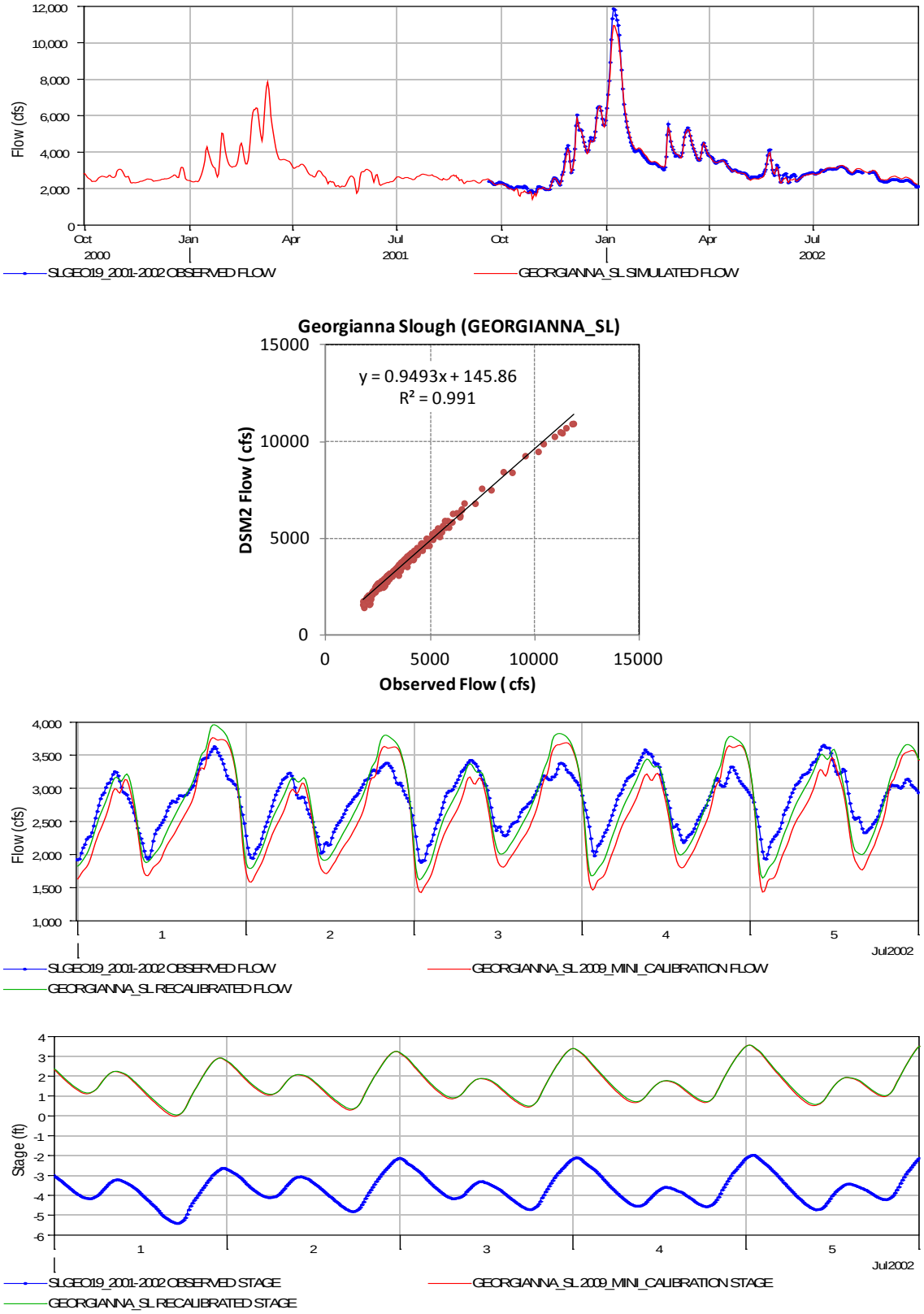

Figure 3-11 Hydro Calibration, Georgiana Slough

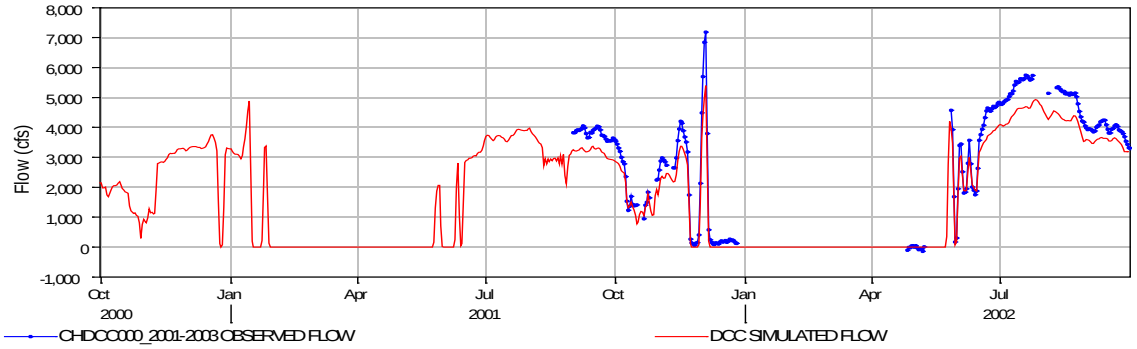

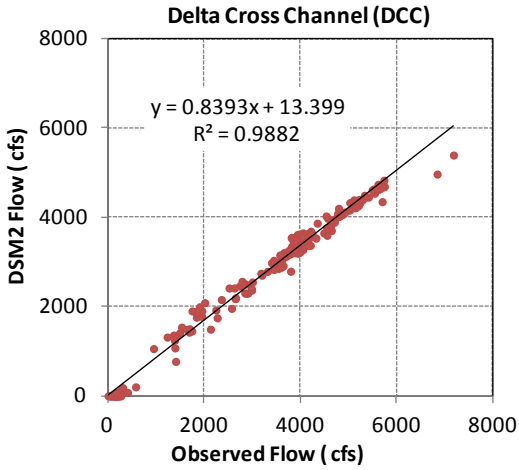

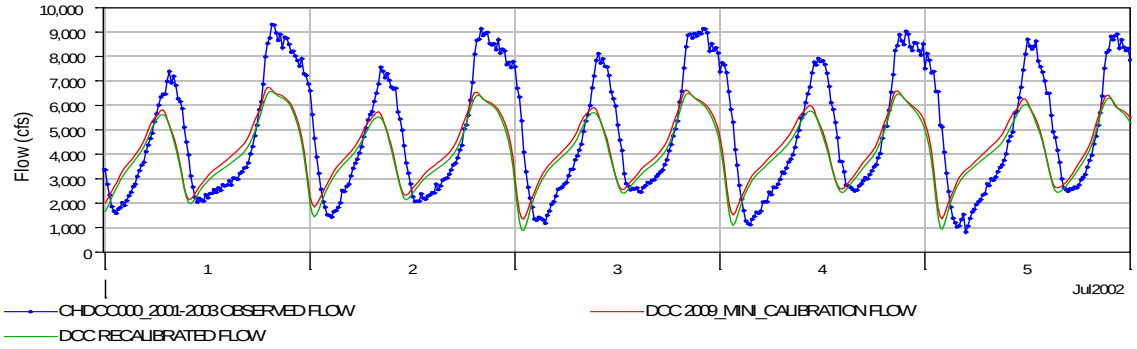

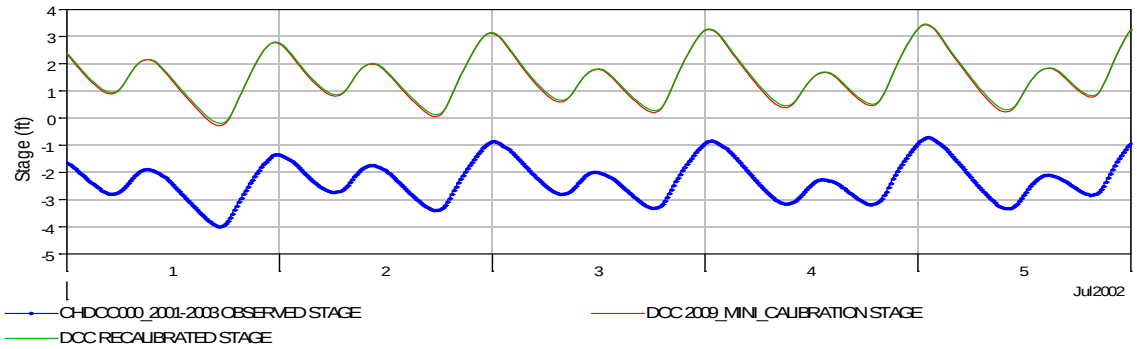

Figure 3-12 Hydro Calibration, Delta Cross Channel

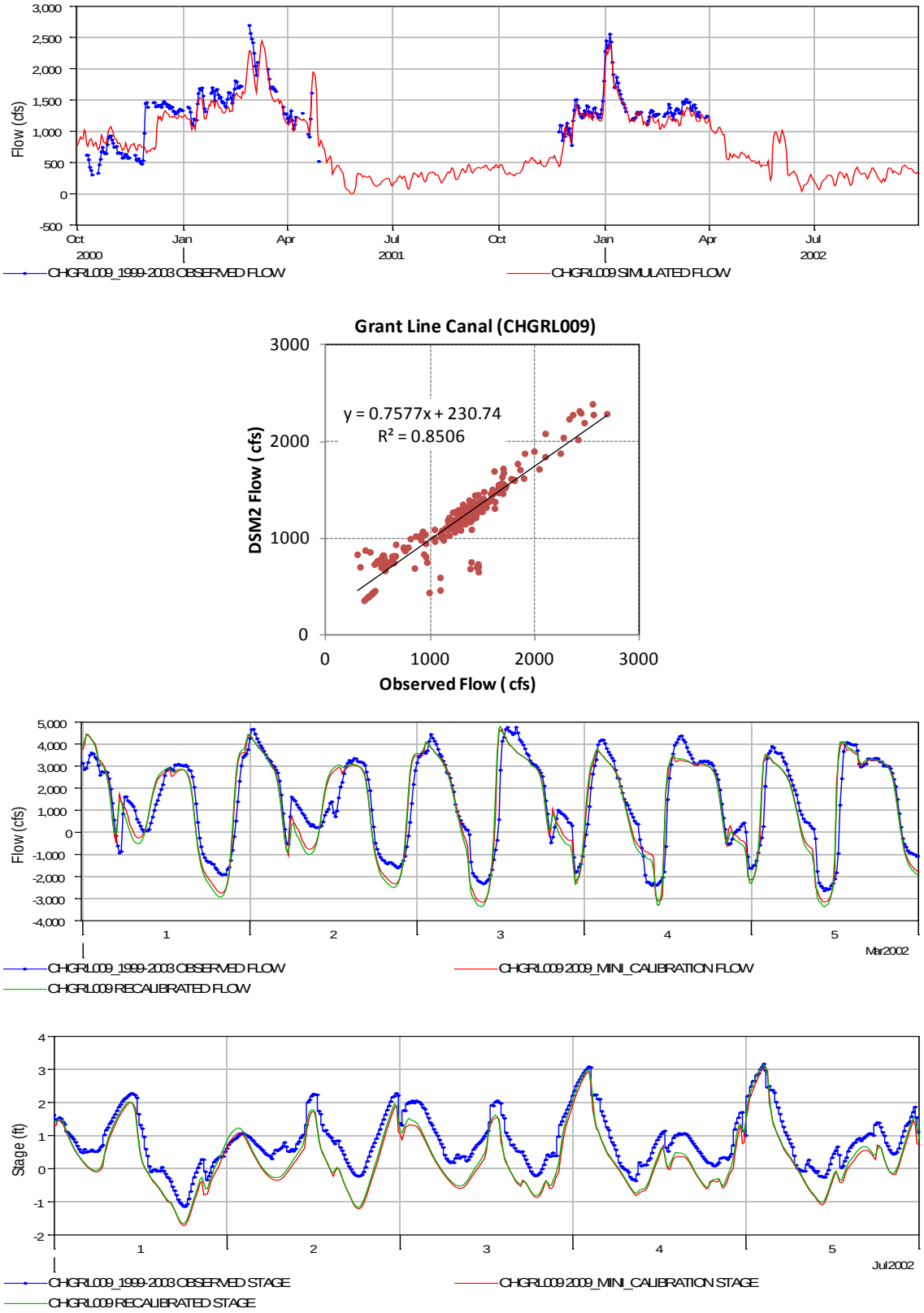

Figure 3-13 Hydro Calibration, Grant Line Canal at Tracy Boulevard Bridge

3.3 EC Recalibration Results

Version 8.1 improved the dispersion formulation to make the model convergent with respect to time step and parcel size, which was described in the 2011 Annual Report (Liu & Ateljevich, 2011) (Liu & Sandhu, 2011). A new dispersion coefficient (DC) was introduced. A limited dispersion recalibration was done and presented in the 2011 DSM2 Users Group newsletter (Liu & Sandhu, 2011 Aug). The calibration was based on the 2009 BDCP Calibration grid by CH2M (CH2M Hill, 2009 Oct). The 2009 calibration by CH2M was done using DSM2 Version 6. The calibration period was from 10/1/2000 to 10/1/2008. The recalibration of version 8.1.1 was done by scaling the previously calibrated dispersion coefficients globally, without fine-tuning, and using the same calibration period. The best result was obtained when new coefficients (DC) were calculated and scaled by 1425, i.e. DC=1425*DQQ. This approach works because the improved dispersion formulation is closely correlated to the original formulation (both versions scaled dispersion with discharge Q).

In this chapter, with the recalibrated Hydro, we reran the previously calibrated Qual model. Key stations are shown in Figure 3-14. The results are presented here at key stations: Collinsville, Emmaton, Jersey Point, Old River at Bacon Island, Clifton Court Forebay, and Montezuma Slough at Beldons Landing (Figure 3-15 to Figure 3-20). The electrical conductivity (EC) results didn't change significantly from the previous calibration. No new adjustments were made.

Three figures are plotted for each station to evaluate the model performance:

- **Linear regression analysis of monthly averaged EC.** This scatterplot with a linear regression trend line shows the simulated vs. observed monthly averaged EC. The intercept is set to zero so that the slope shows the bias of the model for higher EC. The model is over-estimating EC when the slope is higher than 1, and under-estimating EC when the slope is smaller than 1. R2 value gives information about the goodness of fit of the model. A high R2 value close to 1 means best fit, which usually means high quality data and good model prediction.
- **Timeseries comparison of monthly averaged EC.** This plot compares modeled and observed EC month by month, making it easier to see how the model is doing month to month.
- **Timeseries comparison of daily averaged EC.** This plot compares modeled and observed EC on a daily basis, making it easier to see how the model is doing over all.

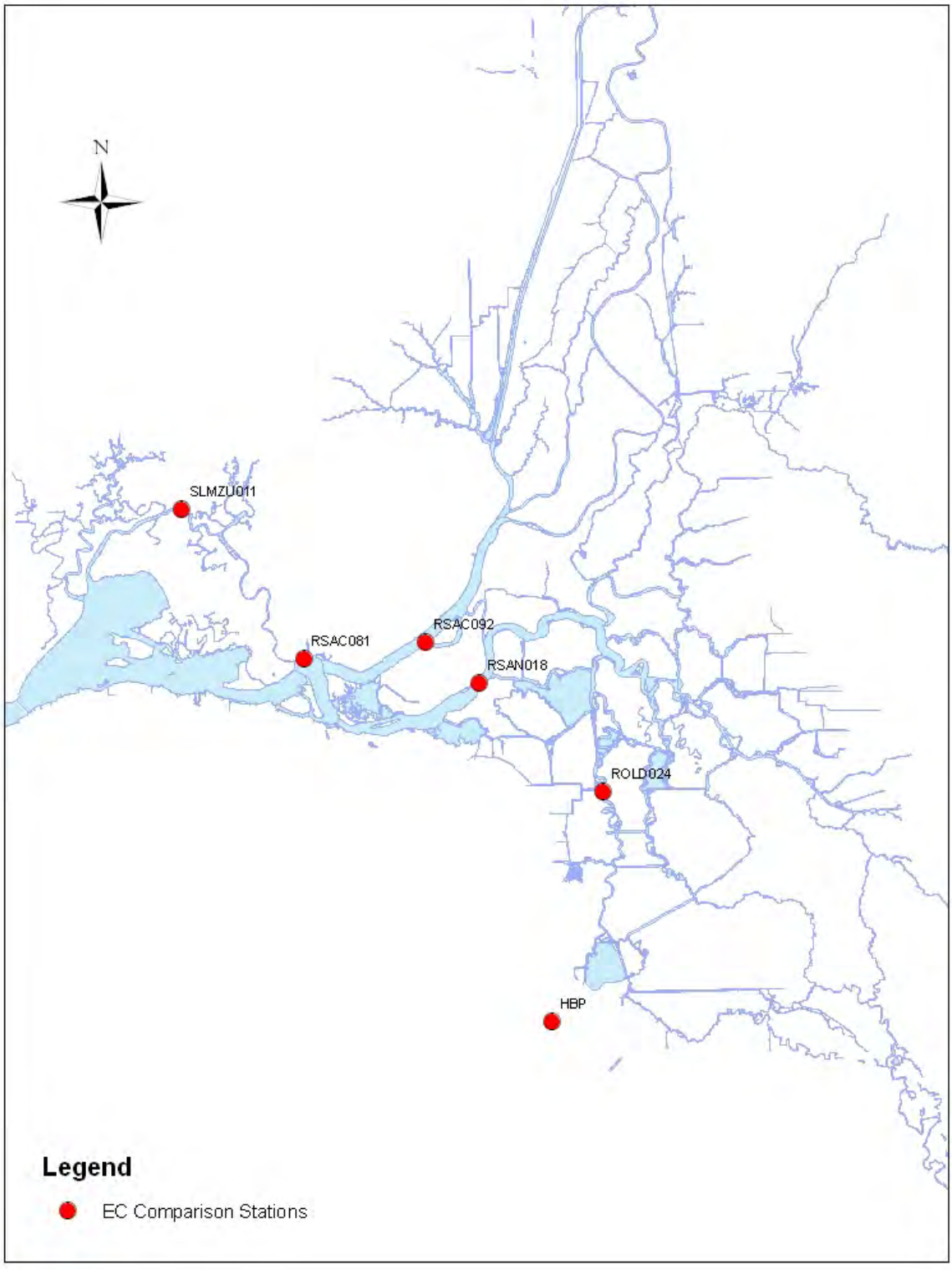

Figure 3-14 Key EC Comparison Stations

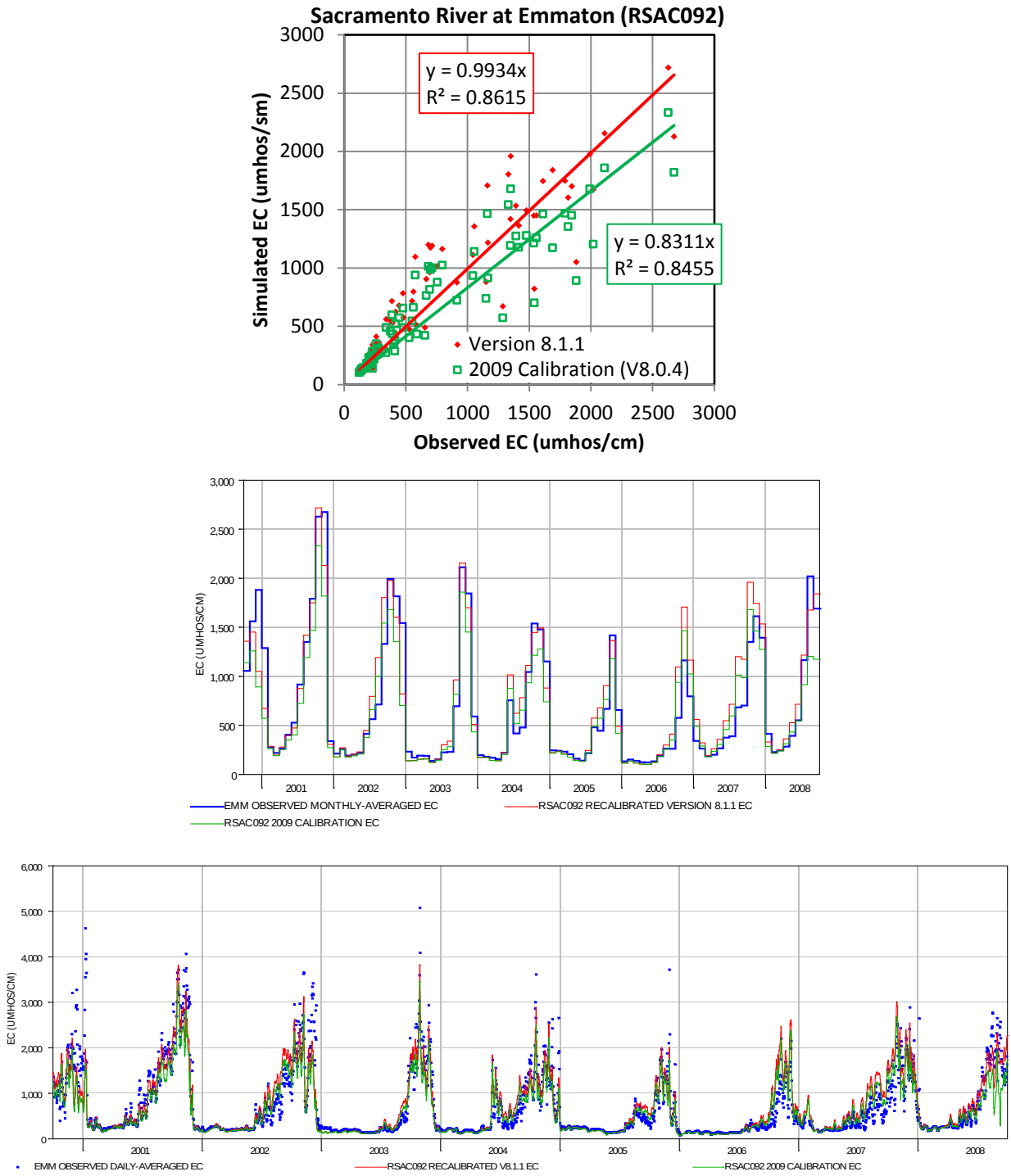

Figure 3-15 Qual Model Performance of EC, Sacramento River at Emmaton

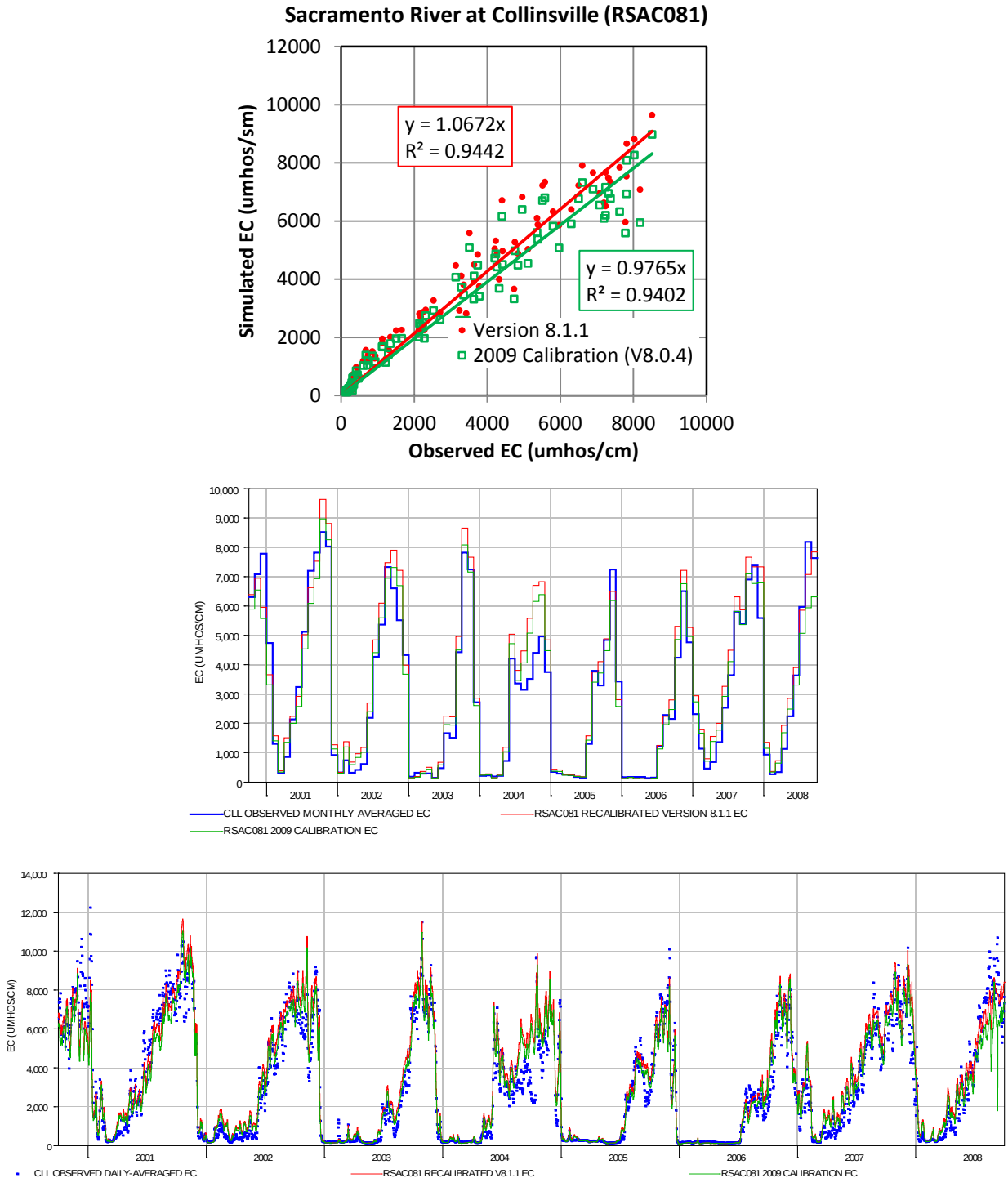

Figure 3-16 Qual Model Performance of EC, Sacramento River at Collinsville

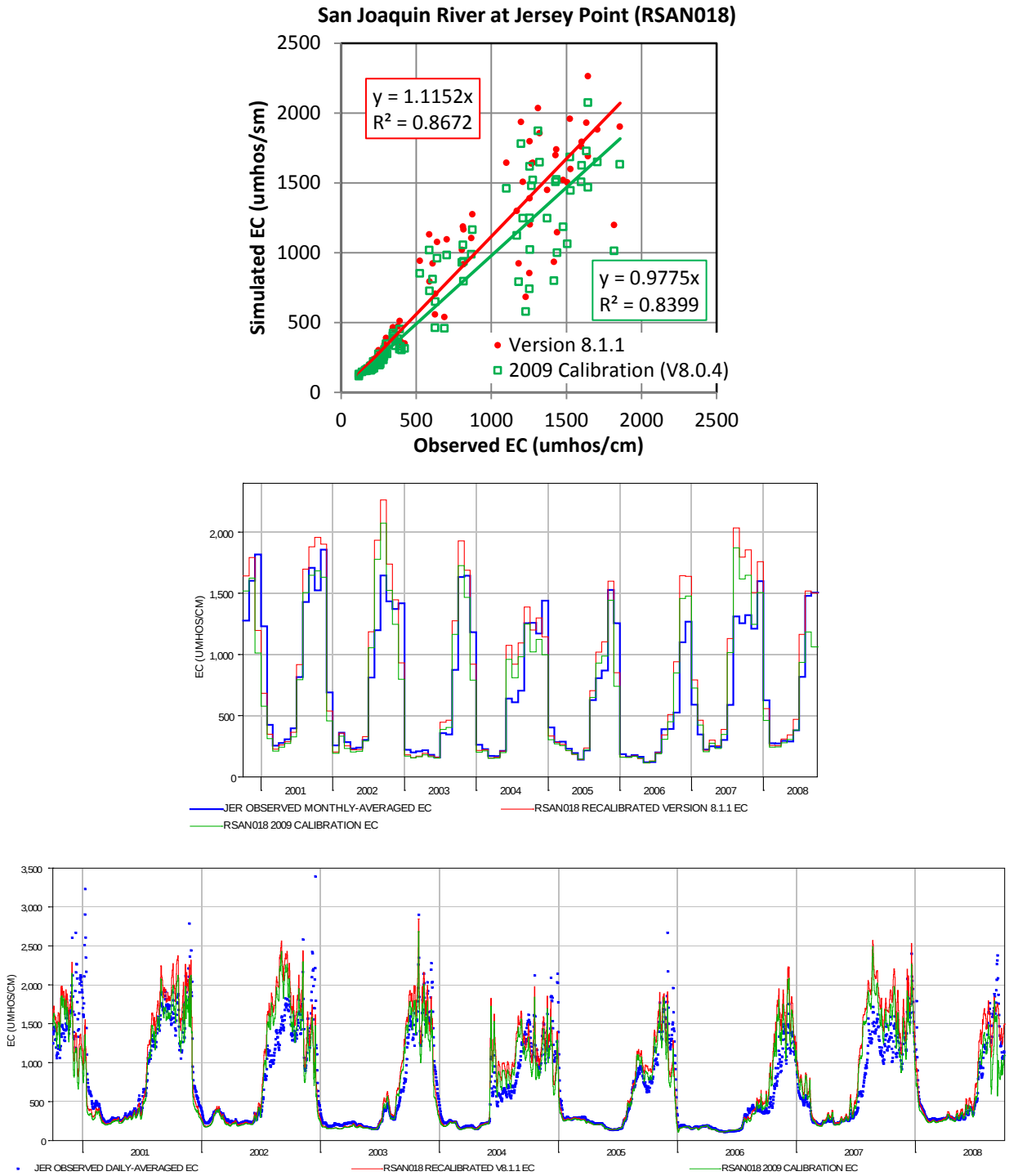

Figure 3-17 Qual Model Performance of EC, San Joaquin River at Jersey Point

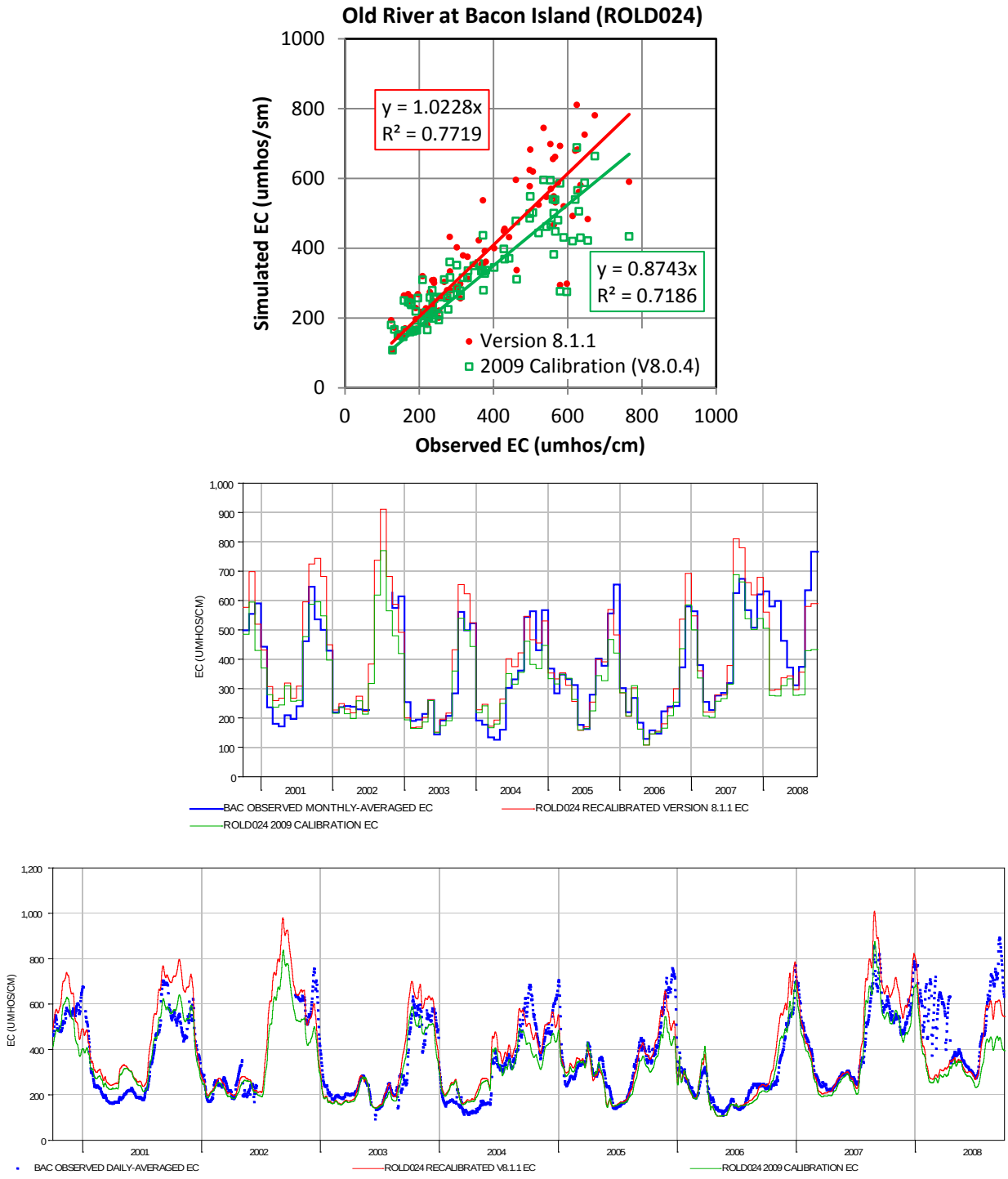

Figure 3-18 Qual Model Performance of EC, Old River at Bacon Island

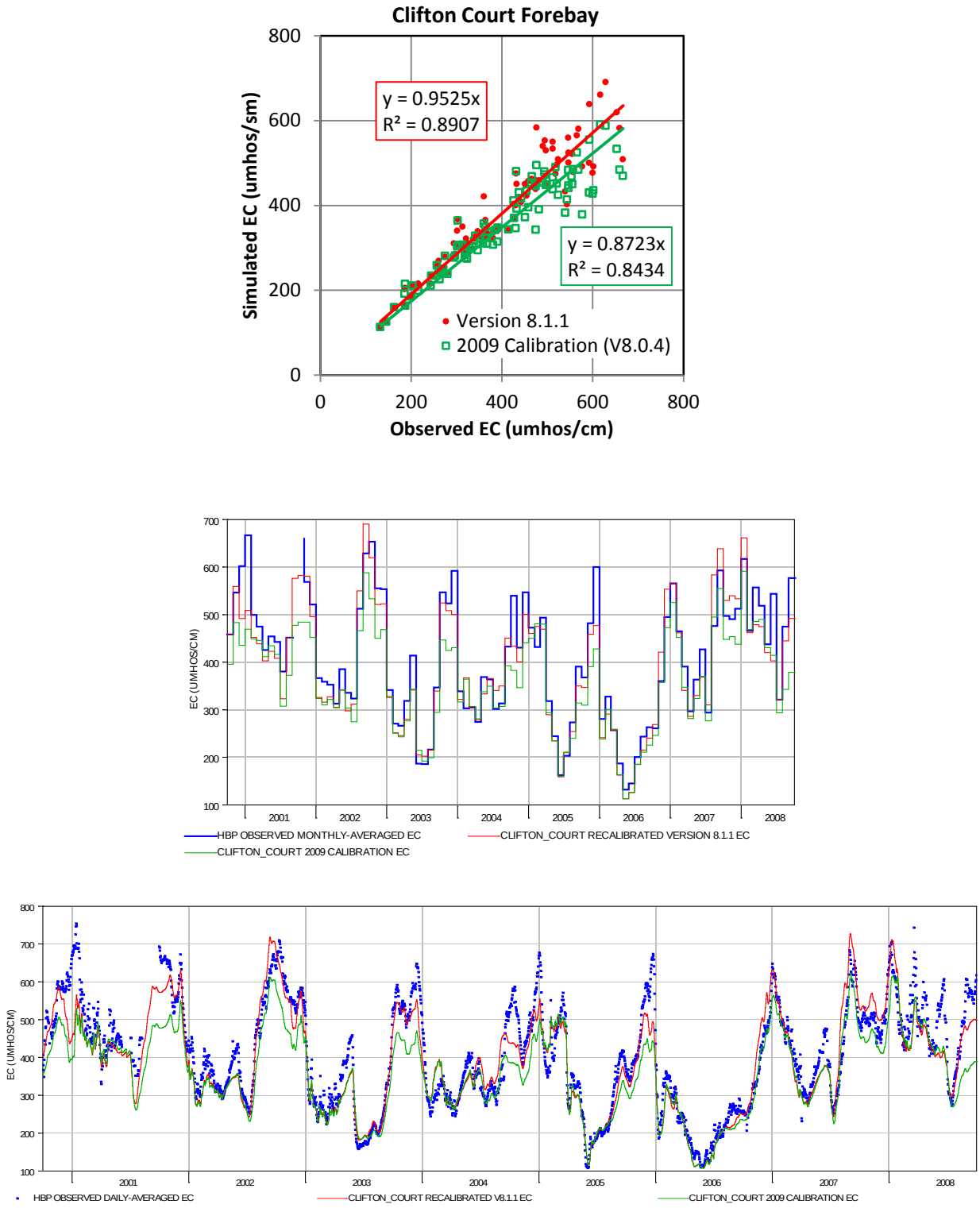

Figure 3-19 Qual Model Performance of EC, Clifton Court Forebay

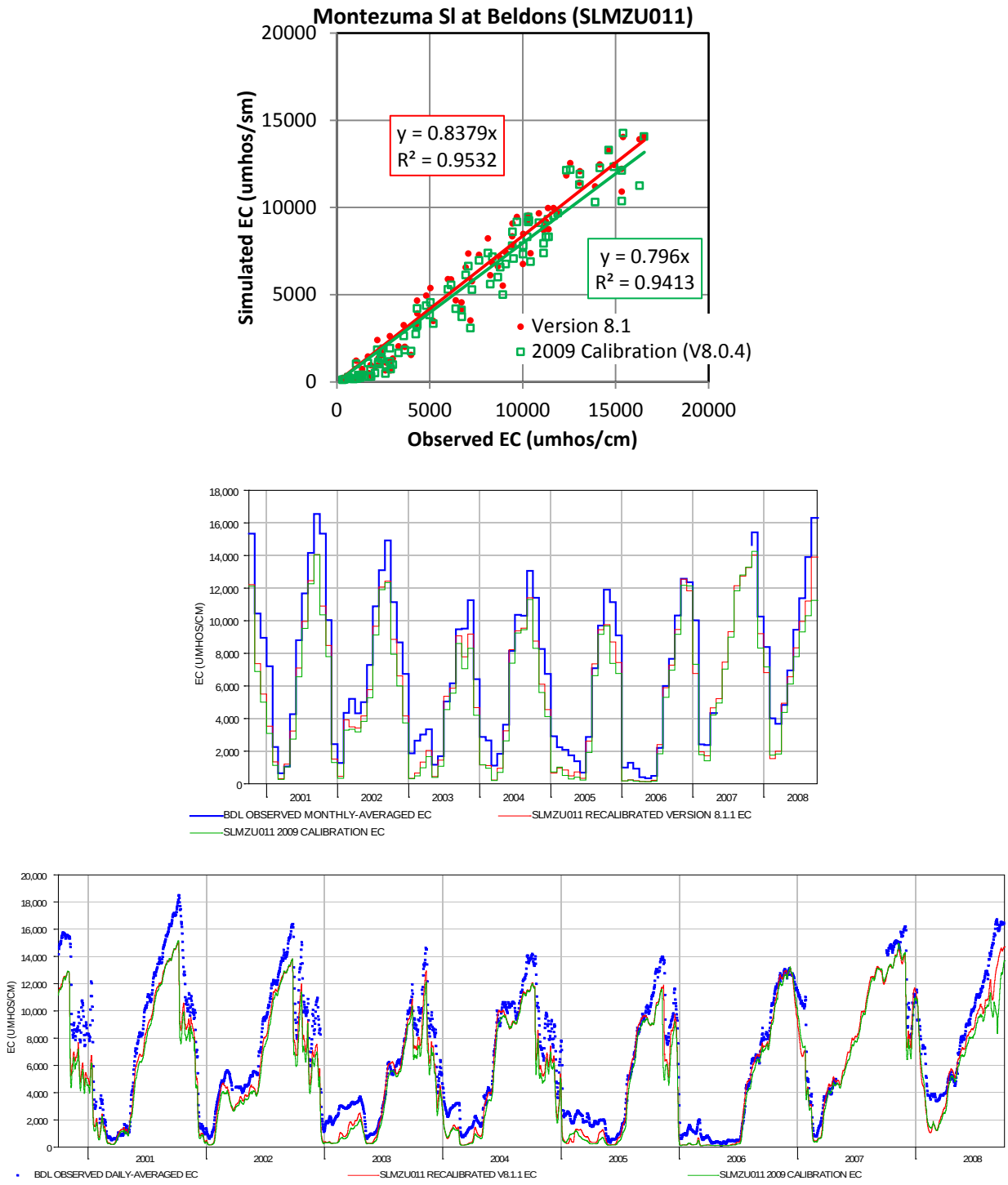

Figure 3-20 Qual Model Performance of EC, Montezuma Slough at Beldons Landing

3.4 Summary

The modifications of channel geometry interpolation and dispersion formulation in Version 8.1 did not result in a significant change in the model results after a brief recalibration. Hydro results are very close to the 2009 calibration, although there are significant changes of Manning's n values. EC results are generally higher than 2009 calibration values. Simulated EC at Clifton Court Forebay matches observed data better than in 2009 calibration.

We are working to improve the calibration by making changes and corrections to the model setup and input. The areas that need improvement and that we have been working on include Martinez EC discrepancy, Delta Cross Channel flow, lower minimum stage than observed at most stations, and Franks Tract representation. We found that NAVD88 is better than NGVD29 when comparing stages at Delta stations. The next improved version of recalibration will use NAVD88. Auto-Calibration will be used to optimize calibration coefficients.

Finally, a full recalibration would involve bigger changes, e.g., improve the channel schematic, regenerate cross sections based on better bathymetry data; improve estimates of diversions, return flows, and return flow water quality; improve Clifton Court gate modeling, etc.

3.5 References

CH2M Hill. (2009 Oct). *DSM2 Recalibration.* Sacramento, CA: Prepared for the California Department of Water Resources.

Liu, L., & Ateljevich, E. (2011). Improvements to the DSM2-Qual: Part 1 (Chapter 1). In *Methodology for Flow and Salinity Estimates in the Sacramento-San Joaquin Delta and Suisun Marsh: 32nd Annual Progress Report.* Sacramento: California Department of Water Resources, Bay-Delta Office, Delta Modeling Section.

Liu, L., & Ateljevich, E. (2011 Oct). Improved geometry interpolation in DSM2-Hydro. *Presentation at DSM2 Users Group meeting*. Sacramento: California Department of Water Resources.

Liu, L., & Sandhu, N. (2011 Aug). Dispersion Recalibration with DSM2 Version 8.1.1. *DSM2 Users Group Newsletter*. Sacramento: California Department of Water Resources, Delta Modeling Section.

Liu, L., & Sandhu, P. (2011). Improvements to DSM2-Qual: Part 2 (Chapter 2). In *Methodology for Flow and Salinity Estimates in the Sacramento-San Joaquin Delta and Suisun Marsh: 32nd Annual Progress Report.* Sacramento: California Department of Water Resources, Bay-Delta Office, Delta Modeling Section.

Liu, L., Ateljevich, E., & Sandhu, P. (2012). Improved Geometry Interpolation in DSM2-Hydro (Chapter 2). In *Methodology for Flow and Salinity Estimates in the Sacramento-San Joaquin Delta and Suisun Marsh: 33rd Annual Progress Report.* Sacramento: California Department of Water Resources, Bay-Delta Office, Delta Modeling Section.

Methodology for Flow and Salinity Estimates in the Sacramento-San Joaquin Delta and Suisun Marsh

33rd Annual Progress Report
June 2012

Chapter 4
South Delta Null Zone Study

Authors: **Ming-Yen Tu**
Delta Modeling Section
Bay-Delta Office
California Department of Water Resources

Page left blank for two-sided printing

Contents

Figures

Table

Page left blank for two-sided printing

4 South Delta Null Zone Study

4.1 Background

The State Water Resources Control Board (SWRCB) is in the process of reviewing and updating the 2006 Water Quality Control Plan for the San Francisco Bay/Sacramento-San Joaquin Delta Estuary (Bay-Delta Plan). The review may result in the potential amendments to the South Delta (Figure 4-1) salinity objectives in the Bay-Delta Plan. Under the review process, SWRCB states that poor water circulation (null zones) contributes to bad water quality in the South Delta, and that the Central Valley Project (CVP) and State Water Project (SWP) are responsible for improving the water circulation conditions while raising water stage so that the farmers are able to divert water (State Water Resources Control Board, 2009).

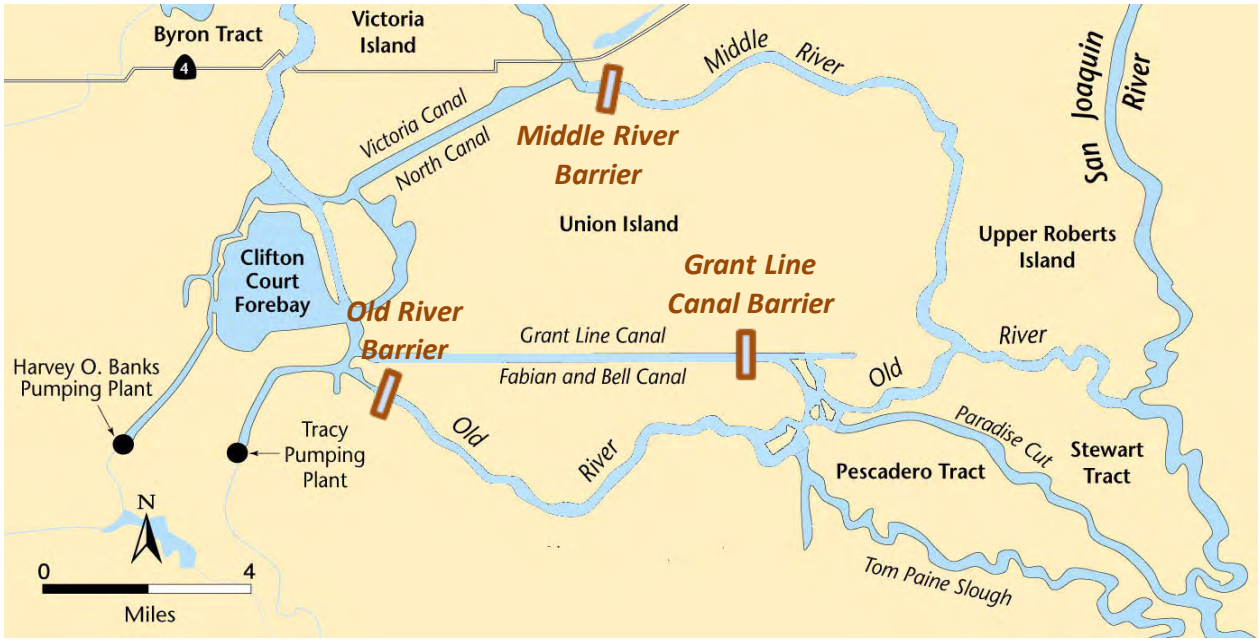

Figure 4-1 South Delta

4.2 Purpose

The purpose of this study is to analyze through hydrodynamic modeling whether and to what extent CVP and SWP exports and the agricultural temporary barriers actually influence the water levels (stage) and water circulation in South Delta. Specifically, the modeling analysis will address the following questions:

- How are null zones defined?
- Where are null zones (historically and with CVP/SWP exports)?
- How often do null zones occur (historically and with CVP/SWP exports)?
- How do CVP/SWP exports and barriers affect null zones?
- What are the stage impacts due to CVP/SWP exports and agricultural barriers?

4.3 Modeling Analysis Approach

The potential effect of CVP/SWP exports on water circulation and stage in the South Delta was examined using the Delta Simulation Model 2 (DSM2) (Delta Modeling Section, Online). A historical hydrology and barrier configuration was used as input and modified for each modeling scenario to evaluate the impacts of CVP/SWP exports and agricultural barriers. This model simulates flow, stage, and water quality in the Delta for both historical and hypothetical conditions. DSM2 has been calibrated or "tuned" to represent observed Delta flows, stages, and salinity (Nader-Tehrani & Shrestha, 2000). The model has a long history of applications for planning and management purposes in the Delta. Enhancements to the model are documented in annual reports to the SWRCB (annual reports available online at http://baydeltaoffice.water.ca.gov/modeling/deltamodeling/annualreports.cfm).

DSM2 version 8.0.6 was used for this study. Specifically, the DSM2-HYDRO module was run with associated assumptions to produce flow and stage results; the model results were later post-processed for analysis and interpretation purposes (Figure 4-2).

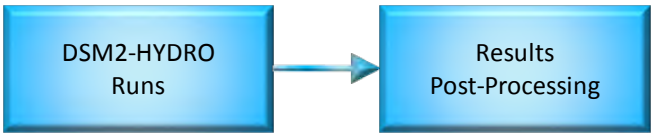

Figure 4-2 Process of DSM2 Modeling Analysis

4.3.1 Modeling Scenarios

Scenarios examined for this study include the combinations of three major factors:

- SWP export from the South Delta (Banks pumping plant)
- CVP export from the South Delta (Jones pumping plant)
- Operations of 3 barriers (Old River near Tracy, Middle River, and Grant Line Canal, generally installed between April and November)

Five modeling scenarios were investigated for this study. For each scenario, the model input for a historical simulation was modified so that the effects of that change could be analyzed. The 5 scenarios are listed below and are shown in Table 4-1:

- **NO_CVP_SWP_BARRIERS**: without CVP/SWP exports and without agricultural barriers[1].
- **NO_BARRIERS**: with historical CVP/SWP exports, but without agricultural barriers.
- **NO_SWP_BARRIERS**: with historical CVP export, but without SWP export and agricultural barriers.
- **NO_CVP_BARRIERS**: with historical SWP export, but without CVP export and agricultural barriers.
- **HISTORICAL**: with historical CVP/SWP exports and agricultural barrier operations.

[1] The Head of Old River Barrier (fish barrier) was not modified from its historical operation for any of the scenarios.

Table 4-1 Summary of Modeling Scenarios

Scenarios	SWP	CVP	Agricultural barriers
NO_CVP_SWP_BARRIERS	-	-	-
NO_BARRIERS	√	√	-
NO_SWP_BARRIERS[a]	-	√	-
NO_CVP_BARRIERS[a]	√	-	-
HISTORICAL	√	√	√

√ : Included - : Not Included
[a] The results of these two scenarios are available, but not presented in this report.

4.3.2 Modeling Assumptions and Considerations

Conceptually a null zone occurs at locations in the South Delta channels where flow and velocity in the channel approaches zero (or the flow is stagnant) and water quality degrades. This is a general definition of a null zone as it applies to the South Delta channels. However, according to DWR staff and stakeholders, there is no specific null zone definition that can easily be modeled. This definition would need to include the rate of velocity or flow, whether the flow or velocity is averaged over a tidal cycle, the time period over which that flow is near that low value, and the amount of water quality degradation. A clear definition is needed to carry out a thorough modeling analysis. Absent this definition and due to the limitations of accuracy in Delta diversion and return flows and quality, a simplified definition has been created for this study. This limited definition of a null zone can still provide information on the impacts of CVP/SWP exports and agricultural barriers on flow movement.

In this study, a null zone is defined if either of the following two conditions is met:

- **Condition 1**: in a DSM2 channel, if the tidal-averaged flow at the upstream end is flowing downstream and the tidal-averaged flow at the downstream end is upstream. (Figure 4-3, flows are shown as horizontal red arrows)
- **Condition 2**: in a DSM2 channel, if the tidal-averaged flow at the upstream end is flowing upstream and the tidal-averaged flow at the downstream end is downstream. (Figure 4-4, flows are shown as horizontal red arrows)

Figure 4-3 Condition 1 of Assumed Null Zone Definition

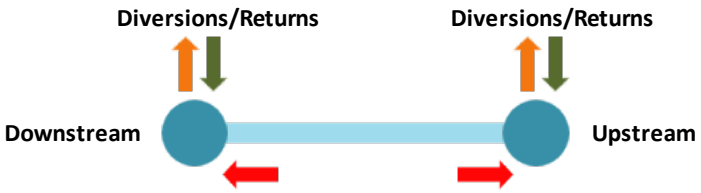

Figure 4-4 Condition 2 of Assumed Null Zone Definition

Also, for this modeling analysis, it is very important to recognize the following two considerations:

- The Without-CVP/SWP export simulations do not incorporate possible changes in upstream reservoir releases or other system operations as a result of cutting exports.
- DSM2 is limited by sparsely observed data for In–Delta diversions and returns. This may affect the null zone calculations.

Figure 4-5 shows the study area that is in the vicinity of the Old River and Middle River for assessing the null zone in this study. The area covers DSM2 channels 70 to 82 for Old River (about 10.9 miles in total), and channels 125 to 139 for Middle River (about 16.1 miles in total).

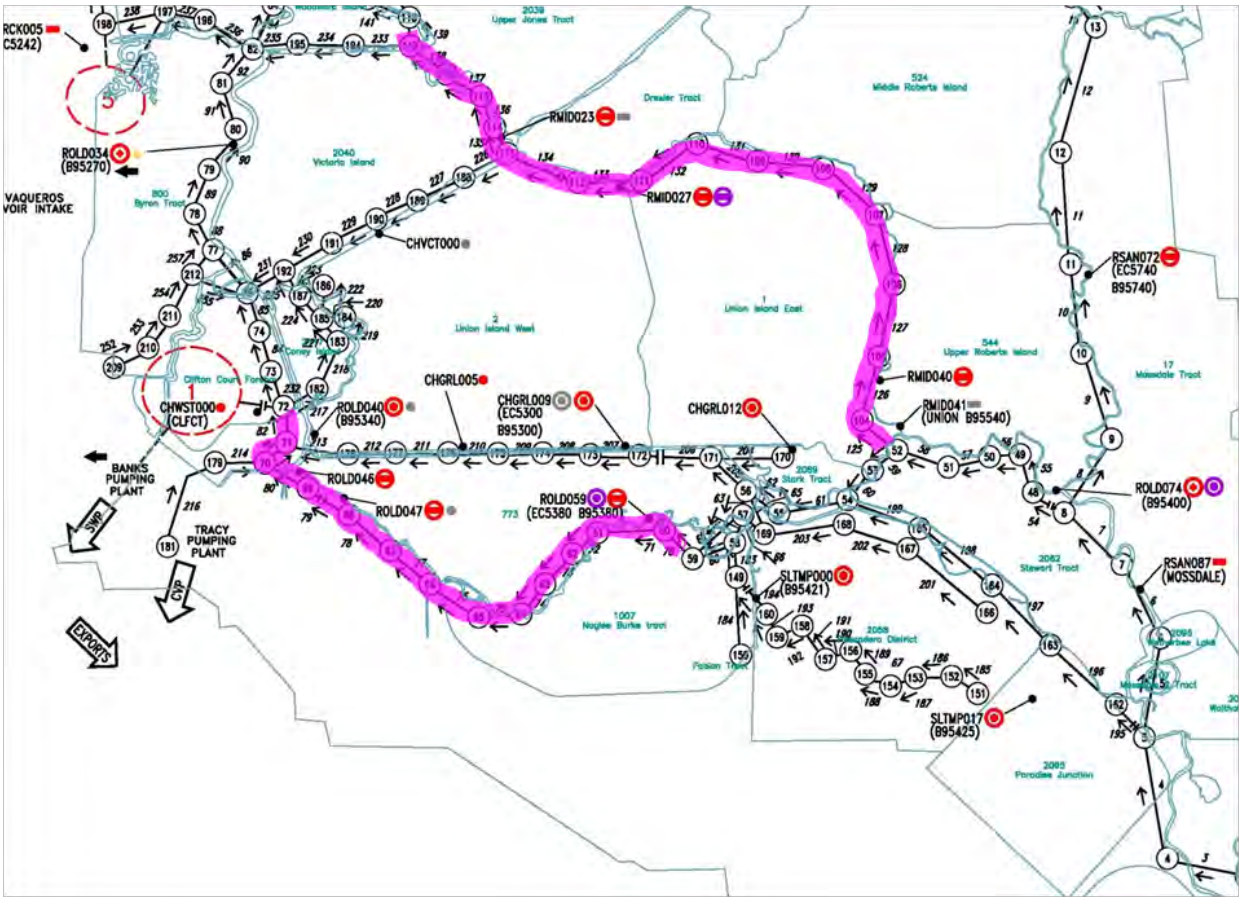

Figure 4-5 South Delta Channels included in Null Zone Assessment (Highlighted Area)

4.3.3 Simulation Periods

The model simulation period starts from January 1990 to December 2010 (21 years in total). These 21 years cover various hydrologic conditions, including 6 Wet years, 4 Above Normal years, 2 Below Normal years, 4 Dry years, and 5 Critical years according to the Sacramento Valley Index (California Department of Water Resources, 2011).

4.3.4 Model Results Interpretation

Because no historical records clearly identify where and how often null zones happen, no available data validate the adequacy of the assumed null zone definition and the associated model results. Therefore,

in this study, the model results are mainly used for comparison purposes. That is, the analysis focuses on the differences between scenarios, not the absolute values of the model results.

The model results are presented in terms of flow and stage for this study. Two scenario comparisons are discussed to assess the effects of CVP/SWP exports and/or the agricultural barriers' operations on water circulation and stage:

- A comparison between NO_CVP_SWP_BARRIERS and NO_ BARRIERS scenarios: this comparison shows the effects of CVP/SWP exports when no agricultural barriers are in place.
- A comparison between NO_CVP_SWP_BARRIERS and HISTORICAL scenarios: this comparison shows the effects of both CVP/SWP exports and the agricultural barriers.

4.4 Results and Findings

4.4.1 Flow

The DSM2 simulation results were post-processed to calculate the tidally-averaged flow (using the Godin filter method) for assessing the null zone conditions under different scenarios.

Figure 4-6 shows the null zone results for Old River and Middle River under the NO_CVP_SWP_BARRIERS and NO_ BARRIERS scenarios. The channel numbers in the DSM2 grid and the number of days in the 21 years simulation when a null zone is happening in each channel are shown and color-coded for the reader's convenience. Based on the assumed null zone definition, the results show that:

- Null zones occur in Old River and Middle River even when the CVP/SWP exports and the agricultural barriers are not in place (see results for the NO_CVP_SWP_BARRIERS scenario). The frequency of the null zone occurrence is relatively small when considering the entire 21 years (7,670 days in total). For example, in Middle River, the maximum number of days when a null zone happens is in channel 133 (134 days), which is about 1.75% of time over the 21 years.
- When the CVP/SWP exports are in place, the location and timing of null zone occurrences changes (see results for the NO_BARRIERS scenario). Similar to the NO_CVP_SWP_BARRIERS scenario, the frequency of null zone occurrences is relatively small when considering the entire 21 years. For example, in Middle River, the maximum number of days when a null zone happens is in channel 133 (141 days), which is about 1.84% of time over the 21 years.
- Comparing the NO_CVP_SWP_BARRIERS and the NO_BARRIERS scenario, in the entire 21-year simulation, the changes of occurrence frequency are between -22 to 4 days in Old River, and between -19 to 58 days in Middle River. The scale of the changes is considered relatively small.

Figure 4-7 shows the null zone results for Old River and Middle River under the NO_CVP_SWP_BARRIERS and HISTORICAL scenarios. The results show that when the CVP/SWP exports and agricultural barriers are in place, null zones happen; and compared with the NO_CVP_SWP_BARRIERS scenario, the timing and frequency of null zone occurrences change. In the entire 21-year simulation, the differences in frequency are between -22 to 13 days in Old River, and between -21 to 51 days in Middle River. The scale of the changes is considered relatively small.

The difference in null zone occurrences is further investigated for each month. The findings show that the changes are small when comparing scenarios under Without- and With-CVP/SWP exports and/or barriers (Figure 4-8 and Figure 4-9 show the results for July, when barriers are in place, as an example).

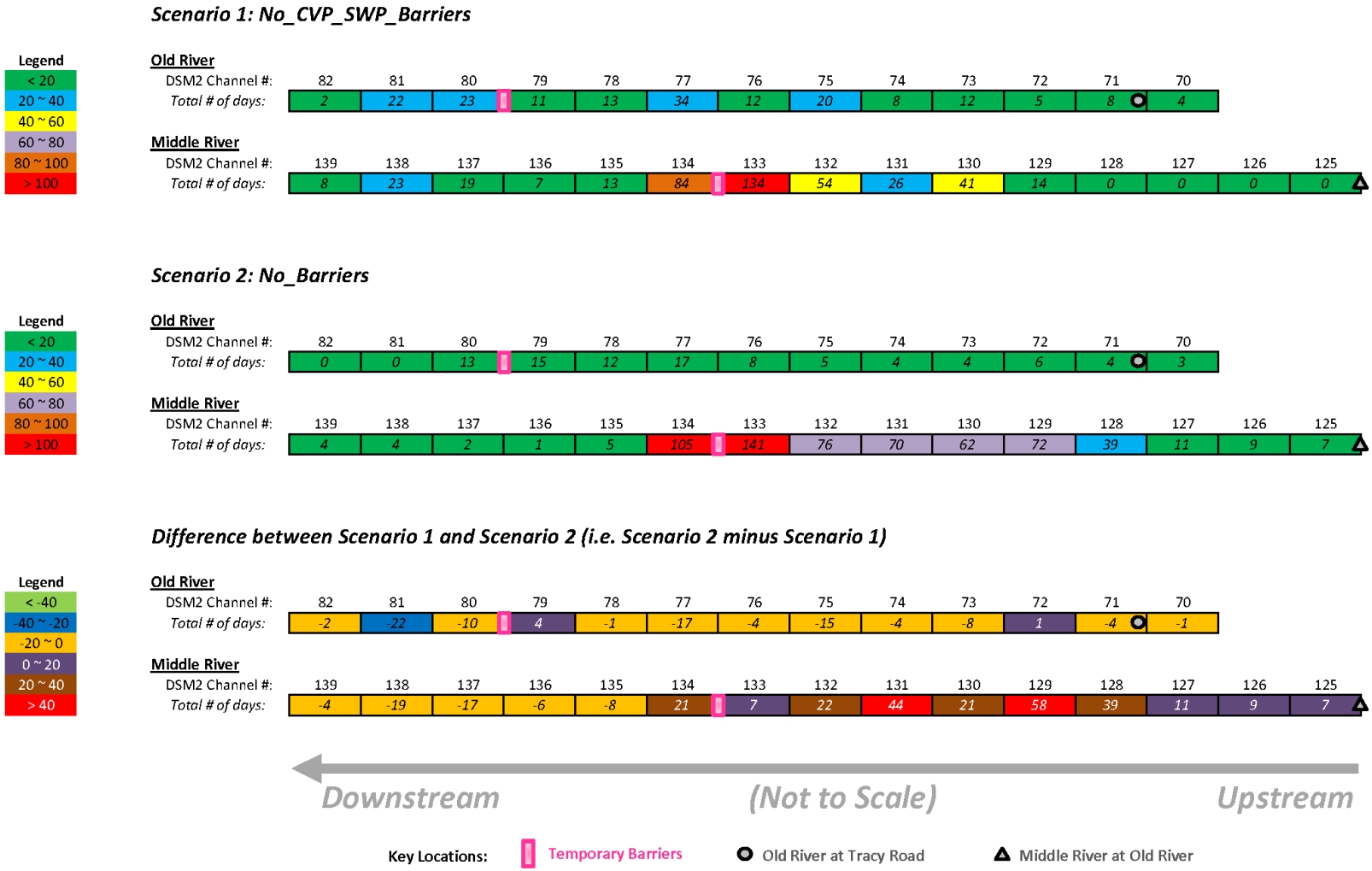

Figure 4-6 Model Results of Null Zone Occurrence for NO_CVP_SWP_BARRIERS and NO_BARRIERS Scenario (January 1990 to December 2010)

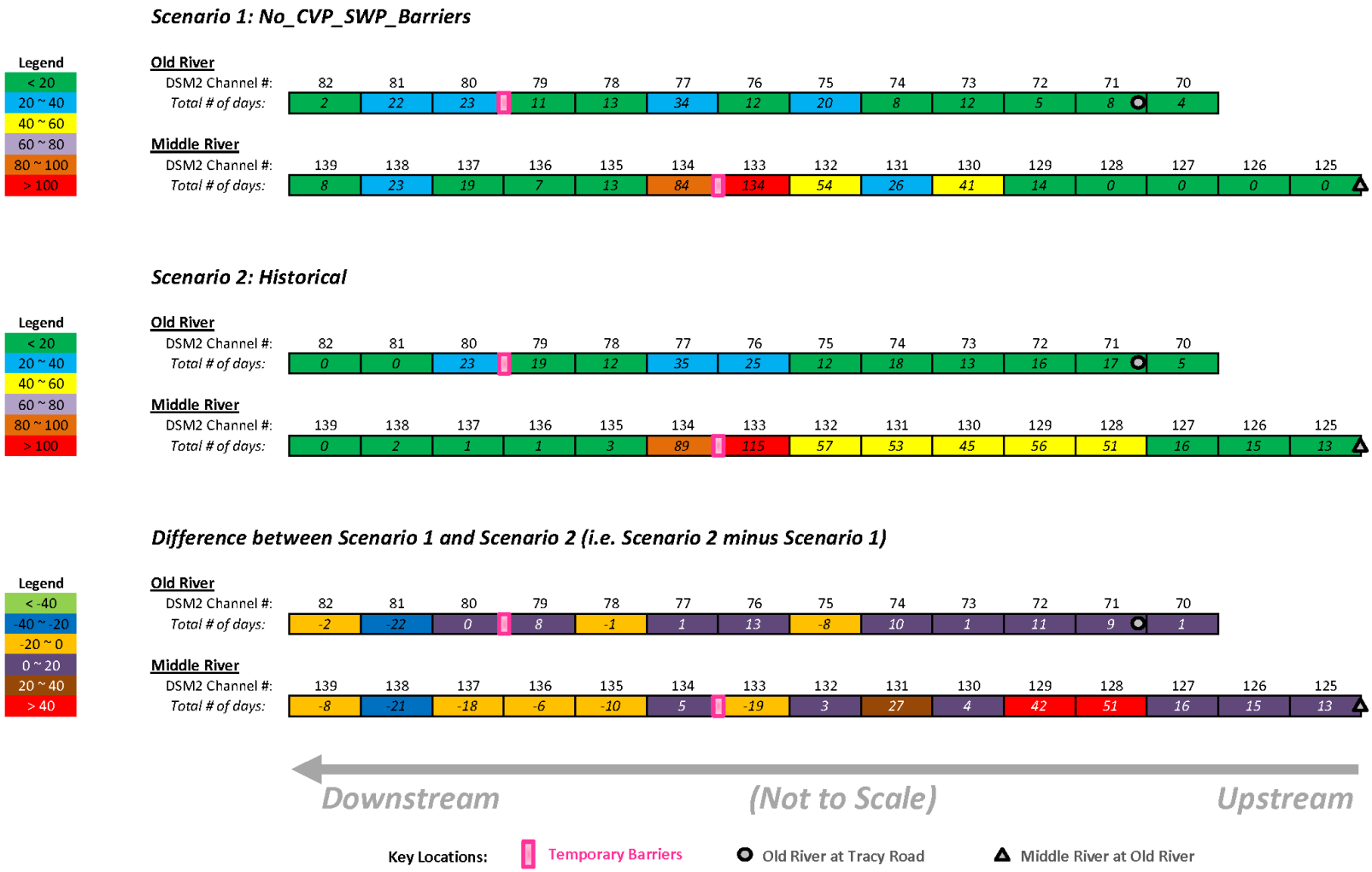

Figure 4-7 Model Results of Null Zone Occurrence for NO_CVP_SWP_BARRIERS and HISTORICAL Scenario (January 1990 to December 2010)

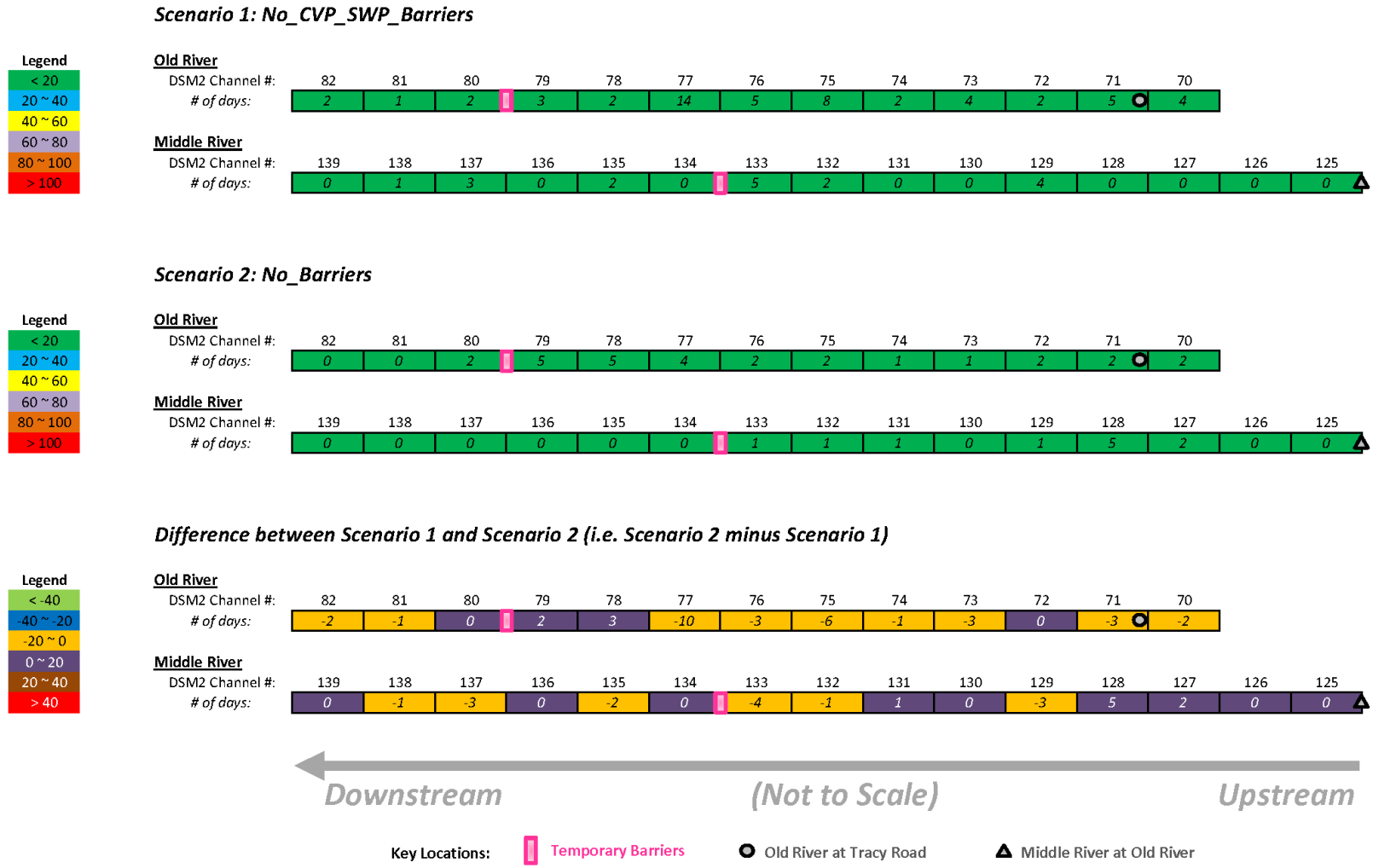

Figure 4-8 Model Results of Null Zone Occurrence for NO_CVP_SWP_BARRIERS and NO_BARRIERS Scenario for July Only (1990 to 2010)

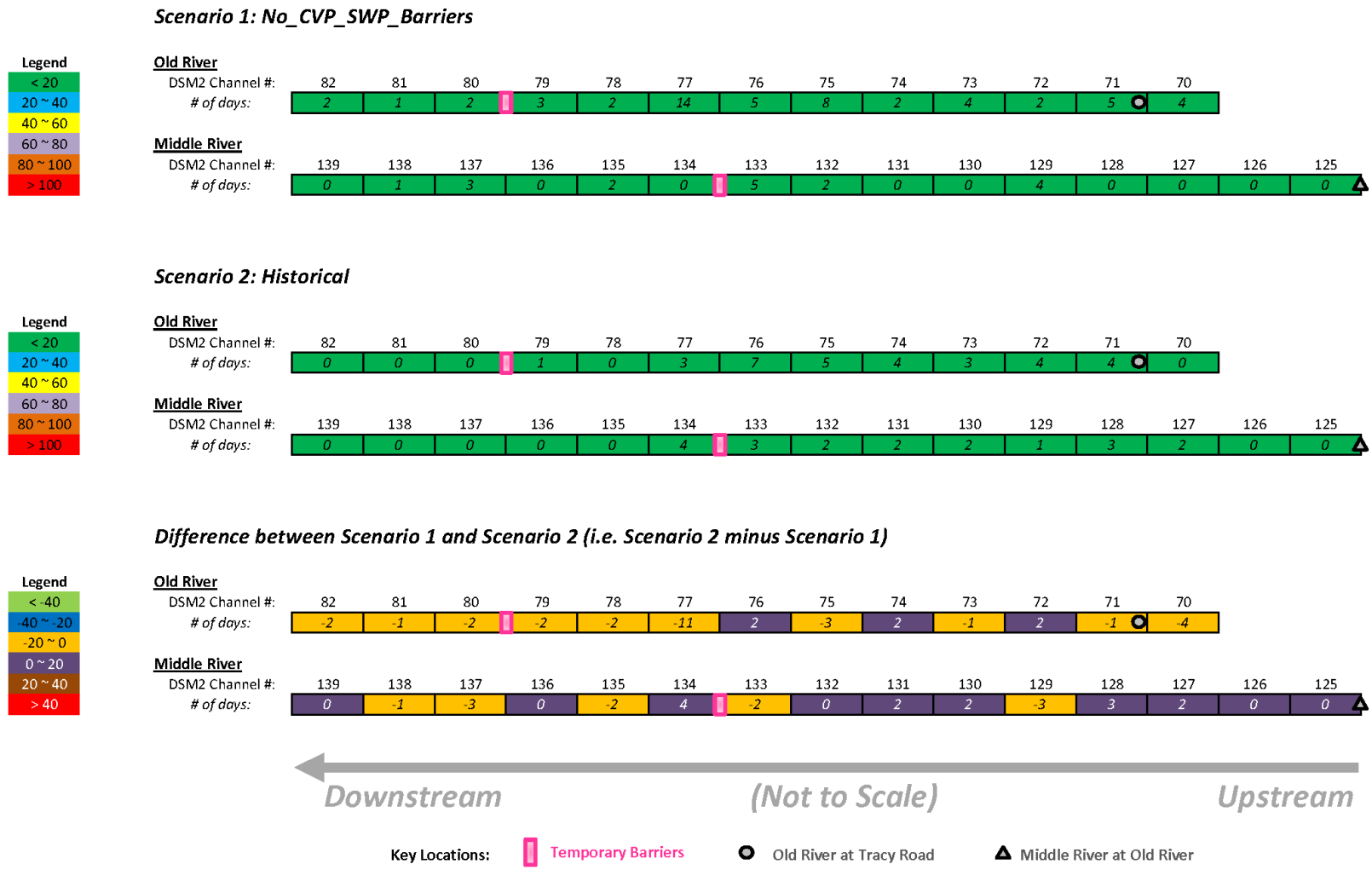

Figure 4-9 Model Results of Null Zone Occurrence for NO_CVP_SWP_BARRIERS and HISTORICAL Scenario for July Only (1990 to 2010)

4.4.2 Stage

In this study, the stage results are evaluated in terms of the daily minimum stage at 5 locations in the South Delta (Figure 4-10): (1) Old River at Tracy Road, (2) Middle River at Old River, (3) Old River Barrier, (4) Middle River Barrier, and (5) Grant Line Canal Barrier.

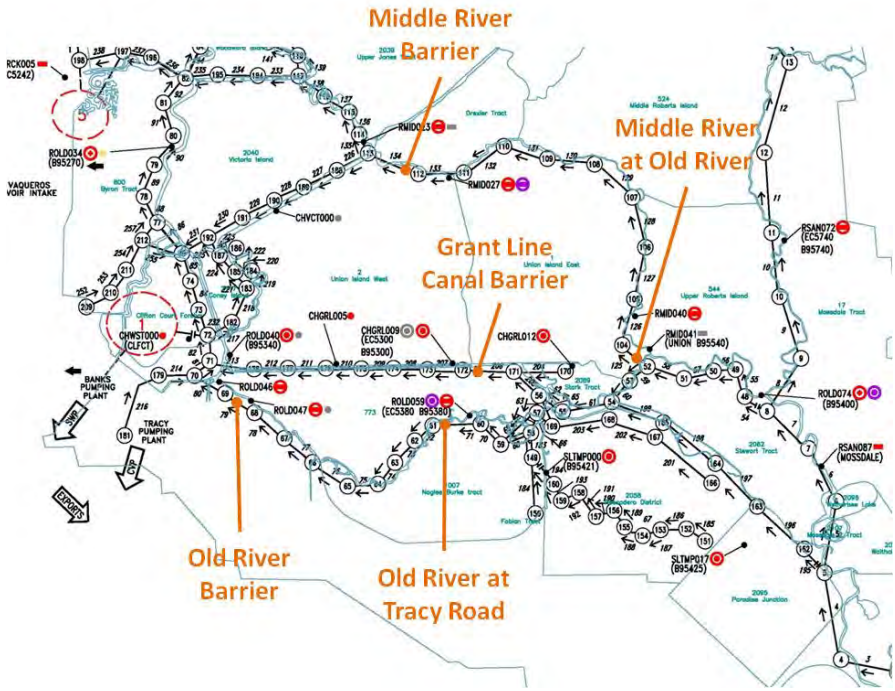

Figure 4-10 Locations of Stage Assessment in South Delta

Figure 4-11 shows the exceedence probability of the daily minimum stage results for the 21-year simulation. The plots on the left-hand side show the results under 3 scenarios. The plots on the right-hand side show the differences after comparing scenarios.

(a) Old River at Tracy Road

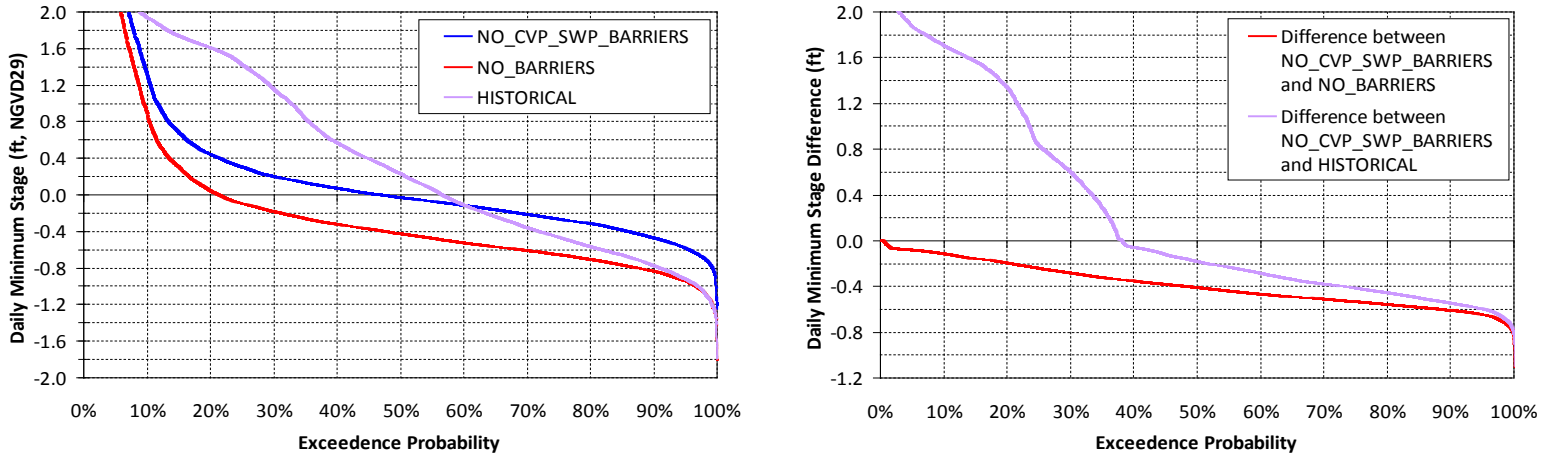

(b) Middle River at Old River

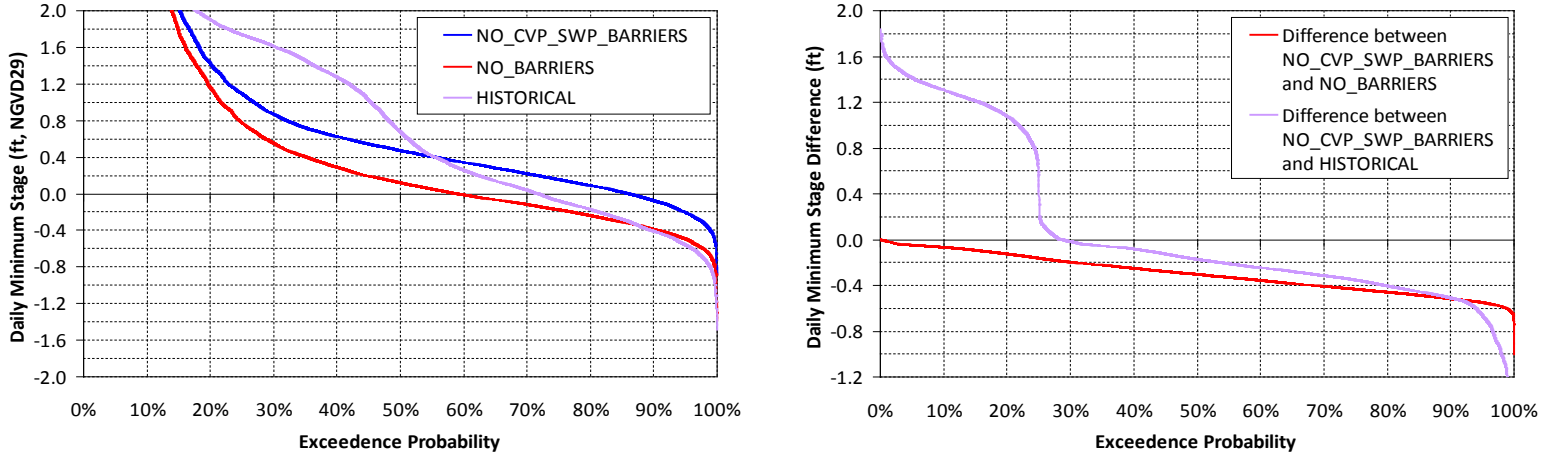

Figure 4-11 Daily Minimum Stage Results for the Entire 21 Years (1990 to 2010)

(c) Old River Barrier

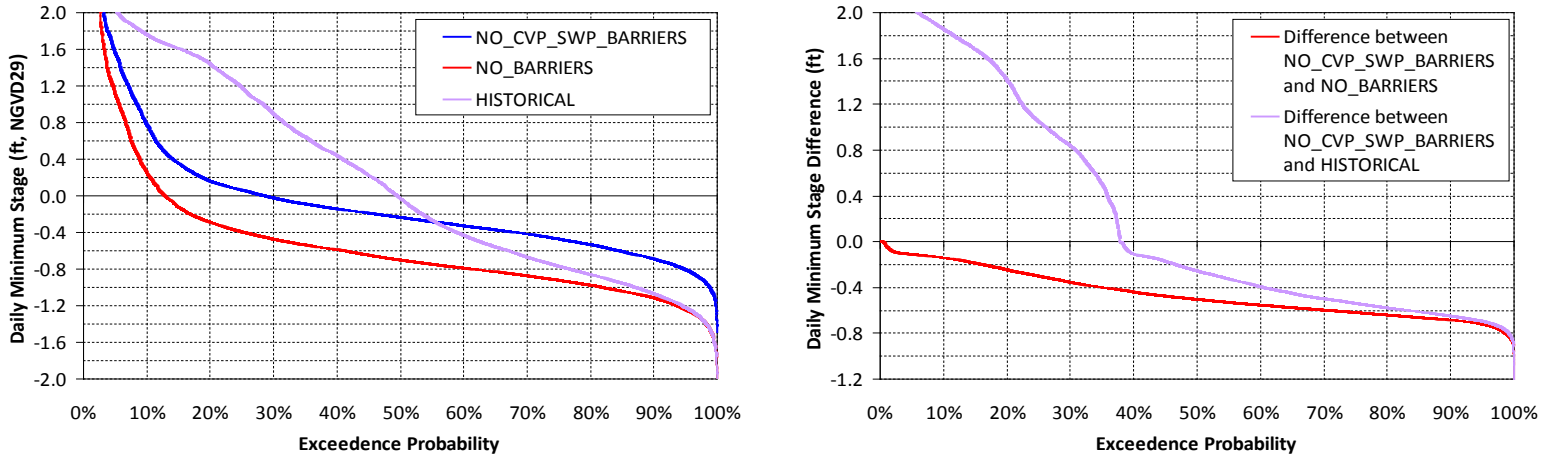

(d) Middle River Barrier

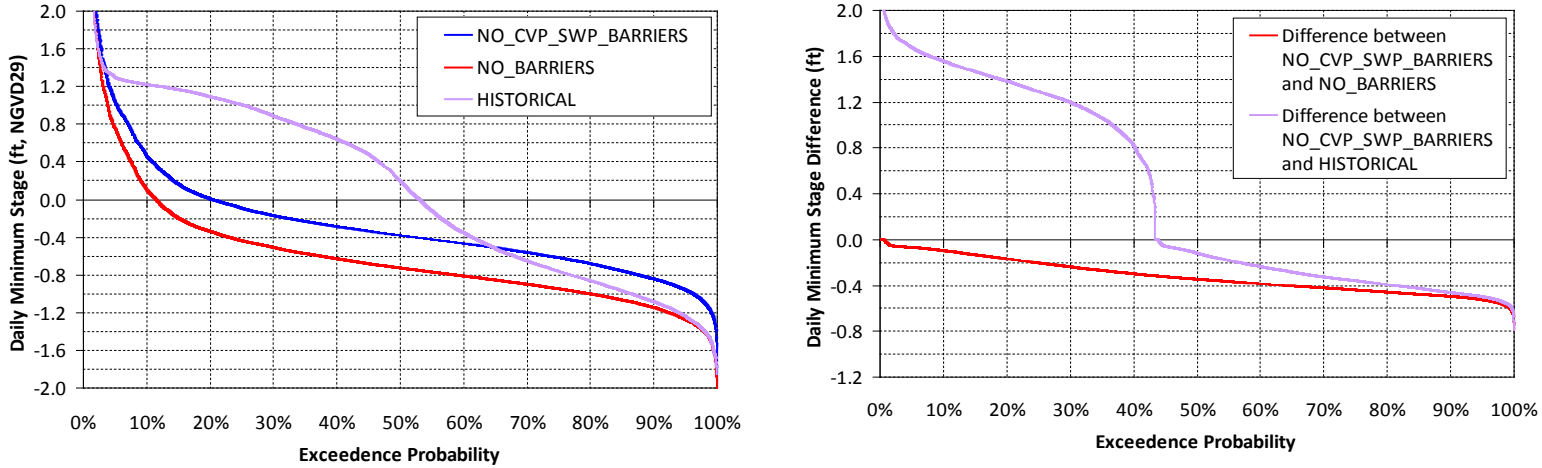

Figure 4-11 (cont'd) Daily Minimum Stage Results for the Entire 21 Years (1990 to 2010)

(e) Grant Line Canal Barrier

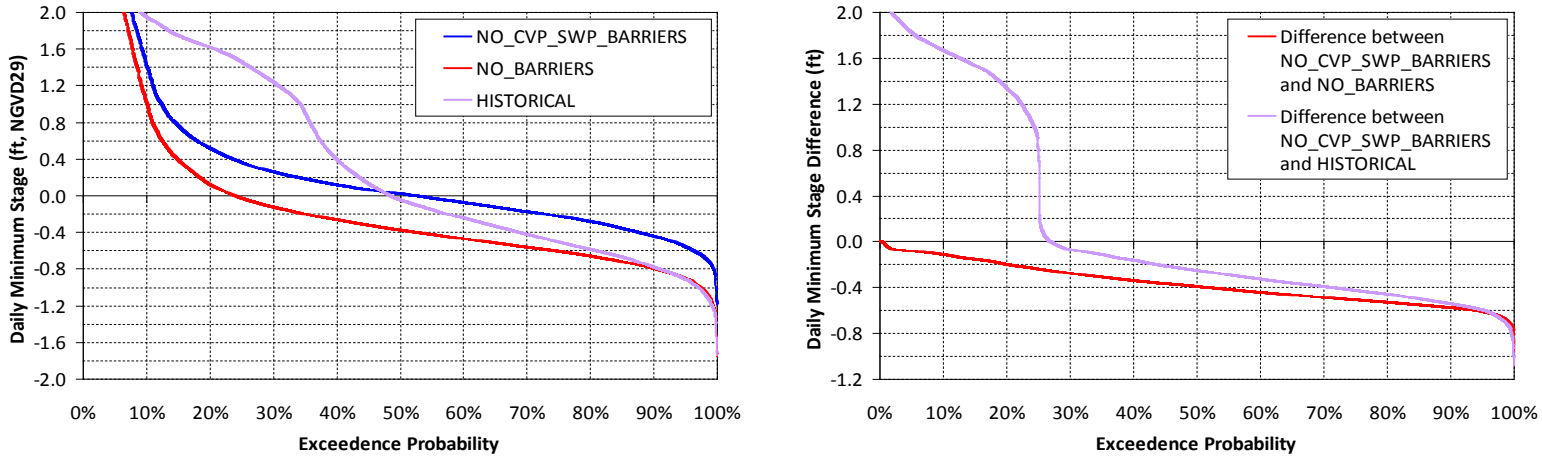

Figure 4-11 (cont'd) Daily Minimum Stage Results for the Entire 21 Years (1990 to 2010)

The results show that:

- When comparing the stage of NO_CVP_SWP_BARRIERS and NO_BARRIERS scenarios, the stage of the former is higher than that of the latter, i.e., the stage is lower when the CVP/SWP exports are in place. The exceedence probability curves provide the information of the frequency of stage and the differences between scenarios. For example, for the location of Old River at Tracy Road,
  - under the NO_BARRIERS scenario, the daily minimum stage that is equal to or less than zero (which is sometimes considered as a threshold for farmers so that water can be diverted) is about 79% of the time; and
  - the stage reduction (difference between the two scenarios) that is equal to or less than 0.4 feet occurs about 45% of the time.

- When comparing the stage of NO_CVP_SWP_BARRIERS and HISTORICAL scenarios, the stage of the latter could be either higher or lower than that of the former depending on if the agricultural barriers are operated. The stage is higher when both CVP/SWP exports and agricultural barriers are considered; the stage is lower when only CVP/SWP exports are in place. The exceedence probability curves provide the information of the frequency of stage and the differences between scenarios. For example, for the location of Old River at Tracy Road,
  - under HISTORICAL scenario, the daily minimum stage that is equal to or less than zero (which is sometimes considered as a threshold for farmers so that water can be diverted) occurs about 44% of the time; and
  - the stage reduction (difference between the two scenarios) that is equal to or less than 0.2 feet is about 50% of the time.

The daily minimum stage is further investigated for each month. Figure 4-12 shows the results for July (when agricultural barriers are in place) as an example.

- When comparing the stage of the NO_CVP_SWP_BARRIERS and NO_BARRIERS scenarios, the stage under the former is higher than that of the latter. For example, the exceedence probability curves for the location of Old River at Tracy Road show that
  - under the NO_BARRIERS scenario, the daily minimum stage that is equal to or less than zero occurs about 91% of the time; and
  - the stage reduction (difference between the two scenarios) that is equal to or less than 0.6 feet occurs about 71% of the time.

- When comparing the stage under the NO_CVP_SWP_BARRIERS and HISTORICAL scenarios, the stage of the latter is higher than that of the former most of the time because the agricultural barriers are operated. For example, the exceedence probability curves for the location of Old River at Tracy Road show that
  - under the HISTORICAL scenario, the daily minimum stage that is equal to or less than zero occurs about 14% of the time; and
  - the stage increase (difference between the two scenarios) that is equal to or greater than 0.4 feet occurs about 70% of the time.

(a) Old River at Tracy Road

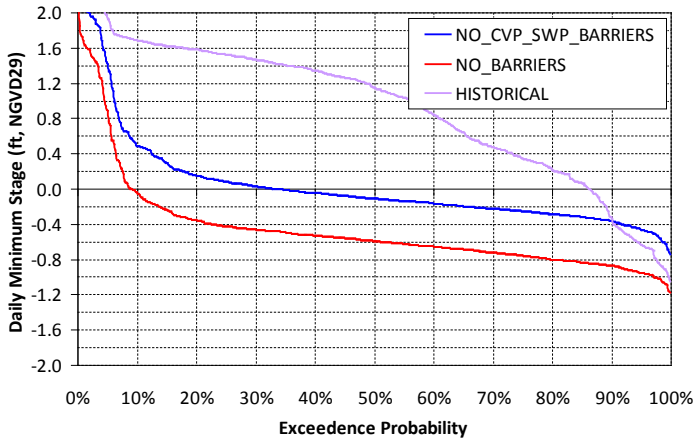

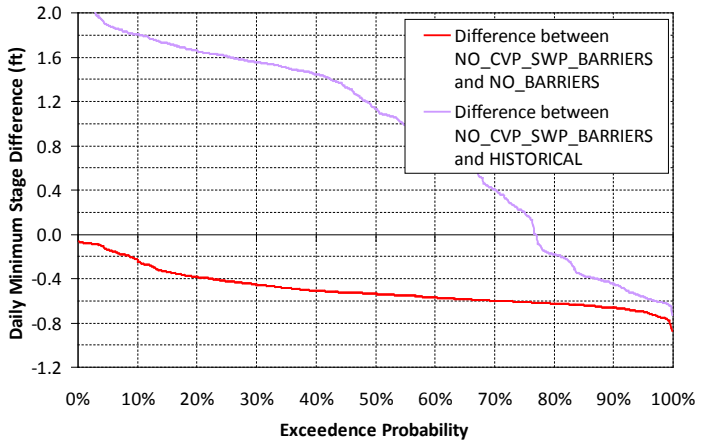

(b) Middle River at Old River

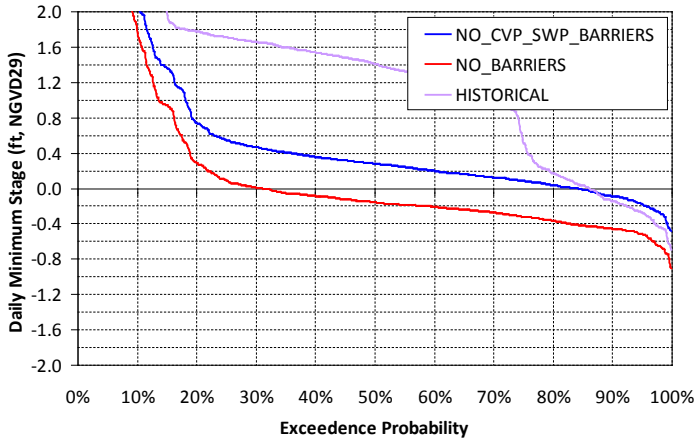

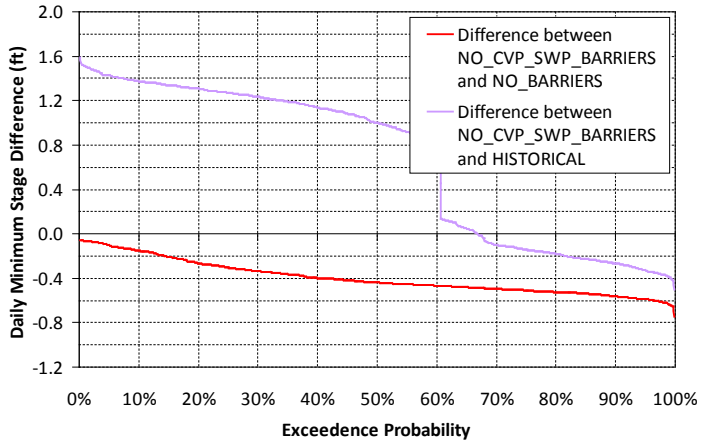

Figure 4-12 Daily Minimum Stage Results for July Only (1990 to 2010)

(c) Old River Barrier

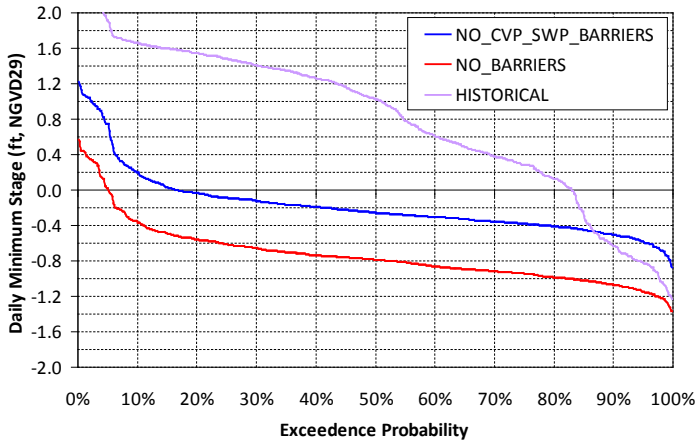

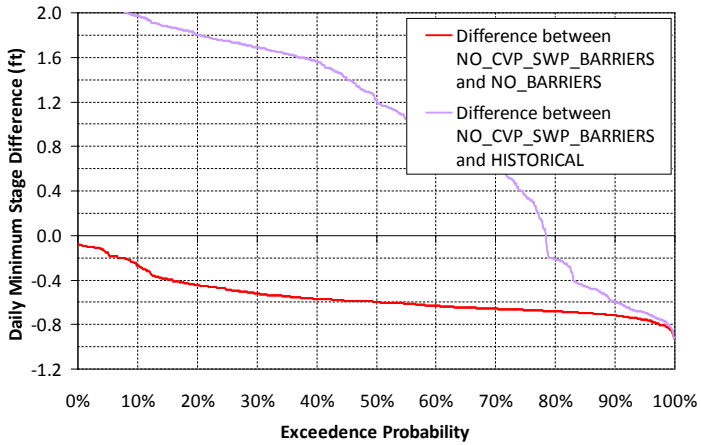

(d) Middle River Barrier

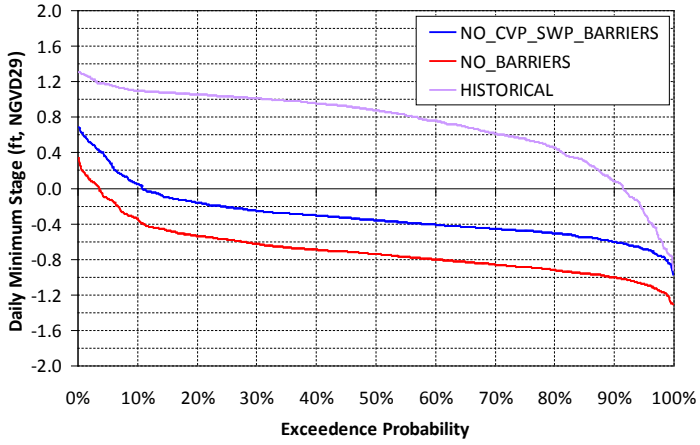

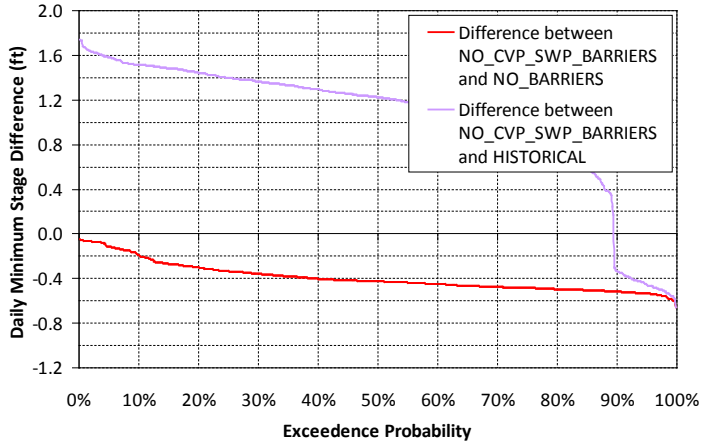

Figure 4-12 (cont'd) Daily Minimum Stage Results for July Only (1990 to 2010)

(e) Grant Line Canal Barrier

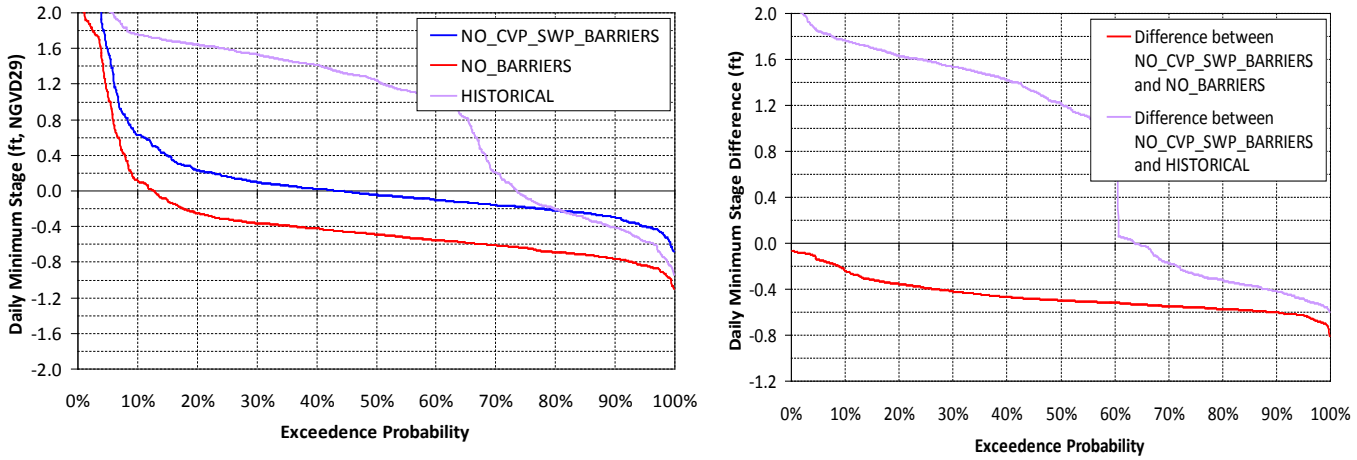

Figure 4-12 (cont'd) Daily Minimum Stage Results for July Only (1990 to 2010)

4.5 Conclusions

The following summarizes the conclusions of this study:

- Based on the assumed null zone definition, the modeling results show that null zones could happen even when CVP/SWP exports and/or barriers are not in place.
- When CVP/SWP exports are in place, the locations and occurrence frequency of null zones change. When compared to the Without-CVP/SWP exports scenario, the difference is relatively small.
- When CVP/SWP exports and agricultural barriers are in place, the locations and occurrence frequency of null zones change. When compared to the Without-CVP/SWP exports scenario, the difference is relatively small.
- Agricultural barrier operations raise the daily minimum water levels during irrigation seasons.

4.6 References

California Department of Water Resources. (2011). *Historical Water Year Type Indexes.* Retrieved March 2012, from California Data Exchange Center: http://cdec.water.ca.gov/cgi-progs/iodir/WSIHIST

Delta Modeling Section. (Online). *Delta Simulation Model II -- DSM2*. (California Department of Water Resources) Retrieved 2012, from Bay-Delta Office: http://baydeltaoffice.water.ca.gov/modeling/deltamodeling/models/dsm2/dsm2.cfm

Nader-Tehrani, P., & Shrestha, B. (2000). DSM2 Calibration (Chapter 10). In *Methodoogy for Flow and Salinity Estiimates in the Sacramento-San Joaquin Delta and Suisun Marsh: 21st Annual Progress Resport.* California Department of Water Resources.

State Water Resources Control Board. (2009). Periodic Review of the 2006 Water Quality Control Plan for the San Francisco Bay/Sacramento-San Joaquin Delta Estuary. Sacramento, CA. Retrieved from http://www.waterboards.ca.gov/waterrights/water_issues/programs/bay_delta/periodic_review/docs/periodicreview2009.pdf

Methodology for Flow and Salinity Estimates in the Sacramento-San Joaquin Delta and Suisun Marsh

33rd Annual Progress Report
June 2012

Chapter 5
Estimating Delta-wide Bromide Using DSM2- Simulated EC Fingerprints

Authors: Siqing Liu and Bob Suits
Delta Modeling Section
Bay-Delta Office
California Department of Water Resources

Page left blank for two-sided printing

Contents

Figures

Tables

Page left blank for two-sided printing

5 Estimating Delta-wide Bromide Using DSM2-Simulated EC Fingerprints

5.1 Introduction

This chapter compares 6 methods to determine bromide concentrations at select locations in the Sacramento-San Joaquin River Delta (the Delta). The results of the methods are compared to observed grab sample bromide data at those Delta locations. The 6 methods examined are shown in Table 5-1.

Table 5-1 Methods to Determine Bromide Concentrations

No.	Method	Description
1	DSM2 Simulation	Bromide is simulated at various Delta locations using DSM2 with bromide values as input at boundaries.
2	Direct EC-Br regression	Regression using EC and bromide observed data (does not consider source of EC in regression).
3	Previous BDO[a] regression	Linear regression using observed data (considered Volumetric fingerprint from Martinez).
4	Site-specific regression	DSM2 EC fingerprint simulations[b]. Results from multiple linear regressions developed from site data and from fingerprint results.
5	Regional regression	DSM2 EC Fingerprint simulations. Results from multiple linear regressions developed from regional data that include several sites and from DSM2 fingerprint output.
6	Delta-wide regression	DSM2 EC Fingerprint simulations. Results from multiple linear regressions developed using fingerprint output and with full Delta data.

[a] BDO Bay Delta Office

[b] Fingerprints provide the amount of electrical conductivity (EC) contributed by different sources of salinity, such as the ocean, agricultural returns, and river inflows. These sources contain different combinations of cations and anions. For example, the salinity coming from the ocean contains a higher proportion of bromide than that coming from river inflows.

5.2 Background

The dispersion coefficients in the current version of QUAL, the water quality module of DSM2, were calibrated using electrical conductivity, which measures the water's ability to conduct electrical current. At high salinity concentration, as usually occurs at DSM2's downstream boundary at Martinez, EC underestimates true salinity[1]. This has raised concerns about directly simulating truly conservative water quality constituents with DSM2's EC-based dispersion coefficients. Although no actual test has been conducted to evaluate this as a potential problem, some analysis has been done.

Recently, direct simulation of historical Delta bromide using DSM2 was conducted and reported by Montgomery Watson Harza (2011) as part of a larger analysis of DSM2's current capability to simulate various cations and anions. Cations and anions values were developed at model boundaries, including Martinez, by applying regressions developed by the California Department of Water Resources to DWR's historical EC simulation time series. Based on model results, MWH concluded that using DSM2 to simulate historical Delta cation and anion concentrations does not introduce additional error beyond the baseline error in EC.

As part of our review of MWH's report, we reproduced the direct simulation of bromide and compared values to observed bromide, but at more locations. In addition, we compared simulated bromide to bromide derived from multiple linear regressions based on simulated EC fingerprints and grab samples containing both EC and bromide. We considered 3 regressions: a single Delta-wide, site-specific, and regional.

As presented below, our analysis confirms MWH's conclusion that direct simulation of bromide with DSM2 and the current version of dispersion coefficients is equivalent to estimating bromide based on DSM2-simulated EC and applying multiple linear regressions based on simulated EC fingerprints. However, using observed EC and multiple linear regressions provides significantly better estimates of bromide. Multiple linear regressions based on Delta regions perform nearly as well as site-specific regressions and allow for converting from EC to bromide at nearly any location in the Delta.

[1] "An important drawback to using EC to calibrate dispersion factors is its acknowledged failure to behave as a truly conservative constituent of salinity. As salinity and ionic concentration increases, electrical conductance increases. For high concentrations, however, the proximity of ions to each other depresses their activity and consequently their ability to transmit electrical current. As a result, EC increasingly underestimates true salinity at higher concentrations, a trend manifest in a nonlinear relationship between EC and any conservative constituent." (Suits, Calibrating DSM2-QUAL Dispersion Factors to Practical Salinity (Chapter 6), 2002)

5.3 Directly Simulating Delta Bromide

We followed MWH's approach in setting up the DSM2 model to simulate bromide directly. Boundary conditions for bromide were generated using regression equations developed by the Bay-Delta Office (BDO) (work by Bob Suits, not published) based on grab sample bromide and EC data. The regressions for all boundaries are in the linear form

$$Br = A + B * EC \qquad \text{(Equation 1)}$$

where Br is the bromide concentration in mg/L; A and B are regression coefficients (y-axis intercept and slope, respectively); and EC is electrical conductivity in microsiemens per centimeter (µS/cm), or equally, micromhos per centimeter (µmhos/cm).

Figure 5-1 through Figure 5-3 show the scatterplots of EC and bromide and linear EC-bromide regressions represented by equation (1) at Martinez, Sacramento River at Freeport, and San Joaquin River at Vernalis. The regression for Sacramento River is also applied to Eastside Streams. The EC and bromide data used to derive the regression at Martinez were grab sample EC and bromide data at Mallard Island and Jersey Point downloaded from Water Data Library (WDL). The data used to develop the Sacramento River bromide-EC regression came from grab sample data at Delta Cross Channel, and Jersey Point and Mallard Island when EC < 300 uS/cm. The EC and bromide data used to derive the regression at San Joaquin River at Vernalis were grab sample data at San Joaquin River at Vernalis.

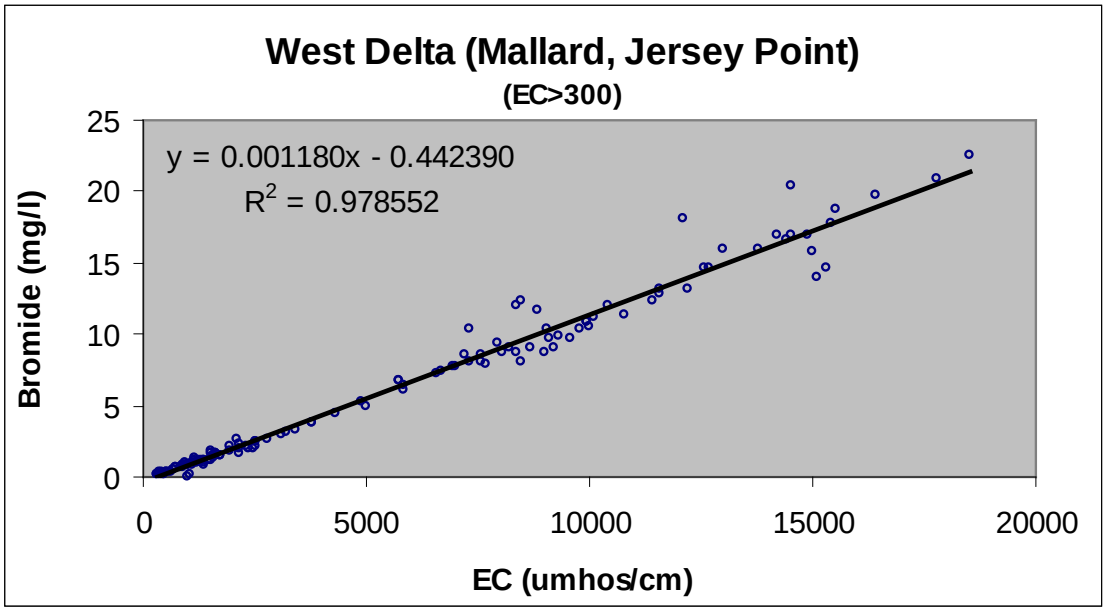

Figure 5-1 Martinez Regression Used for Converting from EC to Bromide

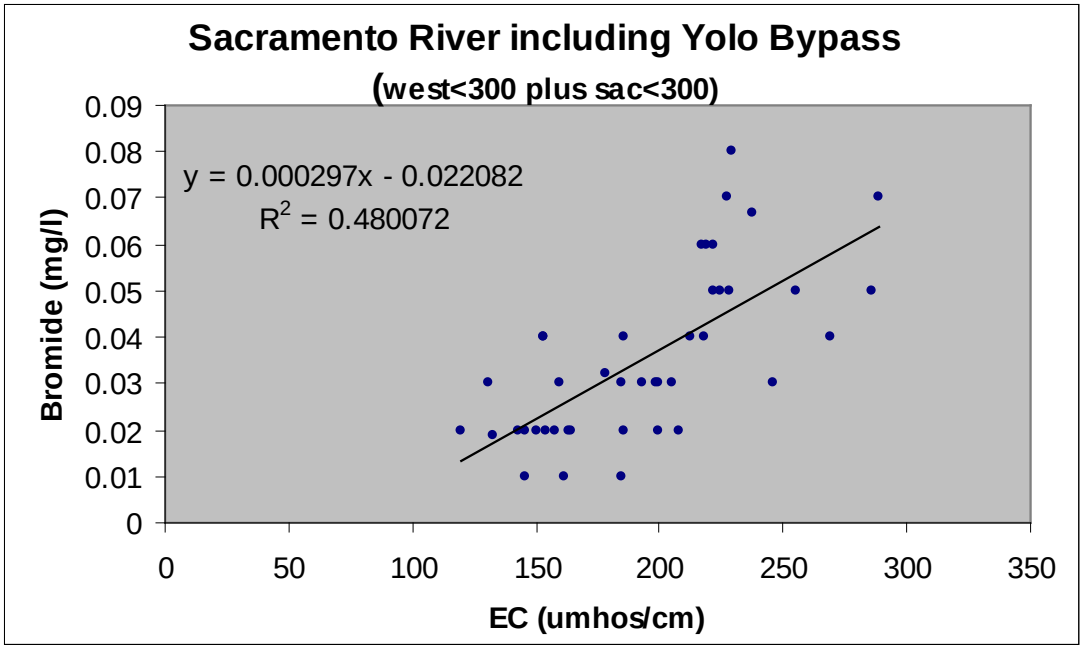

Figure 5-2 Sacramento River Boundary Regression Used for Converting from EC to Bromide

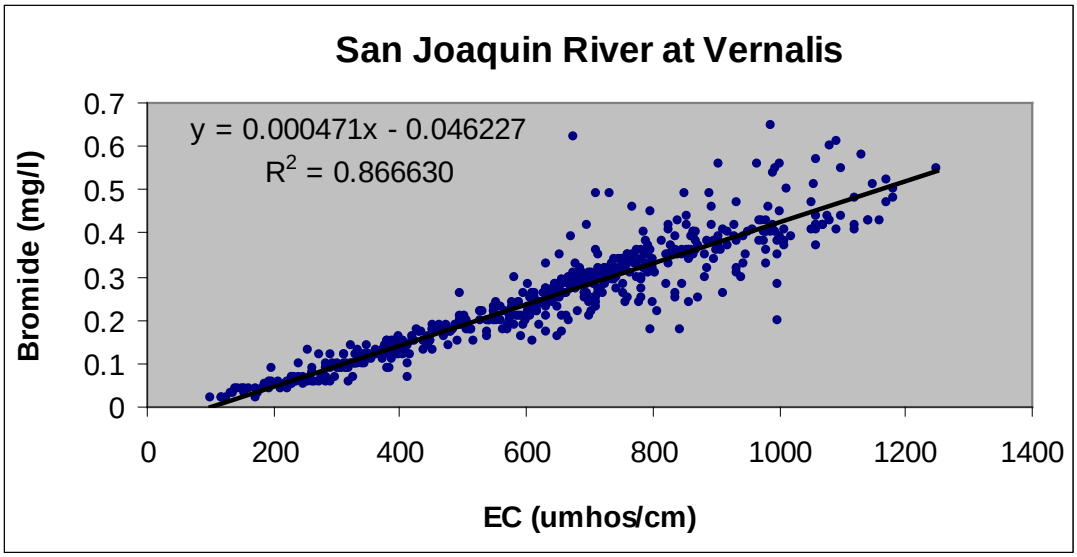

Figure 5-3 San Joaquin River Boundary Regression Used for Converting from EC to Bromide

Besides water quality at boundaries, DSM2 also requires that water quality for Delta island return flows be specified. Bromide data for Delta island return flows is scarce. Thus, in the current DSM2 bromide simulation, bromide data for Delta island return flows was based upon a memorandum report(California Department of Water Resources, 1995). The data was reported for 2 Delta regions shown (with lighter and darker shades) in Figure 5-4.

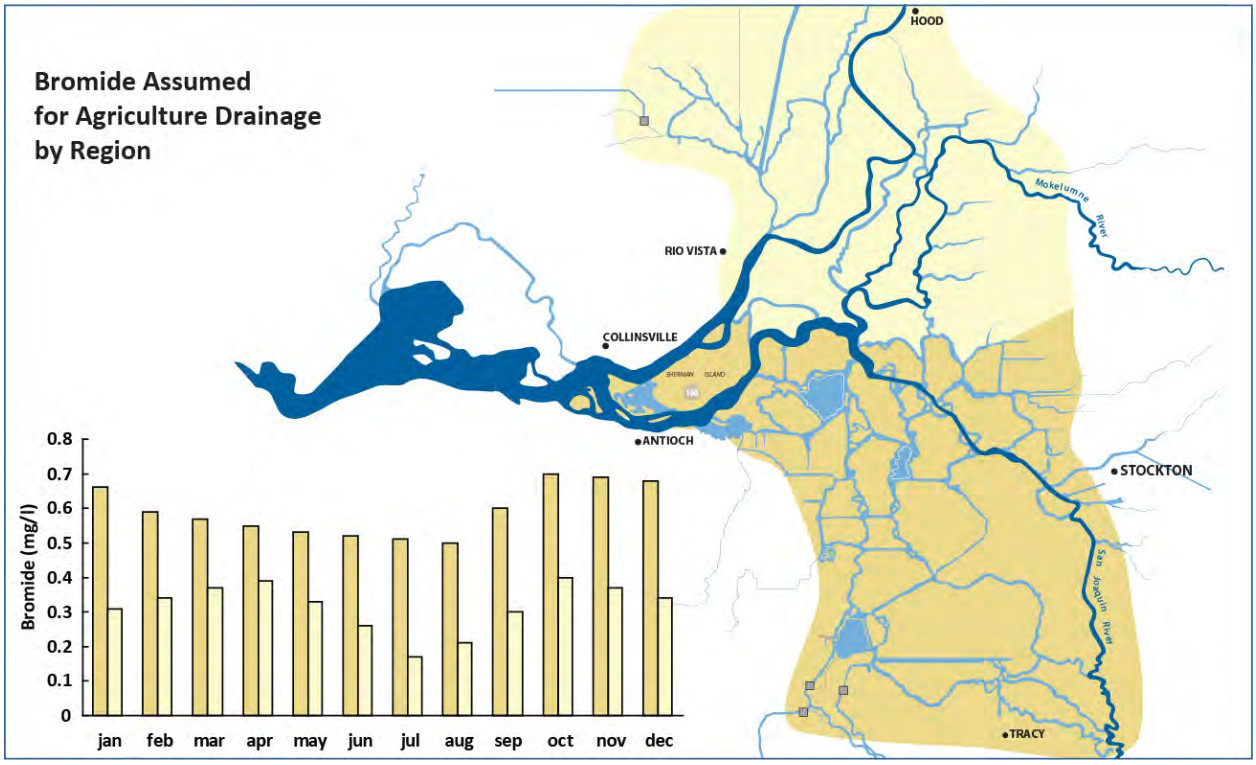

Figure 5-4 Bromide Assumed for Agricultural Drainage by Region

5.4 Estimating Historical Bromide Based on Simulated EC

Analysis in the past, based on grab sample EC and other constituents (bromide, chloride, magnesium, calcium, TDS, sulfide, total alkalinity, potassium, and sodium), has consistently shown certain patterns. At low EC values, the concentration of other constituents is bounded within a small range. But at higher EC values, the possible concentration of other constituents can vary over a larger range. The source of water when there are higher EC values will affect the percentage of bromide present in the concentration. For water from the ocean boundary, there will be a higher concentration of bromide. For water that is more influenced by the San Joaquin River or by Delta agricultural returns, the concentration of bromide will be lower, but the concentration of other constituents will be higher.

As shown in Figure 5-5, the concentration of a constituent can be bounded within two lines. This is the result of the complex mixing of water from different sources. Figure 5-5 shows two points with almost the same EC values but quite different bromide concentrations. The main graph shows a scatterplot between measured bromide and EC. A linear regression is made through the points and the R^2 value is 0.79, indicating that there is a spread in the data which becomes larger at greater EC and bromide levels. The two bar charts (fingerprints) show the makeup of EC and the percentage of water by volume from the different sources that contribute to Jones Pumping Plant water. At point 1, water from the Martinez boundary contributed most EC, so bromide concentration is high. At point 2, water from the San Joaquin

River contributed most EC, contribution from the Martinez boundary is negligible, and thus bromide concentration is much less.

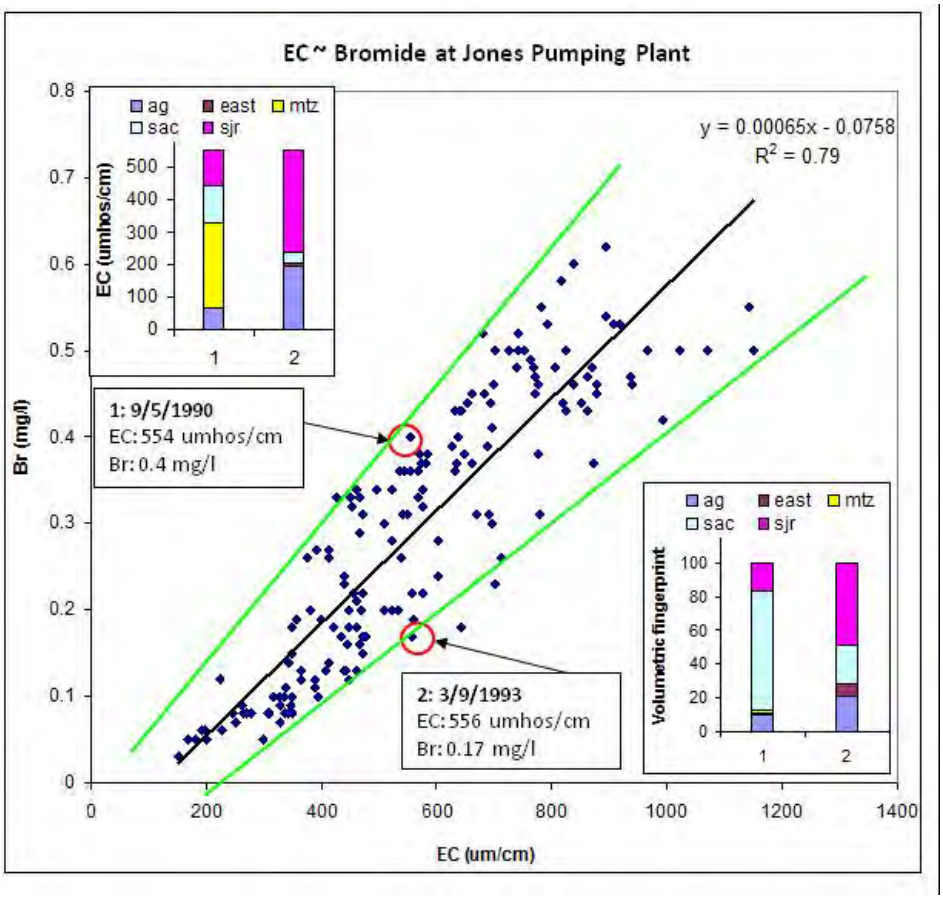

Figure 5-5 Illustration of Change of Bromide Concentration with Change of Water Sources

Based on the previous observation and the close EC-bromide relationship at boundaries, it is reasoned that it is very feasible that the bromide concentration at any location can be derived from the EC fingerprint of water from boundary sources. The following is the mathematical form that calculates bromide concentrations from EC fingerprints using multiple linear regressions,

$$Br = EC * (A*EC_{fp,mtz} + B*EC_{fp,sac} + C*EC_{fp,sjr} + D*EC_{fp,east} + E*EC_{fp,agr}) / EC_{all} \quad \text{(Equation 2)}$$

where *Br* is the bromide concentration in mg/L; EC can be observed EC or modeled EC at a location; A, B, C, D, and E are coefficients; and $EC_{fp,mtz}$, $EC_{fp,sac}$, $EC_{fp,sjr}$, $EC_{fp,east}$, $EC_{fp,agr}$ are EC fingerprints at a specific location in the Delta from the 5 boundary sources: Martinez, Sacramento River, San Joaquin River, Eastside streams and Delta return flows. EC_{all} is total model simulated EC, i.e.,

$$EC_{all} = EC_{fp,mtz} + EC_{fp,sac} + EC_{fp,sjr} + EC_{fp,east} + EC_{fp,agr} \quad \text{(Equation 3)}$$

Equation (2) can be re-organized as

$$Br = A*(EC*EC_{fp,mtz}/EC_{all}) + B*(EC*EC_{fp,sac}/EC_{all}) + C*(EC*EC_{fp,sjr}/EC_{all}) + D*(EC*EC_{fp,east}/EC_{all}) + E*(EC*EC_{fp,agr}/EC_{all}) = Br_{mtz} + Br_{sac} + Br_{sjr} + Br_{east} + Br_{agr} \quad \text{(Equation 4)}$$

Equation (4) indicates that bromide concentration at each specific location is the sum of bromide concentrations from each source. Thus multiple linear regressions can be used to estimate not only total bromide concentrations, but also bromide fingerprints.

A multiple linear regression can be developed for different regional scales. It can be developed using all grab sample data available within the Delta so a Delta-wide regression can be obtained, in which case, one set of coefficients can be used for all stations in the Delta. It can also be conducted for each station using limited data at that station so there will be a set of coefficients for each site-specific regression.

Without doubt, best results can be achieved by using the site-specific regression approach. However, this can only be done for locations with grab sample data. For locations without grab sample data, it is difficult to use this approach. The Delta-wide regression is elegant and the simplest, but at the cost of sacrificing accuracy for some locations.

Several years ago, BDO analyzed EC and bromide relationships [(Suits, 2001), (Suits, 2002), (Hutton, 2006)]. It was found that a close relationship between EC and bromide exists for boundary locations and all stations in the Delta. Further study indicated that it is not necessary to have a regression for each single station. Instead, several stations may have characteristics in common and can be grouped to form a region; and as a result, a regression will apply to all locations within the region.

Figure 5-6 is a map of the regions that were defined based on available grab sample locations. It is anticipated that by grouping stations into regions, accuracy at each station can be maintained with regressions only conducted for regions. Therefore, the number of regressions is reduced considerably compared with the number of site-specific regressions.

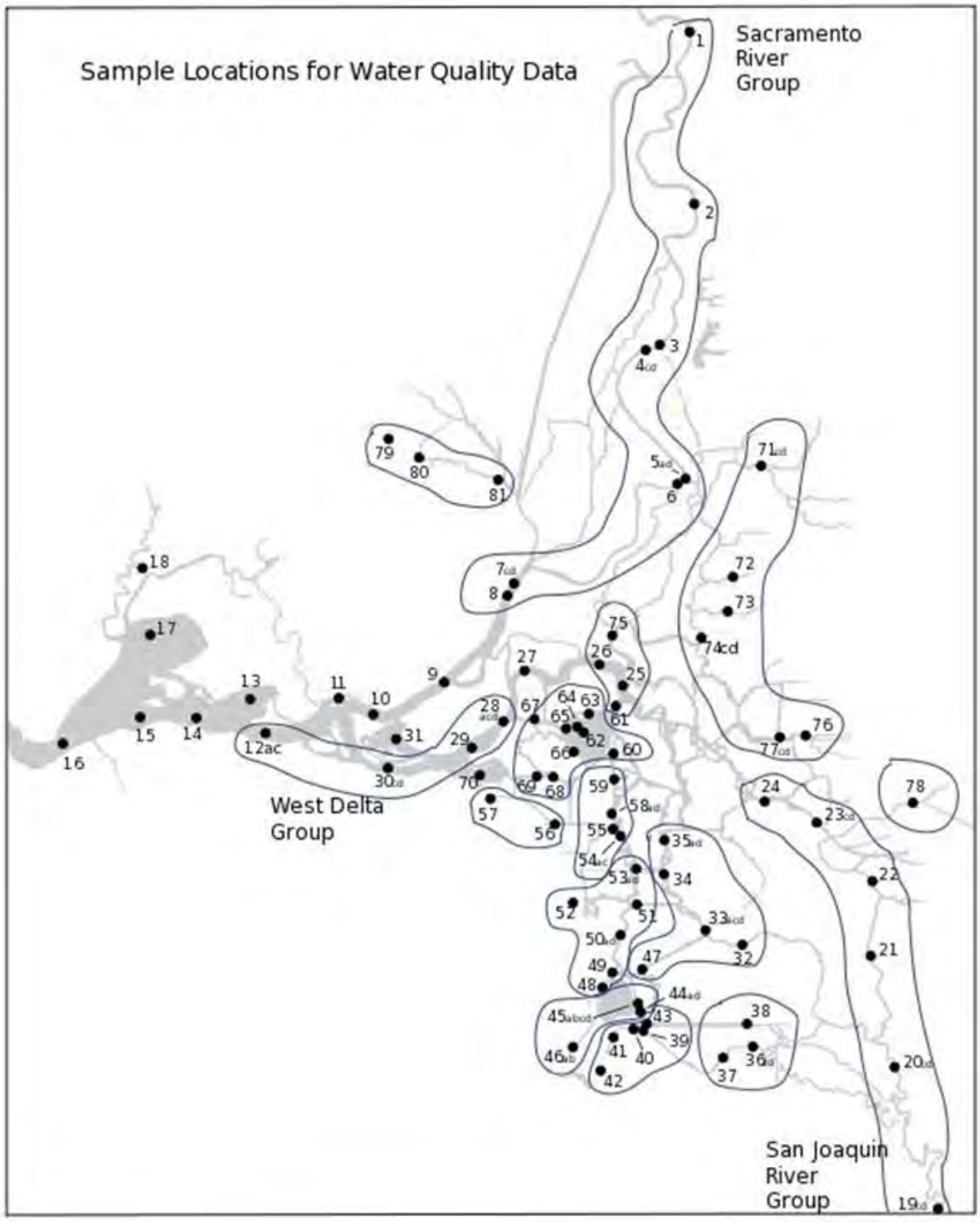

Figure 5-6 Grab Sample Locations and Groupings for Derivation of Regressions

5.5 Comparison of Direct Bromide Simulation and Delta-wide Regression

Figure 5-7 through Figure 5-12 show the following:

- Grab sample bromide (observed)
- DSM2 modeled bromide (direct simulation)
- DSM2 modeled EC and then converted to bromide using a Delta-wide multiple linear regression
- Grab sample (observed) EC converted to bromide using a Delta-wide multiple linear regression

Because the bromide concentration can vary a lot within one day, the graphs also show the range of bromide values for each day. For Jones Pumping Plant and the Sacramento River at Mallard Island, the ranges can be seen clearly. For other locations, the changes of bromide concentration within a day are not significant.

From the figures, we can see that most of the time the grab sample bromide concentrations (green, filled circles) fall within or close to the bromide range simulated by DSM2 (gray area). Bromide concentrations estimated by using the multiple linear regression that used EC fingerprint and DSM2-simulated EC (red triangles) are very close to DSM2-calculated bromide concentrations (gray area). This is anticipated because the bromide concentrations at boundaries were estimated using linear regressions between bromide and EC. However, better results can be obtained by using a multiple linear regression and grab sample EC (blue asterisks), which better matches the grab sample bromide concentrations (overall the blue asterisks are nearer to the green circles). It is apparent that this approach can decrease errors caused by the limitations of the DSM2 model. A comparison of the different methods of determining bromide is analyzed mathematically following the figures.

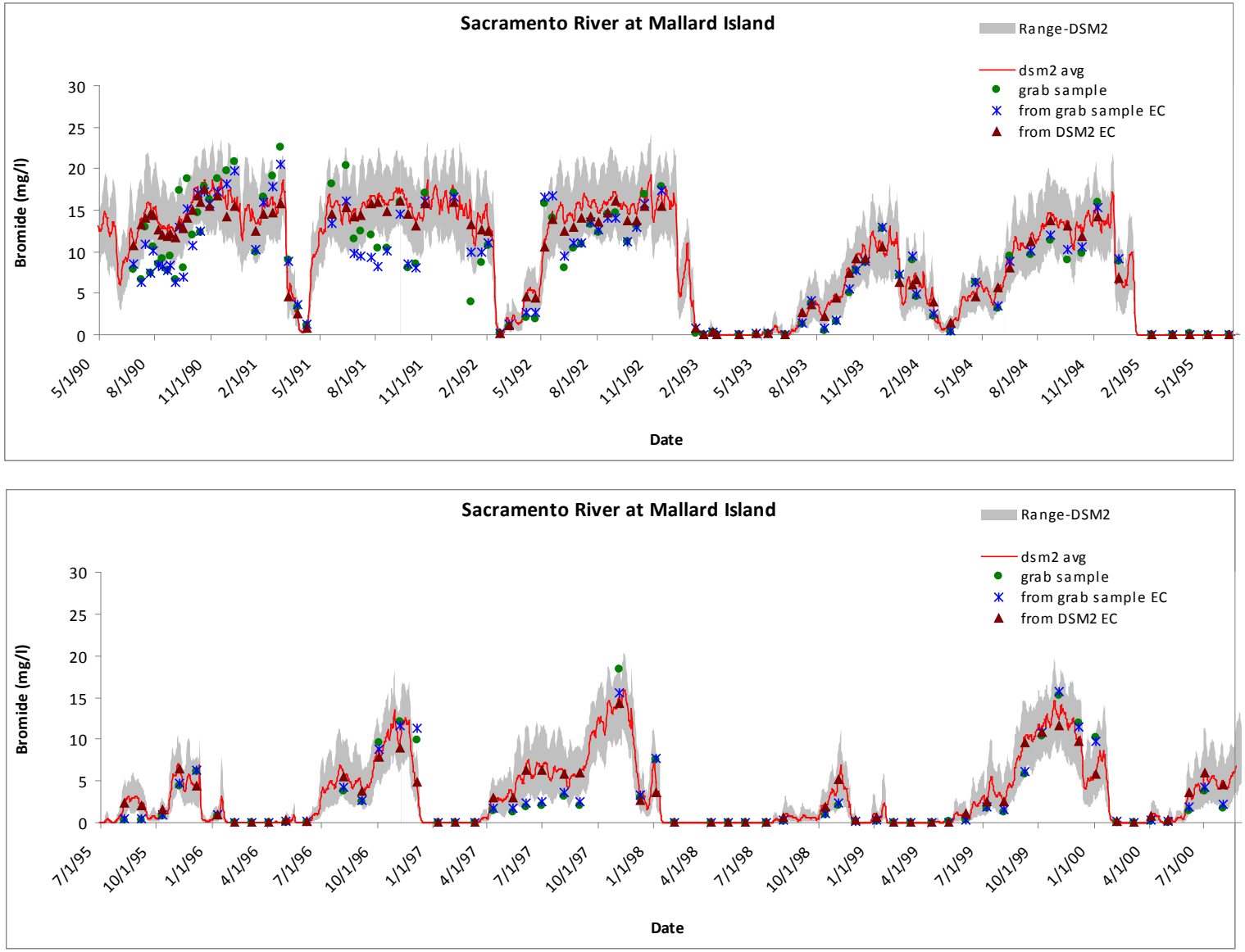

Figure 5-7 Comparison of Grab Sample Data and Calculated Bromide Concentration at Sacramento River at Mallard Island (four figures total)

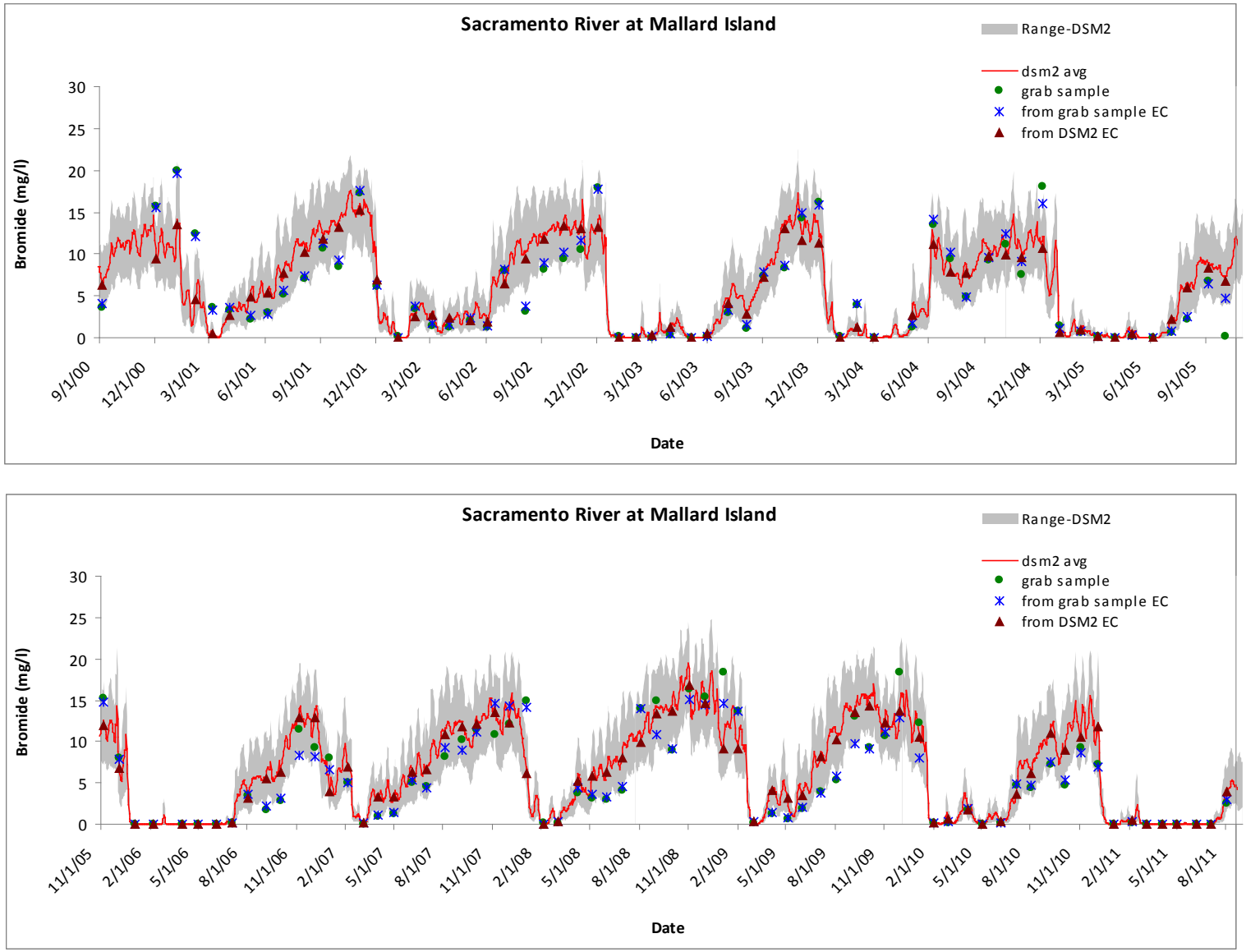

Figure 5 7 (cont'd) Comparison of Grab Sample Data and Calculated Bromide Concentration at Sacramento River at Mallard Island

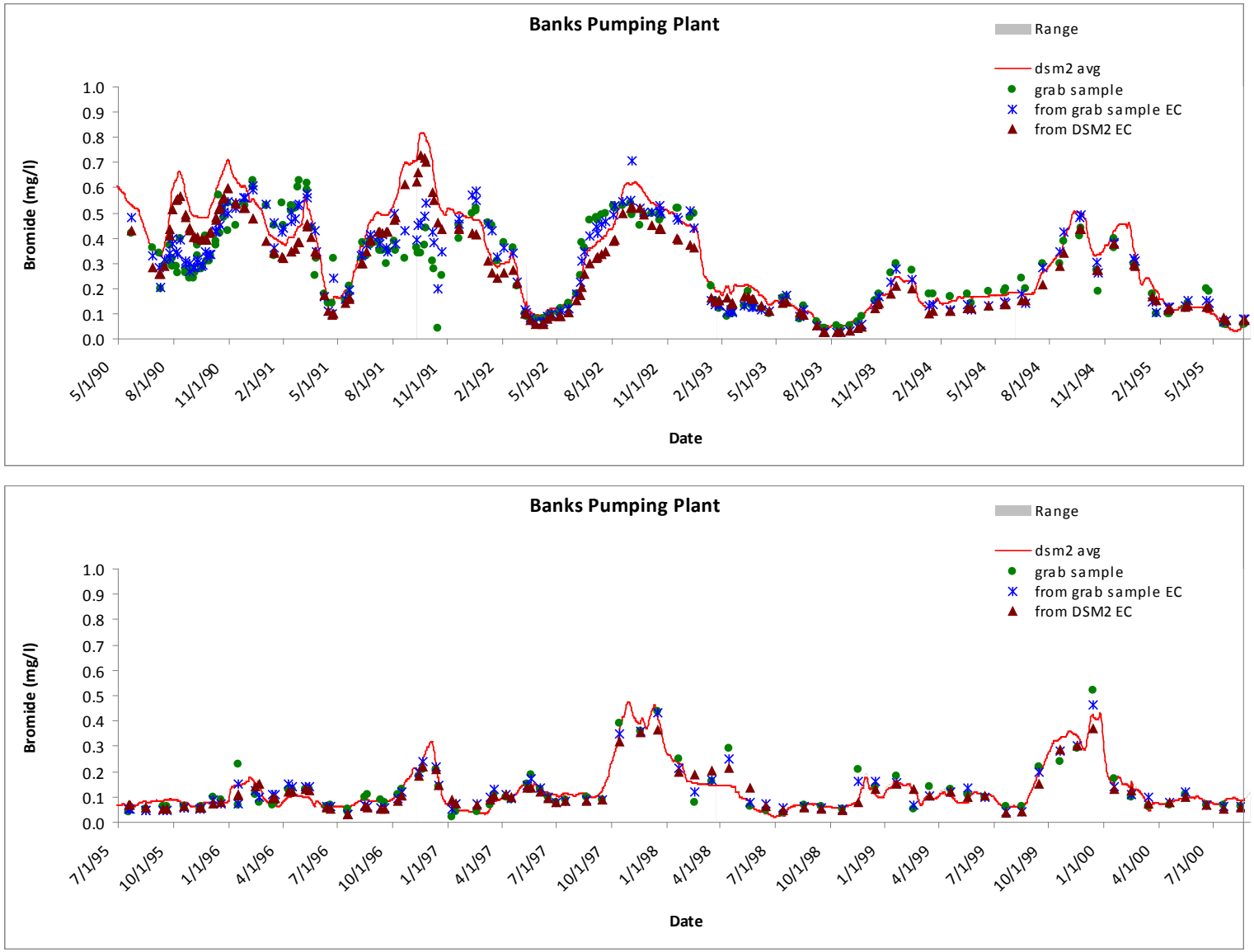

Figure 5-8 Comparison of Grab Sample Data and Calculated Bromide Concentration at Banks Pumping Plant (four figures total)

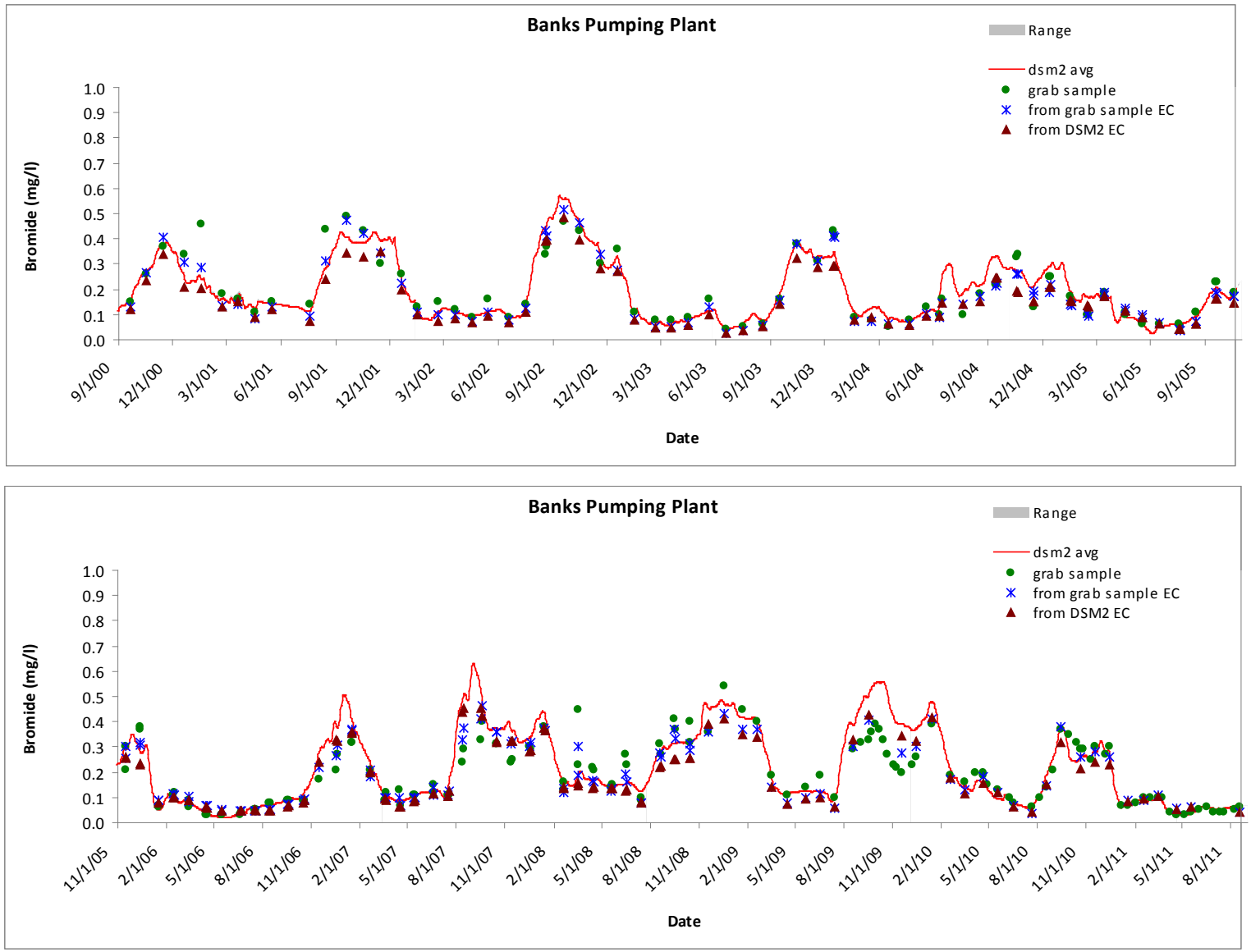

Figure 5-8 (cont'd) Comparison of Grab Sample Data and Calculated Bromide Concentration at Banks Pumping Plant

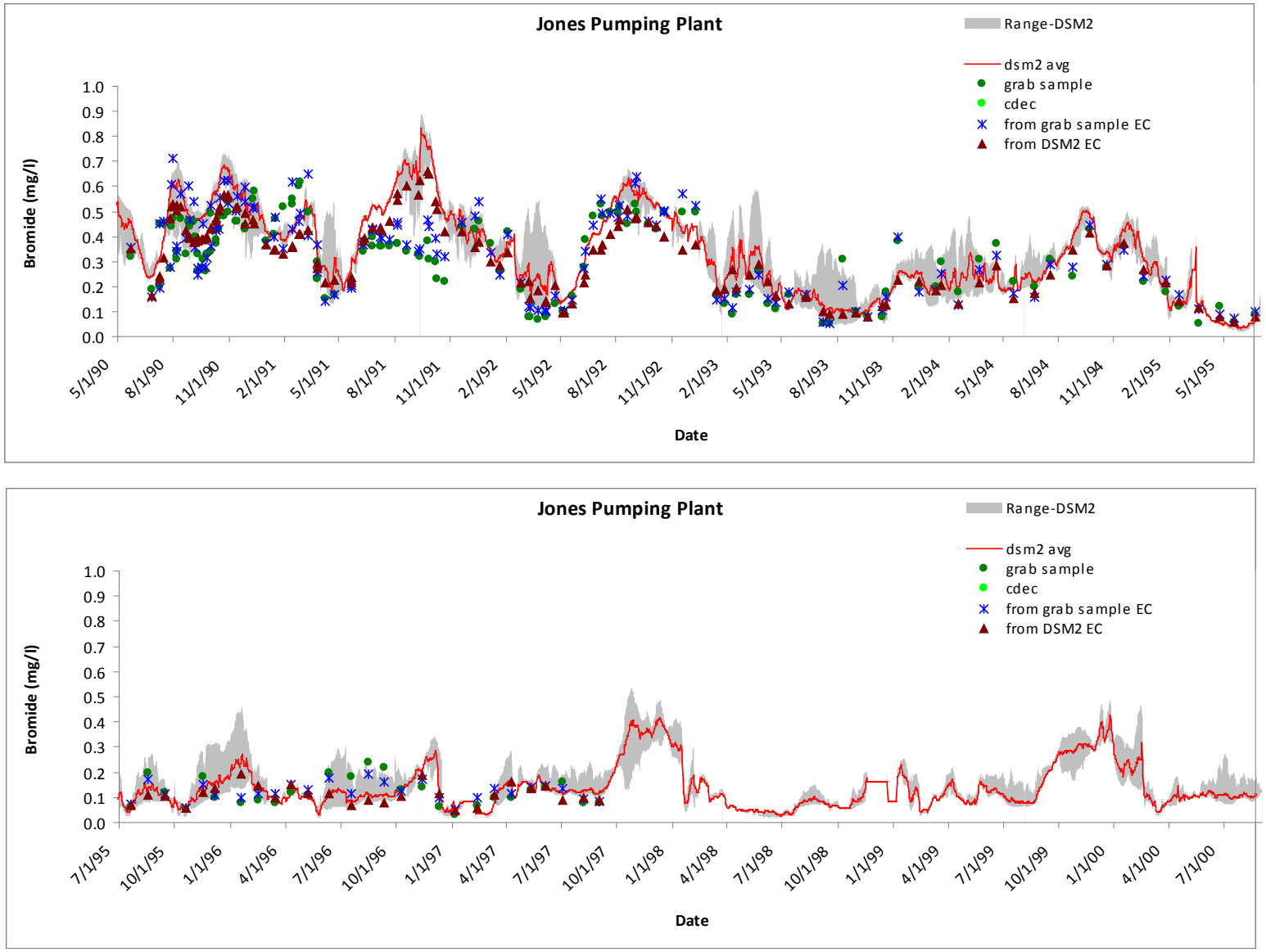

Figure 5-9 Comparison of Grab Sample Data and Calculated Bromide Concentration at Jones Pumping Plant (four figures total)

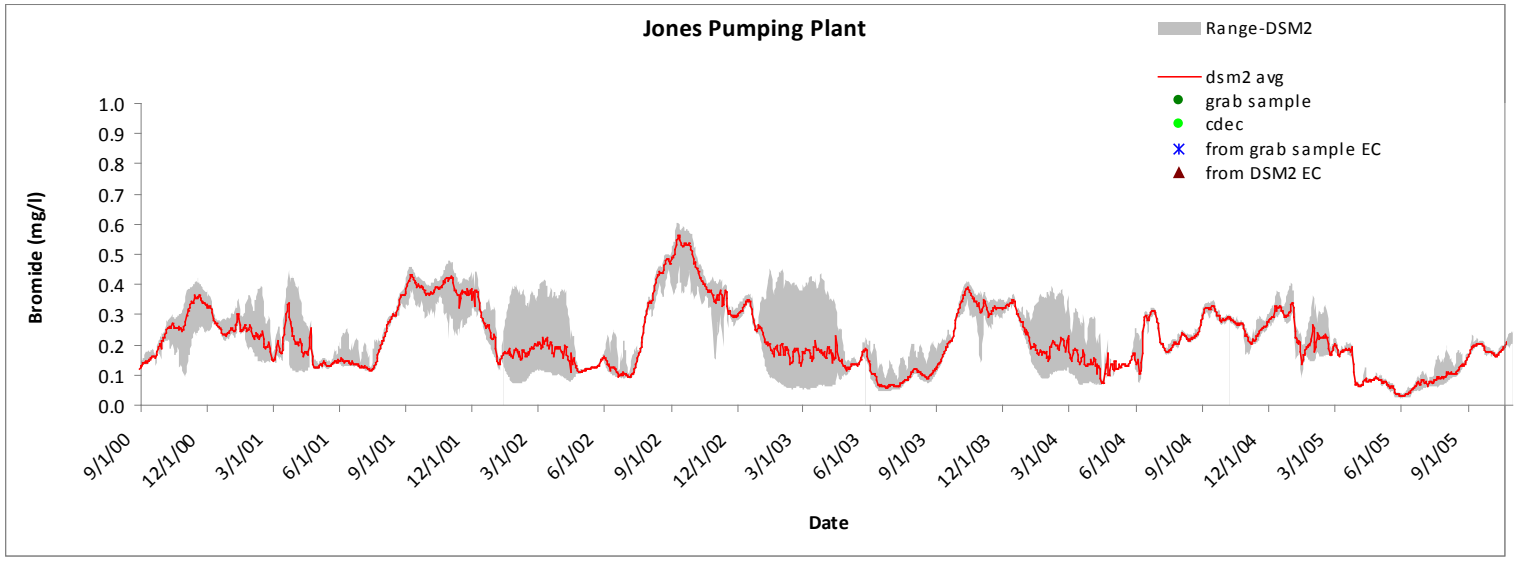

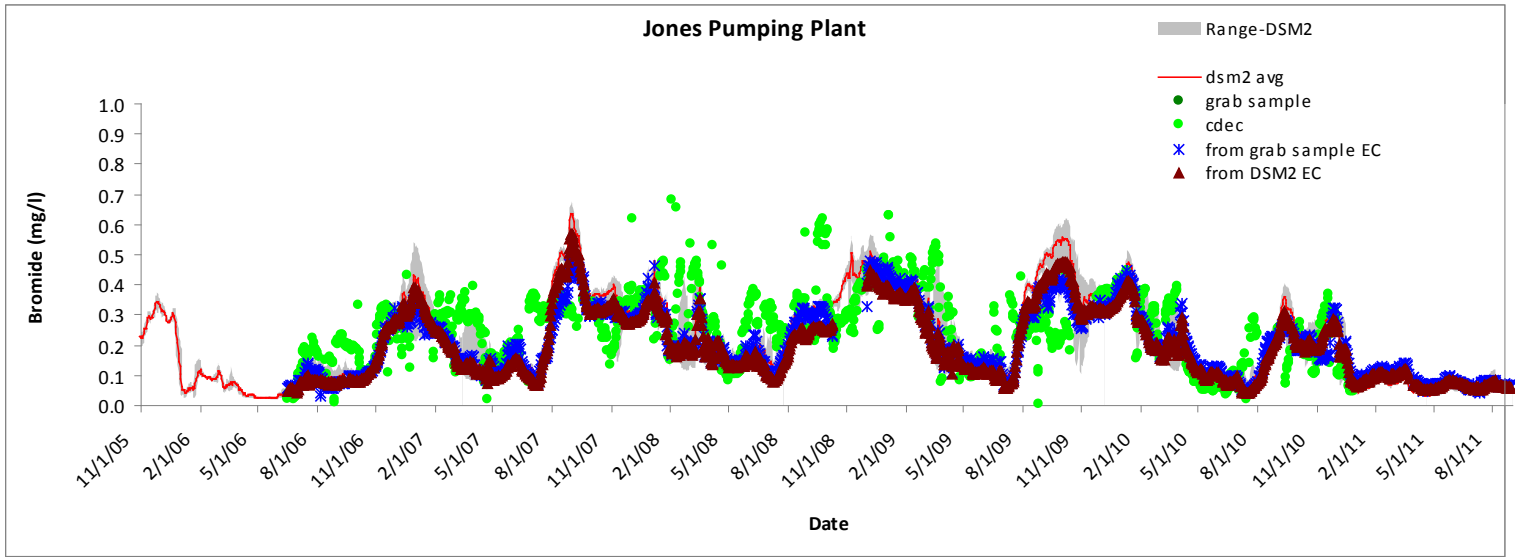

Figure 5-9 (cont'd) Comparison of Grab Sample Data and Calculated Bromide Concentration at Jones Pumping Plant

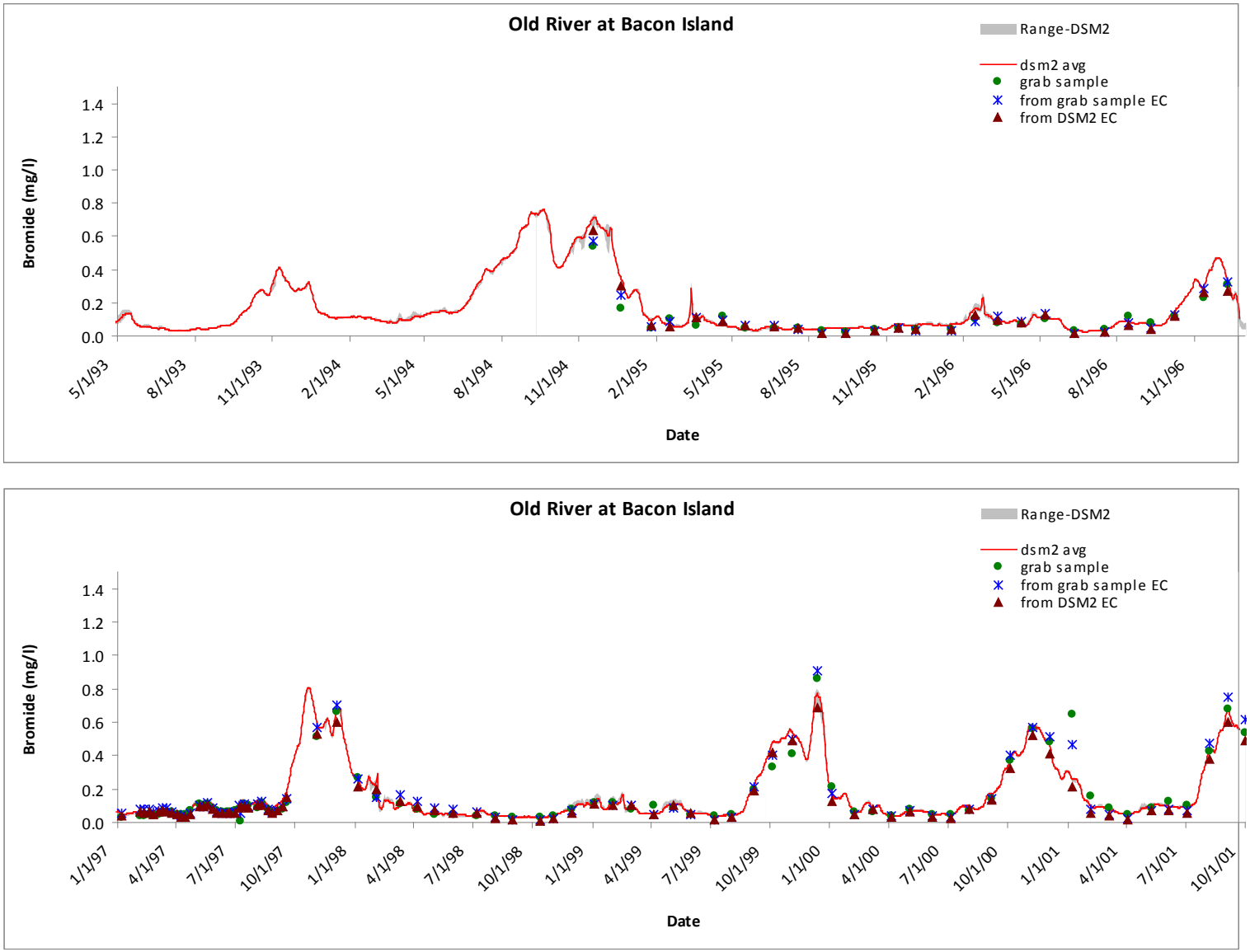

Figure 5-10 Comparison of Grab Sample Data and Calculated Bromide Concentration in Old River at Bacon Island (four figures total)

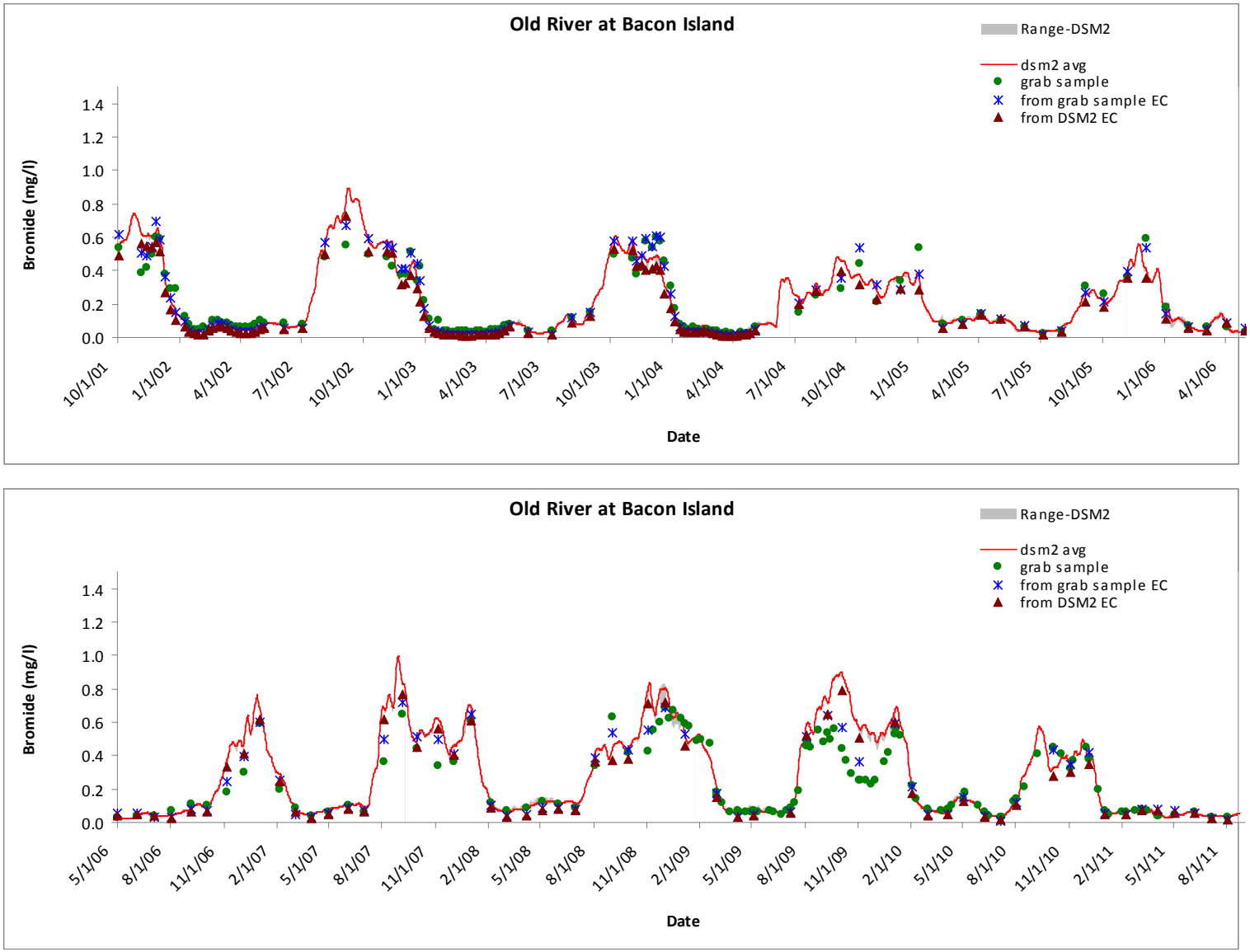

Figure 5-10 (cont'd) Comparison of Grab Sample Data and Calculated Bromide Concentration in Old River at Bacon Island

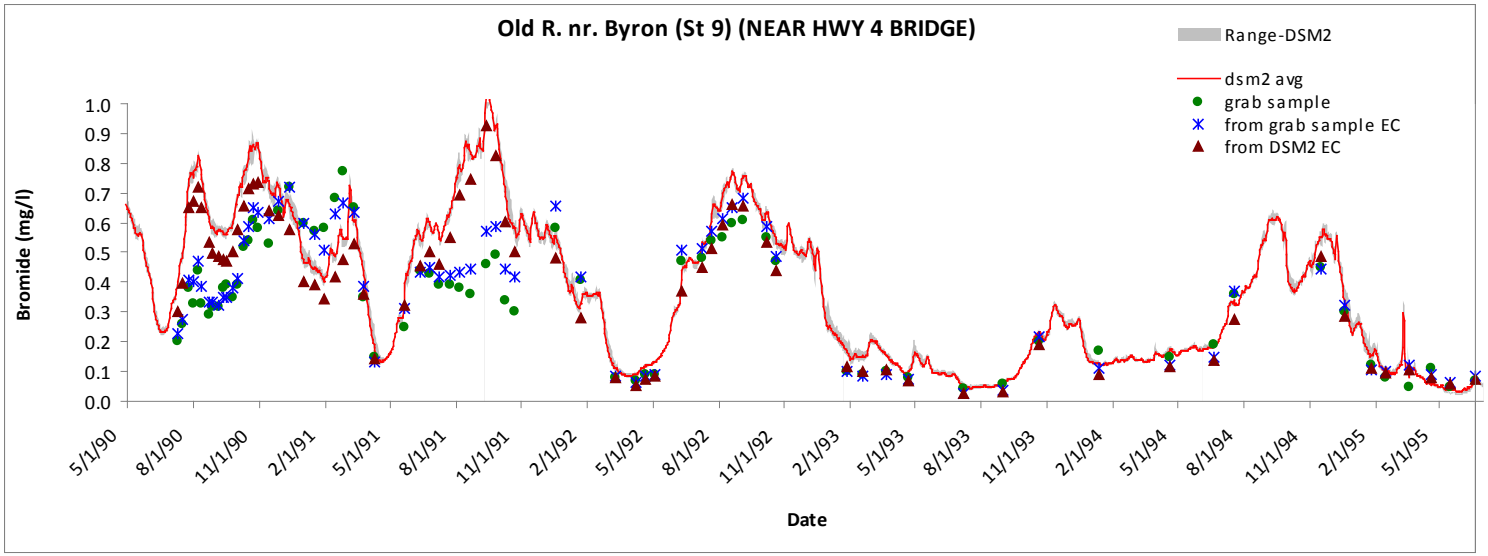

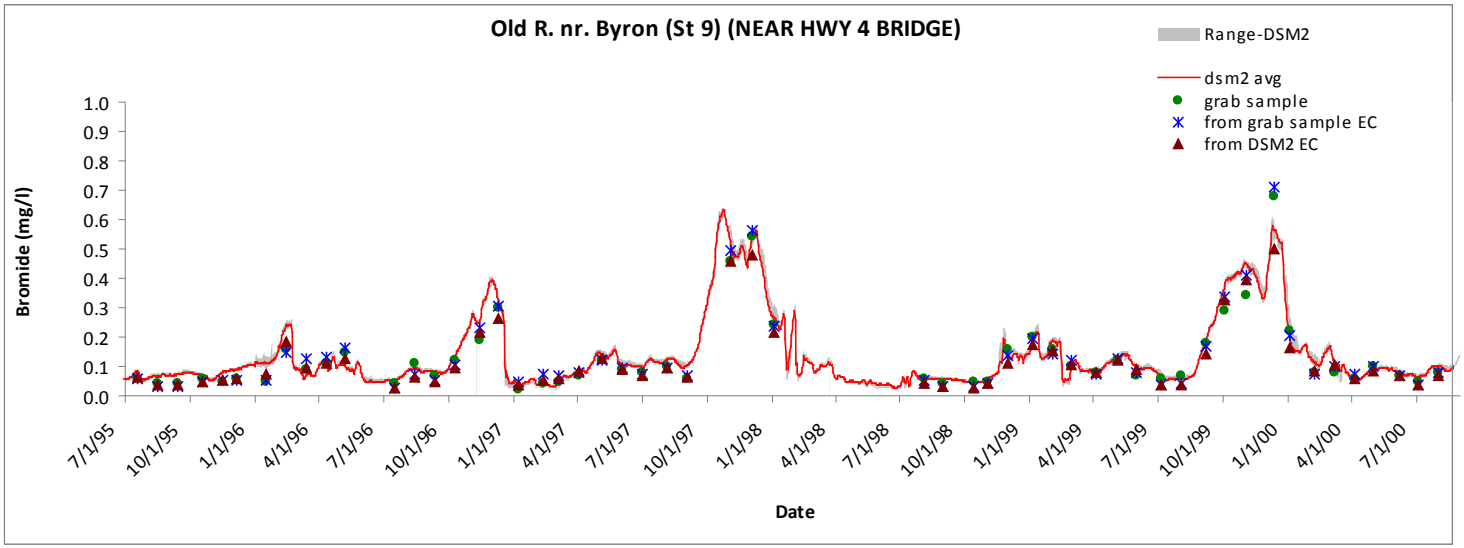

Figure 5-11 Comparison of Grab Sample Data and Calculated Bromide Concentration in Old River near Highway 4 Bridge (four figures total)

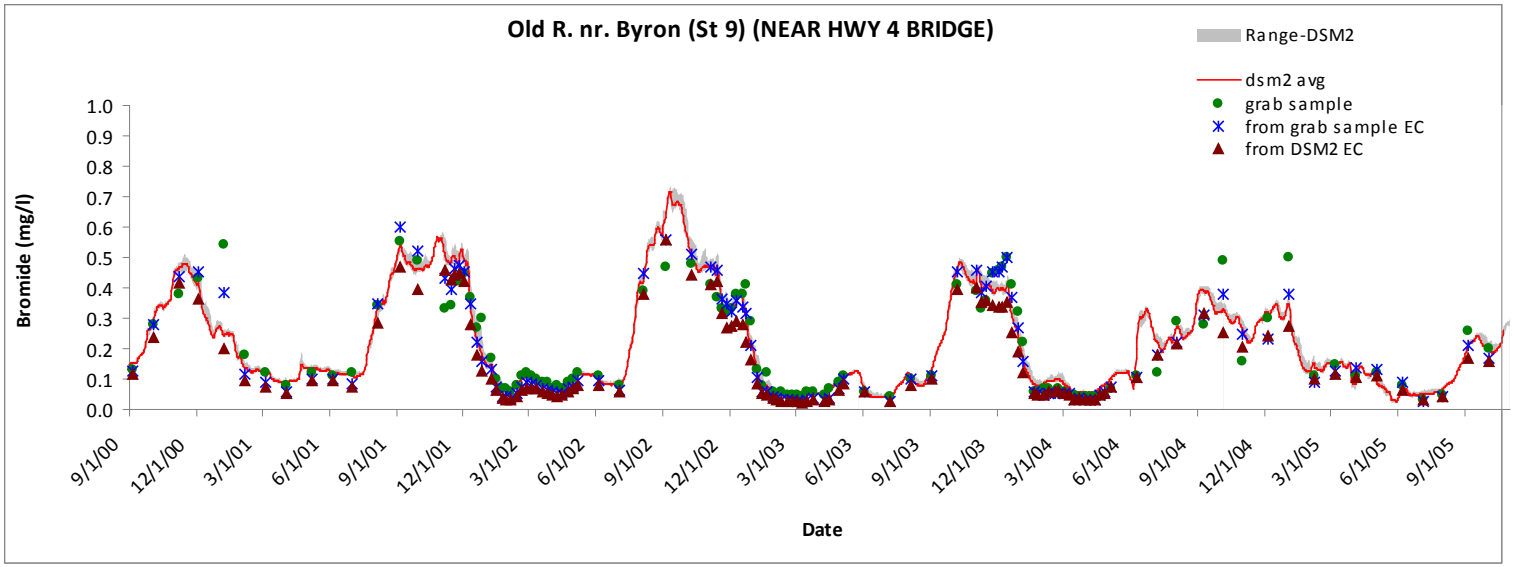

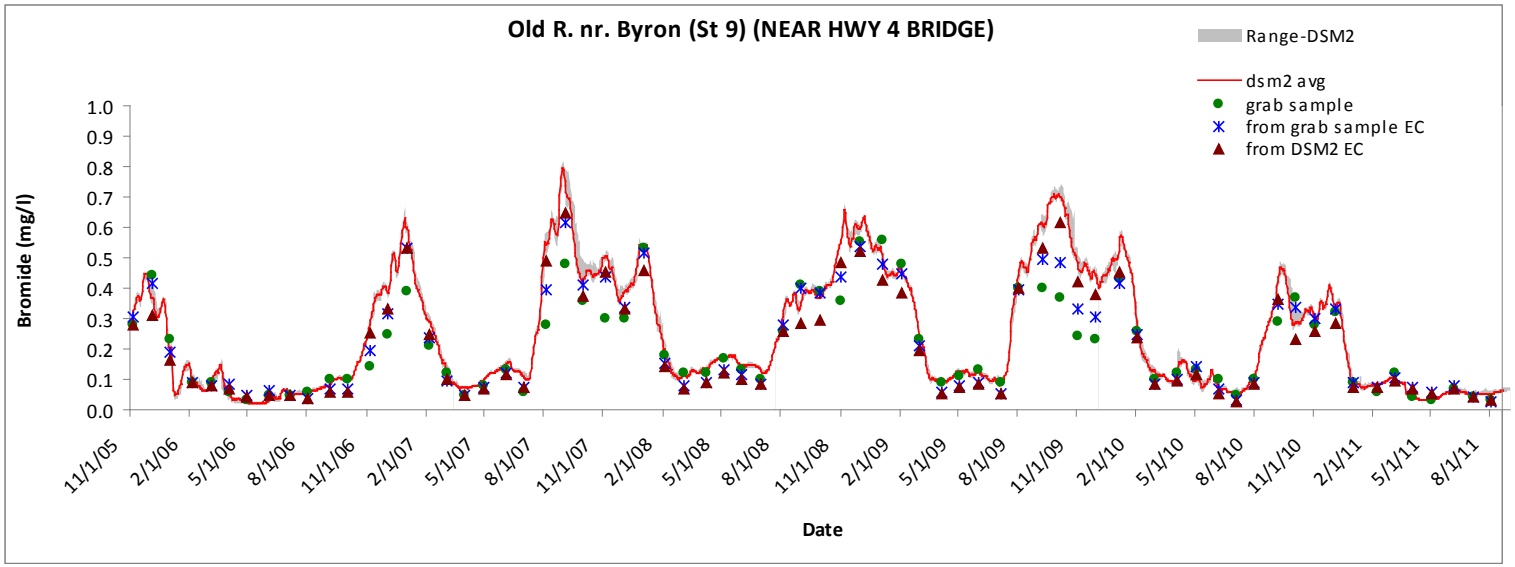

Figure 5-11 (cont'd) Comparison of Grab Sample Data and Calculated Bromide Concentration in Old River near Highway 4 Bridge

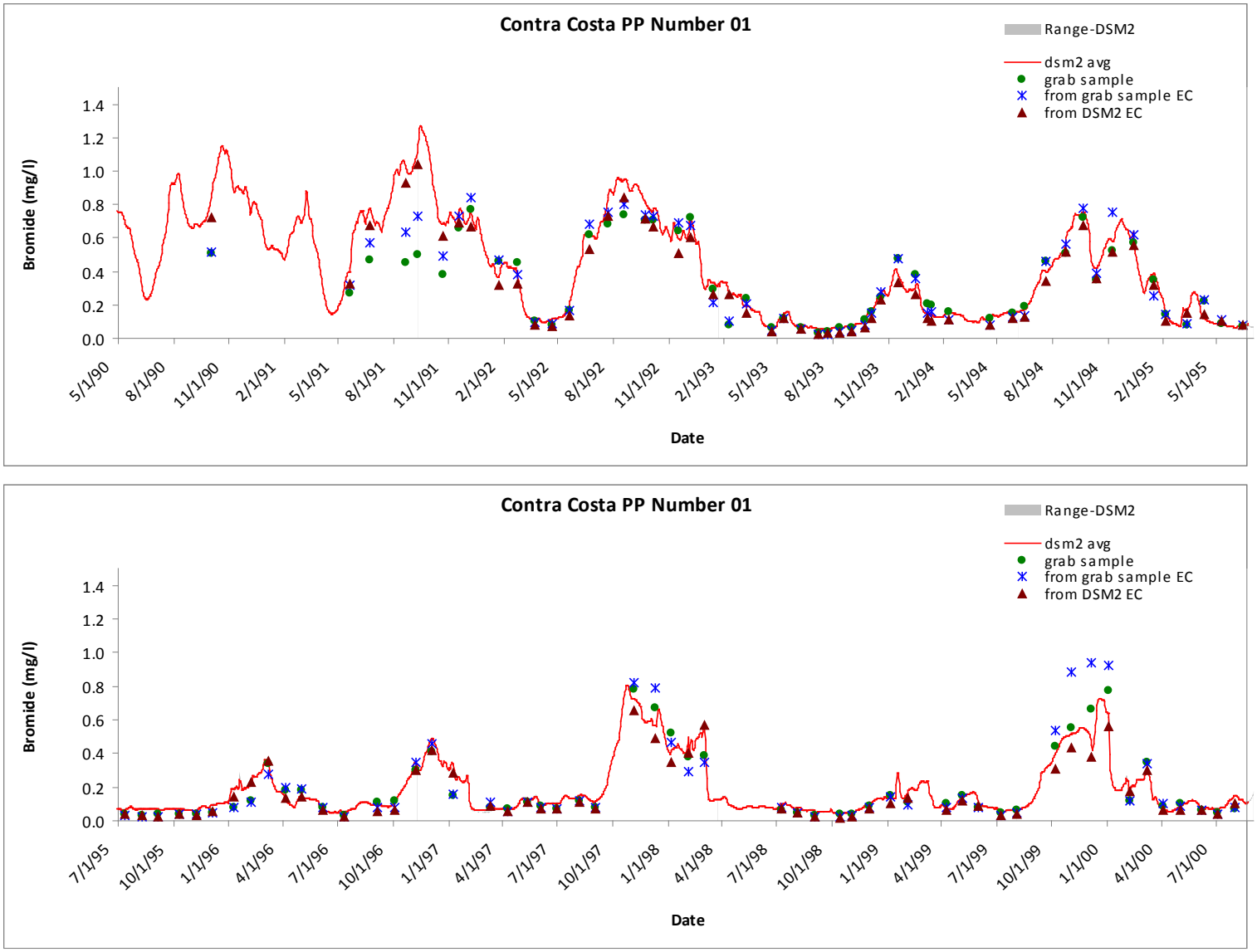

Figure 5-12 Comparison of Grab Sample Data and Calculated Bromide Concentration at Contra Costa Pumping Plant 1 (four figures total)

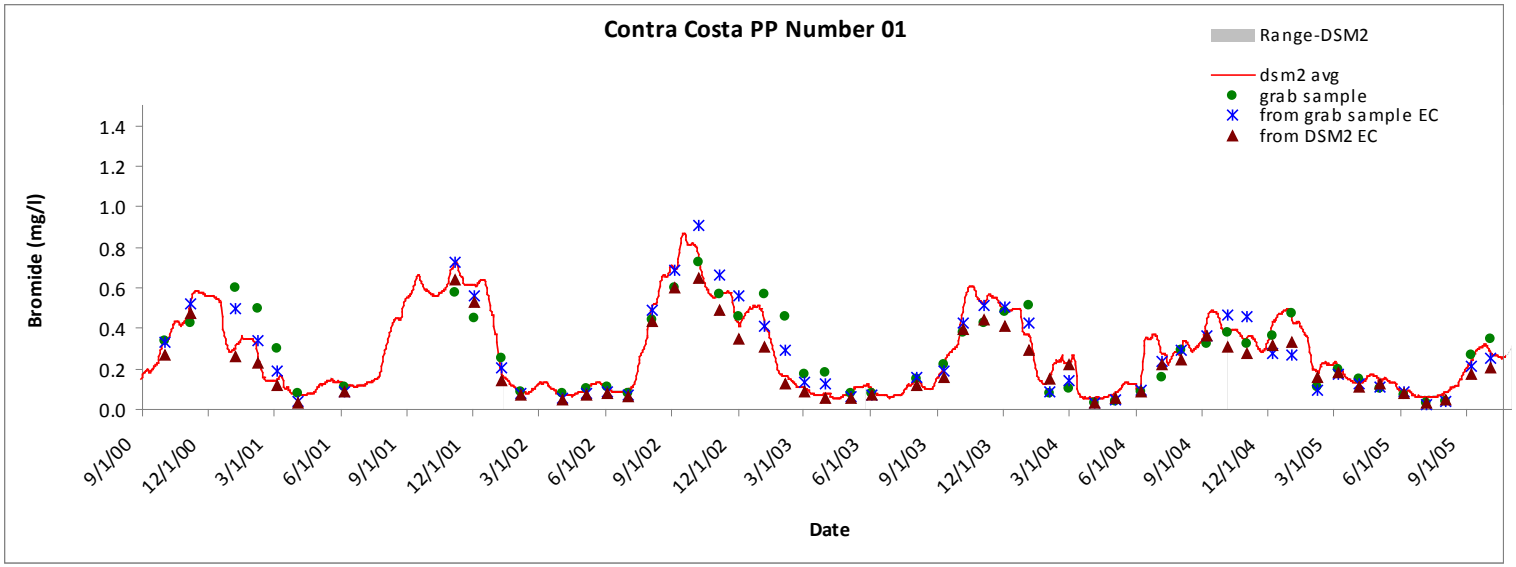

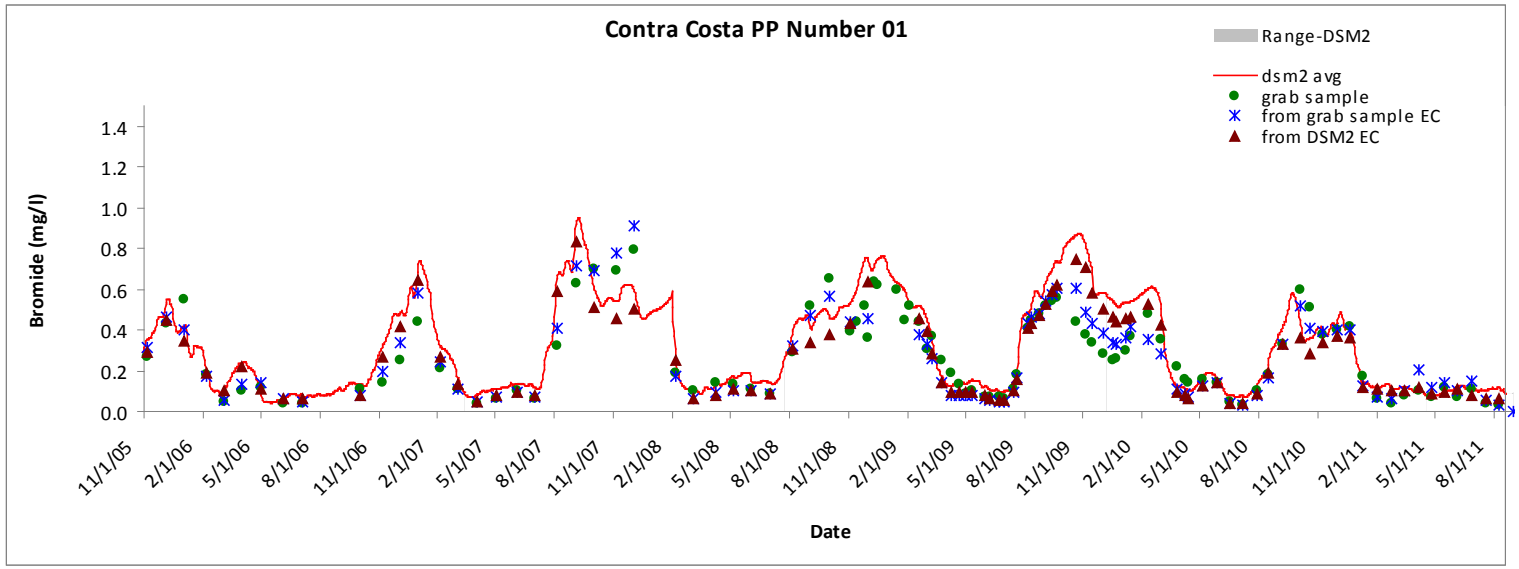

Figure 5-12 (cont'd) Comparison of Grab Sample Data and Calculated Bromide Concentration at Contra Costa Pumping Plant 1

5.6 Comparison of Performance of Different Methods in Estimating Bromide

To compare the performance of each method, the Nash–Sutcliffe model efficiency coefficient is used. It is defined as

$$E = 1 - \frac{\sum_{t=1}^{T}(Q_o^t - Q_m^t)^2}{\sum_{t=1}^{T}(Q_o^t - \overline{Q_o})^2} \quad \text{(Equation 5)}$$

where E is the Nash–Sutcliffe model efficiency coefficient; Q_o^t is observed value at time *t;* Q_m^t is model calculated value at time *t;* and $\overline{Q_o}$ is the average of the observed values.

Nash–Sutcliffe (N-S) efficiencies can range from −∞ to 1. An efficiency of 1 (E = 1) corresponds to a perfect match of estimated bromide to the observed data. An efficiency of 0 (E = 0) indicates that the model predictions are as accurate as the mean of the observed data, whereas an efficiency less than zero (E < 0) occurs when the observed mean is a better predictor than the model (Wikipedia, 2011).

Table 5-2 is a summary of the N-S efficiencies estimated from 6 methods at 17 grab sample locations. The first column shows all the stations used in this study for comparison of different methods. Column 2 lists N-S efficiencies from direct DSM2 simulation. It must be pointed out that the daily bromide values from DSM2 output were used to calculate the N-S efficiencies, but grab sample bromide concentrations are instantaneous values. So the actual N-S efficiencies for DSM2 simulation may be better than those listed in the table. Column 3 lists N-S efficiencies from direct EC ~ bromide regression. The site-specific regression did not consider the fingerprint of each source.

Column 4 lists N-S efficiencies from a regression developed in BDO in the past (Hutton, 2006) using equation (6). The regression was developed mainly for Banks Pumping Plant. However, in this memorandum, it was also used to calculate N-S efficiencies at other locations to see how it does at locations other than Banks Pumping Plant. The method consists of 2 expressions for 2 cases, corresponding to the condition that Martinez volumetric fingerprint at a location is more or less than 0.4%, the following are the 2 expressions,

$$Br = \begin{cases} -0.0364 + 0.0004 * EC & Vol_{MTZ} < 0.4 \\ -0.1117 + 0.0000827 * EC & Vol_{MTZ} > 0.4 \end{cases} \quad \text{(Equation 6)}$$

In columns 5, 6, and 7 are N-S efficiencies from multiple linear regressions that use EC fingerprint and grab sample EC. The difference is that different data sets were used in regression. For site-specific regression, only grab sample data at a location was used to get regression coefficients. For regional regression, grab sample data at all locations within a region was used to get regression coefficients for that region; and the same coefficients were used for all locations within the region. For Delta-wide regression, all grab sample data at locations within the Delta was used to get regression coefficients; and the same coefficients were used for all locations.

It is true that the N-S efficiencies for direct bromide DSM2 simulation may be underestimated because daily values of bromide calculated by DSM2 were compared against grab sample bromide data. But it is not expected that N-S efficiencies for direct DSM2 bromide simulation at Banks and Jones Pumping Plants are greater than 0.8 because the N-S efficiencies for direct EC simulation at Banks and Jones Pumping Plants are 0.72 and 0.76 respectively, based on historical EC simulation from January 1, 1990,

to August 31, 2011. It is assumed that the N-S efficiencies for bromide simulation will be quite similar to the N-S efficiencies for EC simulation.

As expected, the site-specific regression did the best for all locations. The direct EC-bromide regression did very well for some locations, but not so well for other locations. Surprisingly, the previous BDO regression did well for a lot of locations including Banks Pumping Plant, Contra Costa Pumping Plant, and Old River at Bacon Island. Without doubt, Delta-wide regression did better than direct EC ~ bromide regression, especially for such locations as Banks Pumping Plant, Jones Pumping Plant, and Contra Costa Pumping Plant. The regional regression performed almost as well as the site-specific regression, but can be used more conveniently.

Table 5-2 Comparison of Performance of Different Methods in Estimating Bromide

Grab sample locations	Direct EC-Br Regression (2)	Previous BDO Regression (3)	Site-specific Regression (4)	Regional Regression (5)	Delta-wide Regression (6)
SJRJERSEY	0.89	0.80	0.92	0.91	0.87
MALLARD	0.97	0.80	0.96	0.96	0.96
BANKS	0.87	0.94	0.95	0.95	0.93
DMC	0.79	0.77	0.91	0.91	0.86
MRIVBACON	0.75	0.88	0.92	0.91	0.87
MIDDLER	0.83	0.94	0.93	0.93	0.92
GRANTOLD	0.71	0.33	0.84	0.83	0.77
FALSETIP-WEBB	0.94	0.85	0.95	0.95	0.90
NORTHCAN	0.85	0.89	0.92	0.91	0.89
NVICWOOD	0.90	0.93	0.94	0.92	0.93
OLDRIVBACISL	0.96	0.97	0.98	0.98	0.95
ROCKSL	0.95	0.91	0.97	0.97	0.93
SANDMOUND	0.95	0.90	0.96	0.96	0.87
SANTAFEBACON	0.92	0.92	0.94	0.93	0.93
STATION09	0.94	0.97	0.97	0.97	0.94
STATION04B	0.95	0.89	0.97	0.96	0.93
CONCOSPP1	0.85	0.92	0.95	0.94	0.90

Table note: Numbers 2, 3, 4, 5, and 6 in column heads refer to method numbers as shown in Table 5-1. A number shown in gray box is the highest N-S value for that grab sample location.

5.7 Conclusions

Based on the comparison of grab sample data, modeling results, and calculated bromide concentrations, the following conclusions can be made:

1. BDO confirmed MWH's conclusion that the DSM2 model performs equally well in simulating bromide concentrations in the Delta as it does in modeling EC.
2. Delta-wide multiple linear regression based on EC fingerprints and DSM2-calculated EC performs as well as direct bromide simulation using DSM2.
3. Overall, Delta-wide multiple linear regression based on EC fingerprints and grab sample EC performs better than direct bromide simulation using DSM2.
4. Site-specific multiple linear regression performs the best at all locations. However, this approach cannot be used for locations without both measured bromide and EC data.
5. Regional multiple linear regression has close performance as site-specific regression, and can be used for locations without measured bromide data.
6. Multi-variable regression can be used to fingerprint bromide from each source.

5.8 References

California Department of Water Resources. (1995). *Representative Delta Island Return Flow Quality for Use in DSM2.* Memorandum Report, Sacramento.

Hutton, P. (2006). Validation of DSM2 Volumetric Fingerprints Using Grab Sample Mineral Data. *California Water and Environmental Modeling Forum (CWEMF) Annual Meeting.*

Montgomery Watson Harza. (2011). *Validation of DSM2 QUAL for Simulation of Various Cations and Anions.* Prepared for the Metropolitan Water District of Southern California.

Suits, B. (2001, May 29). Relationships between EC, chloride, and bromide at Delta export locations. *Office memo to Paul Hutton, Availability: www.baydeltaoffice.water.ca.gov/modeling/deltamodeling/models/misc/EC_chloride_bromide_05_29_01.pdf*, 8 pages. California Department of Water Resources.

Suits, B. (2002, June). Calibrating DSM2-QUAL Dispersion Factors to Practical Salinity (Chapter 6). In *Methodology for Flow and Salinity Estimates in the Sacramento-San Joaquin Delta and Suisun Marsh, 23rd Annual Progress Report.* Sacramento: California Department of Water Resources.

Suits, B. (2002, June). Relationships between Delta Water Quality Constituents as Derived from Grab Samples (Chapter 5). In *Methodology for Flow and Salinity Estimates in the Sacramento-San Joaquin Delta and Suisun Marsh, 23rd Annual Progress Report.* Sacramento: California Department of Water Resources.

Wikipedia. (2011, April 5). Nash–Sutcliffe model efficiency coefficient. Retrieved 2012, from http://en.wikipedia.org/wiki/Nash%E2%80%93Sutcliffe_model_efficiency_coefficient

Methodology for Flow and Salinity Estimates in the Sacramento-San Joaquin Delta and Suisun Marsh

33rd Annual Progress Report
June 2012

Chapter 6
A Continuous Surface Elevation Map for Modeling

Authors: Rueen-Fang Wang and Eli Ateljevich
Delta Modeling Section
Bay-Delta Office
California Department of Water Resources

Page left blank for two-sided printing

Contents

Figures

Page left blank for two-sided printing

6 A Continuous Surface Elevation Map for Modeling

6.1 Introduction

Bed elevation is an important input to any hydrodynamics model, and the Delta Modeling Section has maintained a database of bathymetry soundings and levee surveys for decades. In recent years, new data have become available; technology has shifted to very dense multibeam sonar soundings; and the demands on accuracy have increased due to increasingly common multidimensional modeling of the region. In some locations, such as near the Burlington Northern Santa Fe (BNSF) Railway Bridge shown in Figure 6-1, newer elevation data differ from earlier elevation models by as much as 50% to 100%. The differences can be due to evolution of the bed, improved sounding, and georeferencing techniques, or denser coverage of areas that were previously interpolated.

This chapter documents the development of an elevation data set for multidimensional modeling developed under the REALM project, synthesizing LiDAR, single- and multibeam sonar soundings and surveys and integrating them with existing integrated maps that themselves were collated from multiple sources.

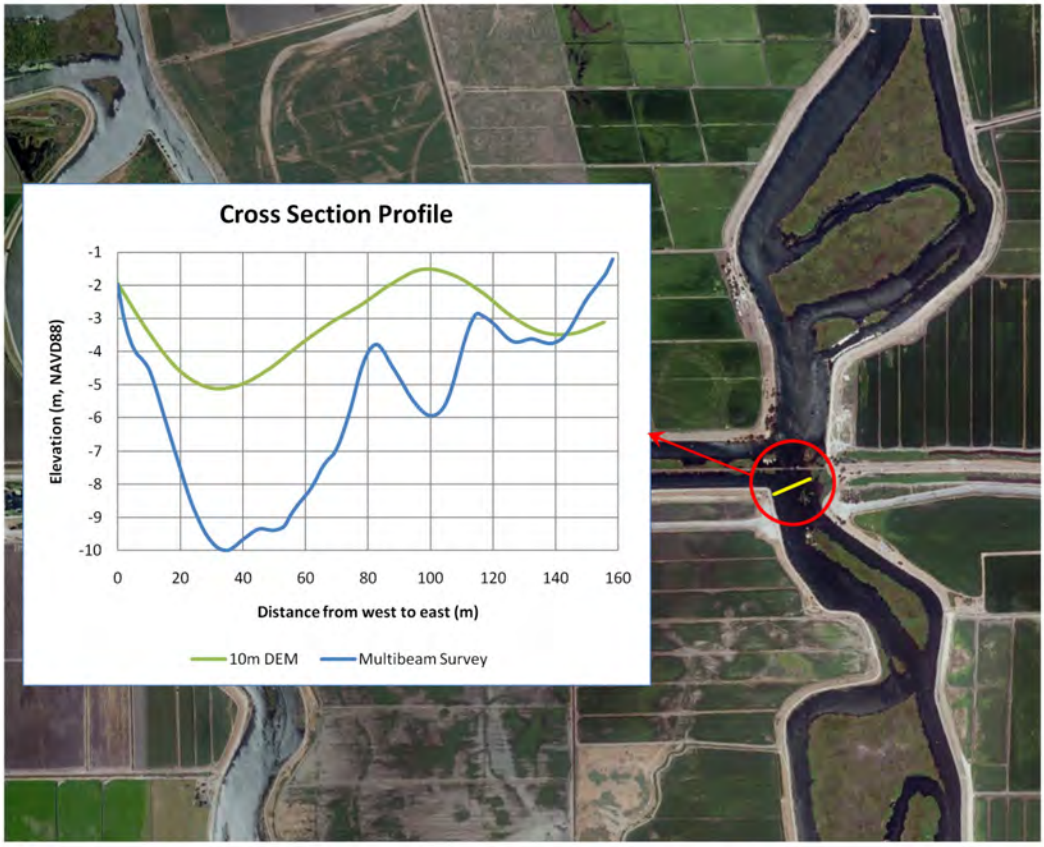

Figure note: DWR Central District shows the magnitude of the discrepancy between older (green, 10 m Digital Elevation Map [DEM]) elevations data and more recent high resolution (blue, Multibeam Survey) soundings. The region is near a bridge abutment, but the magnitude of discrepancy is typical of the stretch of Middle River for several kilometers south.

Figure 6-1 Cross Section Profile near BNSF Railway Bridge

The result is a continuous surface—terrestrial and water—in meters using the NAVD88 vertical datum. The initial release of this map was in the form of a 10 m Digital Elevation Map (DEM) for the entire Bay-Delta and parts of the coast to the Farallones, supplemented by a 2 m model of the South Delta in a region where the channel features are poorly resolved at 10 m. These data are raster data sets, meaning they are defined on a rectangular mesh with square cells, some of which may be declared missing. Raster data are compatible with data formats used for modeling and allow a greater variety of Geographical Information System (GIS) analysis. However, in regions where high resolution LiDAR and multibeam coincide, we are moving some of our analysis to ArcGIS Terrain data sets. A Terrain is a collection of dense points, lines, and polygons. It is a form of data that makes good use of disparate data and is efficient for huge clusters of points. However, it is a proprietary data structure not directly usable by hydrodynamic models.

One requirement of the project is to always have a product and to release updates as frequently as 2 times per year. During each release, the products are essentially rebuilt from the base maps, adding newer data sets on top of the old in a systematic way. Users of the map are urged to join an issue tracking system, as the faults they find are addressed in each iteration.

The remainder of this chapter outlines the data sources we use for the project, the method of preparation, and challenges involving both data and modeling applications. Only modest attention is given to a traditional subject: interpolation. In the course of the project, we have made use of promising, robust interpolators to fill gaps when there is supporting data (hand soundings and digitized photos). However, we are concerned about spending too much effort near the point of decreasing returns. The newer bathymetric and LiDAR data present a dichotomy between data that is either very dense or is entirely missing, and it is hard to increase the information content in a gap under those circumstances.

6.2 Data Sources

The work presented here is based largely on elevation models, which themselves were stitched together from multiple sources. Figure 6-2 shows the core data, comprising mainly DWR LiDAR (Dudas, 2010), the Foxgrover 10 m bathymetry in the Delta (Foxgrover, Smith, & Jaffe, 2003) and the NOAA San Francisco Bay DEM (Carignan, et al., 2010). Some outlying regions are covered only by the USGS National Elevation Dataset (http://ned.usgs.gov/)—the NED data are less accurate and congruent with the other data, but are only employed in places that are fairly remote from tidal water bodies. The figure also shows additional point data sets that were incorporated in Version 1. Most are single beam soundings (DWR, Towill, Inc. 2009, and CSDP bathymetry data, online), but some are hand digitized contour maps (Smith). The DEM for the San Joaquin River near Vernalis is created based on the 1988 COE survey (CSDP bathymetry data, online). The transects for this survey were closely spaced and realistic; but due to morphological changes, the data had to be manipulated ("rubbersheeted") to coincide with the recent channel bed. The 2 m South Delta also contains a modest number of synthetic points estimated along channel centerlines. This 2 m effort was undertaken not so much because the data at the time justified it in all places, but rather because we believe that certain locations in the South Delta are too narrow to be represented at 10 m. Resolution of elevation maps for modeling is discussed later.

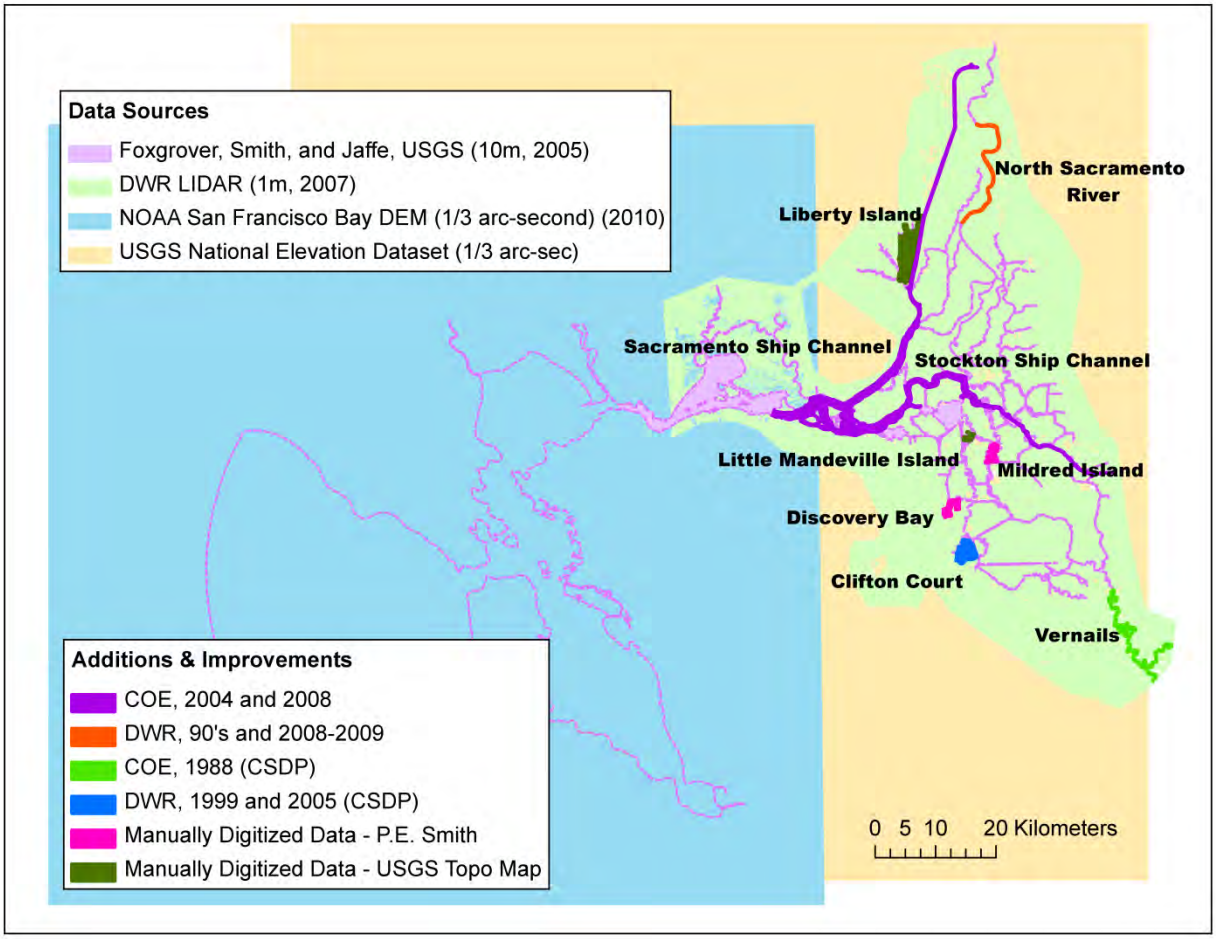

Figure note: References for data sources in version 1.0 DEM:

Foxgrover, Smith, and Jaffe, USGS (10m, 2005)	Foxgrover, Smith, & Jaffe, 2003
DWR LiDAR (1m, 2007)	Dudas, 2010
NOAA San Francisco Bay DEM (1/3 arc-second) (2010)	Carignan, et al., 2010
USGS National Elevation Dataset (1/3 arc-sec)	http://ned.usgs.gov/
COE, 2004 and 2008	Towill, Inc., 2009
DWR, 90's and 2008-2009	DWR
COE, 1988 (CSDP)	CSDP bathymetry data (online)
DWR, 1999 and 2005 (CSDP)	CSDP bathymetry data (online)
Manually Digitized Data - P.E. Smith	Smith
Manually Digitized Data - USGS Topo Map	http://services.arcgisonline.com/arcgis/services

Figure 6-2 Data Sources for Version 1.0 of the 10 m DEM

Version 2 of the elevation model is being prepared and is slated for release in late summer 2012. For the new version, a number of additional high resolution data sets have been identified and are being vetted for inclusion. Figure 6-3 shows a map of these data sets. The updates are being prepared as a set of discrete 2 m "patches" on the base map. Most of the data for Version 2 are multibeam or exceptionally high resolution single beam observations.

Finally, we expect a round of enhancements to be released in each of our base data sets. The USGS is currently creating a 2 m DEM including both terrestrial and soundings data. DWR is creating an

enhanced release of the terrestrial Delta LiDAR data set that solves some interpolation and missing data issues with the original release.

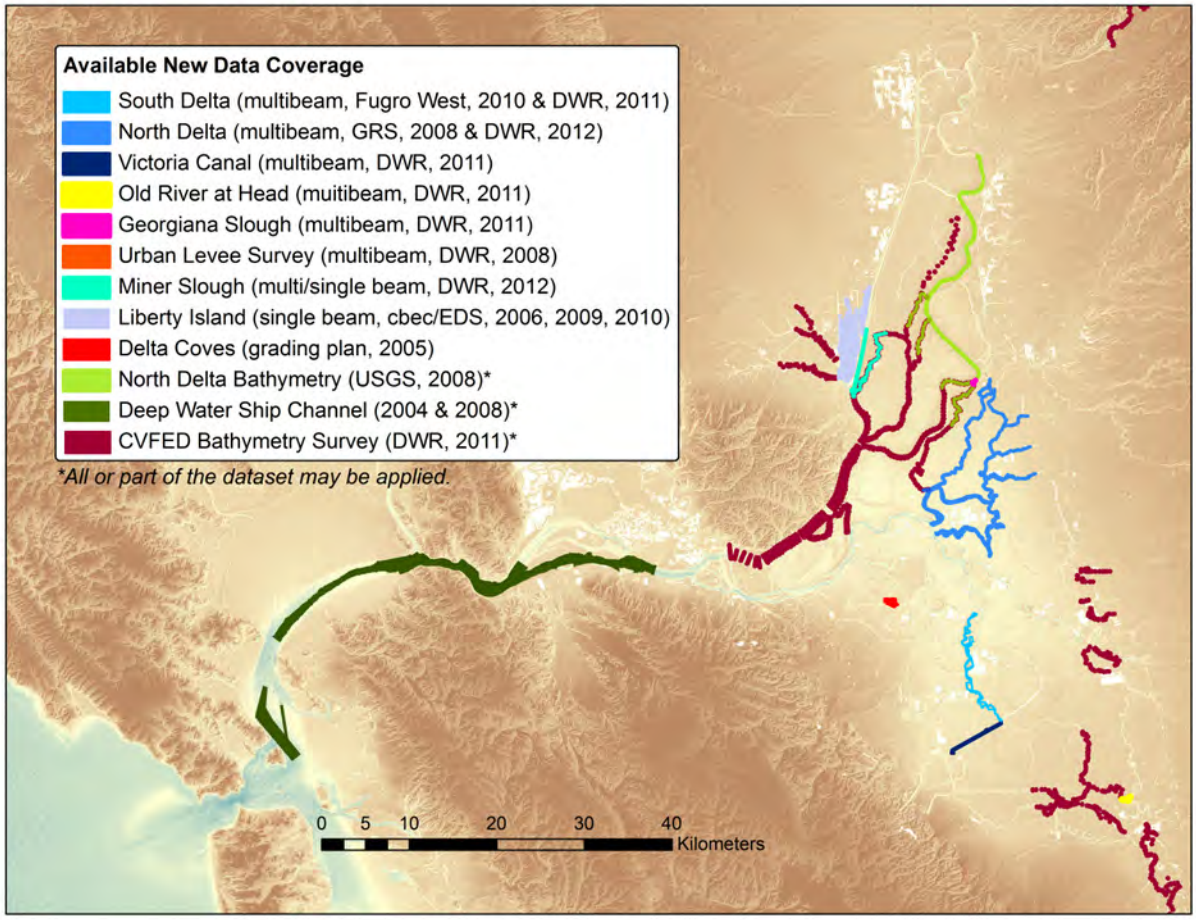

Figure note: References for the available new data:

South Delta (multibeam, Fugro West, 2010 & DWR, 2011)	(Mayr, 2011), (Fugro West, Inc., 2008)
North Delta (multibeam, GRS, 2008 & DWR, 2012)	(GRS, 2008), Mayr, 2011-2010
Victoria Canal (multibeam, DWR, 2011)	(Mayr, 2011)
Old River at Head (multibeam, DWR, 2011)	Mayr, 2011-2012
Georgiana Slough (multibeam, DWR, 2011)	Mayr, 2011-2012
Urban Levee Survey (multibeam, DWR, 2008)	(Fugro West, Inc., 2008)
Miner Slough (multi/single beam, DWR, 2012)	Mayr, 2011-2012
Liberty Island (single beam, cbec/EDS, 2006, 2009, 2010)	(EDS, 2006), (EDS, 2009), (Campbell, 2012)
Delta Coves (grading plan, 2005)	(Ruggeri-Jensen-Azar & Associates, 2005)
North Delta Bathymetry (USGS, 2008)	(USGS, 2008)
Deep Water Ship Channel (2004, 2008)	(Towill, Inc., 2009)
CVFED Bathymetry Survey (DWR, 2011)	(HDR, 2011); (PBS&J, An Atkins Company, 2010)

Figure 6-3 Data Sources Being Added for Version 2.0 of Elevation Model

6.3 Methodology Overview

Before outlining the methodology of preparation, it is useful to reiterate the end products. We produce a 10 m DEM everywhere plus 2 m standalone point or raster models of special focus regions such as the South Delta. The finer DEM is obtained from a terrain model. In the process of preparing the 2 m patch, the background 10 m model is improved and edge-matched to the 2 m data.

6.4 10 m Base Map

The method for producing the 10 m map is shown in Figure 6-4. The main steps are discussed below.

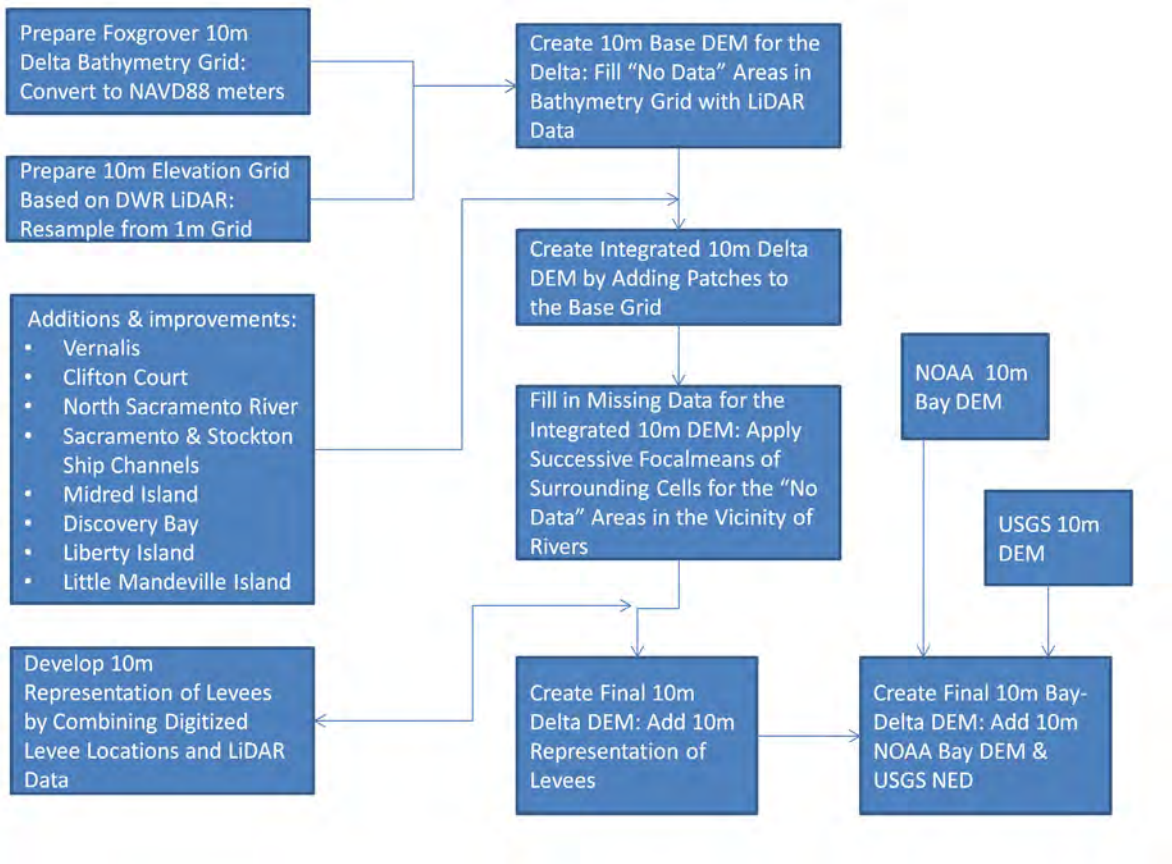

Figure 6-4 Preparation of 10 m DEM

6.4.1 Prioritization of Core Data and Supplemental Data Sets

To reconcile the base data, LiDAR is resampled or interpolated to a common 10 m grid, the bathymetry and LiDAR are overlain, and overlapping regions are determined by priority. In Version 1, we prioritized the bathymetry over terrestrial data; and we continue to do this for our 2 m maps. But in Version 2, we are prioritizing terrestrial data at 10 m.

The additional low-medium resolution data listed in Figure 6-2 then nested within the 10 m grid. In Version 1, the ArcGIS topo-raster was used in most places to complete a raster where point data were sufficiently dense. Topo-raster is a thin plate spline with enforcement of contours and drainage directions frequently used with hydrologic features.

6.4.2 Filling at 10 m and Missing Values

Both LiDAR and our base bathymetry maps contain missing data; and because neither captures the shoreline reliably, there is a gap between them. Where gaps and missing values can be appropriately filled, successive applications of kernel averages (*focal means* in ArcGIS) were used to fill holes from the edges in—each new kernel average would fill one new cell working toward the interior of the "hole" in the data, a technique we are currently reconsidering. Missing regions remote from water were left missing. No large regions in the Delta were left without some form of estimate, mostly because the Foxgrover 10 m DEM itself contains a lot of estimated data and fill values which we left intact. In some cases with missing LiDAR returns, we had little basis for guesses besides what we could see from aerial photos.

Most remaining missing values are on land, and some are behind levees. Although it is certainly not an infallible generalization, users who need to fill the remaining missing data in our model should use a mild dry elevation above the threshold of sea level rise (we often use 8 m, NAVD).

6.4.3 Transitions between Data Sources

Except for the LiDAR, data sources informing the 10 m map are not highly accurate and were collected over the course of decades. There is no guarantee of smoothness between them, and discontinuities occasionally occur at transitions. We fixed the transitions by hand, using local kernel averages to smooth the map. The transition zone over which we smooth is approximately 100 m.

6.4.4 Orthogonal Levee Reinforcement

One of the hazards of an integrated 10 m land-water elevation model is that the width of a levee crest is slightly under-resolved. And some aspect of the sampling or data processing can cause a low-lying raster cell to develop along a narrow levee crest, creating a false numerical "leak" in the elevation model between channels and islands. Such a numerical leak is shown in Figure 6-5 and is more common when the levee runs at an angle to the raster.

The levee refinement problem goes away when the data are finer. Levee crests are always well resolved by 2 m data. We enforce them in the 10 m model by reference to the finer data:

1. Levees are digitized into a vector (line) feature.
2. 10 m and 2 m raster cells are identified that intersect the levee.
3. The 10 m cells are set to the maximum of
   a. their own value or
   b. the elevation of the highest 2 m cell inside the 10 m cell that also intersects the levee.

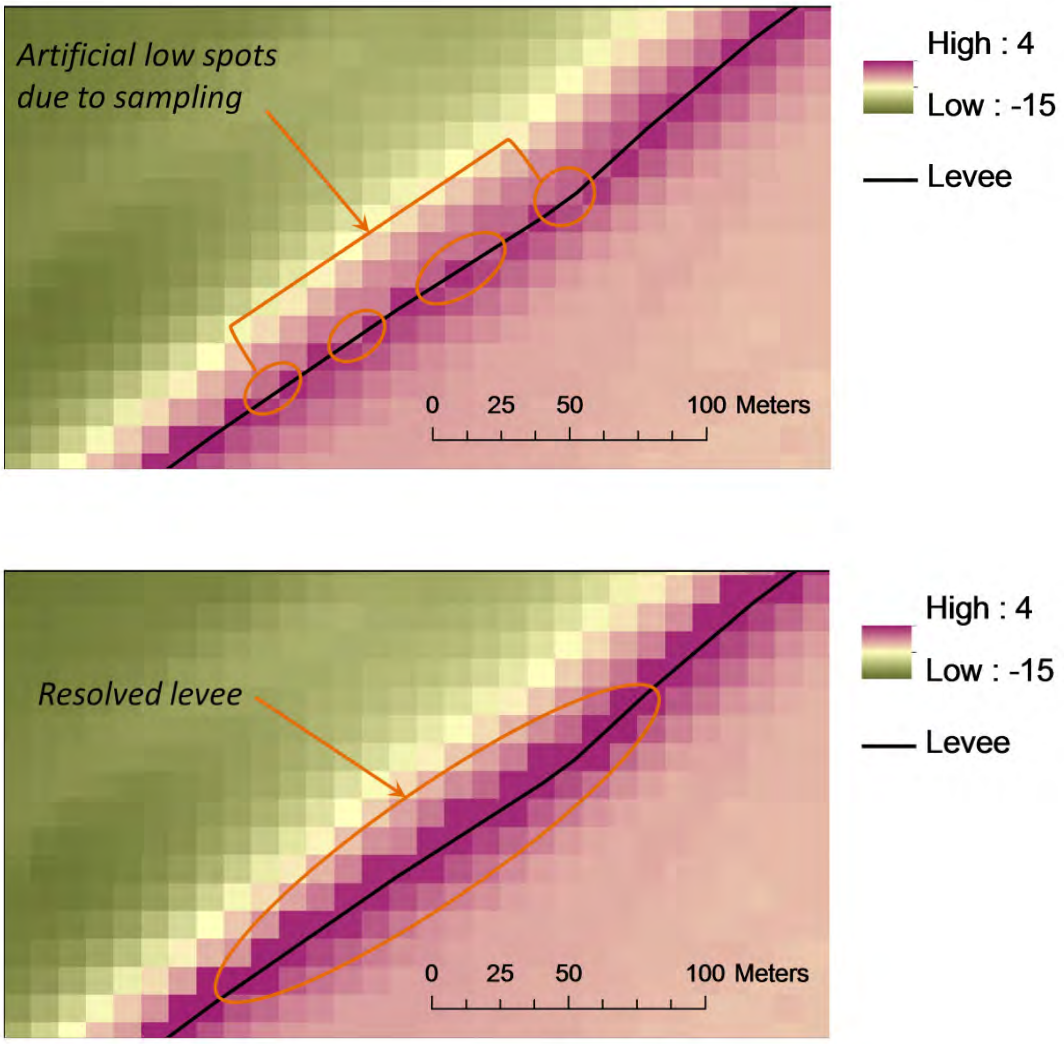

Figure note: (Top) Levees with artificial low spots in the elevation model due to coarse sampling. (Bottom) Orthogonal reinforcement of levees using finer data so that the levees do not have low spots in the elevation model.

Figure 6-5 Examples of False Numerical 'Leaks' in Levee Elevation Models

6.5 High Resolution Model

In Version 2, we have begun to introduce 2 m high resolution patches where LiDAR and dense (often multibeam) data coincide. The patches have value as standalone products, though the usefulness of data at this resolution for modeling should not go unquestioned; and we assume that users of the finer data are acquainted with the sampling issues raised at the end of the chapter.

The finer data are prepared using their own fill techniques. The nominal vertical accuracy of the soundings and terrestrial data is submeter—hence the accuracy of the 2 m patch is determined for the most point by the size and complexity of the gaps between them.

6.5.1 Gaps

The most vexing issue that arises in deriving a continuous surface model is that the land-base LiDAR and water-based soundings do not meet. The shoreline determines the tidal prism, and its width is arguably one of the most critical parameters for modeling. There is also often an abrupt change in slope near the interface between land and water, and the change is almost never observed or resolved. In channels, the region of missing data is routinely 10 to 20 m wide, but the gap can be much larger for islands with poor LiDAR returns or in shallows that are not navigable by boats collecting multibeam soundings.

Our approach is to categorize the gaps according to nature and complexity and to apply a simple and automatable method for gaps that are narrow and tractable. We have methods to treat the special cases depending on the width of the gap, the complexity of the water body, available supporting data such as hand soundings or prior collections and which data source (land or water) is causing the gap. We also prune away the hardest gaps when interpolation seems to compromise most of the benefits of updating the data.

6.5.1.1 Simple Gaps

A typical case is shown in Figure 6-6 where a narrow sliver of missing data 10 to 40 m wide separates the land and water data on either side of a small island near the junction of Victoria Canal and Old River. A 3-segment transect is indicated crossing both sides of the island where we performed a comparison of interpolants. An abrupt slope change exists on 2 of the 4 banks (this is more apparent in Figure 6-7), and trying to fit the break in slope is the only technical challenge. We have indicated the apparent location of the shore according to aerial photos. The images available to us are vague and shadowy, but we believe our guess is accurate to ± 5 to 15 m laterally.

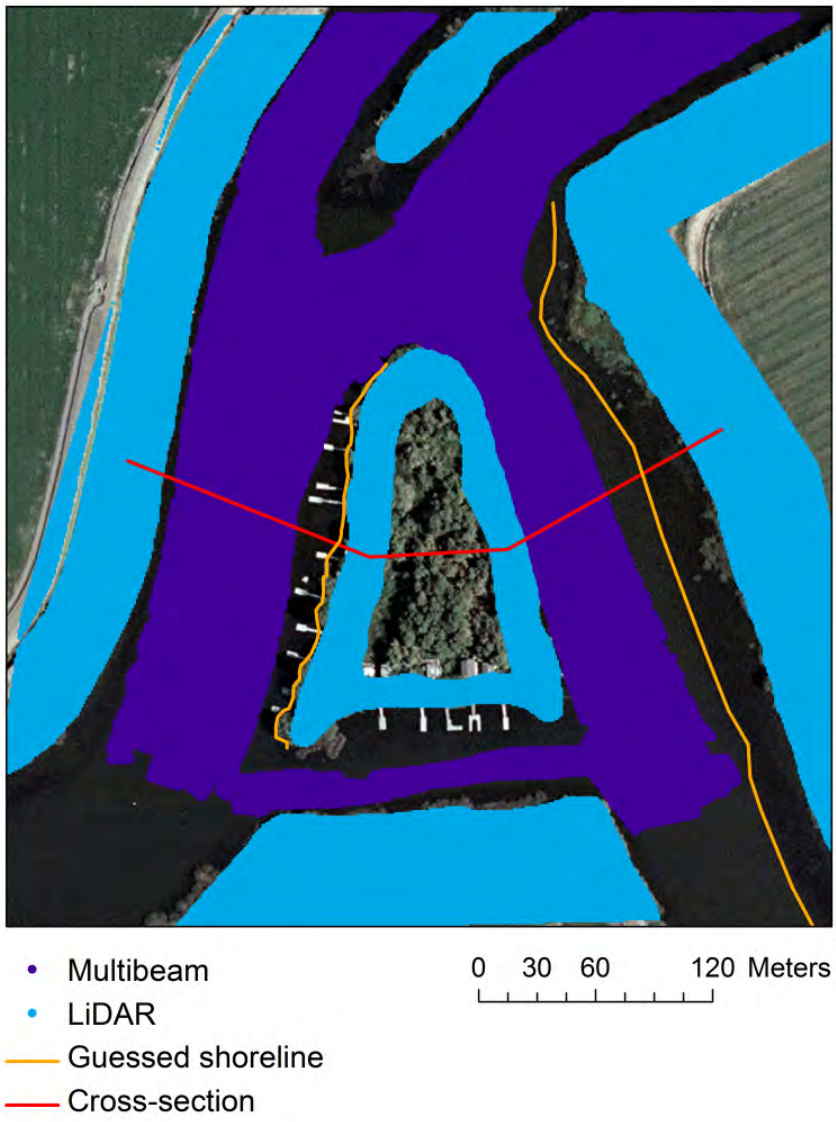

Figure note. Simple gaps between multibeam (purple) and LiDAR (blue). A bent transect used for interpolation comparisons is shown in red.

Figure 6-6 Example of Simple Gaps

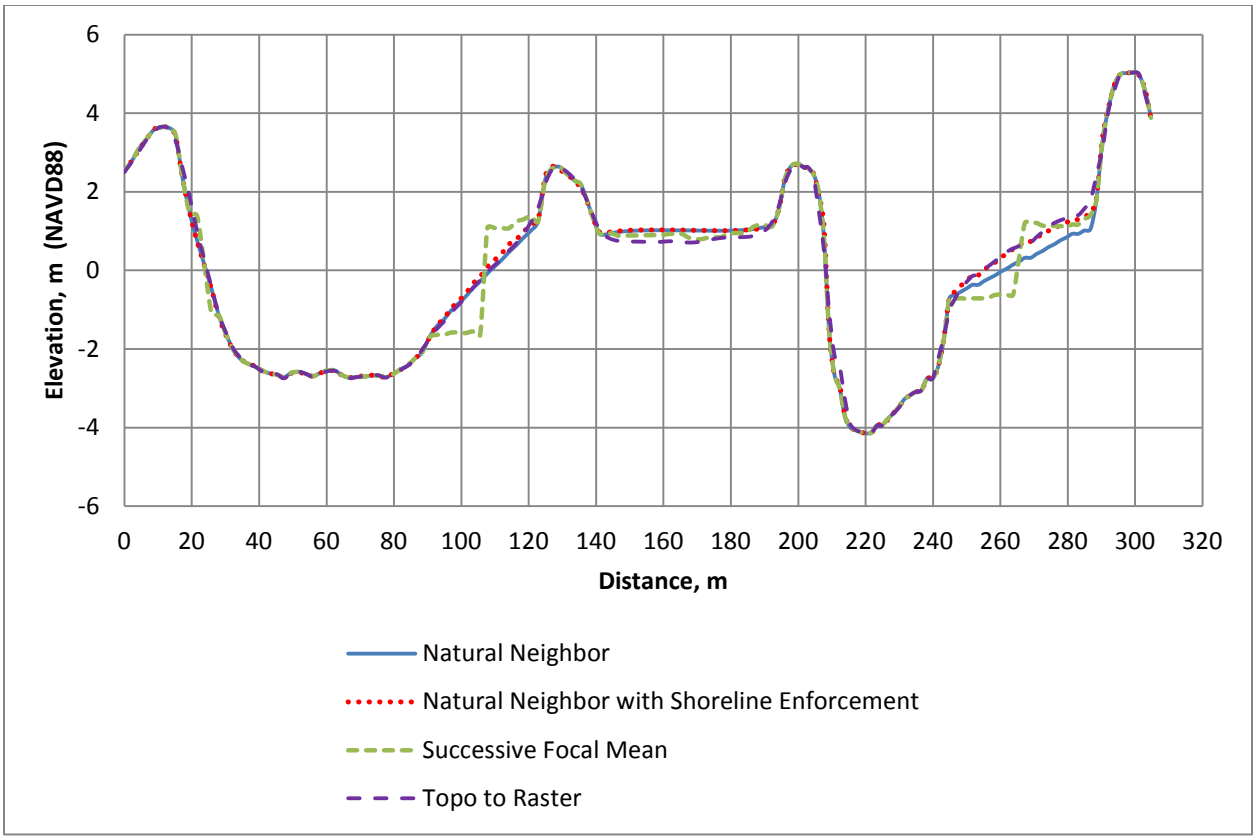

Figure 6-7 Comparison of Interpolation Techniques on Simple Gap

Figure 6-7 shows a vertical profile along the red transect in Figure 6-6 given by several different interpolants:

1. natural neighbor;
2. natural neighbor with reinforcement of a guess (0.75 m NAVD) at the shoreline from photos;
3. successive application of kernel averages (*focal means* in ArcGIS) in no data areas from the outside in;
4. thin plate splines using topo-raster, a method that handles a small amount of local anisotropy in the streamwise and cross-stream direction.

With the exception of successive focal means, there is little to distinguish the methods. The interpolants all resolve the fairly continuous shore gradients near 20 m and 210 m, and they all suffer from the missing data and ambiguous gradients at 100 m and 260 m. Methods (1) and (2) are particularly economical, as they can be applied automatically when converting data from ArcTerrain data sets to 2 m raster. Method (3) seemed successful and expedient on coarser 10 m data where the gaps were only 1 to 2 raster cells wide. It produces a discontinuity in the middle of the gap that tends to force inundated area to a medium value, but it also looks odd at higher resolutions. As with most thin plate and many other families of interpolants, method (4) is known to work well near data that are well balanced in resolution—where the smallest and largest gaps between data are not very different. This assumption is violated here—but perhaps more important to us, topo-raster is designed for smaller data structures and requires more processing for dense terrain data.

6.5.1.2 Missed Returns on Islands

One of the most common large-gap cases occurs when berms and islands go entirely or partially missing in the LiDAR returns. This is common in split channels such as Victoria Canal, and as in the previous example we assume the slope of the bathymetry gives no accurate indication of the slope of the land. In this case our goal is to plausibly fill the water portion and set the island to a missing value that we hope the user will fill using a mild "dry" value. To achieve this result, we digitize the shoreline as a (hard) line feature or breakline in our Terrain model and assign it a locally average elevation—the guess at which may be aided by any patches of non-missing LiDAR. In Figure 6-8, the perimeter of the island is delineated by a polygon—the island itself had no LiDAR returns.

Figure 6-8 Delineation of an Inhabited Island Using Bounds of a Polygon as a Hard Constraint

For our assumed shoreline, we generally choose a value that represents a locally near-mean tidal surface to represent the digitized shore. For instance in the South Delta, this might be 1.0 to 1.5 m NAVD88—the number is based on an informal analysis. Because the enforced shoreline is assigned based on photos taken at an unknown point in the tide cycle, the absolute accuracy of this method at the shore can never be better than the tidal amplitude, or about ± 0.5 to1.0 m. However, the approximation has good qualitative properties: The slope will be accurate (near zero) along the shore,

and the inundated area around small islands is more correct. Figure 6-9 shows how useful island enforcement is in preserving inundated area—the (blue solid) unenforced case simply interpolates from bathymetry to LiDAR, inundating a small community and overestimating the extent of the tidal prism by a large amount.

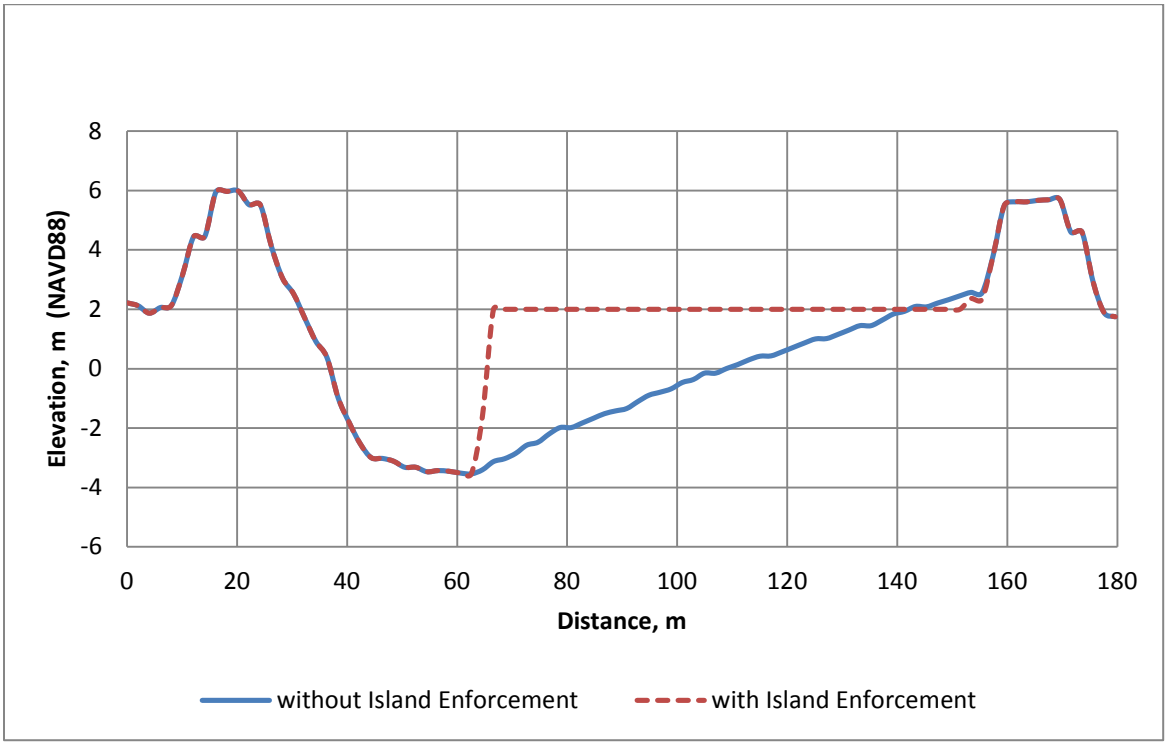

Figure 6-9 Cross Section Profiles with and without Island Enforcement

6.5.1.3 Complex Shallows

A catch-all category for regions that interpolate poorly filled, complex gaps often occur at the fringes of a multibeam collection or in regions where the multibeam collection misses impassible shallows. The issue often coincides with berms and complex geometry around small islands, in which case the LiDAR returns can be missing as well. Our goal in this case is to plausibly fill the water portion of the data and to fill the land if it is adequately represented by LiDAR returns. Whether we are able do this accurately enough to salvage or justify a map of the region in 2 m resolution depends on the supporting data—lacking that, we prefer to trim the difficult regions.

Figure 6-10 shows a hydraulically important junction near the BNSF railway crossing on Middle River, which flows north-south from the top to the bottom of the figure. To the west (left in Figure 6-10), the island supporting the railroad is missing LiDAR returns and was treated using the island breakline method from the previous section. To the east, numerous shallow islands have virtually no soundings between them. In this case, the importance of the rest of the data set prompted us to include the new data—but the islands are completely lost except when we use laborious techniques (Wood, Bravington, & Hedley, Soap film smoothing, 2008). And even then, they are not well resolved. To get any sort of reasonable estimate of inundated area, we will need to resample around the islands in the eastern part of the figure.

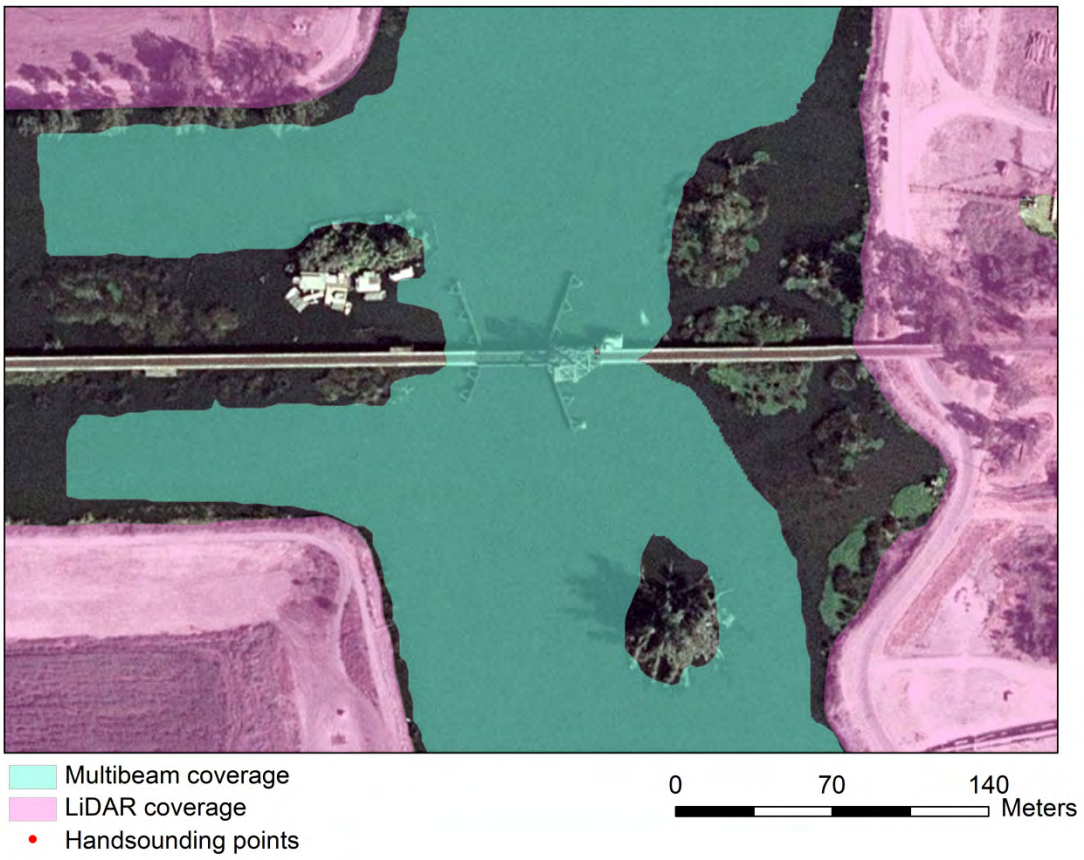

Figure note: The gap in the west side of the figure is due to an island with no LiDAR returns. The gap in the east is more complex, involving shallows, small islands, and structures. In this case, there were few recent hand soundings to support interpolation near the islands.

Figure 6-10 Complex Shallows near BNSF Railroad Bridge Crossing Middle River near Bullfrog Marina

The horseshoe bend in Figure 6-11 is less complex than the railway crossing, but some of it is still too complex and undersampled for out-of-the-box *terrain* interpolation. The region has more auxiliary data than the previous example, including hand soundings and a digitized estimate of the shoreline.

Figure 6-12 shows the improvement in drawing a cross section that can be expected from including supporting data, particularly near the tidal prism. Without supporting data, natural neighbor interpolation gives a nearly straight line fit between the multibeam and LiDAR when there is no shoreline enforcement. However, when a shoreline is imposed as in this example and hand soundings are included, it brings about a 1 m or greater change in vertical elevations and a significantly different characterization of the tidal prism.

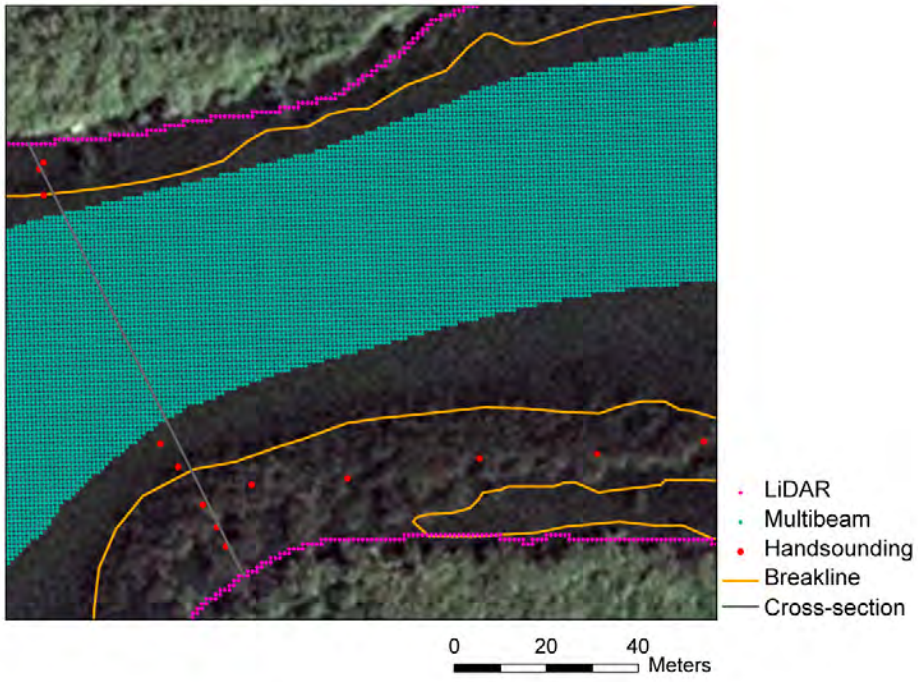

Figure note: Shoreline estimates from photos and locations of some supporting hand soundings are also indicated.

Figure 6-11 Shallow Horseshoe Bend on Middle River North of Bullfrog Marina (top) and Close-up of Southern Part of Bend where Interpolation was Compared (bottom)

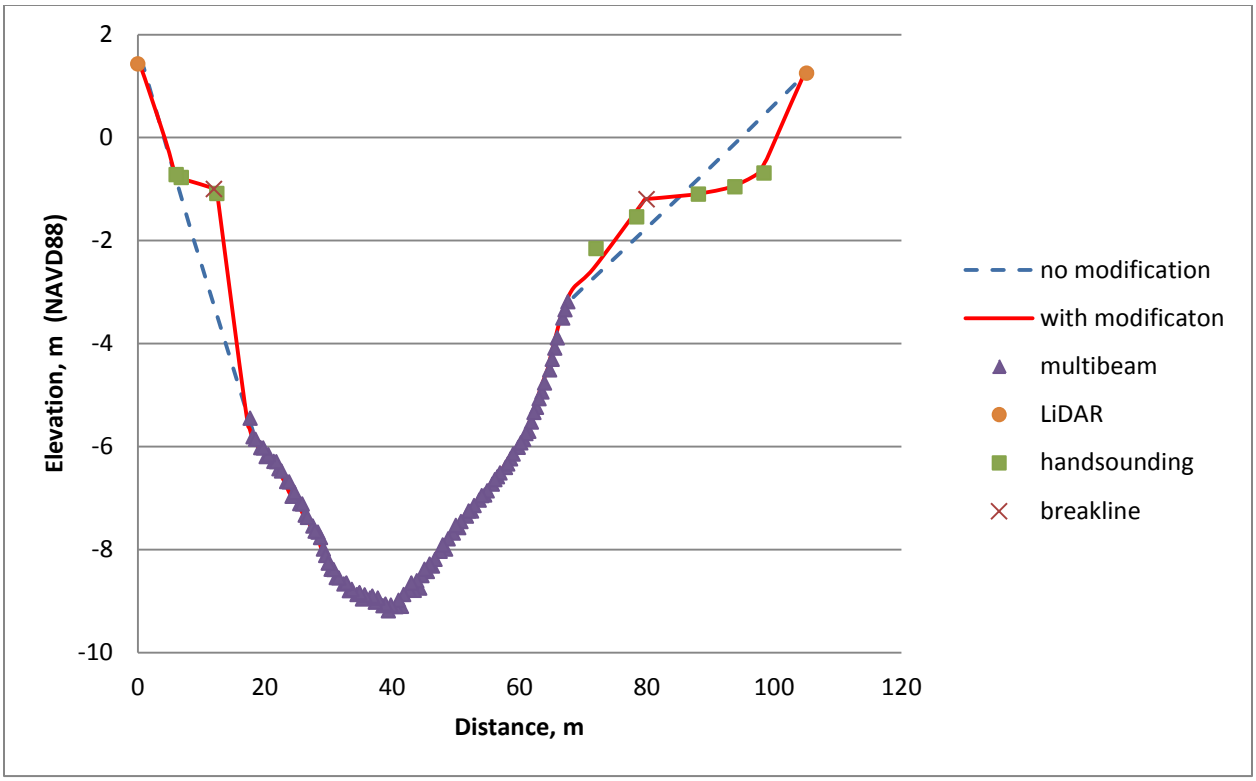

Figure note: Comparison of vertical cross sections on the bend constructed using bathymetry and LiDAR alone (dashed blue) and including hand soundings and hand-drawn breaklines at the shoreline from photography (solid red).

Figure 6-12 Example of Vertical Cross Sections with Supporting Data

Though it makes use of auxiliary data, the fit in Figure 6-12 still comes from a natural neighbor interpolation method that is "out-of-the-box" for an ArcGIS terrain model. When bathymetry is not available, we have to revert to methods that honor boundaries (shores), interpolate realistically, and can robustly handle combinations of fine LiDAR and sparse soundings. In the northern section of the bend, we have been able to fit the channel well qualitatively with multidimensional tensor splines (Wood, 2006) in streamwise and cross-stream coordinates and robustly with soap film smoothers (Wood, Bravington, & Hedley, 2008). Both were implemented in the statistical programming language R. We suspect also that the anisotropic methods of Merwade, Maidment, & Goff (2006) would perform similarly to the tensor splines both in terms of high labor and good performance. However, both methods utilize "streamwise" and "cross-stream" coordinates that are hard to define in many places. We believe that the soap film methods and locally anisotropic methods for shape fitting such as in Casciola, Lazzaro, Montefusco, and Morigi (2005) and (2006) will generalize better to junctions and clusters of islands. We will compare the accuracy and realism of some of these interpolants over complex bathymetry in a future report.

6.6 Fine-coarse Transitions

In a previous section, we noted the possibility of discontinuities between different coarse (10 m) data sources. The same issue arises when 2 m and 10 m products need to agree at their boundaries.

We use the 2 m data to improve the 10 m data locally. Hence, 10 m data that is covered by 2 m data tends to naturally agree with the finer data. The issue is on the border region Figure 6-13. There we created synthetic transitions that allow 2 m and 10 m to nest well. Our goal in this case is that the 2 m

data and underlying 10 m model be left unaltered. The "patching" is done by manipulating the bordering 10 m data within a 100 m distance using successive passes of isotropic kernel smoothers (focal mean) (Figure 6-14).

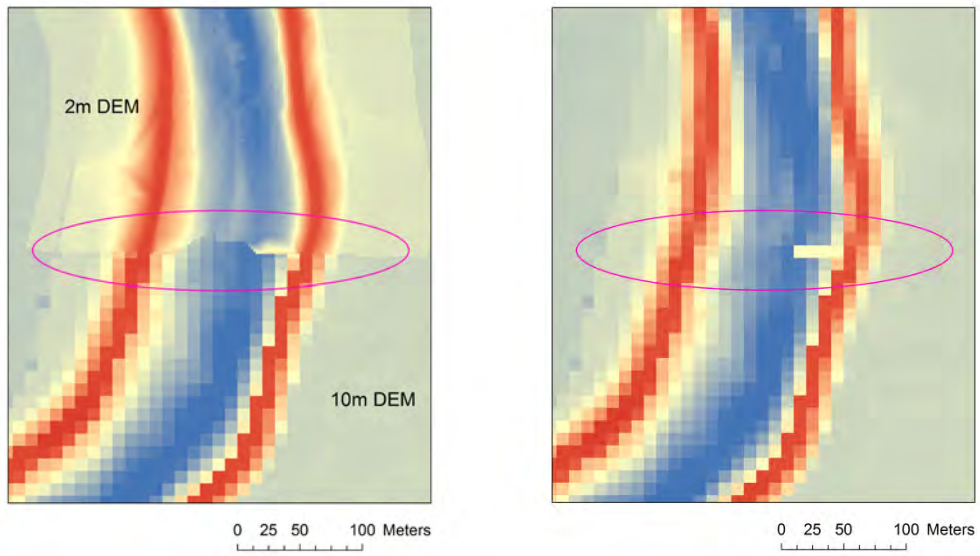

Figure note: (Left) Disagreement at coarse-fine interface between 2 m and 10 m maps. (Right) 10 m map updated using 2 m data with no adjustment at the interface.

Figure 6-13 Example of Fine-coarse Transitions

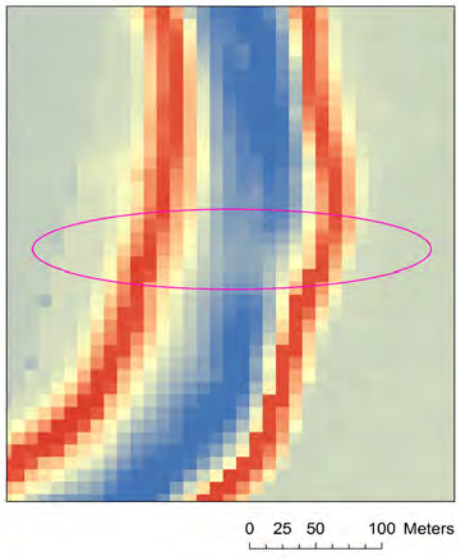

Figure 6-14 Result of Stitching and Smoothing Discontinuity at 10 m

6.7 Time and Spatial Sampling

It is necessary as a modeling assumption to treat an integrated bathymetry map as a synoptic view of the entire domain. In fact, the Delta is constantly changing, including subsidence of land and survey benchmarks, moving bed forms, and morphological change from extreme events. We encountered this evolution in several contexts:

1. **Morphological evolution over decades.** On the San Joaquin River, more than a few kilometers upstream of Old River, only one historical bathymetric survey sampled transects spaced closely enough longitudinally to resolve the channel meanders in the region (approximately 150 m is required, and COE and other institutions have sampling standards much more distant). The one survey available was made in the late 1990s and did not line up with the channel bed suggested by the LiDAR and photos.
2. **Sand wave movement.** Bed forms exist in many areas of the San Francisco Bay and Delta. Relatively few spots have been subject to enough repeated high density monitoring to describe changes over time. Figure 6-15 shows the evolution of sand waves near the Middle River railroad bridge over 3 multibeam surveys that were spaced over 18 months. Within that time, the bed forms appear to evolve and come out of phase with another between the first DWR survey and the Fugo survey; and then the bed forms moved only slightly by the second DWR collection. The absolute difference in elevation at a point between the collections can be over a meter, although there is clearly an "average" bed that is more stable.

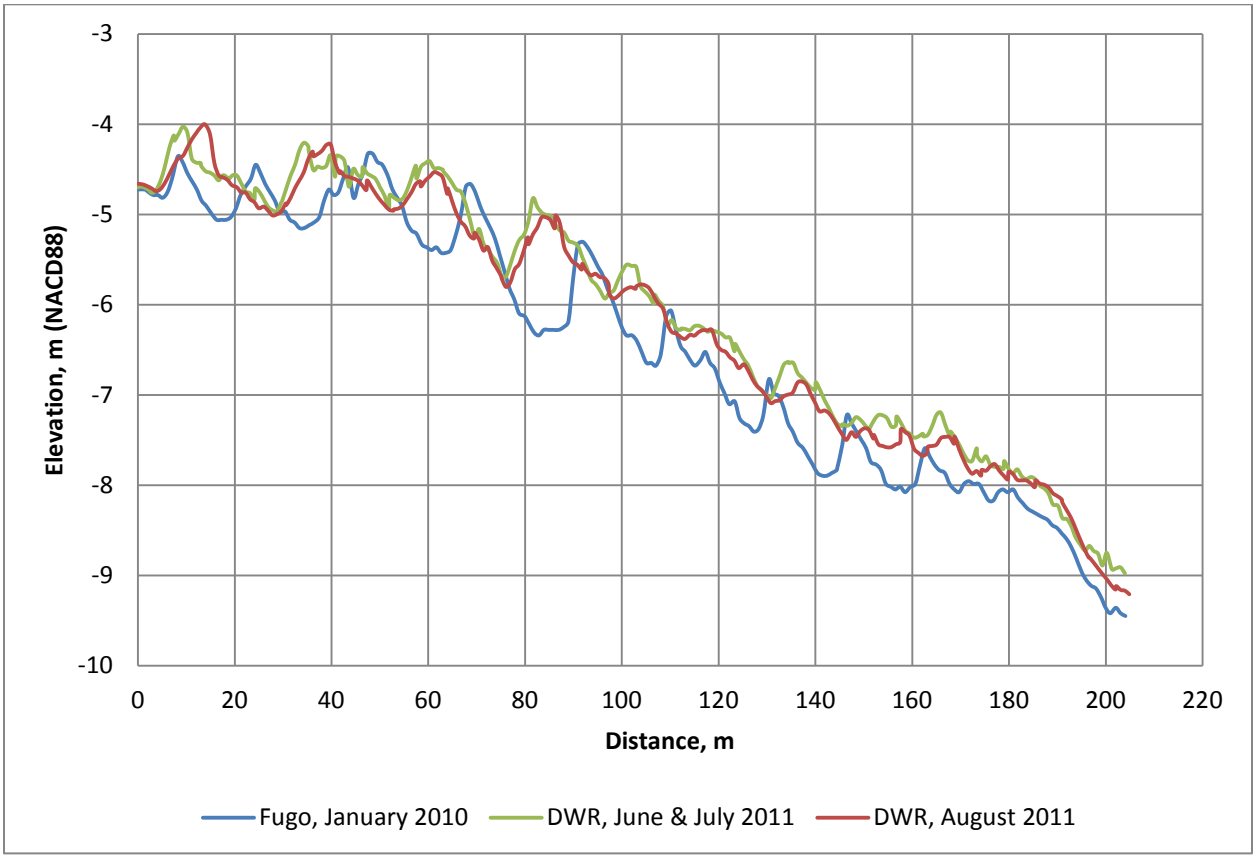

Figure 6-15 Evolution of Channel Bedforms over 3 Data Collections in 2010 and 2011

3. **Methodology discrepancies**. Differences between successive multibeam surveys are almost always interpreted by practitioners as a physical change. The nominal error and precision of the data warrants this, and changes in spatial patterns are often bona fide. On the other hand, errors due to equipment setup and quirks of the day can amount to several tenths of a meter, and the error is often systematic—affecting much of the data collected in one outing in a similar way. It is beyond the scope of this chapter and the available data to quantify this effect. We believe it amounts to between 0.1 m and 0.2 m in the railway bridge region, which is not enough to affect our results.
4. **Spatial sampling goals.** The original LiDAR and multibeam data are observed at a resolution of 1 m or less. To properly down-sample or decimate the original data to 2 m or 10 m, we must remove noise and eliminate high frequency variation that the coarser destination resolution cannot represent. Decimation is supported by ArcGIS Terrain models when they are converted to a DEM—information is averaged or filtered over a "window." The effect on longitudinal and lateral profiles of using different window sizes for filtering is demonstrated in Figure 6-16.
5. **The standard (Nyquist) distance** for aggregation suggests the window size should be at least equal to the destination resolution. We found that a small additional amount of smoothing gave a visually more pleasing shape without losing longitudinal detail. We use this window size for our production work.

Figure 6-17 shows the longitudinal and lateral profiles derived from DEMs at different resolutions, in each case fixing the relative window size. Medium-fine resolution multidimensional models would probably have a discretization length of 10 to 15 m laterally and 40 m longitudinally for this region, certainly no finer than 10 m. Hence, our interpretation of Figure 6-17 is that a 10 m DEM not only captures the stable bathymetric features in this region, it is the finest (not coarsest) level of detail appropriate for the region.

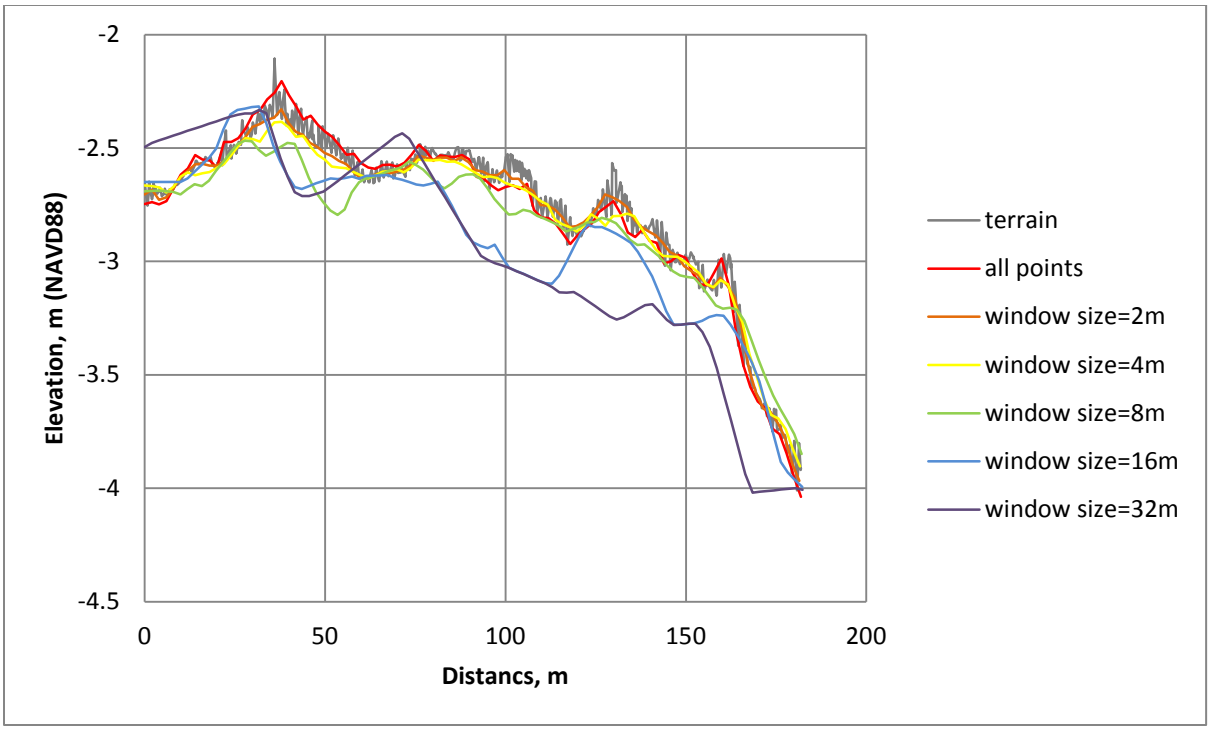

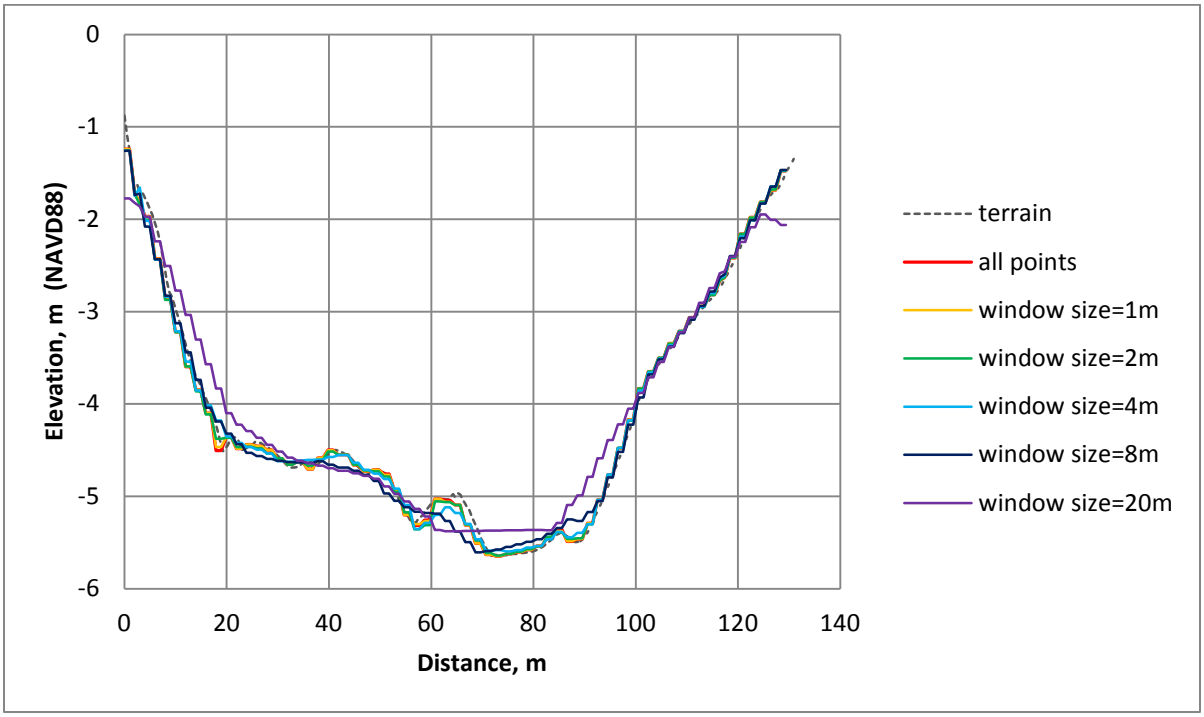

Figure note: The "window" size represents the extent over which averaging or aggregation is filtered.

Figure 6-16 Longitudinal Profile (top) and Lateral Profile for 2 m DEM Derived from Terrain Using Different Window Sizes

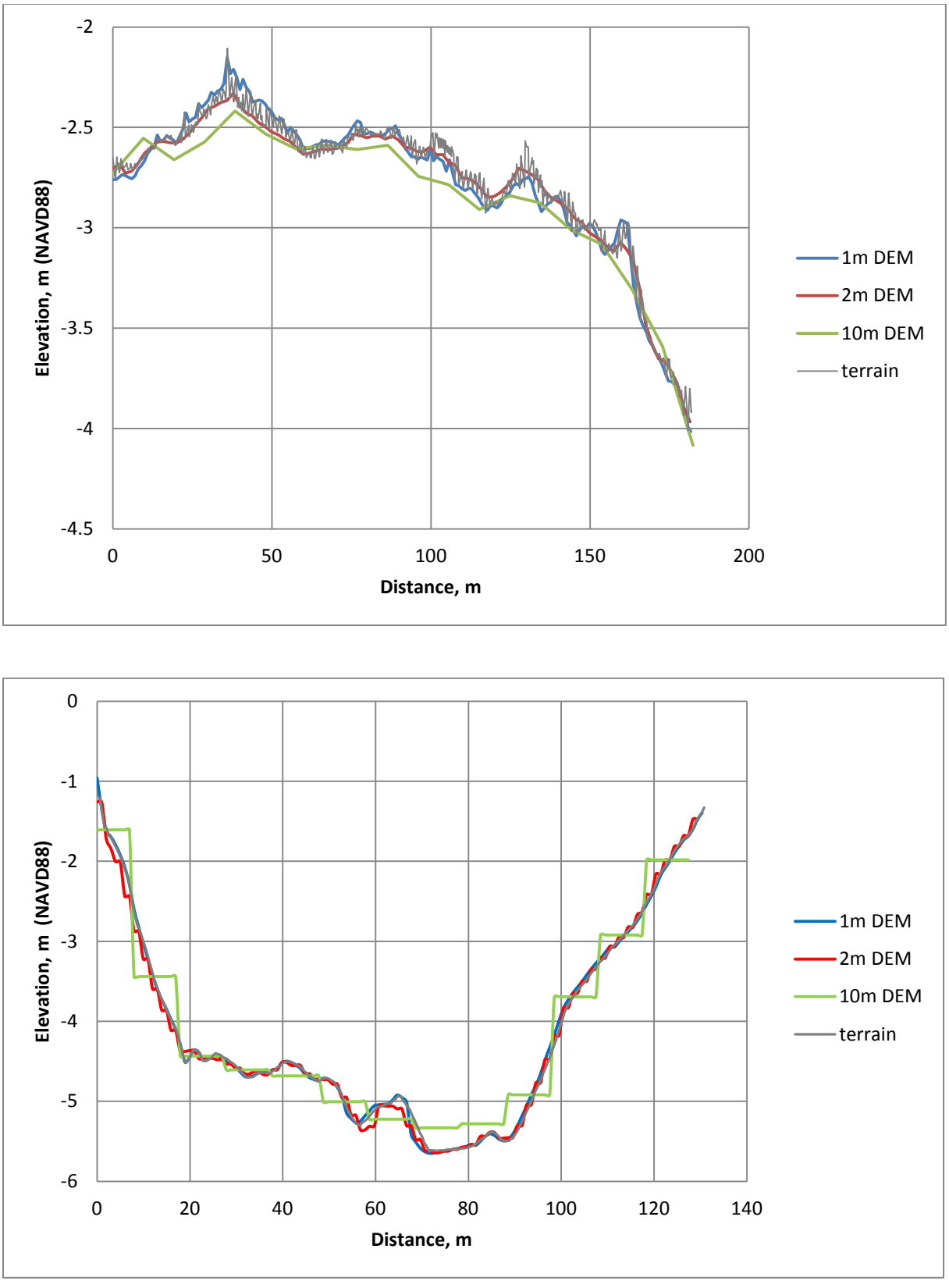

Figure 6-17 Longitudinal Profile (top) and Lateral Profile Generated from Different Resolution DEMs Using Same Proportional Window Size

6.8 Summary and Conclusions

Geometry is important to hydrodynamic models. In some locations, data used in the Bay-Delta is still in need of serious improvement. The authors have systemized the production of a 10 m/2 m elevation model for the Bay-Delta, borrowing strength from work done previously by the DWR, USGS, and NOAA and integrating new data when it becomes available. In many locations, the new geometry improves the quality of information we use in our hydrodynamic models, a point that will be amplified by the release of Version 2, which has many new sources of data. Some areas such as Mildred Island and the upper San Joaquin are still not well understood. The authors are hopeful that new soundings data will be collected before morphological change makes integration with LiDAR difficult.

The challenges of elevation mapping have changed since we began this work in 2010. Previously, our primary challenge was how to interpolate a realistic surface from sparse, poorly geo-referenced soundings often taken at intervals that seemed to have more to do with budget and technology than the scale of underlying features. Now, new data are over-resolved in space, and the quality of the integrated data set is determined by the handling of omissions and gaps. We are unaware of metrics for digital elevation models that are useful in the case where the distribution of error is concentrated in a small section of the tidal prism and where inundated area (for a given water surface) is quantified. We have some promising techniques for fixing the gaps in cases where out-of-the-box GIS techniques fail and where there is supporting data and aerial photography, which we will write about in a future report. However, the point of decreasing returns is easy to reach—good interpolants add realism and robustness to an elevation model, but they don't give new information.

Lastly, as resolution goes up, sampling frequency must be properly accounted for when a geographic elevation model is shaped into a bathymetry model for hydrodynamics. We have attempted to stage our products in such a way that we retain most of the detail of the raw data in our terrain models and point data, but correctly down-sampled products for applications.

We would like users to acquire our elevation model—and help criticize it! The data are distributed under a copyleft license with the understanding that we are interested in collaboration and improvement and improvements should be shared. Collaborators are asked to join our issue tracking system.

6.9 References

Campbell, C. (2012). Tule Canal and Toe Drain Bathymetry - Data Collection Procedures.

Carignan, K. S., Taylor, L. A., Eakins, B. W., Caldwell, R. J., Friday, D. Z., Grothe, P. R., et al. (2010). *Digital Elevation Models of Central California and San Francisco Bay: Procedures, Data Sources and Analysis.* NOAA Technical Memorandum NESDIS NGDC-52.

Casciola, G., Lazzaro, D., Montefusco, L. B., & Morigi, S. (2005). Fast surface reconstruction and hole filling using Radial Basis Functions. *Numerical Algorithms, 39*(1-3), 289-305.

Casciola, G., Lazzaro, D., Montefusco, L. B., & Morigi, S. (2006). Shape preserving surface reconstruction using locally anisotropic radial basis function interpolants. *Computers and Mathematics with Applications, 51(8)*, 1185-1198.

EDS [Environmental Data Solutions]. (2006). Draft Filed Data Report - Barker Slough, Calhoun Cut, Lindsey Slough and Cache Creek, Solano County, CA - Bathymetric Survey.

EDS [Environmental Data Solutions]. (2009). West Delta Condition Bathymetric Surveys: Field Data Collection Procedures. Prepared for cbec, Inc.

Foxgrover, A., Smith, R. E., & Jaffe, B. E. (2003). Suisun Bay and Delta Bathymetry: Production of a 10m Grid. *CALFED Science Conference.*

Fugro West, Inc. (2008). Bathymetric Surveys in Support of Urban Levees, Geotechnical Evaluation. Prepared for URS Corporation and California Department of Water Resources, DWR Task Order 32.

Fugro West, Inc. (2010). Multibeam Hydrographic Survey Middle River. Prepared for Storesund Consulting.

GRS [Global Remote Sensing LLC]. (2008). Mokelumne River (California Delta), California Hydrographic Survey Report. Prepared for the law offices of Herum Crabtree Brown.

HDR. (2011). Bathymetry Surveying in Support of Hydraulic Model Development Summary Report. DWR Task Order 18, Contract No. 4600007990, Lower San Joaquin River System.

Mayr, S. (2011). Multibeam Bathymetry Survey Report: Middle River - North Canal - Victoria Canal. Bathymetry and Technical Support Section, North Central Region Office, Division of Integrated Regional Water Management, California Department of Water Resources.

Merwade, V. M., Maidment, D. R., & Goff, J. A. (2006). Anisotropic considerations while interpolating river channel bathymetry. *Journal of Hydrology, 331(3-4)*, 731-741.

CSDP bathymetry data. (online). Retrieved from Bay-Delta Office, California Department of Water Resources: http://baydeltaoffice.water.ca.gov/modeling/deltamodeling/models/csdp/csdp.cfm

PBS&J, An Atkins Company. (2010). WR TO18 FINAL Technical Memo/Quality Control Report. DWR Task Order 18. Contract No. 4600007989, Lower Sacramento River Basin.

Ruggeri-Jensen-Azar & Associates. (2005). Grading Plans Subdivision 6013 – Delta Coves, Bethel Island, Contra Costa County, California, for DUC Housing Partners, Inc.

Smith, P. E. (n.d.). 10 m digitized bathymetry map. Sacramento, CA.

Towill, Inc. (2009). Sacramento DWSC 3D Models and San Francisco to Stockton DWSC 3D Models.

US Geological Survey. (2008). Northern Sacramento River Detailed Modeling Survey, Jun - 08 (online). Availability: https://sites.google.com/site/bathmapperwiki/Home/bathymetry-surveys/northern-sacramento-river-detailed-modeling-survey-june---07.

Wood, S. N. (2006). *General Additive Models.* Chapman and Hill.

Wood, S. N., Bravington, M. V., & Hedley, S. L. (2008). Soap film smoothing. *Journal of the Royal Statistical Society, Series B; 70*(5), pp. 931-935.

Methodology for Flow and Salinity Estimates in the Sacramento-San Joaquin Delta and Suisun Marsh

33rd Annual Progress Report
June 2012

Chapter 7
DSM2-PTM Simulations of Particle Movement

Authors: Yu Zhou and Tara Smith
Delta Modeling Section
Bay-Delta Office
California Department of Water Resources

Page left blank for two-sided printing

Contents

Figures

Tables

7 DSM2-PTM Simulations of Particle Movement

7.1 Summary

The National Marine Fisheries Service (NMFS) requested the California Department of Water Resources (DWR) Modeling Support Branch perform a DSM2-PTM modeling study to investigate the impact of various factors on salmon/steelhead migration behaviors in the Sacramento-San Joaquin River Delta (the Delta). Those factors include San Joaquin River (SJR) flows, exports from the State Water Project (SWP) and Central Valley Project (CVP), and the Head of Old River Barrier (HORB). The report documents the assumptions, model setups, and simulation results and could be used to help studies on HORB installation/operation and export adaptive management for salmonid outmigration protections.

7.2 Study Scenario Determination and Modeling Configuration

7.2.1 Hydrodynamic Boundary and Source Flows Configuration

The assumed flow and operations for these scenarios are synthetic but based on Delta historical hydrodynamic record and facilities operations. Although representing historical conditions, the synthetic hydrology allows only one flow or operation to be varied so that the impacts on particle movement due to the various changes can be more easily analyzed. The factors of concern are SJR flow, exports (CVP, SWP), and HORB operation; other boundaries and facilities are configured as fixed, using values associated with the selected intermediate SJR condition (red in Table 7-1).

May 2007 SJR monthly flow at Vernalis is closest to 3,000 cfs, a historical average flow in May (Table 7-1), so May–June 2007 was selected as the simulation period. Other boundaries, which are not of this study's concern, were set constant in the above simulation period. Figure 7-1 and Table 7-2 show the details of the Delta flow and stage boundary conditions.

Table 7-1 Monthly Average of San Joaquin and Sacramento River Flows in May, 1990 to 2010

	MAY monthly average flow (cfs)			MAY monthly average flow (cfs)			MAY monthly average flow (cfs)	
Year	SJR	SAC R.	Year	SJR	SAC R.	Year	SJR	SAC R.
1990	1,279	10,402	1997	4,530	11,349	2004	2,684	12,487
1991	1,049	7,332	1998	17,834	48,250	2005	10,380	40,079
1992	892	6,414	1999	5,681	19,723	2006	26,708	52,804
1993	3,610	24,955	2000	4,881	20,406	2007	3,033	9,204
1994	1,973	8,848	2001	3,637	9,082	2008	2,748	8,819
1995	22,187	63,181	2002	2,798	12,921	2009	2,185	15,436
1996	8,422	40,113	2003	2,691	40,514	2010	4,889	17,238

SJR: San Joaquin River flow at Vernalis; SAC R.: Sacramento River flow at Freeport; Red: selected; Green: max/min

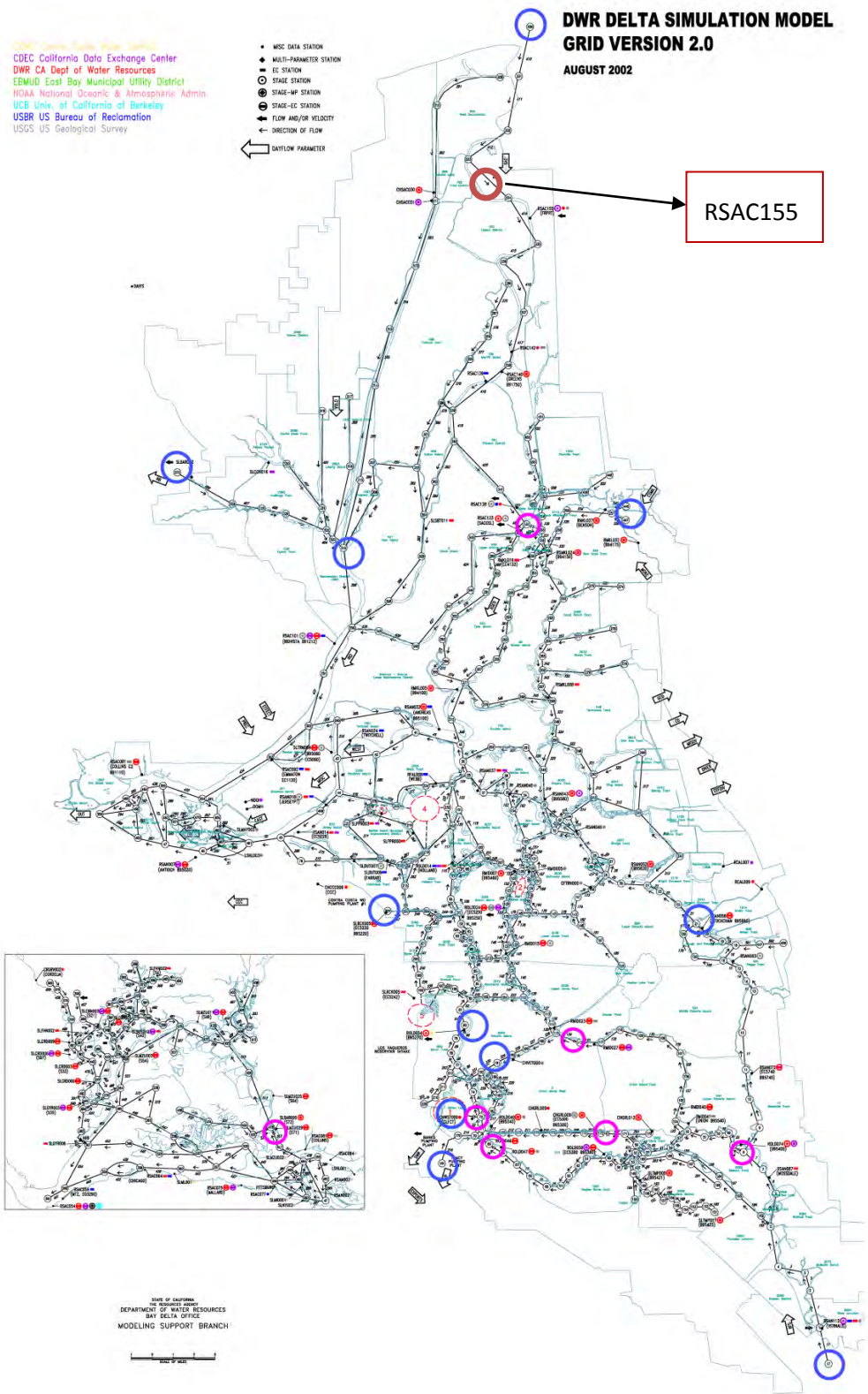

Figure 7-1 Delta Boundaries Showing Flows (blue circles) and Temporary Barriers and Gates (purple circles)

Table 7-2 DSM2-HYDRO Configuration for the Delta Boundaries and Source Flows

Source	DSM2			Flow (cfs)
	Name	Station	Node	
San Joaquin River	SJR	RSAN112	17	Vary for specific scenario
Sacramento River	SAC	RSAC155	330	Determined from sensitivity study[1]
Calaveras River	CALAVERAS	RCAL009	21	167.39
Cosumnes River	COSUMNES	RCSM075	446	214.58
Mokelumne River	MOKE	RMKL070	447	212.32
North Bay	NORTH_BAY	SLBAR002	273	99.871
Yolo Bypass	YOLO	BYOLO040	316	581.32
Contra Costa Canal	CCC	CHCCC006	206	96.636
Contra Costa Canal at Old River	CCCOLDR	ROLD034	80	87.164
Contra Costa Canal at Victoria Canal	CCW	CHVCT001	191	0
Central Valley Project	CVP		181	Vary for specific scenario
California State Water Project	SWP		Clifton Court	Vary for specific scenario
Martinez (stage)	May-June 2007 historical stage data			
DICU	May 2007 historical data			

7.2.2 Operable Barrier and Gate Configuration

The effect of HORB operations is the focus of this study. Two HORB operations were considered in the modeling studies: HORB is installed (HORB IN) and HORB is not installed (HORB OUT). When HORB is installed, all 6 HORB culverts are modeled as open to allow partial flow through the barrier into Old River (Le, 2004) (Division of Operations and Maintenance, 1989).

For the other temporary barriers, Middle River Barrier (MIDB), Grant Line Canal Barrier (GLCB), and Old River Barrier at Tracy (ORTB) were set in place with their pipes allowing one-directional flow to capture the incoming tide. Delta Cross Channel (DCC) was closed during the entire simulation period.

Historical May-Jun 2007 operations were used for Montezuma Salinity Control Structure (MTZSL).

The Priority 3 operation schedule was used for Clifton Court Forebay Gates (CLFCT). The Priority 3 gate operation is open 1 hour after the low-low tide, closed 2 hours after the high-low tide, reopened 1 hour before the high-high tide, and closed 2 hours before the low-low tide (Figure 7-2). Martinez historical tidal cycle stage data was delayed 5.5 hours for CLFCT to identify the peak, High-High tide (HH), Low-High tide (LH), Low-Low tide (LL), and High-Low tide (HL)).

Table 7-3 and Figure 7-1 show the barriers and gates operations discussed above.

[1] In order to identify an acceptable fixed value for SAC R. flow, a sensitivity analysis was conducted. The sensitivity analysis examines the effects of SAC R. flows at Freeport on the particle flux.

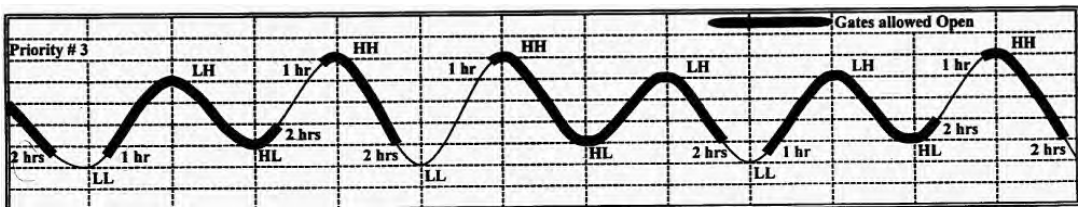

Figure 7-2 Priority 3 Operation Rule

Table 7-3 Facilities Configuration for the Delta Temporary Barriers and Important Gates

Facility	DSM2			INSTALL	weir		pipe		Flow direction
	name	node	chan		Elev (ft)	Width (ft)	number	Elev (ft)	
Head of Old River Barrier	HORB	8	54	IN/OUT	10	167	6	-4	both
Old River Barrier at Tracy	ORTB	69	79	IN	2	180	9	-6	Chan -> Node
Middle River Barrier	MIDB	112	134	IN	1	140	6	-4	Node -> Chan
Grant Line Canal Barrier	GLCB	206	172	IN	1	125	6	-6.5	Chan -> Node
Delta Cross Channel	DCC	342	365	CLOSED					both
Montezuma Salinity Control	MTZSL	418	512	historical op configuration					both
Clifton Court Forebay Gate	CLFCT	72	clifton_ court	'Priority 3' apply on 5.5 hrs delayed MTZ historical stage					Node -> Reservoir

7.2.3 Hydrodynamic Scenario Configuration

There are 2 sets of hydrodynamic scenarios in this study. For a given scenario, SJR flows and combined CVP+SWP exports will be the same (Table 7-4).

The first set of simulations is based on the ratio of the SJR flow at Vernalis to the export level (IE ratio) as defined in the NMFS Reasonable Prudent Alternatives (RPA). This set of simulations consists of:

- 4 levels of Vernalis flows
- Exports according to the IE ratio in the NMFS RPA
- 2 different configurations of the Head of Old River barrier (HORB-IN and HORB-OUT)

The second set of simulations is based on different combinations of SJR flow at Vernalis, and Old and Middle River flows (OMR). This set of simulations consists of:

- 4 levels of Vernalis flows
- 3 levels of OMR flows
- 2 different configurations of the Head of Old River barrier (HORB-IN and HORB-OUT)

For both sets of the scenarios, exports were equally split between CVP and SWP, i.e., CVP = SWP. Because of flood safety concern, HORB is not installed when SJR flow is equal to or greater than 12,000 cfs. This safety restriction reduced the total scenarios to 36.

Aside from the specific combinations above, these 2 scenario categories are different in the way in which input variables vary. These could bring in very different hydrodynamics, especially for SJR branches to the South Delta. This may result in very different particle movement:

- SJR_IE scenarios could reflect the export directly, and could vary SJR flow and export together, i.e., proportionally when fixing IE ratio (in the following analysis expressed as 'varying SJR flow' for convenience);
- SJR_OMR scenarios could vary SJR flow and exports independently, and could use OMR to reflect the hydro conditions close to the exports more directly.

Table 7-4 Simulation Hydro Combinations of sjr_ie Scenarios and sjr_omr Scenarios

SJR_IE			SJR_OMR		
SJR Flow (cfs)	**IE Ratio**	**Total**	**SJR flow (cfs)**	**OMR (cfs)**	**Total**
1,500	1:1	16 scenarios	1,500	-2,500, -3,500, -5,000	24 scenarios
3,000	1:1, 2:1		3,000	-2,500, -3,500, -5,000	
4,500	2:1, 3:1		6,000	-2,500, -3,500, -5,000	
6,000	3:1, 4:1		12,000 (only HORB-OUT)	-2,500, -3,500, -5,000	
12,000 (only HORB-OUT)	4:1				

7.2.4 DSM2-PTM Configuration

For the particle insertion locations selection, there are 2 scenarios: Three Basins and Southern Delta (Table 7-5, Figure 7-3); each scenario has its own flux outputs configuration (Table 7-6).

Each insertion location is treated as 1 PTM simulation in every Hydro scenario. Thus, there are in total 36 x (3 + 7) = 360 PTM simulations. For each PTM simulation, 10,000 particles are inserted at a fixed rate such that they are all inserted within the 24 hours of the start of the simulation.

Table 7-5 PTM Particle Insertion Location Scenarios

Scenario	Insertion	DSM2 node	Description	Output group
Three Basins	Mossdale	6	Mossdale	Standard output; SJR junctions output;
	Calaveras	21	San Joaquin River at Calaveras River	
	Rio Vista	351	Rio Vista	
Southern Delta	HOR	48	Just inside Head of Old River	Standard output
	Turner	140	Just inside Turner Cut	
	Columbia	31	Just inside Columbia Cut	
	Mmid	134	Just inside mouth of Middle River	
	Mold	103	Just inside mouth of Old River	
	Jersey	469	San Joaquin River just downstream of Jersey Point	
	3mile	240	Just inside Threemile Slough	

The PTM running period is set as 45 days. The starting time is set as the midpoint between the neap and spring tides.

Figure 7-4 shows the historical Martinez tidal stage at Station RSAC054. May 7 is in the middle between its spring and neap. Figure 7-5 shows that the corresponding San Joaquin flow is 3,012 cfs, which is close to our required May monthly average. Therefore, May 7 is selected as the PTM simulation starting date. June 20 is selected as the ending date.

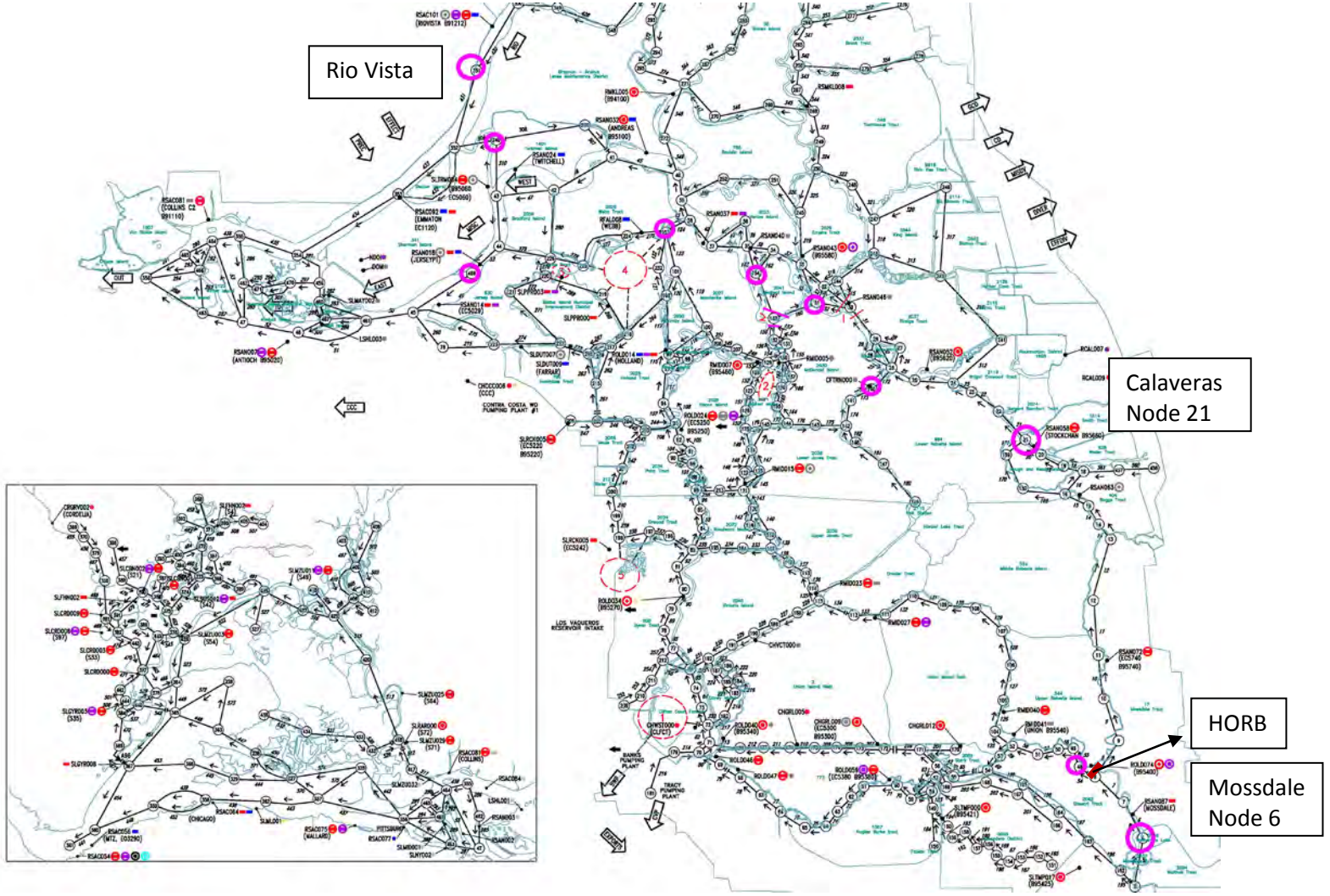

Figure note: Big circles indicate 3 locations of the 'three basins' scenario; small circles indicate 7 locations of the Southern Delta scenario

Figure 7-3 PTM Particle Insertion Locations (purple circles)

Table 7-6 PTM Flux Output Groups and Specification

Scenario	Name	Description	DSM2 water body		Related Hydro chan
			From	To	
PTM Standard Boundary Output * particle fate for Delta	DIVERSION_AG	Particles by agricultural facilities (DICU)	all	ag_div	N/A
	DIV_CCC	Particles diverted by Contra Costa Canal	ccc_chan	ccc_div	
	EXPORT_CVP	Particles diverted by CVP	216	CVP	
	EXPORT_SWP	Particles diverted by SWP	clifton_court	SWP	
	PAST_MTZ	Particles passing Martinez	441	mtz	
	WHOLE	Particles remaining in Delta (not yet diverted)	whole		
South Delta SJR Output * particle split pattern for SJR junctions	hor_sjr	San Joaquin River at Head of Old River to just inside Head of Old River	7,8	54	54
	sjr_hor	San Joaquin River at Head of Old River to San Joaquin River just downstream of Head of Old River	7,54	8	8
	turner_sjr	San Joaquin River at Turner Cut to just inside Turner Cut	25,26,27,30	172	-172
	sjr_turner	San Joaquin River at Turner Cut to San Joaquin River just downstream of Turner Cut	25,172	26,27,30	26-27+30
	columbia_sjr	San Joaquin River at Columbia Cut to just inside Columbia Cut	32,33,35	160	-160
	*sjr_columbia_up	San Joaquin River upstream at Columbia Cut to San Joaquin River just downstream of Columbia Cut (indirectly apply)	31,314	32,34, 315,316	31+314
	sjr_columbia	San Joaquin River at Columbia Cut to San Joaquin River just downstream of Columbia Cut	sjr_columbia_up - columbia_sjr		
	mmid_sjr	San Joaquin River at Mouth of Middle River to just inside Mouth of Middle River	162,163	161	161
	sjr_mmid	San Joaquin River at Mouth of Middle River to San Joaquin River just downstream of Mouth of Middle River	40,41	42	40+41
	rold_sjr	San Joaquin River at Mouth of Old River to just inside Mouth of Old River	42,43	124	-124
	sjr_rold	San Joaquin River at Mouth of Old River to San Joaquin River just downstream of Mouth of Old River	42,124	43	43
	jersey	Past Jersey Point	83	49	49
	3mile_sac	Sacramento River at Threemile Slough to just inside Three Mile Slough *(For Rio Vista insertion point only)*	431,432,433	309	-309
	sac_3mile	Sacramento River at Threemile Slough to Sacramento River just downstream of Three Mile Slough *(For Rio Vista insertion point only)*	431,309	432,433	432+433

Table note: Blue (shaded) cells indicate SJR junction mainstream branch downstream to Martinez.

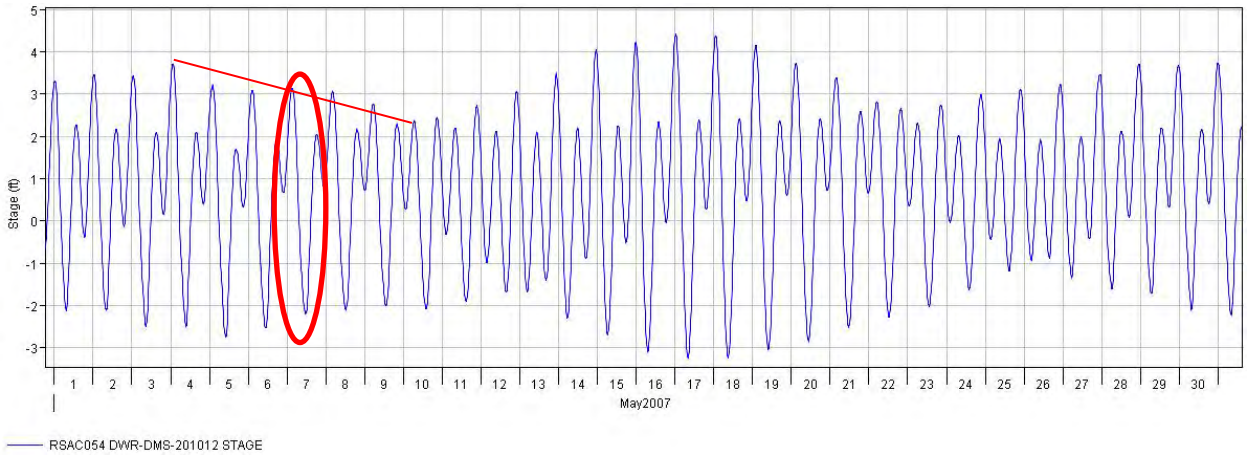

Figure 7-4 Stage at Martinez at Station RSAC054

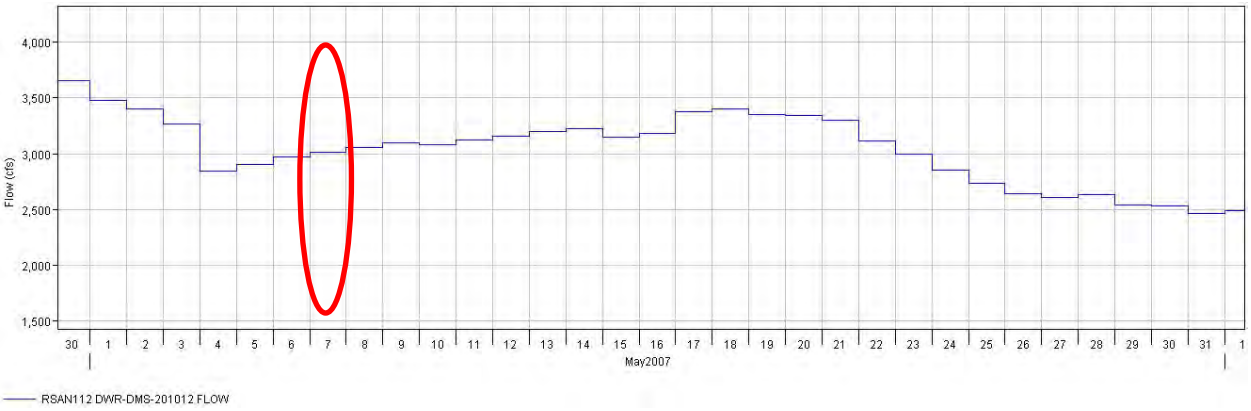

Figure 7-5 San Joaquin River Flow at Station RSAN112

7.3 Sacramento River Flow Sensitivity Test

7.3.1 Simulation Configuration

In order to examine the influence of Sacramento River (SAC R.) flows on particle movement and fate, a sensitivity analysis was conducted with a range of Sacramento River flows. This sensitivity analysis was done to see if it was necessary to add an additional matrix of runs where the Sacramento River flow varied. If the sensitivity simulations indicate that the impact of the Sacramento River is not significant then only one value of Sacramento flow would be used in the simulations and the other parameters such as San Joaquin River flow, exports, and Old River at Head Barrier configuration varied.

This sensitivity analysis is configured with the intermediate SJR flow condition (3000 cfs), IE ratio of 1:1 (both CVP and SWP exports are at 1500 cfs). The other inputs including boundary conditions and barriers/gates operations are the same as described in the previous Section of this report.

To cover the varying range of the SAC R. flows, the following values were selected (Table 7-7):

- 6400 cfs: historical minimum SAC R. May monthly-average flow, Year 1992
- 63200 cfs: historical maximum SAC R. May monthly-average flow, Year 1995
- 9200 cfs: historical SAC R. May monthly-average flow with the medium SJR flows, Year 2007
- 20000 cfs and 40000 cfs: 2 values in the middle between the minimum and maximum

Particles are inserted at DSM2 nodes 6, 21, and 351 (i.e., 3 basin insertion scenario in Table 7-5 and Figure 7-3) with the standard PTM flux output configuration.

Table 7-7 HYDRO Configuration for SAC R. Sensitivity Analysis

Source	DSM2			Flow (cfs)
	Name	Station	Node	
San Joaquin River	SJR	RSAN112	17	3000
Sacramento River	SAC	RSAC155	330	6400, 9200, 20000, 40000, 63200
Central Valley Project	CVP		181	1500
State Water Project	SWP		clifton_court	1500

7.3.2 Result Summary

The Sacramento flow amount only has significant influence on the percentage of particles moving past Martinez. With Sacramento River flow increased, the percentage of particles moving past Martinez increases. The influence of the Sacramento River flow amount on other output locations are relatively small and not uniform. (Please refer to the authors for detailed analysis on each insert location).

The effect of the Head of Old River Barrier depends on the particle insertion location.

- With HORB-IN, the percentage of particles moving into the CVP decreases for Mossdale insertion location and increases for Calaveras insertion location.
- The barrier's influence on SWP is relatively small, possibly due to the operation effect of the tidal operation gate at Clifton Court Forebay.
- The barrier's influence on the percentage of particles moving past Martinez (increase) is significant only for Mossdale insertion. Its influence on other fluxes is relatively small.

Understanding the relative impacts of Sacramento flow levels and using that understanding in interpreting the results, the remainder of simulations for the requested sets of studies used 18,000 cfs for Sacramento boundary flow.

7.4 Hydrodynamic Scenario Results and Analysis

A series of Hydro simulations were conducted for both SJR_IE and SJR_OMR scenarios. OMR flow and flow splits at some key junctions of San Joaquin River were recorded.

7.4.1 Old and Middle River (OMR)

The combined flow of Old River and Middle River (OMR) is used as one criterion to decide the 2nd set of hydrodynamic scenarios. In DSM2, OMR is determined by adding flows at the following 3 channels:

OMR = $Q_{144} + Q_{145} - Q_{106}$. Note that negative flow in channel 106 is due to the channel direction defined in DSM2. (Table 7-8)

The calculated OMR timeseries are processed with Godin filter and 14-day forward moving average; then average over the entire period. This final average is used as the indicator for OMR criterion.

Table 7-8 Locations Required for OMR Calculation in DSM2 Grid

	Channel	Node	Channel Direction
Old River	106	93	To node 93
Middle River	144	121	To node 121
	145	121	To node 121

7.4.1.1 San Joaquin River Flow – IE Ratio (sjr_ie) Scenarios

Table 7-9 and Figure 7-6 show all the SJR_IE scenarios with corresponding hydro conditions. Detailed OMR comparisons are in Appendix B-1.

a) For the same SJR flow, as IE Ratio increases (lower export, same SJR flow), OMR flow increases (negative flow decreases), for both HORB-IN & OUT.
b) For the same IE Ratio, as SJR flow increases (export increases proportionally), OMR flow decreases (negative flow increases) at smaller SJR, but the decrease rate gradually becomes less, finally reverses to increase (negatively decrease) at higher SJR flow, for both HORB-IN & OUT. This is because SJR flow increases more than export, with the same increase ratio.
c) Concerning the difference between HORB-IN and OUT:

- HORB-OUT has relatively a more stable OMR trend over the entire period.
- OMR IN-OUT difference is always negative, i.e. same sjr_ie conditions would result in more negative OMR for HORB-IN, since HORB-IN block SJR flow entering Old River, then more OMR flow is required for the same export.
- For the same SJR flow, as IE Ratio increases, OMR IN-OUT difference increases a little bit,
  i.e. varying export causes the same OMR change for HORB-IN & OUT.
- For the same IE Ratio, as SJR flow increases, OMR IN-OUT difference negatively increases, i.e. larger SJR flow and export combination has negative larger OMR for HORB-IN.

Table 7-9 Hydro Conditions for sjr_ie Scenarios

Scenario	SJR	CVP+SWP	IE Ratio	OMR		IN-OUT	
				HORB-IN	HORB-OUT	OMR diff	OMR diff ratio (over HORB-OUT)
sjr1500_ie11	1500	1500	1	-2045.14	-1648.64	-396.50	0.24
sjr3000_ie11	3000	3000	1	-3282.05	-2415.77	-866.28	0.36
sjr3000_ie21	3000	1500	2	-1887.96	-1036.87	-851.09	0.82
sjr4500_ie21	4500	2250	2	-2438.21	-1092.27	-1345.94	1.23
sjr4500_ie31	4500	1500	3	-1741.27	-397.38	-1343.89	3.38
sjr6000_ie31	6000	2000	3	-2085.88	-163.00	-1922.88	11.80
sjr6000_ie41	6000	1500	4	-1621.03	302.79	-1923.82	-6.35
sjr12000_ie41	1500	3000	4	N/A	1864.19	N/A	

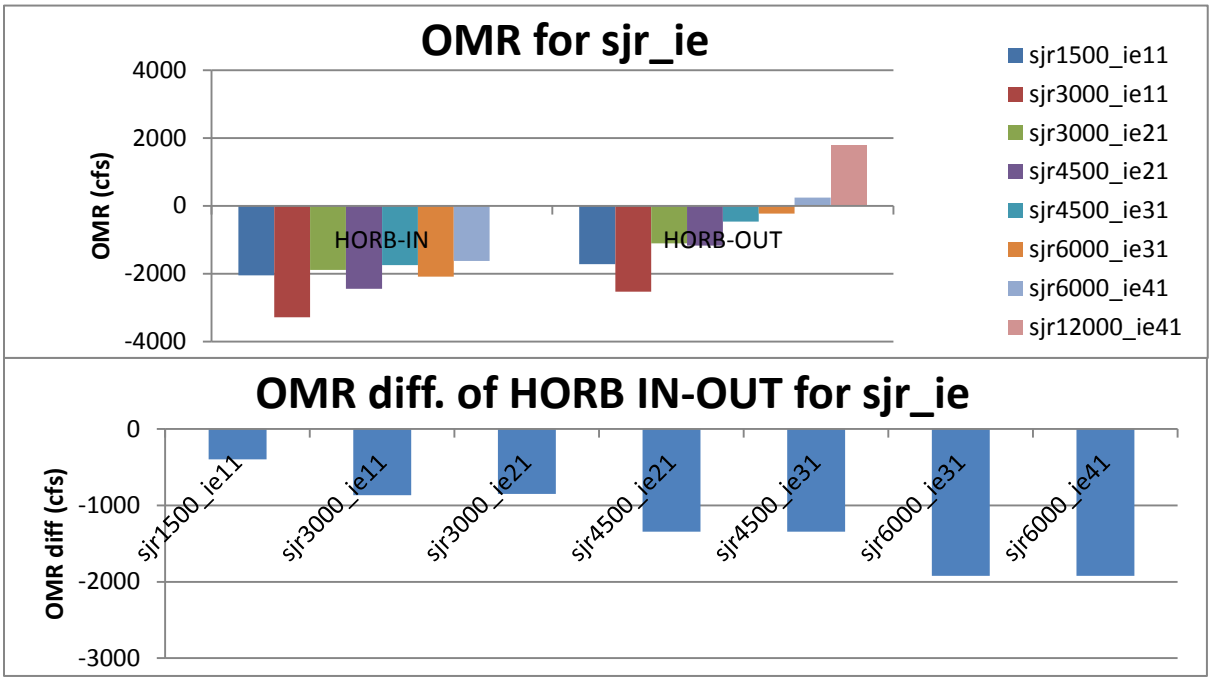

Figure 7-6 OMR and its HORB IN-OUT Difference for sjr_ie Scenarios

7.4.1.2 San Joaquin River Flow – OMR (sjr_omr) Scenarios

Because OMR flow is an output of DSM2, not an input, a trial-and-error iteration method is applied to achieve the required OMR flow with boundaries inputs (CVP, SWP) varying.

Table 7-10 and Figure 7-7 list all the sjr_omr scenarios with the corresponding hydro conditions. Detailed OMR comparisons are in Appendix B-2.

a) For the same SJR flow, as OMR negatively increases, export increases, IE ratio decreases, for both HORB IN and OUT; i.e., higher negative OMR standard allow larger export, especially for HORB-OUT.
b) For the same OMR, as SJR flow increases, HORB-IN export slightly increase, HORB-OUT export increases, IE ratio increases, for both HORB IN and OUT; i.e. for the same OMR standard, higher SJR flow allow more export.
c) Concerning the differences between HORB-IN and OUT:

- Export IN-OUT difference is always negative, IE Ratio IN-OUT difference is always positive, i.e., same sjr_omr conditions could allow more exports for HORB-OUT, since there is another water source (Old River) for export in addition to OMR.
- For the same SJR flow, as OMR negatively increases, export IN-OUT difference negatively increases slightly, IE Ratio IN-OUT difference decreases; i.e., higher OMR standard allows higher export, but similar increase for both HORB IN & OUT.
- For the same OMR flow, as SJR flow increases, export IN-OUT difference negatively increases and IE Ratio IN-OUT difference increases; i.e., for the same OMR, higher SJR flow could allow exports increase for both HORB IN & OUT, but more for HORB-OUT.

Table 7-10 Hydro Conditions for sjr_omr Scenario

Scenario	SJR	Target OMR	HORB IN		HORB OUT		IN - OUT	
			CVP+SWP	Approx. IE Ratio	CVP+SWP	Approx. IE Ratio	CVP+SWP	IE Ratio
sjr1500_omr2500	1500	-2500	2000	3/4	2400	5/8	-400	0.13
sjr1500_omr3500		-3500	3100	1/2	3500	3/7	-400	0.06
sjr1500_omr5000		-5000	4700	1/3	5200	2/7	-500	0.03
sjr3000_omr2500	3000	-2500	800	4/3	1700	1/1	-900	0.40
sjr3000_omr3500		-3500	2200	1/1	3100	5/7	-1000	0.22
sjr3000_omr5000		-5000	3200	5/8	4200	1/2	-1000	0.11
sjr6000_omr2500	6000	-2500	4800	5/2	5800	4/3	-2100	1.17
sjr6000_omr3500		-3500	2400	12/7	4500	1/1	-2100	0.64
sjr6000_omr5000		-5000	3500	7/6	5600	5/6	-2100	0.34
sjr12000_omr2500	12000	-2500	N/A		3850	14/9	N/A	
sjr12000_omr3500		-3500			4350	11/8		
sjr12000_omr5000		-5000			5150	7/6		

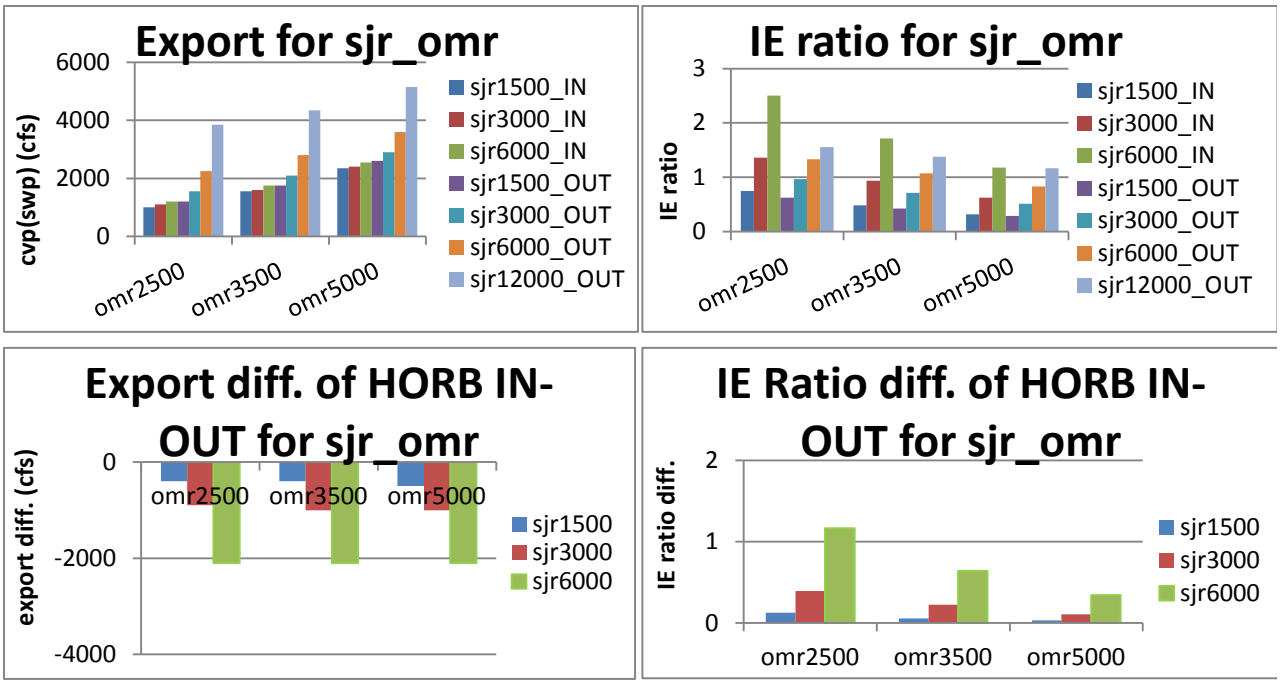

Figure 7-7 Export and IE Ratios and Their HORB IN-OUT Difference for sjr_omr Scenarios

7.4.2 Flow Splits at San Joaquin River Junctions to South Delta

The current version of the DSM2-PTM uses a purely flow-volume-driven particle movement model. In order to better investigate the particle movement environment at San Joaquin River key junctions—main stem downstream and branches to South Delta junctions include Head of Old River (hor), Tuner, Columbia (col), Middle River mouth (mmid), and Old River mouth (rold)—average flows of the entire 45-day simulation period were recorded for these locations (the last column of Table 7-6). Detailed comparative bar charts are included in Appendix B-3 (sjr_ie scenario), B-4, and B-5 (sjr_omr scenario).

- SJR (SAC R.) main stem usually takes the major flows, due to the large cross-section area.
- Flow ratios of downstream / (downstream + southward branch) are calculated to better represent the flow split pattern. This ratio is only calculated when both branch flows are positive. A negative ratio happens when one of the branches has flow direction inverse from specified direction, and cannot be used for the analysis & comparison.

7.4.2.1 San Joaquin River Flow – OMR (sjr_omr) Scenarios

The flow information of Appendix B-4, Appendix B-5 is summarized for all sjr_omr scenarios in the following ways: Table 7-11 lists the average flow ranges (minimum-maximum) of SJR junctions, as well as the flow ratios of downstream / (downstream + southward branch), and their IN-OUT difference. Table 7-12 and Table 7-13 list these flow variation patterns to SJR flow and OMR.

- As SJR flow increases (higher SJR flow, same export), usually both downstream and southward Delta branches increase in flow. There are some exceptions that experience flow decreases such as mmid and 3mile. This pattern is similar for both HORB-IN and OUT.
- As OMR increases (higher export, same SJR flow), usually downstream flow decreases and southward branch flows increase. This pattern is similar for both HORB-IN and OUT.

- Negative downstream flow appears at some output locations, including columbia, mmid, and rold, especially for high OMR and low SJR flow scenarios, i.e., more flows to South Delta. And usually the closer the locations to Chipps, the larger the negative flows, i.e., rold > mmid > columbia. Figure 7-8 shows the flow directions of channels around ROLD for sjr1500_omr11 scenario, other scenarios are similar.

HORB IN-OUT differences of average flows in sjr_omr scenarios:

- Usually have positive values, i.e., HORB-IN has more flow for both downstream and southward branches.
- Have some negative exceptions: (1) HOR branch – this is the branch after HORB; when HORB-OUT, flow passes through it. (Please refer to the authors for the detailed analysis) (2) Mmid, 3mile branch.
- Usually the closer the specified location to Chipps, the smaller the difference; e.g., jersey, 3mile have the difference < 10 cfs.
- Variation pattern is non-uniform. Usually all locations downstream increase with SJR flow.

The ratio of flow downstream / (downstream + branch) could indicate the flow split pattern more directly (the larger the ratio, the more particles flow to downstream):

- As SJR flow increases (higher SJR flow, similar export), the ratio usually increases, i.e., higher SJR flow increases both downstream and southward branch flows, but the latter more.
- As OMR flow increases (higher export, same SJR flow), the ratio usually decreases, which corresponds to larger downstream flow and smaller southward branch flow.
- Flow ratio IN-OUT difference is usually positive, i.e., HORB-IN direct more flows downstream. Variation pattern: (1) As OMR increases, IN-OUT difference usually increases, i.e., higher export with HORB-IN direct more flow downstream. (2) Its variation pattern to SJR flow is not uniform. As SJR flow increases, ratio decreases for Turner, Columbia, increases for 3mile.

7.4.2.2 San Joaquin River Flow – IE Ratio (sjr_ie) Scenarios

The flow information of Appendix B-3 is summarized for all sjr_ie scenarios, but not included in this report. (Please refer to the authors for the detailed analysis.)

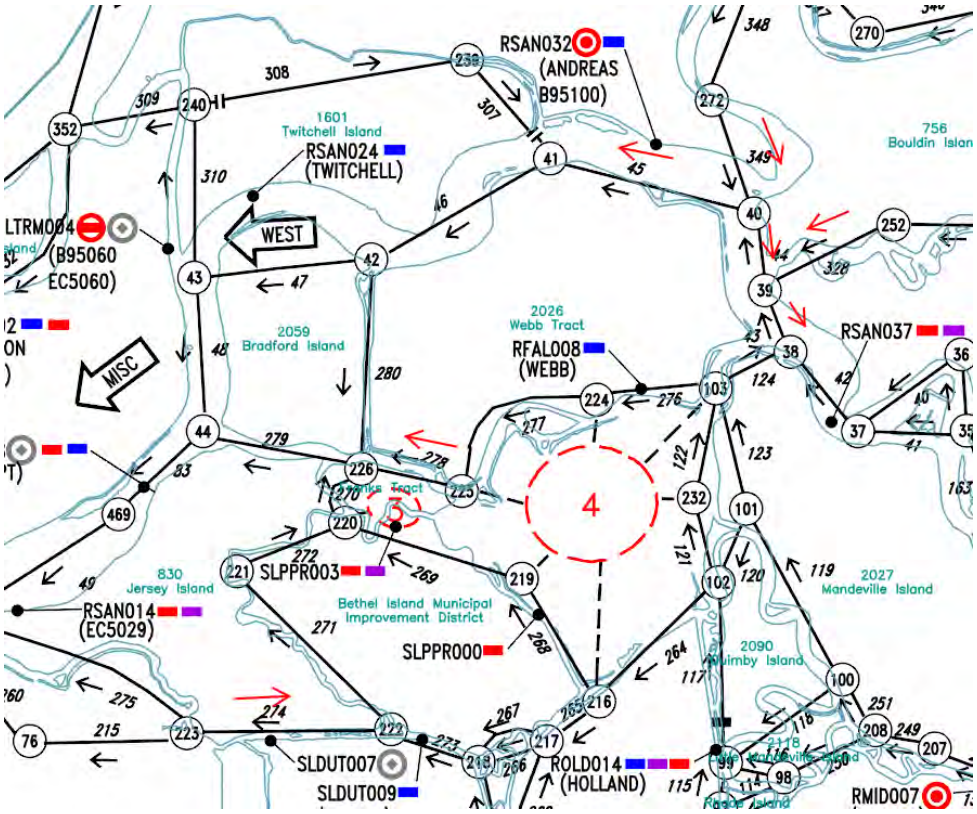

Figure 7-8 Flow Directions (red arrows) of Channels around ROLD for sjr1500_ie11 Scenario

Table 7-11 Average Flow (cfs) Range (min, max) for SJR Junctions in sje_omr Scenarios

Junctions	IN			OUT			IN-OUT		
	branch	downstream	ratio	branch	downstream	ratio	branch	downstream	ratio
HOR	(328.9, 794.9)	(987.9, 5033.2)	(0.7, 0.9)	(767.9, 2854.7)	(508.5, 2983.4)	(0.4, 0.5)	(-2059.8, -439.0)	(438.3, 2053.6)	(0.3, 0.4)
Turner	(374.3, 757.3)	(386.0, 4182.1)	(0.4, 0.9)	(346.5, 660.3)	(-33.0, 2344.9)	(0.2, 0.8)	(27.9, 97.0)	(381.2, 1837.2)	(0.0, 0.3)
Columbia	(331.0, 1396.5)	(-387.6, 3049.7)	(0.4, 0.8)	(259.3, 1084.1)	(-712.0, 1587.7)	(0.3, 0.7)	(71.8, 312.5)	(298.0, 1462.0)	(0.1, 0.3)
Mmid	(521.8, 1485.2)	(-1054.8, 2824.0)	(0.0, 0.8)	(706.6, 1539.9)	(-1386.4, 1383.1)	(0.2, 0.7)	(-200.6, -23.1)	(279.3, 1440.9)	(0.2, 0.4)
Rold	(3067.2, 4090.4)	(-4760.5, -653.1)	(0.0, 0.0)	(3011.3, 3909.0)	(-5056.6, -1901.6)	(0.0, 0.0)	(35.5, 192.2)	(223.4, 1257.8)	(0.0, 0.0)
Jersey	(0.0, 0.0)	(1014.5, 6306.5)	(0.0, 0.0)	(0.0, 0.0)	(611.9, 4653.1)	(0.0, 0.0)	(0.0, 0.0)	(312.3, 1663.0)	(0.0, 0.0)
3mile	(743.8, 1815.0)	(12303.4, 13468.2)	(0.9, 0.9)	(1069.2, 1885.3)	(12231.8, 13118.9)	(0.9, 0.9)	(-325.4, -57.0)	(57.9, 349.3)	(0.0, 0.0)

*Ratio is flow of downstream / (downstream + southward branch)

Table 7-12 Average Flow Variation Pattern with SJR Flow Increasing for SJR Junctions in sjr_omr Scenarios

Junctions	IN			OUT			IN-OUT		
	branch	downstream	ratio	branch	downstream	ratio	branch	downstream	ratio
HOR	increase	increase	increase	increase	increase	increase	negatively increase	increase	mixed
Turner							increase		decrease
Columbia									
Mmid	decrease			decrease			negatively increase		
Rold	increase		N/A	increase		N/A	increase		N/A
Jersey	N/A			N/A			N/A		
3mile	decrease		increase	decrease		increase	negatively increase		increase

*Yellow cell indicate negative values for most scenarios

Table 7-13 Average Flow Variation Pattern with OMR Increasing for SJR Junctions in sjr_omr Scenarios

Junctions	IN			OUT			IN-OUT		
	branch	downstream	ratio	branch	downstream	ratio	branch	downstream	ratio
HOR	increase	decrease	decrease	increase	decrease	decrease	negatively increase	increase	increase
Turner							mixed	mixed	
Columbia									
Mmid							negatively increase		
Rold			N/A			N/A	decrease	increase	N/A
Jersey	N/A			N/A			N/A		
3mile	increase		decrease	increase		decrease	negatively mixed	mixed	increase

*Yellow cell indicate negative values for most scenarios

7.5 PTM Scenarios Results and Analysis

A series of PTM simulations were conducted as described in Section 7.2.4, with insertion locations as in Table 7-5 and Figure 7-3. Simulation results are summarized in the following sections, with corresponding analysis. Detailed Flux plots can be found in Appendixes C and D.

Particle fates at the 45-day end of the simulation period are also recorded and summarized. Compared to the time curve, particles' "final" fates could reflect their movements more directly. Comparison is made between different Hydro scenarios, to identify the effect of SJR flow, IE Ratio, OMR.

7.5.1 Particle Fate Comparison for PTM Standard Boundary Outputs

PTM standard output locations are investigated for the particles' fate at Delta boundaries (Table 7-6):

- Focus is on PAST_MTZ (MTZ), EXPORT_CVP (CVP), EXPORT_SWP (SWP), and DIVERSION_AG (AG).
- DIV_CCC is usually very stable and only takes a small percentage of total flux (0-2%).
- WHOLE could be viewed as a corresponding result related to the other outputs, and its variation trend is usually not obvious to analyze.

For this study, both Three Basins and Southern Delta insertions are investigated (Table 7-5). These insertion locations cover a large part of the Central and South Delta, and could be grouped into 4 categories:

- Insertion 6—on SJR mainstream before HORB
- Insertions 21, 140, 31, 134, 103—on SJR mainstream after HORB (upstream -> downstream).
- Insertions 351, 469, 240—close to Chipps. Usually the particle flux is very large (60-98%) for **MTZ**, very small (1-10%) for CVP, SWP, i.e., most of the particles flow to MTZ, no opportunity to exports.
- Insertion 48—on Old River just after HORB. Usually **AG, export** (mostly CVP) are very large, taking almost 100% (HORB-IN with AG as majority because particles stay longer in Old River due to the very low flows; HORB-OUT with CVP as majority), i.e., most of the particles flow to agricultural facilities and exports, no opportunity to Chipps. Insertion 48 could be viewed as a special insertion, with variation pattern different from other insertions, and won't be included in the following analysis.

7.5.1.1 San Joaquin River Flow – OMR (sjr_omr) Scenarios

Table 7-14 and Table 7-15 summarize the PTM standard output particle fate variations to OMR and SJR flow for sjr_omr scenarios (Appendix C-2, C-3). Both HORB-IN & OUT have a similar pattern most of the time:

a) As OMR increases (higher export, same SJR flow), MTZ decreases for all the insertions, almost all the CVP and SWP increase; almost all the AG decreases for insertions farther from Chipps, increases for insertions close to Chipps.
b) As SJR flow increases (higher SJR flow, same OMR), MTZ increases for all the insertions. CVP, SWP, and AG variation patterns are usually not uniform: with CVP and SWP increases, AG decreases for insertions farther from Chipps and low SJR flows; with CVP and SWP decrease, AG increases for insertions close to Chipps and high SJR flows.

7.5.1.2 San Joaquin River Flow – IE Ratio (sjr_ie) Scenarios

The PTM standard output particle fate range and variation patterns for IE Ratio and SJR flow for sjr_ie scenarios (Appendix C-1) are summarized for all sjr_ie scenarios, but not included in this report. (Please refer to the authors for the detailed analysis.)

7.5.2 HORB IN-OUT Difference of Particle Flux at Martinez

In order to investigate the effect of HORB and HORB IN-OUT, differences of Martinez particle flux are examined for the required insertions. Similar analysis has been conducted for other outputs, e.g., CVP, SWP, but is not included in this report due to space limits. The results could be used for helping decision making of HORB installation in spring season.

- For insertion 6 (SJR upstream before HORB), usually HORB-IN brings more particles to Martinez, and IN-OUT differences increase as SJR flow increases and export decreases (OMR flow negatively decreases).
- For insertion 48, most of the particles flow to exports (CVP/SWP) or AG, that is, usually not to MTZ (except for high SJR flows, like 12,000 cfs, but it does not have HORB-IN for comparison).

7.5.2.1 San Joaquin River Flow – IE Ratio (sjr_ie) Scenarios

Table 7-16 and Figure 7-9 summarize Martinez particle fate at 45-days for different particle insertions of sjr_ie scenarios (details in Appendix C-1).

a) For insertions 21, 140, 31, 134, 103, 351, 469, and 240 (SJR downstream after HORB), HORB-OUT usually has much greater particle movement to Martinez, especially at higher SJR flows. This is probably because HORB-OUT results in lower flows at SJR junctions to the south Delta. Insertions 140, 31, 134, and 103 could have differences of -5% to -20% for SJR flow > 4,500 cfs. HORB's effect are small on insertions 351, 240, and 469; since insertions are very close to Chipps, most particles (usually >85%) go to MTZ.
b) Increasing SJR flow could negatively increase this IN-OUT difference.

7.5.2.2 San Joaquin River Flow – OMR (sjr_omr) Scenarios

Table 7-17 and Figure 7-10 summarize MTZ particle fate at 45 days for different particle insertions of sjr_omr scenarios. (Details in Appendix C-2 and C-3)

- IN-OUT difference is always positive (or zero) in the specified ranges. This is probably because HORB-OUT results in lower SJR flows, but the flows at SJR junctions to the South Delta do not change much with the same OMR flow in each hydro scenario.
- For particle flux HORB IN-OUT difference, the effect on OMR and SJR flow depends on the distance of the insertion location from Chipps:
  - Higher negative OMR usually reduces the difference for farther insertions (6, 21, 140, 31, 134, and 103), but enlarges the difference for the closer insertions (351, 469, and 240).
  - Higher SJR flow usually enlarges the difference for farther insertions (6, 21, 140, 31, 134, and 103), but non-uniform effect for the closer insertions (351, 469, and 240).
  - IN-OUT difference can be very large (5%-25%) for many insertions with higher SJR flow and negatively higher OMR.

Table 7-14 Particle Fates' Ranges (min, max) of PTM Standard Outputs at 45-days' End for sjr_omr Scenarios, Unit %

Insert	MTZ		CVP		SWP		AG	
	IN	OUT	IN	OUT	IN	OUT	IN	OUT
6	(0.0, 30.1)	(0.0, 5.8)	(15.7, 31.4)	(26.5, 47.4)	(10.0, 28.4)	(5.8, 29.0)	(17.4, 40.5)	(14.5, 42.0)
21	(0.0, 35.5)	(0.0, 12.0)	(14.2, 37.1)	(7.8, 32.1)	(16.7, 35.8)	(20.6, 51.1)	(10.4, 22.2)	(12.4, 21.7)
140	(0.0, 10.7)	(0.0, 5.0)	(28.4, 42.3)	(13.8, 42.2)	(26.9, 44.2)	(33.4, 60.0)	(8.0, 19.4)	(7.1, 16.0)
31	(0.2, 37.6)	(0.1, 21.2)	(15.7, 42.0)	(8.4, 39.1)	(17.9, 41.6)	(27.9, 57.7)	(8.4, 17.5)	(7.2, 14.4)
134	(0.6, 50.3)	(0.3, 30.8)	(11.1, 41.5)	(7.0, 38.4)	(12.8, 40.5)	(24.9, 52.1)	(8.3, 15.9)	(7.5, 13.7)
103	(20.7, 67.0)	(18.0, 57.7)	(5.8, 26.1)	(3.8, 26.2)	(8.1, 26.5)	(13.5, 31.0)	(7.3, 11.3)	(7.5, 10.1)
351	(81.9, 96.2)	(79.7, 94.6)	(0.1, 2.8)	(0.0, 3.4)	(0.1, 2.3)	(0.3, 3.2)	(1.2, 2.2)	(1.2, 2.6)
469	(65.4, 95.6)	(60.6, 92.9)	(0.3, 6.0)	(0.2, 7.5)	(0.2, 5.4)	(0.7, 6.9)	(1.4, 4.7)	(1.7, 4.7)
240	(64.1, 95.6)	(60.9, 91.2)	(0.4, 7.9)	(0.2, 8.4)	(0.3, 7.2)	(1.0, 9.3)	(1.2, 4.4)	(1.9, 4.3)
48	(0.0, 0.0)	(0.0, 0.0)	(4.9, 42.8)	(36.5, 75.0)	(0.0, 0.0)	(0.0, 17.4)	(48.4, 85.3)	(16.5, 53.7)

Table 7-15 Particle Fates' Variation Patterns of PTM Standard Outputs with OMR and SJR Flow for sjr_omr Scenario

<table>
<tr><th rowspan="2">Insert</th><th colspan="2">MTZ</th><th colspan="2">CVP</th><th colspan="2">SWP</th><th colspan="2">AG</th></tr>
<tr><th>As OMR increases</th><th>As SJR flow increases</th><th>As OMR increases</th><th>As SJR flow increases</th><th>As OMR increases</th><th>As SJR flow increases</th><th>As OMR increases</th><th>As SJR flow increases</th></tr>
<tr><td>6</td><td rowspan="5">decrease</td><td rowspan="5">increase</td><td rowspan="4">increase</td><td>increase</td><td rowspan="4">increase</td><td rowspan="2">increase</td><td rowspan="4">decrease</td><td rowspan="4">decrease</td></tr>
<tr><td>21
140
31</td><td rowspan="3">decrease</td></tr>
<tr><td>134
103</td><td>IN: decrease;
OUT: increase -> decrease</td></tr>
<tr><td>351
469
240</td><td>increase
(very small)</td><td>decrease
(very small)</td><td>Increase
(very small)</td><td>decrease
(very small)</td><td>increase
(very small)</td><td>decrease
(very small)</td></tr>
<tr><td>48</td><td colspan="2">No particle</td><td>increase</td><td>increase</td><td>decrease</td><td>increase</td><td>decrease</td><td>decrease</td></tr>
</table>

Table 7-16 HORB IN-OUT Difference of Martinez Particle Flux Fate at 45-day's End for sjr_ie Scenarios

Insert		sjr1500 _ie11	sjr3000 _ie11	sjr3000 _ie21	sjr4500 _ie21	sjr4500 _ie31	sjr6000 _ie31	sjr6000 _ie41
Three Basins	6	0.20	1.92	5.31	6.29	10.27	13.62	15.12
	21	0.85	0.74	1.51	3.37	4.42	-2.35	-1.47
	351	0.25	0.04	0.09	-0.11	-0.33	0.34	1.12
Southern Delta	48	0.00	0.00	0.00	0.00	0.00	0.00	-0.60
	140	0.29	-0.02	-1.14	-3.64	-5.88	-15.14	-18.52
	31	0.19	1.00	-0.61	-5.32	-5.84	-17.08	-16.30
	134	0.53	0.22	0.36	-3.24	-4.30	-10.24	-10.67
	469	-0.26	0.01	-0.21	-0.38	-0.14	-0.16	-0.34
	240	0.41	0.86	0.06	-0.21	-0.21	-0.01	-0.54
	103	-0.98	-2.97	-4.93	-6.10	-6.84	-11.04	-10.34

*Red cell indicate particle flux IN-OUT difference larger than 5%; Green cell indicate particle flux IN-OUT difference less than -5%

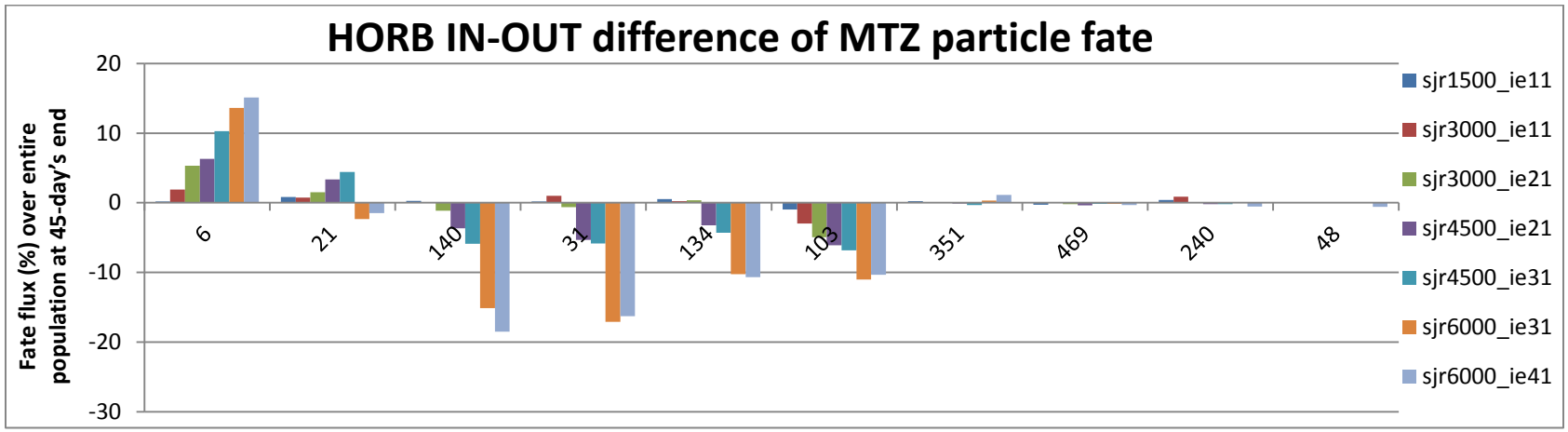

Figure 7-9 HORB IN-OUT Difference of Martinez Particle Flux Fate at 45-day's End for sjr_ie Scenarios

Table 7-17 HORB IN-OUT Difference of Martinez Particle Flux Fate at 45-day's End for sjr_omr Scenarios

Insert		sjr1500 _omr2500	sjr1500 _omr3500	sjr1500 _omr5000	sjr3000 _omr2500	sjr3000 _omr3500	sjr3000 _omr5000	sjr6000 _omr2500	sjr6000 _omr3500	sjr6000 _omr5000
Three Basins	6	0.12	0.08	0.00	4.36	2.16	0.46	24.30	17.09	7.43
	21	0.69	0.18	0.00	4.12	1.89	0.25	23.46	17.31	8.97
	351	0.78	1.74	2.30	1.87	2.46	4.59	1.57	4.09	4.25
Southern Delta	48	0.00	0.00	0.00	0.00	0.00	0.00	0.00	0.00	0.00
	140	0.43	0.08	0.01	1.49	0.43	0.07	5.75	4.14	1.89
	31	1.36	0.24	0.11	7.94	3.82	0.86	16.43	14.25	8.76
	134	2.51	0.72	0.31	9.18	7.00	2.11	19.47	19.66	14.44
	469	3.07	3.80	4.87	3.34	5.11	8.45	2.76	4.37	9.14
	240	2.83	2.77	3.18	4.41	7.10	6.79	4.44	5.63	11.05
	103	3.95	3.17	2.70	6.34	8.21	5.93	9.32	10.33	10.01

*Red cell indicates particle flux IN-OUT difference larger than 5%

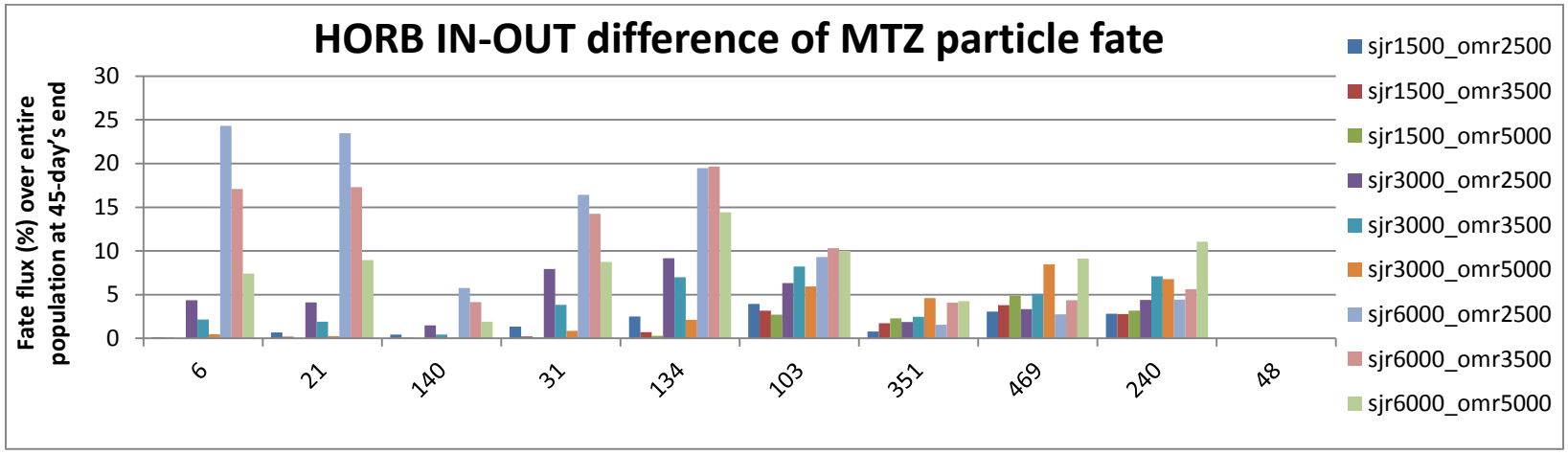

Figure 7-10 HORB IN-OUT Difference of Martinez Particle Flux Fate at 45-day's End for sjr_omr Scenarios

7.5.3 Particle Flux Split at San Joaquin River Junctions to Southward Branch

Another concern of this study is the particle flux split at SJR junctions of their main stem downstream and branches to South Delta (explained in Section 7.4.2). This split analysis is only for 3basins insertions: 6 (Mossdale), 21 (Calaveras), and 351 (Rio Vista).

Detailed comparative plots of particle fate at 45-days are included in Appendix D:

- For insertion 351, 3mile usually has particle flux 85-90% for sac_3mile, 10-15% for 3mile_sac, for both HORB-IN and OUT, both sjr_ie and sjr_omr scenarios. The variation pattern is stable and non-uniform with respect to SJR flow, IE ratio, and OMR. Therefore, 3mile is not considered further in this section.
- The downstream particle flux ratio is only included in the analysis when both branch particle fluxes are positive. A negative ratio happens when one of the branches has a net particle flux inverse from specified direction, and cannot be used for the analysis and comparison.

Average flow split analysis (Section 7.4.2) over the entire simulation period could be used as a reference for the particle movement environment. It cannot reflect the particle fluxes directly, because particles' split only take place at some specific times, e.g., HOR particles' split only take place in the first 2 days, thus only these 2 days flow split affects the particles' split pattern directly.

What should be clarified is the particle flux of DSM2-PTM is not based on particles, but connected water bodies (usually channels); e.g., one particle flowing through channel 1->2 would be counted 1, flowing through channel 2->1 would be counted -1. But one particle may be counted more than once if it reflows the same route; e.g., one particle flowing through channel 1->2->3->1->2 would be counted twice.

This situation may happen due to the complexity of the water bodies' grid and tide effect. As for the 2 categories outputs of this study (Table 7-6):

- Standard output locations (the previous 2 subsections) don't have this problem, since they are boundaries of the model, i.e., once out of boundaries, particles will never be counted again.
- SJR junctions (this subsection) have this problem, since they are intersection grids, and Martinez tide causes flows back and forth all the time. Their counts cannot reflect the exact real percentage of the entire inserted particle population.

However, this issue does not matter for the split analysis in this section. What is important is how particles split at those branch junctions, not which specific particles. Therefore, even if one reflow particle is recounted, it still reflects particles' split pattern at that junction, at that time. And the amount of these reflow particles is relatively limited due to the previous studies.

7.5.3.1 San Joaquin River Flow – OMR (sjr_omr) Scenarios

The particle flux information of Appendix D-3, D-4, D-5, and D-6 is summarized for all sjr_omr scenarios in the following ways: Table 7-18 lists the range (minimum, maximum) of particle flux fates at the 45-days, for SJR junctions, both HORB-IN & OUT and IN-OUT differences, as well as particle flux ratios of downstream / (downstream + southward branch), and their IN-OUT difference. Table 7-19 and Table 7-20 list the particle flux variation patterns to SJR flow and OMR.

- As SJR flow increases (higher SJR flow, similar export), usually downstream particle flux increases, southward branch particle flux increases for junctions close to Chipps (e.g. rold), decreases or non-uniform for junctions farther from Chipps (e.g. hor). This variation is similar for both HORB-IN and OUT, insertion 6 and 21.
- As OMR increases (higher export, same SJR flow), usually downstream particle flux decreases, southward branch particle flux decreases for junctions close to Chipps, increases for junctions farther from Chipps, non-uniform for junctions in-between. This variation is similar for both HORB-IN and OUT, insertions 6 and 21.

For HORB IN-OUT particle flux differences in sjr_omr scenarios,

- Usually positive difference value, i.e., HORB-IN has more flow for both downstream and southward branches since HORB-IN directs more flow to SJR mainstream.
- Some negative exceptions: (1) Insertion 6, HOR branch—this is the branch channel after HORB; HORB-OUT enables half SJR flows to enter interior Delta with almost half particles' fluxes. (2) Insertion 21, turner, columbia, and mmid have negative difference for high SJR flow, i.e., HORB-OUT has more southward flow than HORB-IN.
- Variation pattern is non-uniform. Usually insertions 6 and 21 have downstream increase with SJR flow for many junctions; insertion 6 has downstream decrease with OMR for junctions farther from Chipps.

Particle flux ratio of downstream / (downstream + southward branch) could indicate the particle flux split pattern more directly:

- As SJR flow increases (higher SJR flow, similar export), ratio of many junctions (both insertion 6 and 21) usually increase, i.e., higher SJR flow increases both south-branch and downstream particle flux, but the latter more.
- As OMR increases (higher export, same SJR flow), ratio of many junctions (both insertion 6 and 21) usually decrease, which corresponds to larger downstream particle flux and smaller south-branch particle flux.
- Ratio IN-OUT difference of many junctions is usually positive, i.e., HORB-IN makes larger downstream particle flux. Yet negative values also exist, especially for low SJR flow. This variation pattern is non-uniform to SJR flow and OMR.

7.5.3.2 San Joaquin River Flow – IE (sjr_ie) Scenarios

The particle split information of Appendix D-1 and D-2 is summarized for all sjr_ie scenarios, but not included in this report. (Please refer to the authors for the detailed analysis.)

Table 7-18 Particle Fate Ranges (min, max) at 45-day's End at SJR Junctions for sjr_omr Scenarios, Unit %

Loc	IN			OUT			IN-OUT		
	branch	downstream	ratio	branch	downstream	ratio	branch	downstream	ratio
6									
HOR	(13.0, 24.2)	(74.4, 86.7)	(75.4, 86.9)	(48.2, 56.5)	(42.0, 51.5)	(42.7, 51.6)	(-35.2, -29.0)	(29.1, 35.2)	(29.4, 35.3)
Turner	(7.7, 34.6)	(3.6, 39.2)	(9.4, 83.7)	(6.5, 24.4)	(24.0, 70.5)	(49.5, 91.5)	(-1.9, 10.2)	(-33.5, -20.4)	(-40.1, -7.9)
Columbia	(13.2, 25.4)	(8.6, 53.9)	(37.0, 80.4)	(1.8, 16.6)	(1.2, 25.5)	(39.6, 68.7)	(1.6, 14.1)	(7.4, 28.4)	(-3.5, 14.2)
Mmid	(8.0, 22.4)	(0.1, 44.5)	(1.1, 79.9)	(1.0, 14.9)	(0.0, 17.8)	(1.0, 66.9)	(2.1, 15.2)	(0.1, 26.6)	(0.1, 28.5)
Rold	(0.1, 30.6)	(0.0, 13.7)	(-11.1, 30.9)	(0.0, 14.3)	(0.0, 3.4)	(-5.9, 100.0)	(0.1, 18.1)	(0.0, 10.3)	(-111.1, 13.7)
Jersey	N/A	(0.0, 25.7)	N/A	N/A	(0.0, 7.7)	N/A	N/A	(0.0, 18.0)	N/A
21									
Turner	(15.6, 56.6)	(12.9, 78.3)	(18.5, 83.4)	(10.9, 72.6)	(32.8, 79.5)	(31.1, 88.0)	(-16.8, 4.7)	(-20.1, -1.2)	(-12.6, 5.7)
Columbia	(15.3, 33.2)	(12.4, 59.9)	(39.1, 79.7)	(7.6, 34.5)	(4.1, 52.7)	(34.8, 72.1)	(-11.6, 11.8)	(5.1, 13.3)	(1.6, 17.6)
Mmid	(10.2, 24.8)	(0.2, 51.3)	(1.5, 83.4)	(3.8, 28.5)	(0.0, 34.7)	(0.5, 62.0)	(-11.2, 8.7)	(0.2, 20.2)	(1.0, 34.7)
Rold	(0.2, 35.5)	(-0.1, 15.7)	(-27.8, 30.7)	(0.0, 28.7)	(0.0, 5.7)	(-0.5, 16.5)	(0.2, 17.2)	(-0.1, 10.0)	(-27.8, 14.7)
Jersey	N/A	(0.1, 29.9)	N/A	N/A	(0.0, 14.4)	(0.0, 0.0)	N/A	(0.1, 15.6)	N/A
351									
Jersey	N/A	(2.4, 13.8)	N/A	N/A	(0.9, 12.1)	N/A	N/A	(0.7, 3.4)	N/A
3mile	(10.7, 14.0)	(85.2, 89.1)	(85.9, 89.3)	(10.5, 12.7)	(86.0, 89.2)	(87.3, 89.5)	(-0.4, 1.5)	(-1.5, 0.4)	(-1.5, 0.4)

* Downstream & southward branch: percentage over the entire release particle population. Ratio: particle flux of downstream / (downstream + southward branch)

Table 7-19 Variation Pattern of Particle Fate (45-days' end) with SJR Flow Increasing at SJR Junctions for sjr_omr Scenarios

Loc	IN			OUT			IN-OUT		
	branch	**downstream**	**ratio**	**branch**	**downstream**	**ratio**	**branch**	**downstream**	**ratio**
6									
HOR	decrease	increase	increase	mixed	mixed	mixed	negatively increase	increase	increase
Turner	mixed				increase		mixed		mixed
Columbia				increase			mixed		increase
Mmid				mixed		increase			mixed
Rold	increase		decrease	increase		mixed			mixed
Jersey	N/A		N/A	N/A		N/A	N/A		N/A
21									
Turner	mixed	increase	mixed	mixed	increase	mixed	mixed	mixed	mixed
Columbia			increase			increase			mixed
Mmid							decrease	increase	increase
Rold	increase		mixed	increase		mixed	increase		mixed
Jersey	N/A		N/A	N/A		N/A	N/A		N/A
351									
Jersey	N/A	increase	N/A	N/A	increase	N/A	N/A	increase	N/A

*Yellow (shaded) cells indicate negative values for most scenarios

Table 7-20 Variation Pattern of Particle Fate (45-days' end) with OMR Increasing at SJR Junctions for sjr_omr Scenarios

Loc	IN			OUT			IN-OUT		
	branch	downstream	ratio	branch	downstream	ratio	branch	downstream	ratio
6									
HOR	increase	decrease	decrease	increase	decrease	decrease	negative increase	increase	increase
Turner				mixed		mixed	increase	mixed	mixed
Columbia						decrease		decrease	
Mmid	mixed						mixed		
Rold	decrease		mixed	decrease		mixed	decrease		
Jersey	N/A		N/A	N/A		N/A	N/A		N/A
21									
Turner	increase	mixed	decrease	mixed	mixed	mixed	mixed	mixed	mixed
Columbia		decrease			decrease			mixed	increase
Mmid	mixed								mixed
Rold	decrease		mixed	decrease		mixed	mixed		mixed
Jersey	N/A		N/A	N/A		N/A	N/A	decrease	N/A
351									
Jersey	N/A	decrease	N/A	N/A	decrease	N/A	N/A	increase	N/A

*Yellow cells indicate negative values for most scenarios

7.6 Conclusions

This study provides a sensitivity investigation on the movement of neutrally buoyant particles due to variations of San Joaquin River inflow, Jones and Banks exports, and the Head of Old River barrier, in the Sacramento-San Joaquin Delta during the spring season. Simulation results created a Delta hydrodynamic database for better understanding the boundary inputs' effects.

Although different particle insertions and output retrieval locations affect the results substantially, some general variation patterns could be found:

- Higher SJR inflows and smaller OMR (higher export) carry more particles to Martinez and less to CVP/SWP exports, which usually corresponds to SJR junctions split pattern of more flux to mainstem downstream. SJR flow usually has dominant contribution at its high flow level.
- HORB's effect depends on insertion locations, boundary inputs, and adaptive management selection (sjr_ie or sjr_omr).
- The scenarios simulation result matrix could be used to obtain the detailed variation patterns and ranges, which are helpful in understanding different variables' contributions.
- Insertion locations play a key role in particle behaviors' change under the effect of other boundary/facility operations. Locations farther from Chipps, especially upstream of HOR could have very different (even opposite) patterns from downstream or locations very close to Chipps.

For detailed simulation configuration and result data files and plots, please refer to the website: https://msb.water.ca.gov/delta-modeling/-/document_library/view/95707

7.7 Acknowledgments

We thank Yu Min and Xiaochun Wang for their helps in report revisions, Kijin Nam and Prabhjot Sandhu for their help in quality checks.

7.8 References

Division of Operations and Maintenance. (1989). Standing Operating Order PC 200.7-A. Sacramento: California Department of Water Resources.

Le, K. (2004). Calculating Clifton Court Forebay Inflow (Chapter 12). In *Methodology for Flow and Salinity Estimates in the Sacramento-San Joaquin Delta and Suisun Marsh, 22nd Annual Progress Report to the State Water Resources Control Board.* California Department of Water Resources, Bay-Delta Office, Delta Modeling Section.

Appendixes A-1 through D-6

Note: All appendixes are stored in DWR Bay-Delta Office DSM2 User Group website.

http://baydeltaoffice.water.ca.gov/downloads/DSM2_Users_Group/PTM_NMFS/

The following links are accesses to the each appendix respectively.

Appendix A-1: Sacramento Sensitivity Test for Particle insertion at Mossdale (node 6) HORB-IN

http://baydeltaoffice.water.ca.gov/downloads/DSM2_Users_Group/PTM_NMFS/A1_sac_6_IN.docx

Appendix A-2: Sacramento Sensitivity Test for Particle insertion at Mossdale (node 6) HORB-OUT

http://baydeltaoffice.water.ca.gov/downloads/DSM2_Users_Group/PTM_NMFS/A2_sac_6_OUT.docx

Appendix A-3: Sacramento Sensitivity Test for Particle insertion at Calaveras (node 21) HORB-IN

http://baydeltaoffice.water.ca.gov/downloads/DSM2_Users_Group/PTM_NMFS/A3_sac_21_IN.docx

Appendix A-4: Sacramento Sensitivity Test for Particle insertion at Calaveras (node 21) HORB-OUT

http://baydeltaoffice.water.ca.gov/downloads/DSM2_Users_Group/PTM_NMFS/A4_sac_21_OUT.docx

Appendix A-5: Sacramento Sensitivity Test for Particle insertion at Rio Vista (node 351) HORB-IN

http://baydeltaoffice.water.ca.gov/downloads/DSM2_Users_Group/PTM_NMFS/A5_sac_351_IN.docx

Appendix A-6: Sacramento Sensitivity Test for Particle insertion at Rio Vista (node 351) HORB-OUT

http://baydeltaoffice.water.ca.gov/downloads/DSM2_Users_Group/PTM_NMFS/A6_sac_351_OUT.docx

Appendix B-1: OMR over time of SJR_IE Scenarios

http://baydeltaoffice.water.ca.gov/downloads/DSM2_Users_Group/PTM_NMFS/B1_OMR_sjr_ie.docx

Appendix B-2: OMR over time of SJR_OMR Scenarios

http://baydeltaoffice.water.ca.gov/downloads/DSM2_Users_Group/PTM_NMFS/B2_OMR_sjr_omr.docx

Appendix B-3: SJR junctions split of average flow over 45-days of SJR_IE Scenarios

http://baydeltaoffice.water.ca.gov/downloads/DSM2_Users_Group/PTM_NMFS/B3_SD_sjr_ie.docx

Appendix B-4: SJR junctions split of average flow over 45-days of SJR_OMR Scenarios by OMR sequence

http://baydeltaoffice.water.ca.gov/downloads/DSM2_Users_Group/PTM_NMFS/B4_SD_sjr_omr.docx

Appendix B-5: SJR junctions split of average flow over 45-days of SJR_OMR Scenarios by SJR sequence

http://baydeltaoffice.water.ca.gov/downloads/DSM2_Users_Group/PTM_NMFS/B5_SD_sjr_omr_by_sjr.docx

Appendix C-1: Standard particle flux fates at 45-days' end of SJR_IE Scenarios

http://baydeltaoffice.water.ca.gov/downloads/DSM2_Users_Group/PTM_NMFS/C1_PTM_sjr_ie_std.docx

Appendix C-2: Standard particle flux fates at 45-days' end of SJR_OMR Scenarios by OMR sequence

http://baydeltaoffice.water.ca.gov/downloads/DSM2_Users_Group/PTM_NMFS/C2_PTM_sjr_omr_std.docx

Appendix C-3: Standard particle flux fates at 45-days' end of SJR_OMR Scenarios by SJR sequence

http://baydeltaoffice.water.ca.gov/downloads/DSM2_Users_Group/PTM_NMFS/C3_PTM_sjr_omr_std_by_sjr.docx

Appendix D-1: SJR junctions split of particle flux fates (%) at 45-days' end of SJR_IE Scenarios

http://baydeltaoffice.water.ca.gov/downloads/DSM2_Users_Group/PTM_NMFS/D1_PTM_sjr_ie_sd.docx

Appendix D-2: SJR junctions split ratio of particle flux fates at 45-days' end of SJR_IE Scenarios

http://baydeltaoffice.water.ca.gov/downloads/DSM2_Users_Group/PTM_NMFS/D2_PTM_sjr_ie_sd_ratio.docx

Appendix D-3: SJR junctions split of particle flux fates (%) at 45-days' end of SJR_OMR Scenarios by OMR sequence

http://baydeltaoffice.water.ca.gov/downloads/DSM2_Users_Group/PTM_NMFS/D3_PTM_sjr_omr_sd.docx

Appendix D-4: SJR junctions split ratio of particle flux fates at 45-days' end of SJR_OMR Scenarios by OMR sequence

http://baydeltaoffice.water.ca.gov/downloads/DSM2_Users_Group/PTM_NMFS/D4_PTM_sjr_omr_sd_ratio.docx

Appendix D-5: SJR junctions split of particle flux fates (%) at 45-days' end of SJR_OMR Scenarios by SJR sequence

http://baydeltaoffice.water.ca.gov/downloads/DSM2_Users_Group/PTM_NMFS/D5_PTM_sjr_omr_sd_by_sjr.docx

Appendix D-6: SJR junctions split ratio of particle flux fates at 45-days' end of SJR_OMR Scenarios by OMR sequence

http://baydeltaoffice.water.ca.gov/downloads/DSM2_Users_Group/PTM_NMFS/D6_PTM_sjr_omr_sd_ratio_by_sjr.docx